

NUCLEAR MUON CAPTURE

NIMAI C. MUKHOPADHYAY

*CERN, Geneva, Switzerland and
Swiss Institute for Nuclear Research (SIN),
Villigen, Switzerland*



NORTH-HOLLAND PUBLISHING COMPANY — AMSTERDAM

NUCLEAR MUON CAPTURE*

Nimai C. MUKHOPADHYAY

CERN, Geneva, Switzerland and
Swiss Institute for Nuclear Research** (SIN), Villigen, Switzerland

Received July 1976

Contents:

1. Introduction	3	7. Muon capture and symmetry of the nuclear Hamiltonian	80
2. Atomic capture of the negative muons and its history prior to nuclear capture	6	8. Nucleon emissions following muon capture, fission and rarer reaction modes	88
3. Capture of muons by hydrogen nucleus	25	9. Beyond the impulse approximation	110
4. Theoretical strategy for treating muon capture in complex nuclei	38	10. Résumé and outlook	122
5. Allowed transitions in complex nuclei	46	Appendices	127
6. First- and higher-forbidden transitions, total capture rates	65	Notes added in proof	130
		References	132

Abstract:

This report attempts to survey our present knowledge of the *nuclear* muon capture reactions. Starting from the formation of the muonic atom, various phenomena, having a bearing on the nuclear capture, are reviewed. The nuclear reactions are then studied from two angles – to learn about the basic muon–nucleon weak interaction process, and to obtain new insights on the nuclear dynamics. Future experimental prospects with the newer generation muon “factories” are critically examined. Possible modification of the muon–nucleon weak interaction in complex nuclei remains the most important open problem in this field.

Single orders for this issue

PHYSICS REPORTS (Section C of PHYSICS LETTERS) 30, No. 1 (1977) 1-144.

Copies of this issue may be obtained at the price given below. All orders should be sent directly to the Publisher. Orders must be accompanied by check.

Single issue price Dfl. 52.-, postage included.

*Survey of literature pertaining to this review has been concluded in June, 1976. See notes added in proof for references to works published after this date.

**Present address.

1. Introduction*

The *raison d'être* of the muon as a “heavy electron”, in the ever-increasing family of “elementary” particles, continues to remain a mystery. The only fundamental attributes that distinguish a muon from an electron, are its mass (about 207 times the electron mass), and its “muonness”, described by a muon quantum number \mathcal{L}_μ (equal to +1, for the negative muon in the additive scheme). Basic questions as to why there should be a “heavy electron” at all, and why it should not decay electromagnetically, emitting a photon, to the less massive “light” (ordinary) electron, are still with us. Here we are going to study *how a negative muon interacts weakly with a nucleus*. In this, both the muon mass and the “muonness” play fundamental roles. The underlying theme has one striking aspect that is going to be emphasized repeatedly: the identical strength with which muons and electrons interact weakly, either with leptons or with hadrons (the *muon-electron universality*).

The objective of the present paper is to review our current knowledge of the capture of negative muons by atomic nuclei, starting from the most “elementary” nucleus, the proton, and project its experimental and theoretical horizons. This task is not easy, in view of the many accomplishments in this field in the last three decades, and the widespread anticipations from the experimental possibilities in the newer generation muon facilities (appropriately called “meson factories”, for the copious number of pions produced by them). While plenty of familiar footprints are visible in the survey of the well-trodden ground, an attempt will be made to focus on the recent experimental and theoretical efforts in expanding the boundaries of this field. Hopefully, this will stimulate new experiments in the “meson factories”.

Muons are produced, for the purpose of the physics discussed in this review, by the decay of slow pions. They rapidly slow down in the stopping target materials and then are captured in an atomic orbit. Fast electromagnetic cascades ensue, bringing the muon down to the innermost 1S Bohr level. In this “parking” orbit, the muon waits for its disappearance, either by decay ($\mu^- \rightarrow e^- + \bar{\nu}_e + \nu_\mu$) or by nuclear capture. The history of the muon, from its nascence to disappearance, takes us through vastly different domains of physics. Thus, its slowing-down and capture in an outer atomic orbit are in the domain of chemistry, molecular – or solid-state physics and atomic physics. Early part of the electromagnetic cascade may be influenced by the atomic environment, while the later part provides valuable tests on quantum electrodynamics. As the muon comes closer to the nucleus, various nuclear effects, such as those of the nuclear charge distribution, come into prominence. Finally, the decay of the muon or its nuclear capture, well-separated in the time scale from the former episodes, is the domain of weak interaction. The electromagnetic cascade of the muon will be given only a passing attention here**, focusing on the properties relevant to the nuclear weak interaction process. The nuclear dynamics, brought into play, due to a not-so-gentle tickle by the muon absorption, will be discussed at length, together with the consideration of the basic weak interaction itself, of the muon with the nucleons in the nucleus.

1.1. Historical remarks

The subject of our review spans roughly three periods of research activity, i) the cosmic-ray period beginning with the discovery of “mesotrons” (the archaic name first given to the muons) by

*We shall refer to section x in the text by § x and a subsection y of section x by § x.y. A subsection can be further divided as in § x.y.z.

**This will be covered in depth in a forthcoming report by F. Scheck.

Anderson and Neddermeyer, and by Street and Stevenson in 1936–38, ending in the late fifties, ii) the “low-intensity” period of the sixties in which the laboratory accelerators produced not-so-copious quantities of muons, and iii) the “meson-factory” period, just begun in the middle seventies. Below we make a few historical remarks tracing the development of the field in the first two periods.

The physics of the four-fermion weak interaction began with the appearance of Fermi’s classic paper [1] in 1934. Tomonaga and Araki [2] discussed the possibility of the Coulomb capture of the negatively charged particles in 1940. A few years later, Conversi, Pancini and Piccioni [3] published their finding that muons, in the secondary cosmic radiations, interact “weakly” with the nucleus, thereby ruling out the possibility that they are Yukawa’s predicted carriers of the strong interaction. This experiment was thus the first indication of the *scale* involved in the muon–nucleon weak interaction.

The paper of Fermi and Teller [4] was the first comprehensive attempt to understand the capture of negative muons by atoms and molecules, and the processes that muon undergoes, immediately preceding and following the atomic capture. However, the study of *nuclear* muon capture can be said to have truly begun with the appearance of the paper by Tiomno and Wheeler [5], presented at the 1948 Pasadena Conference on Cosmic Rays. This paper, entitled “Charge-exchange reaction of the μ -meson with the nucleus”, studied the following reaction, and its analogs in the nucleus:



in which μ_0 was shown not to be a photon, and was taken to be “a neutral meson – without thereby ruling out the possibility that it is a neutrino”. The analogy of the process to the neutron β -decay was exploited and μ_0 was correctly assigned spin $1/2$. The importance of electric dipole analog transitions in nuclear muon capture was immediately recognized. Camerini and others [6] studied the analogy of the reaction (1.1) in emulsions exposed to cosmic rays, and Godfrey [7] succeeded in studying muon capture in ^{12}C nuclei. However, the first direct observation of muon capture in hydrogen was made only in 1962, by Hildebrand [8]. At the 1948 Pasadena meeting, Wheeler presented a paper [9] containing the famous Z^4 law: the nuclear muon capture rate Λ is proportional to the fourth power of the *effective* atomic number Z for the target nucleus. He also anticipated [9] the possibility that, in heavy nuclei, muon can induce fission, either by the radiationless $2\text{P}-1\text{S}$ transition, or by direct 1S capture.

The discovery of parity-violation in weak interactions [10] and the identification of its V–A structure [11], together with the ideas of the conserved vector current [12], partially conserved axial vector current [13] and G invariance [14], all produced new interest in the problem of nuclear muon capture. A particularly important contribution was made by Goldberger and Treiman [15], and independently by Wolfenstein [16], on the role of the pseudoscalar form factor in the muon–nuclear weak interaction. Lee, Yang, Bernstein and Primakoff [17] showed that a natural consequence of the V–A theory would be a dramatic hyperfine effect in muon capture by the hydrogen nucleus. Primakoff’s classic review article [18] provides a beautiful summary of the theoretical efforts stimulated by the discovery of the parity violation and other aspects of weak interaction.

The second stage of muon capture studies has spanned the sixties. Hildebrand’s [8] observation of the reaction (1.1) in bubble chamber has been followed by the measurement of the singlet capture rate in hydrogen, by the CERN–Bologna Collaboration [19], to a precision of $\pm 15\%$, obtaining excellent agreement with the prediction of the V–A theory. Numerous experiments in complex nuclei have been performed, measuring capture rates and other variables, looking at diverse

reaction channels, yielding neutrons, charged particles, photons, and, in heavy nuclei, fission products. Major experimental contributions have been made at Berkeley, Carnegie-Tech, Chicago, Columbia, William and Mary, Dubna, and by Bologna, Louvain, and other groups at CERN. On the theoretical side, particularly important in this period is the work of Foldy and Walecka [20], discussing the connection of the giant dipole excitation in muon capture to the nuclear super-multiplet symmetry, and by Fallieros and collaborators [21] on the isospin splitting of the giant resonances in the non-isospin-zero targets.

The current phase of the development of the subject under review has begun with the seventies. The usefulness of the muon induced reactions to probe the nuclear structure is now well-established. The relationships of muon capture with other electromagnetic and weak processes are being increasingly exploited. We are now interested in learning more about the muon–nucleon weak coupling constants *in the nuclear context*, and about new information on nuclear excitations. Rarer modes of nuclear excitations can now be studied with relative ease due to the vastly increased muon intensity currently available. Exotic reactions, apparently forbidden by the known lepton number selection rules, can be searched at levels of extremely small probability for occurrence, setting the scene for discovering possible violations of these selection rules.

1.2. Plan of the review

We begin this review with a consideration of the history of muonic atoms from the instant of capture of the muon in an outer atomic orbit, to that of its arrival in the IS orbit (section 2). Sections 3 to 9 will be devoted solely to the problem of *nuclear* muon capture in the following order: capture by hydrogen nucleus (§3), theoretical strategies for the treatment of capture in complex nuclei (§4), allowed transitions (§5), first and higher “forbidden” transitions (§6), muon capture and symmetry of the nuclear Hamiltonian (§7), nucleon emissions following muon capture and rarer reaction modes (§8), and going beyond the impulse approximation (§9). In section 10, we attempt to project the future possibilities of the field. Appendices include some theoretical details that can be omitted at the first reading.

1.3. A “review” of the other recent reviews

There are numerous books, monographs, reviews and dissertations already available dealing with some aspects of various subjects of this paper. An attempt has been made to make this review more complete and up-to-date. About half of the material appearing here has not been reviewed earlier.

A long, but not exhaustive, list of earlier reviews is appended in the reference section along with a catalogue of books and dissertations on the subject. Below we mention some recent reviews that supplement the materials covered here, particularly the researches done before 1970.

The atomic physics aspects are discussed by Wu and Wilets [B38], Kim [A9], Vogel et al. [B35] and Hüfner et al. [B14]. Application of muon capture to chemistry, molecular physics, and solid-state physics are discussed by Gershtein and Ponomarev [B12], and Evseev [B9].

Lee and Wu [B16], and Llewellyn Smith [B17] give excellent introductions to the weak four-fermion interaction. Gourdin [B13] and Jarlskog [B14a'] discuss weak form factors of hadrons. Muon capture in hydrogen and deuterium is reviewed by Mukhopadhyay [B19], Primakoff [B22] and Zavattini [B39].

Various channels of nuclear muon capture are emphasized by Singer [B30], and by Überall [B34].

Walecka [B36] discusses the sum rule techniques and relationships to other processes. Kim [B15] and Primakoff [B21] address themselves to the difficulties with the so-called “elementary particle” approach. Ericson and Rho [B7], Brown and Weise [B1b], and Hüfner [B13a] review soft-pion and related techniques relevant for the post-impulse approximation development. Frankel [B11a] surveys rare and ultra-rare muon capture processes.

Some of the above reviews appear in the three-volume monograph entitled “Muon Physics”, edited by Wu and Hughes [A13]. Several lectures of the 1976 Zuoz topical meeting on the Intermediate Energy Physics emphasize the future research directions of the nuclear muon capture physics [B17a].

2. Atomic capture of the negative muon and its history prior to nuclear capture

In this section, we review briefly the formation and evolution of muonic atoms, in particular the muon decay from the bound orbit, and the phenomena of particular importance to nuclear muon capture studies such as muon depolarization and hyperfine effects. Mesoatomic and mesomolecular reactions, particularly in hydrogen and deuterium, with or without impurities, are also discussed because of their importance in choosing physical conditions desirable for nuclear experiments in certain liquid or gaseous targets. We survey new techniques for the production of muonic atoms that are likely to be used in future for some nuclear capture experiments. See references [A9, B9, B14, B20, B35] for further details about the subjects discussed in this section.

2.1. Formation and evolution of muonic atoms

Fermi and Teller [4] considered in detail the slowing down of negative muons in matter and showed that the time taken by a muon trapped in an atom to cascade down to the lowest Bohr orbit (1S) is negligible ($\sim 10^{-13}$ s for graphite), compared to its natural lifetime ($\sim 2.2 \times 10^{-6}$ s). The entrapment of muons can be described in the following stages [B38]:

1) *High to low (a few keV) energy*: In this step, the muon velocities are *greater* than the velocity of the valence electrons of the atomic scattering centres. Slowing down time in condensed matter is $\sim 10^{-9}$ to 10^{-10} s.

2) *Low energy to rest*: In this phase, the muon velocity is *less* than that of the valence electrons. In metals, muons can exchange energy with the degenerate electron gas in arbitrarily small steps, and they rapidly (in $\sim 10^{-13}$ s) come to a stop. In insulators and gases, the minimum energy loss is fixed by the gap between two Brillouin zones in the former, and the lowest electronic excitation energy in the molecular configuration in the latter. The slowing down time is estimated to be $\sim 10^{-13}$ s in insulators and $\sim 10^{-9}$ s in gases.

3) *Atomic capture*: Once muon reaches a state of no kinetic energy, it is captured by the host atom into high orbital momentum states, forming a muonic atom. *The exact distribution of these states is experimentally unknown.*

The muon atomic orbit with the same size as the K-electron orbit has a principal quantum number n_μ given by

$$n_\mu \simeq (m_\mu/m_e)^{1/2} \simeq 14. \quad (2.1)$$

The time taken for the muon to enter this orbit from the instant of its atomic capture is $\sim 10^{-14}$ s.

4) *Electromagnetic cascade*: Since all low-lying muonic states are unoccupied, the muon cascades down rapidly to the lowest quantum state (1S) available. Auger and radiative transitions are responsible for this de-excitation.

Auger processes are either p-type ($\Delta l = \pm 1$) or s-type ($\Delta l = 0$). Auger probabilities are practically independent of Z , and are greater for larger n , the dominant transition being $(n_1, l_1) \rightarrow (n_2 = n_1 - 1, l_2 = l_1 - 1)$.

Radiative transitions are overwhelmingly electric dipole type, with a transition probability that is proportional to the cube of the energy difference between (n_1, l_1) and (n_2, l_2) orbits and the fourth power of the atomic number Z . *For a given Z, the Auger transitions are dominant for higher n, while, for lower n, radiative transitions become more probable.* As transition energies increase rapidly, the interaction of muons with the atomic electrons becomes less and less important. Thus, for light elements, Auger effects dominate down to $n_1 \sim 3$, while, for a heavy element like Ag, radiative transitions take over at $n_1 \sim 6$.

In heavy nuclear atoms, the 2P–1S transition energy often exceeds the neutron emission or fission threshold. Hence the muonic atom can de-excite without emitting X-rays, by “kicking out” neutrons or fissuring the nucleus. The former is called nuclear Auger effect (as distinguished from the *atomic* Auger effect discussed above) [22], and the latter, “prompt” fission [23] (§ 8.3.1).

5) *Muon disappearance*: After the muon has reached the 1S orbit, it either decays or gets captured by the nucleus. In hydrogen, the capture to decay probability ratio is of the order of 4×10^{-4} . Around $Z = 11$, the capture probability is approximately *equal* to the decay probability. In heavy nuclei ($Z \sim 50$), the ratio of capture to decay probabilities is about 25.

2.1.1. The Fermi–Teller Z-law for atomic capture of muons

Fermi and Teller [4], by simple arguments and the assumption that the atomic capture probability of a muon is proportional to the energy loss of the muon near the atomic species constituting a compound or a gaseous mixture, concluded that the atomic capture rate Λ_a is given by the proportionality relation

$$\Lambda_a \propto Z, \quad (2.2)$$

Z being the nuclear charge of the atom stopping the muon. This so-called “Z law” implies that, for a binary compound A_nB_m , the ratio of atomic capture rates for the constituting species will be given by

$$\Lambda_a(A)/\Lambda_a(B) = [nZ_A]/[mZ_B]. \quad (2.3)$$

Experiments done in the last decade indicate that there is no such simple law as the relation (2.2) valid for all compounds. Deviations from the Fermi–Teller law have been carefully studied, both theoretically [24] and experimentally (figs. 2.1–2.2) [B20, 24a, 25], and are found to be generally associated with the effects of atomic shell-structure and chemical environment. The last effect is also important in the study of intensities of the muonic X-ray spectra [B28, 26].

2.2. Decay of muons in atomic orbits

The muon disappearance rate, Λ_D , which is the sum of muon decay rate Λ_d and nuclear muon capture rate Λ_c , is the quantity often measured in experiments. Hence the muon decay rate in a bound orbit is of our direct interest in extracting Λ_c from Λ_D .

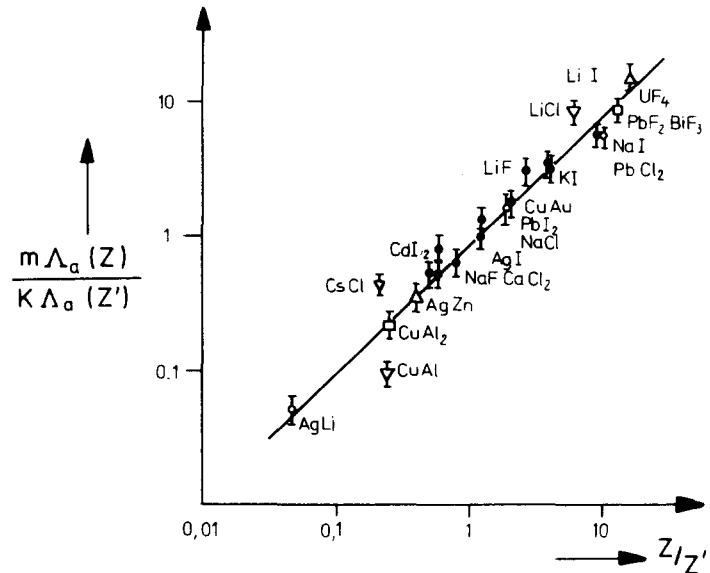


Fig. 2.1. Test of the Fermi-Teller Z law for atomic capture in alloys and halogen compounds of metals, $Z_K Z'_m$. The data are from Zinov et al. [24a]. The straight line represents $0.66 Z/Z'$; $\Lambda_a(Z)$ and $\Lambda_a(Z')$ are the appropriate atomic capture rates.

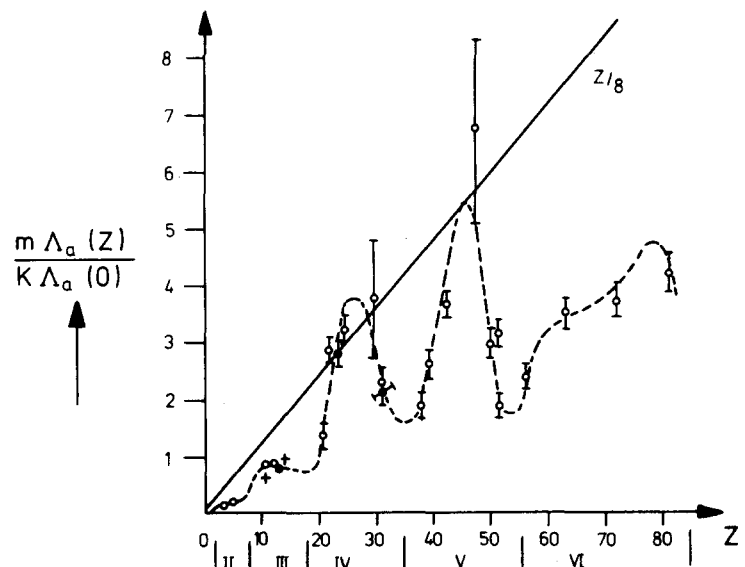


Fig. 2.2. Periodicity of the relative atomic capture probability $m \Lambda_a(Z) / K \Lambda_a(0)$ in the metallic oxides $Z_K O_m$. Numerals II, ..., VI represent the groups in the periodic table to which the metallic atoms belong. The expectation of the Fermi-Teller law is represented by the straight line. Experimental data are from Zinov et al. [24a].

The fact that the probability of μ decay

$$\mu^- \rightarrow e^- + \bar{\nu}_e + \nu_\mu \quad (2.4)$$

is different for bound muons than free ones was pointed out by Porter, Primakoff and others [27]. Recently Hänggi et al. [27] have done an accurate calculation of the decay electron spectrum, using reliable muon and electron wave functions, including the effects of nuclear finite size and vacuum polarization.

Qualitative features:

1) *Decreased decay probability*: This is primarily due to the change of muon mass in the atomic orbit. Since the muon energy in an orbit is

$$E = m_\mu - \Delta E_B < m_\mu, \quad (2.5)$$

the phase space accessible to the muon is smaller than that for the free muon. Hence the decay probability is decreased. Thus, the free decay probability is

$$\Lambda_d^{\text{free}} \propto m_\mu^5, \quad (2.6)$$

while, for the bound case, Λ_d^{bound} is given by

$$\Lambda_d^{\text{bound}} \propto (m_\mu - \Delta E_B)^5, \quad (2.7)$$

where

$$\Delta E_B = \frac{1}{2} m_\mu (Z\alpha)^2. \quad (2.8)$$

For small Z we have

$$\Lambda_d^{\text{bound}} / \Lambda_d^{\text{free}} = 1 - \beta (Z\alpha)^2, \quad (2.9)$$

with $\beta \approx 2.5$. More accurate theoretical estimates confirm the monotonically decreasing trend of the ratio (2.9) with Z , which agree quite well with experiment (table 2.1).

Consideration of relativistic time dilatation due to muon momentum in the 1S orbit also reduces the decay probability, β increasing to about 3.

2) *Doppler shift of the high energy part of the electron spectrum*: Due to orbital motion of the muon in the K-shell, the decay electron spectrum is Doppler-shifted in the high-energy side, thus extending beyond the free muon decay cut-off energy of 52.8 MeV (see fig. 2.3).

Table 2.1

Ratio of bound to free decay rate of negative muons (from Feinberg and Lederman [B10]). Blair's figures are experimental, Huff's are theoretical estimates.

Element	Z	Blair [372]	Huff [27]
Vanadium	23	1.00 ± 0.04	0.98
Iron	26	1.00 ± 0.04	0.98
Cobalt	27	0.94 ± 0.04	0.97
Nickel	28	0.96 ± 0.04	0.97
Zinc	30	0.93 ± 0.04	0.96
Tin	50	0.87 ± 0.04	0.92
Tungsten	74	0.78 ± 0.04	0.85
Lead	82	0.86 ± 0.04	0.84

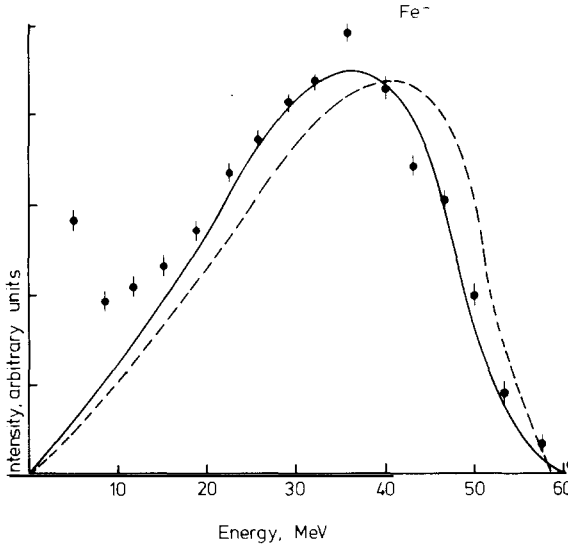


Fig. 2.3. Spectrum of decay electrons from negative muons stopping in iron [A5]. The solid curve represents the theoretical spectrum (Überall, quoted in [A5]). The broken curve gives the electron spectrum from the decay of free muons. Notice the extension of the high-energy tail beyond the free muon decay cut-off limit.

3) *Effect of the nuclear Coulomb field:* This affects both the decay probability of muon and the electron spectrum (analogous to the Fermi effect in β -decay). The latter manifests itself by impeding the emission of low-energy electrons.

2.3. Muon–nuclear magnetic hyperfine interaction

If the nucleus of a muonic atom has non-zero spin, the magnetic moments of the muon and nucleus interact giving rise to the hyperfine (HF) structure in the muonic spectra [28]. The HF interaction width for the 1S state is always larger than or comparable to the muon disappearance width. This has important effects on muon depolarization and nuclear muon capture.

2.3.1. Hyperfine populations for polarized and unpolarized nuclear targets

For generality, let us consider a nucleus of spin I with polarization b , and let a muon enter the 1S orbit* with polarization a . Then the density matrix for the muon and nucleus are given by

$$\rho_\mu = \frac{1}{2} [1 + a \cdot 2S_1], \quad \rho_I = \frac{1}{2I+1} \left[1 + \frac{3}{I+1} b \cdot S_2 \right] + P'_\alpha, \quad (2.10)$$

wherein $S_1 = (\frac{1}{2})\sigma$, $|S_2|^2 = I(I+1)$, and P'_α are higher multipole moments such that $\text{Tr}(1P'_\alpha)$ and $\text{Tr}(S_2 P'_\alpha)$ are zero. Then the HF populations, N_\pm , for the two 1S hyperfine states with angular momenta $F_\pm (= I \pm \frac{1}{2})$ are given by [29]

$$N_\pm \equiv \text{Tr}(P_\pm \rho) = \frac{2F_\pm + 1}{2(2I+1)} \left[1 + \frac{a \cdot b}{I+1} \{ F_\pm(F_\pm + 1) - I(I+1) - \frac{3}{4} \} \right], \quad (2.11)$$

where P_\pm are the projection operators for the hyperfine states with angular momenta F_\pm and ρ is the

*We assume, for simplicity, absence of muon–nuclear magnetic HF interaction in higher orbits

direct product $\rho_\mu \otimes \rho_1$. Thus, in absence of muon or nuclear polarization, eqs. (2.11) reduce to the statistical weights:

$$N_\pm(\alpha \text{ or } b = 0) \equiv N_\pm^s = \frac{2F_\pm + 1}{2(2I + 1)}. \quad (2.12)$$

Hambro and the author [29] have discussed the potential of using *polarized* nuclear targets to probe the difference in nuclear muon capture rates Λ_\pm from the two hyperfine states. The rate of muon capture Λ by a nucleus of spin I is the incoherent average of the HF capture rates Λ_\pm :

$$\Lambda = N_+ \Lambda_+ + N_- \Lambda_-. \quad (2.13)$$

For light nuclei ($3 \leq A < 10$), the HF weights N_\pm are stationary in time, as there is no hyperfine conversion. One can thus measure Λ for two values of nuclear polarization b . Calling $\Lambda^{(1)}$ and $\Lambda^{(2)}$, these values of Λ , we have

$$\Lambda_\alpha = [N_\beta^{(2)} \Lambda^{(1)} - N_\beta^{(1)} \Lambda^{(2)}] / [N_\beta^{(2)} N_\alpha^{(1)} - N_\beta^{(1)} N_\alpha^{(2)}], \quad (2.14)$$

where $\alpha = (+, -)$, $\beta = (-, +)$. Hence, knowing values of α and b , Λ_\pm can be determined separately.

2.3.2. Hyperfine conversion

It was first emphasized by Telegdi [30] that there can be important consequences of the electromagnetic transition between the HF doublet states of angular momenta F_\pm in the muonic $1S$ orbit by radiative M1 decay, which is rather slow, and by emission of conversion electrons. The radiative transition rate R_γ is readily calculable:

$$R_\gamma = \frac{4}{3} \alpha^5 m_\mu^{-2} \epsilon^3 I / (2I + 1), \quad (2.15)$$

where ϵ is the energy difference between the two HF states. The calculation of the electron emission rate is a little more involved [30]. The result is that the internal conversion of electrons begins with $Z = 5$ (^{11}B), and is the main mode of HF conversion for $Z > 5$.

We can thus divide all nuclei, with non-zero spin in four categories: i) very light nuclei ($A = 1, 2$); ii) nuclei with no appreciable HF conversion ($3 \leq A < 10$); iii) nuclei with HF conversion rate R comparable to muon disappearance rate Λ_D ($10 \leq A < 19$); and iv) nuclei with $R \gg \Lambda_D$ ($A \geq 19$). In the first category, the HF conversion is governed by atomic and molecular collision processes (§ 2.5). In the second category, the HF weights are stationary in time and are given by eqs. (2.11). In the third category, the HF weights are functions of time according to the equations

$$N_\alpha = N_\alpha(0) e^{-R t}, \quad N_\beta = 1 - N_\alpha, \quad (2.16)$$

where (α, β) are $(+, -)$ for $\mu > 0$ and $(-, +)$ for $\mu < 0$, μ being the magnetic dipole moment of the target nucleus, R being the conversion rate, $N_\alpha(0)$ being given by eqs. (2.11). Regarding the fourth category, we can write, for the purpose of *nuclear* muon capture estimates,

$$N_\alpha = 0, \quad N_\beta = 1, \quad (2.17)$$

i.e. the capture is *always* taking place from the energetically lower HF state*.

An example of the HF conversion and the resultant time dependence of the HF weights

*Possible exceptions: It has been suggested (see Winston [30]) that the electron conversion may be slow in certain insulators (for example, in red phosphorus), due to the long refilling time of the Auger holes. It would be interesting to test this hypothesis further.

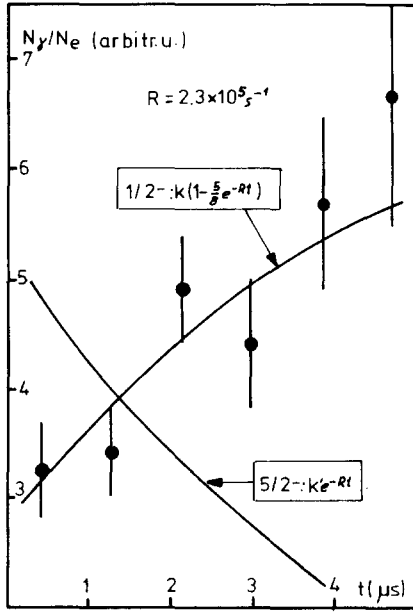


Fig. 2.4. The yield N_γ of the 320 keV γ -line due to the decay of the first excited state of ^{11}Be populated by the nuclear muon capture by ^{11}B . The gamma yield is normalized to the electron yield N_e due to muon decay in the same target (Deutsch et al. [31a]). The experimental points are well-fitted by the function $K(1 - \frac{5}{8}e^{-Rt})$, indicating that the ^{11}Be (320 keV) state has spin 1/2, rather than 5/2.

[eq. (2.16)] is demonstrated in the case of ^{11}B nucleus (fig. 2.4), in which the conversion rate is experimentally determined to be $2.3_{-1.3}^{+2.7} \times 10^5 \text{ s}^{-1}$ [31a]. The HF conversion plays dramatic roles in nuclear capture rates and other observables, particularly in the light nuclei, and should be explored a great deal in future experiments. The depolarization of muon due to HF effects is discussed in the next subsection.

We note here that the magnetic moment of the bound muon is different from that of the free muon. For a point nucleus with charge Ze , this effect is given by Breit [32] for the g -factor:

$$(g^{\text{free}} - g^{\text{bound}})/g^{\text{free}} \approx \frac{1}{3}(\alpha Z)^2. \quad (2.18)$$

Experimental results in light nuclei confirm the Breit trend, while in heavy nuclei finite size effects and other corrections are important [32] (fig. 2.5).

2.4. Muon depolarization before disappearance

The muon residual polarization at the instant of its capture is a fundamental quantity of interest in the consideration of the nuclear capture process. The parity non-conserving effects of the muon–nuclear weak interaction, for example, obtained from the angular asymmetry of the emitted neutrons (or photons in radiative capture), involve the muon residual polarization. Its theoretical evaluation, however, is a very complex matter, as it involves diverse aspects of muon relaxation (μSR) phenomena. The latter also find application in the problem of muon capture in *polarized* nuclear targets [29], and many interesting chemical, solid- and fluid-state studies [B9].

Below we first consider kinematic depolarization suffered by the muon before its atomic capture.

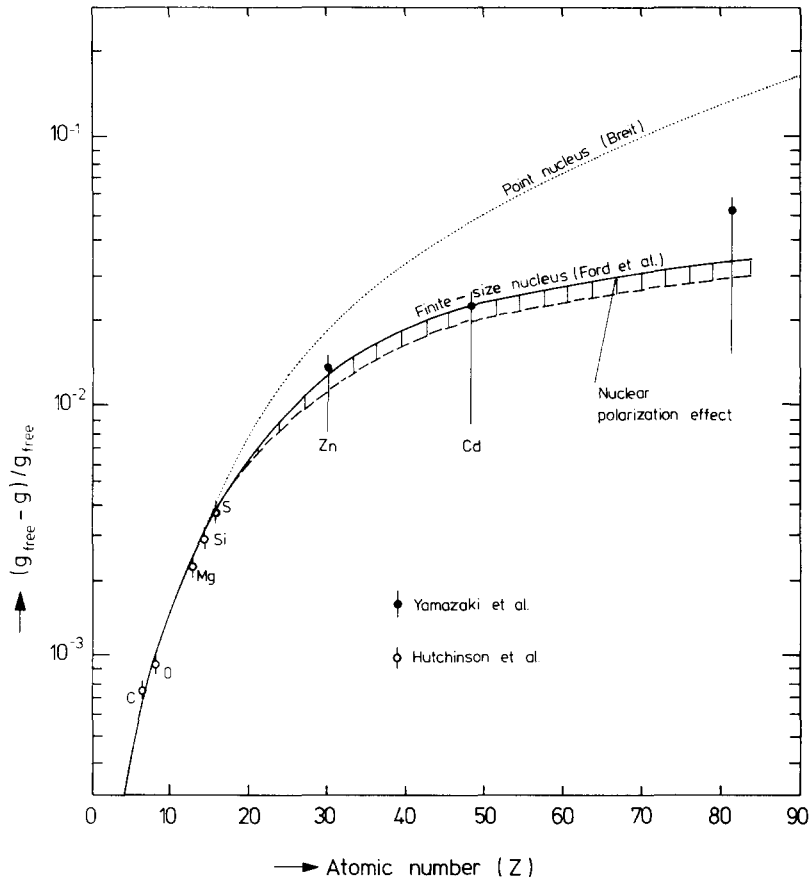


Fig. 2.5. Effect of the atomic binding on the g -factor of muons. Dotted curve is the Breit trend for a point nucleus, while the solid curves take into account the nuclear finite size (see Yamazaki et al. [32] for details).

We then consider depolarization of muons in spin-zero and non-spin-zero nuclear targets, respectively.

2.4.1. Kinematic depolarization

Depolarization suffered by the muon before its capture by an atom is essentially kinematic in origin. Collimated muons available in the laboratory are produced from the decay of pions in flight over a relatively large solid angle. Thus, even though the muon is completely polarized in the pion rest system, there will be kinematic depolarization in the lab, since muons coming forward and backward in the pion rest system have opposite polarizations.

Integrating over the energy spread ΔE_π of pion in the lab, and neglecting the variation of the muon intensity over the corresponding angle range, the average lab polarization of muon is

$$P_1 \simeq 1 - 2\Delta E_\pi/m_\mu, \quad (2.19)$$

putting in explicitly values of various kinematic variables [A5]. With $\Delta E_\pi/m_\mu = 0.1$, $P_1 = 0.8$, i.e. a 20% depolarization of muon. There is practically no depolarization in the process of slowing down of muons before atomic capture [33].

2.4.2. Depolarization in atomic cascade: atoms with spin-zero nuclei

Muons cascade down the atomic levels by Auger and overwhelmingly E1 radiative processes, which, by themselves, do not depolarize the muon, since these processes do not act on the muon spin. However, at some value of the principal quantum number n_0 , the muon de-excitation width Γ_D becomes comparable to, or less than the fine-structure width Γ_{FS} . In this situation, the various (n_0, l_0, j_0) states cannot coherently superpose, and muon depolarization results. Once this situation has been reached, it will continue to hold for lower energy states, except for the orbital angular momenta zero states, for which there is no spin-orbit splitting.

Many authors have considered the spin-orbit depolarization of muons in spin-zero targets [34]. We sketch here the arguments due to Shmushkevich [34], which go in two steps: i) calculation of the polarization of the muon in orbits characterized by the principal quantum number n_0 and total angular momenta $j_0 = l_0 \pm \frac{1}{2}$; ii) determination of the muon polarization as it cascades from the orbit (n_0, l_0, j_0) to the ground state (1S).

Step 1: The probability of occupation of the orbit (n_0, l_0, j_0) , assuming all the magnetic substates to be equally probable, is

$$p_0 = \frac{2j_0 + 1}{2(2l_0 + 1)}. \quad (2.20a)$$

The mean value of σ_Z for the state (n_0, l_0, j_0) is

$$(\bar{\sigma}_Z)_{n_0 l_0 j_0} = \frac{[\frac{3}{4} + j_0(l_0 + 1) - l_0(l_0 + 1)]^2}{3j_0(j_0 + 1)}. \quad (2.20b)$$

Taking the large orbital angular momentum limit ($l_0 \rightarrow \infty$), after substituting $j_0 = l_0 \pm \frac{1}{2}$ in eqs. (2.20), we get

$$\rho_0 \approx \frac{1}{2}, \quad (\bar{\sigma}_Z)_{n_0 l_0 j_0} \approx \frac{1}{3}. \quad (2.21)$$

Step 2: The mean value of spin S_K in the K-orbit can now be calculated by explicitly following the muonic transition from (n_0, l_0, j_0) to 2S and 1S orbits, respectively, and assuming that 2S \rightarrow 1S transition goes by Auger processes having no effect on the muon spin.

This yields

$$\bar{S}_K = \beta_K \bar{S}_0, \quad (2.22)$$

where β_K involves angular momentum factors, partial and total widths for the decay $i \rightarrow i + 1$, a product over the index i , and a sum over the 2S and 1S states. Explicit calculations yield, for large l_0 , the following limits of β_K :

$$\beta_K \rightarrow 1 \quad \text{for } j_0 = l_0 + \frac{1}{2}, \quad \text{and} \quad \beta_K \rightarrow 0 \quad \text{for } j_0 = l_0 - \frac{1}{2}. \quad (2.23)$$

Thus, the decay of the state $j_0 = l_0 + \frac{1}{2}$ preserves the muon polarization completely, while decay of the state $j_0 = l_0 - \frac{1}{2}$ completely depolarizes the muon.

The final muon polarization is given by $P_1 P_2$, where P_1 is given by eq. (2.19), and P_2 is obtained from eqs. (2.21)–(2.23):

$$P_2 = p_0 (\bar{\sigma}_Z)_{n_0 l_0 j_0} = \frac{1}{6}. \quad (2.24)$$

Notice that in heavier nuclei 2S and 2P states are no longer degenerate due to the finite size effect of the nucleus, and the decay 2S \rightarrow 2P \rightarrow 1S will slightly reduce the value of P_2 .

Comparison with experiment: According to eq. (2.24), muon retains $\frac{1}{6}$ ($\approx 17\%$) of its initial polarization at the beginning of the cascade in “isolated atoms” with spin-zero nuclei. Table 2.2 shows the experimental results for this expectation. We notice that the agreement is excellent in all cases except ${}^4\text{He}$ [35]. Studies of muon depolarization in spin-zero atoms in certain atomic environments, however, indicate strong deviations from the “ $\frac{1}{6}$ ” law in many cases [A5, B9, 36]. These deviations can be at least qualitatively understood. The above treatment for isolated systems assumes an idealized situation, in which the electronic shell has no magnetic moment (thus implying absence of its paramagnetic effects and HF coupling between electrons and muon), and the filling of electronic vacancies caused by the Auger processes occurs rapidly compared to the muon de-excitation time. This idealization clearly is not fulfilled in all circumstances. Stark transitions, effects of “denuding” muonic atoms and molecules by ionizations, perturbations due to lattice effects, and mesochemical reactions add to the list of increasingly complex effects having influences on the muon spin relaxation. The exact mechanism of depolarization [35] in the ${}^4\text{He}$ muonic atom is yet to be understood.

Table 2.2

Polarization P_2 of muon in the 1S orbit in various spin-0 targets. P_2 has been defined to be the fraction of the muon polarization at atomic capture (%). The data for ${}^4\text{He}$ comes from Sunder et al. [35], the rest are from Weissenberg [A5].

Target	P_2
${}^4\text{He}$	6 ± 1
${}^{12}\text{C}$	14 ± 4
${}^{16}\text{O}$	15 ± 4
${}^{24}\text{Mg}$	19 ± 5
${}^{28}\text{Si}$	16 ± 4
S	15 ± 3
${}^{64}\text{Zn}$	19 ± 5
Cd	19 ± 5
Pb	19 ± 6

2.4.3. Muon spin relaxation in atoms with non-spin-zero nuclei

The dynamics of the μ SR, in presence of the nuclear HF interaction, is very complex and is discussed in a forthcoming publication by Hambro and the author [29]. For illustration, let us consider a nucleus of spin $\frac{1}{2}$. The density operator for the muon–nucleus system is then of the general form

$$\rho(t) = \frac{1}{4} [1 + 2\alpha(t) \cdot S_1 + 2b(t) \cdot S_2 + 4c^{ij}(t)S_1^i S_2^j], \quad (2.25)$$

where a and b are muon and nuclear polarization. Let us now take the HF interaction Hamiltonian to be just the contact term for simplicity:

$$H = \omega S_1 \cdot S_2, \quad (2.26)$$

which is turned on at time $t = 0$; ω in eq. (2.26) is the HF constant. The initial conditions are

$$\alpha(0) = \alpha_0, \quad b(0) = b_0, \quad c^{ij}(0) = a_0^i b_0^j. \quad (2.27)$$

It is then easy to derive the following set of equations (analogous to the Bloch–Wangsness

equations [37]):

$$\dot{a}^m = -\dot{b}^m = -\frac{1}{2}\omega \epsilon^{ijm} c^{ij}, \quad (2.28)$$

$$\dot{c}^{ij} = \frac{1}{2}\omega \epsilon^{ijk}(a^k - b^k), \quad (2.29)$$

where ϵ^{ijk} is the Levi–Civita tensor.

From eq. (2.29) we immediately get the theorem: *the trace of c is a constant of motion*. Solving eqs. (2.28) is easy and taking the limit $\omega \gg \Gamma$ (i.e. the HF width \gg muon disappearance width), we obtain the time-averaged values of the muon and nuclear polarizations:

$$\bar{a} = \bar{b} = \frac{1}{2}(a_0 + b_0), \quad (2.30)$$

which is the muon physics analogue of the Overhauser effect [38]. For any spin I of the nucleus, the average muon polarization is given by [29]

$$|\bar{a}| = \frac{1}{3} \left[\left\{ 1 + \frac{2}{(2I+1)^2} \right\} a_0 + \frac{12b_0 I}{(2I+1)^2} \right]; \quad (2.31)$$

this equation was obtained originally for unpolarized nuclear targets ($b_0 = 0$) [38]. Generalization of eqs. (2.28)–(2.29) for nuclei with arbitrary spin and for tensor and other muon–nuclear HF interaction is very complex [29].

We get the following conclusions: i) In absence of nuclear polarization, the muon–nuclear HF interaction depolarizes the muon additionally by a factor $\frac{1}{2}$ for spin $\frac{1}{2}$ to $\frac{1}{3}$ for $I = \infty$. ii) *By using polarized targets, it will be possible to repolarize the muon, since the muon and nucleus share their polarizations in the HF interaction.* The second conclusion opens new avenues to exploit the HF interaction and polarized nuclear targets to “regenerate” muon polarization [29]. This should make many difficult correlation experiments attractive in the near future. This technique may also have some application in the experiments looking for neural-current-induced parity violation in muonic atoms [38a].

Recent experiments by Favart et al. [31b] shows that, while eq. (2.31) (with $b_0 = 0$) is enough to explain the additional depolarization of muon in some targets, it is not adequate. In many targets the additional depolarization of muon is much bigger (table 2.3). Origins of the additional depolarization are not clear at the moment.

2.5. Mesomolecular reactions

A study of these reactions, particularly in hydrogen and deuterium with or without impurities, tells us how to use the physical variables (temperature, pressure, impurity, etc.) to choose the condition desirable for the *nuclear* capture experiments. Transfer reactions are suitable to use when one needs to do experiments with trace elements that can be mixed with hydrogen gas at *high pressure* [39]. Transfer reactions are *not* suitable for experiments in which the muon polarization should be retained.

2.5.1. Muon–hydrogen system

A) *Elastic scattering and jump (hyperfine conversion) scattering:* In a system of pure hydrogen, the $\mu^- p$ system can exist in two hyperfine states with total angular momentum (F) equal to 1 (triplet) or 0 (singlet). At time $t = 0$, indicating the arrival of muon in the 1S orbit, the $\mu^- p$ system

Table 2.3

Additional depolarization of muons due to the magnetic hyperfine (HF) interaction between muon and nucleus. P_J and P_0 are polarizations of muon in the 1S orbit, for target nuclei with spin J and zero, respectively. Experimental results are from the sources indicated by superscripts: a, compilations by Weissenberg [A5]; b, Favart [C4]; ca and cb, Ignatenko et al., quoted by Winston [30], for red and black phosphorous, respectively; d, Winston [30] for red phosphorous. The quantity x indicates the expected additional depolarization due to infinite HF coupling in the 1S levels *in absence of any HF conversion* (HFC). Notice the effect of HFC in ^1H , ^{19}F and ^{31}P .

Target nucleus (Spin, sign of the magnetic moment)	P_J/P_0	x
$^1\text{H}(J = 1/2, +)$	$0.18 \pm 0.18^{\text{a}}$	0.50
$^6\text{Li}(J = 1, +)$	$0.45 \pm 0.02^{\text{b}}$	0.41
$^7\text{Li}(J = 3/2, +)$	$0.41 \pm 0.02^{\text{b}}$	0.38
$^9\text{Be}(J = 3/2, -)$	$0.32 \pm 0.02^{\text{b}}$	0.38
$^{10}\text{B}(J = 3, +)$	$0.18 \pm 0.03^{\text{b}}$	0.35
$^{11}\text{B}(J = 3/2, +)$	$0.26 \pm 0.04^{\text{b}}$	0.38
$^{19}\text{F}(J = 1/2, +)$	$0.24 \pm 0.24^{\text{a}}$	0.50
$^{31}\text{P}(J = 1/2, +)$	$\sim 0.50^{\text{ca}}$ $\sim 0^{\text{cb}}$ $\sim 0^{\text{d}}$	0.50

can be assumed to be statistically populated. We can now characterize the scattering process



with three cross-sections: σ_a , σ_b , σ_c ; σ_a is the elastic scattering cross-section for the $\mu^- p$ system having an energy E greater than the hyperfine interval

$$\Delta E_H = 0.195 \text{ eV}; \quad (2.33)$$

σ_b is the cross-section for $E \sim \Delta E_H$, for the conversion of the $\mu^- p$ system from the triplet state to the singlet state by its scattering from p ; σ_c is the elastic scattering cross-section for $\mu^- p$ in the angular momentum $F = 0$ state with energy $E < \Delta E_H$. Theoretical [40a, b] and experimental [41] cross-sections for these reactions are given in table 2.4. In a relatively short time, the $\mu^- p$ system ends up in the $F = 0$ state in a dense hydrogen gas. By varying the pressure of the gas, one can change the lifetime of the triplet state. Thus, for hydrogen gas at $\sim 300^\circ\text{K}$, Matone [42] estimates a triplet lifetime of 82 ns at 8 atm of pressure and of 1.2 μs at 0.5 atm (fig. 2.6).

B) *Molecule formation*: In absence of any impurity, the $\mu^- p$ system can undergo the following processes*:



The process (2.34) has been studied extensively theoretically [40a, b] and experimentally [43]. The conclusions are as follows: i) $p\mu^- p$ forms almost completely in the ortho (relative angular

*We indicate by P(D) a proton (deuteron) *with* an orbital electron.

Table 2.4

Scattering cross-sections for the process $\mu^- p + p \rightarrow \mu^- p + p$. Two experimental values of σ_b and σ_c arise from the ambiguity in the scattering length. See text for definitions of the σ 's.

	$\sigma_a(10^{-21} \text{ cm}^2)$	$\sigma_b(10^{-19} \text{ cm}^2)$	$\sigma_c(10^{-19} \text{ cm}^2)$
Experiment [41]	7.6 ± 0.7	8.7 ± 0.7 4.0 ± 0.5	8.8 ± 0.7 4.1 ± 0.5
Theory [40a] [40b]	1.2 8.2	7.8 3.9	7.9 4.0

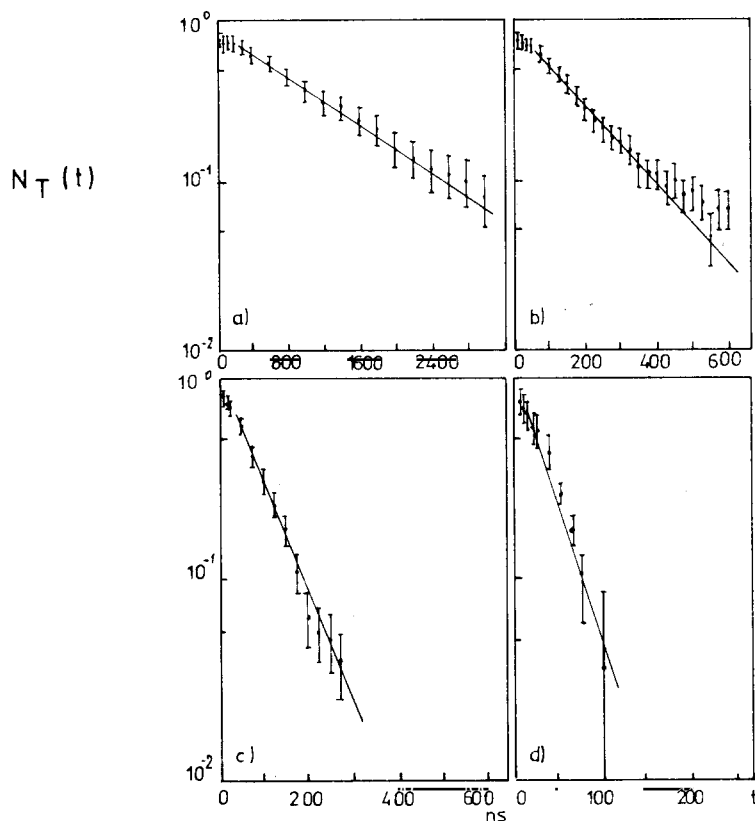


Fig. 2.6. Lifetime of the triplet hyperfine state in the muonic 1S level of hydrogen as a function of pressure, in the Monte Carlo calculation of Matone [42]; pressures are (a) 1/2 atm; (b) 5 atm; (c) 8 atm; (d) 25 atm.

momentum $L = 1$) state at a rate $\sim 2 \times 10^6 \text{ s}^{-1}$ in liquid hydrogen, and $\sim 2 \times 10^4 \text{ s}^{-1}$ in gas at 7 atm [B26]; ii) the conversion rate λ_{op} from an ortho state to a para state ($L = 0$) (which is 148 eV lower in energy) is negligible compared to the decay rate λ_0 of the muon ($\lambda_{op} \leq 5 \times 10^4 \text{ s}^{-1}$ [53]).

Thus the $p\mu^- p$ formation is *unimportant* for gaseous hydrogen, but *extremely important* for liquids. We will utilize this result in the calculation of the nuclear capture rate in liquid hydrogen (§3).

2.5.2. Muon-deuteron system

A) *Elastic scattering and jump (hyperfine conversion) scattering:* At $t = 0$, the μ^-d system is formed with statistical populations for the hyperfine states with total angular momenta $F = \frac{3}{2}$ (quadruplet state) and $F = \frac{1}{2}$ (doublet state), respectively. The hyperfine interval in this case is ΔE_D equal to 0.046 eV. The rate $\lambda_{3/2 \rightarrow 1/2}$ for the jump scattering in the process



is theoretically [40] estimated to be

$$\begin{aligned} \lambda_{3/2 \rightarrow 1/2}(\text{liquid}) &= 7 \times 10^6 \text{ s}^{-1}, \\ \lambda_{3/2 \rightarrow 1/2}(\text{gas}) &= 3.5 \times 10^4 \text{ s}^{-1}. \end{aligned} \quad (2.38)$$

Thus the conversion is negligible in gaseous deuterium compared to muon disappearance rate, and *the initial populations (with which the hyperfine states are formed) are retained.*

B) *Fusion reaction:* Fusion reactions taking place in the deuterium mesic system are



These have been studied experimentally by many authors, most recently by Bystritskii et al. [45]. The experimental results are in excellent agreement with the theoretical predictions of Vesman [46], who has to make a crucial assumption on the existence of an excited rotational-vibrational level of low binding energy (~ 0.7 eV) in the $(\mu^-dd)^+$ system.

2.5.3. Muon-proton system with deuterium impurities

This system has been extensively studied, highlighted by the experimental discovery by the Alvarez group [47] of fusion reactions *involving muons as catalysts*. There was excitement in the early days about the spurious potential of using this reaction as a source of energy*.

A) *Transfer and collision scattering:* Very briefly we sketch here reactions that take place even in presence of a very small deuterium impurity in the hydrogen targets. Due to reduced mass effect, a muon is more tightly bound in a μ^-D atom than in a μ^-P atom by about 135 eV; thus muon has a very high affinity for deuterium. Hence the rate λ_e for the reaction



is very high, about 1.4×10^{10} per sec in liquid hydrogen, higher than any other reaction rate in the system. The μ^-d system then slows down by the collision reaction:



At very low concentrations of deuterium, this reaction (2.42) determines the evolution of the μ^-d atom. The cross-section of this reaction, calculated by Cohen et al. [40b], has a zero at about 0.2 eV centre-of-mass energy of μ^-d system (the *Ramsauer-Townsend effect*).

*How this prospect was missed only “by several orders of magnitude” is described by L.W. Alvarez in his Nobel Lecture [48]. We include here the photographs of muon catalysis, taken by Alvarez et al. (plate 1) in liquid hydrogen bubble chamber at Berkeley, and by Dzhelepov et al. (plate 2) in hydrogen diffusion chamber at Dubna.

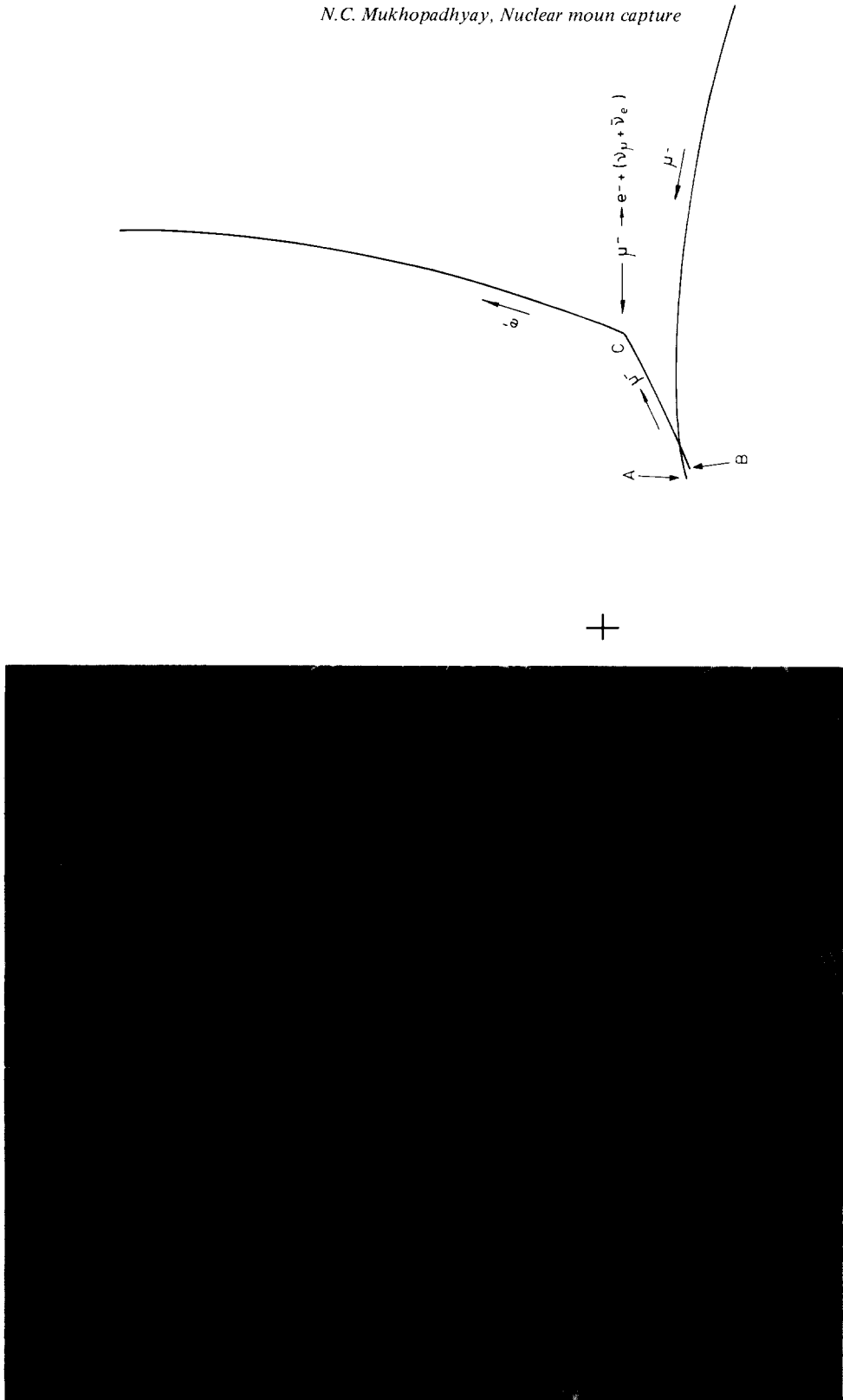


Plate 1. The proton-deuteron fusion reaction catalyzed by muons in the liquid hydrogen bubble chamber, observed by Alvarez et al. [47] (courtesy of Professor Luis W. Alvarez, Lawrence Radiation Laboratory, University of California, Berkeley). The sketch accompanying the plate illustrates the reaction stages: μ^- comes in and $(p\mu^-)^0$ atom is formed at A. It drifts; muon is transferred to D in the HD molecule, forming $(d\mu^-)^0$ atom. The $(d\mu^-)^0$ atom recoils, stopping at B and forming $(pd\mu^-)$ molecular ion. The fusion reaction $(HD)_\mu^+ \rightarrow {}^3\text{He} + \mu^- + 5.46 \text{ MeV}$ takes place. The muon takes off, decaying at C.

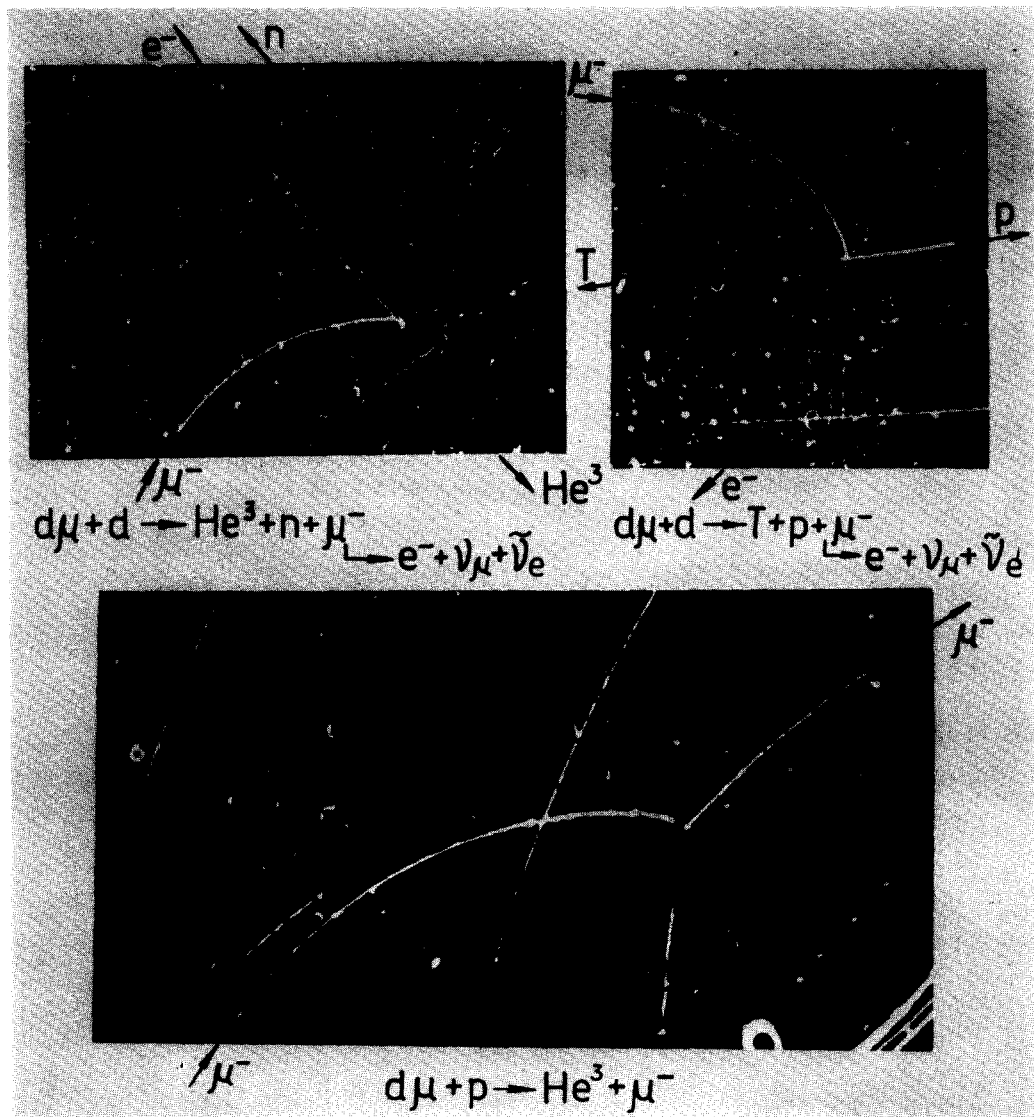


Plate 2. The muon catalyses in the high pressure (20 atm) diffusion chamber filled with hydrogen having deuterium admixture, observed by Dzhelepov et al. [Sov. Phys. JETP 22 (1966) 275] (courtesy of Professor V.P. Dzhelepov, Laboratory of Nuclear Problems, Joint Institute of Nuclear Research, Dubna). As an illustration, the sequence of events in the figure at the bottom of Plate 2 will be given here: reactions occurring between the point of stopping and the point of emergence of the muon ("gap") are (a) $p\mu^- + d \rightarrow d\mu^- + p$, (b) $d\mu^- + p \rightarrow d\mu^- + p$, (c) $d\mu^- + p \rightarrow pd\mu^-$, (d) $pd\mu^- \rightarrow {}^3He + \mu^-$. The "gap" is due to the small cross-section for the elastic scattering reaction (b).

Table 2.5

Important muomolecular processes in competition with muon decay in muonic hydrogen and deuterium systems

Rates	Muonic process	Measured values in units of $10^6/\text{sec}$
λ_0	$\mu^- \rightarrow e^- + \bar{\nu}_e + \nu_\mu$	0.4547 [368]
$\lambda_{1 \rightarrow 0}$	$\mu^- p(F=1) + p \rightarrow \mu^- p(F=0) + p$	12.2 [42] ¹ , 0.83 [42] ²
λ_{pp}	$\mu^- p + p \rightarrow p\mu^- p(L=1)$	2.55 ± 0.18 [43b] ³ , ~ 1.2 [369] ⁴
λ_{op}	$p\mu^- p(L=1) \rightarrow p\mu^- p(L=0)$	1.89 ± 0.2 [43a] ³
λ_e	$\mu^- p + d \rightarrow \mu^- d + p$	≤ 0.05 [44a, 53]
λ_{pd}	$\mu^- d + p \rightarrow p\mu^- d$	$(1.43 \pm 0.13) \times 10^4$ [43a]
λ_{fp}	$p\mu^- d \rightarrow {}^3\text{He} + \mu^+$	6.82 ± 0.25 [43b], 5.8 ± 0.3 [43a]
λ_{dd}	$\mu^- d + D \rightarrow d\mu^- d + e^-$	0.31 ± 0.01 [43a]
	$d\mu^- d \rightarrow T + p + \mu^-$	0.072 ± 0.014 [370] ⁵ , 0.75 ± 0.11 [371] ⁶
	and	0.098 ± 0.001 [45] ⁵ , 0.73 ± 0.07 [45] ⁶
	$d\mu^- d \rightarrow {}^3\text{He} + n + \mu^-$	$> 10^2$ [370]
λ_{fd}	$\mu d \left(F = \frac{3}{2} \right) + d \rightarrow \mu^- d \left(F = \frac{1}{2} \right) + d$	> 1.8 [45]
$\lambda_{3/2 \rightarrow 1/2}$		$7^{5,7}, 0.0035^{6,7}$

¹ Gas at 8 atm pressure and $\sim 300^\circ\text{K}$.² Gas at $\sim 300^\circ\text{K}$ and 0.5 atm pressure.³ Liquid.⁴ Gas at 1000 atm pressure.⁵ Liquid deuterium.⁶ Gaseous deuterium.⁷ Calculated by Zel'dovich and Gershtein.^{1,2} Calculated values.

B) *Fusion reactions* [47, 48]: Fusion reactions consist of the following chain:



In the last reaction, the 5.5 MeV muon is recycled into the chain of getting captured by the proton, forming $\mu^- p$, and following successive stages again.

See table 2.5 for a summary of the determination of rates of the various reactions discussed here.

2.5.4. Muon-proton and muon-deuterium systems with impurities having atomic numbers $Z > 1$ and $Z > 2$, respectively

Transfer reactions: These reactions occur in presence of target materials of mass number A and atomic number $Z (>1)$ in the hydrogen and deuterium systems as impurities:



resulting in the formation of a new muonic atom $(\mu^- {}_Z A)^*$ which then de-excites by Auger and radiative processes described in § 2.1 [49]. Some interesting facts about these reactions can be summarized here:

- 1) The rates of these reactions are high ($\sim 10^{11} \text{s}^{-1}$) except in ${}^4\text{He}\dagger$, where the rates are down by about five orders of magnitude [50] for the reaction (2.47), more for the reaction (2.46).

[†]Theoretical discussion of this exceptional case is involved [see S. Gershtein, Sov. Phys. JETP 16 (1963) 501 for a complete treatment]. This is due to absence of the pseudointersections in the term values for the $p\mu + \text{He}$ and $\text{He}\mu + p$ systems.

2) The ratio of the reaction rates (2.46) and (2.47) is ~ 2 for rare gas impurities [50], except ${}^4\text{He}$.

3) There are definite maximum principal quantum number (n_0) values from which the $(\mu^- {}_Z A)^*$ atom can start the muon cascade; this is governed by the total available energy (2.6 keV) in the μ^- p ground state. This gives $n_0 \leq Z$ [39].

4) Muon residual polarization at the end of the cascade in the muonic atom formed by the transfer reaction should be *much smaller* than that in the case of directly formed muonic atoms of same Z . This is due to the additional fine and hyperfine depolarizations in hydrogen or deuterium, suffered by the muon before its transfer to the final host atom.

Transfer reactions play very important roles in the X-ray intensity anomalies [B28].

2.6. New techniques of producing muonic atoms for nuclear capture experiments

We discuss here two new techniques for producing muonic atoms for nuclear capture experiments. The first method has already been shown to work; the second one is yet to be experimentally tested.

2.6.1. Trapping of muons in gases at low pressures: magnetic bottle technique

A novel method has been utilized recently to demonstrate the practibility of stopping muons in gases at very low pressures (10 to 600 Torr at 300° K) [50a]. In view of the importance of achieving a decent muon stop rate with low-pressure hydrogen for studying the muon capture process at or near statistical hyperfine occupation probabilities, this technique appears very promising.

There exists a “magic” laboratory momentum $p_\pi = (m_\pi^2 - m_\mu^2)/2m_\mu \approx 40 \text{ MeV}/c$, near which pions, decaying in flight, yield very slow muons. This fact has been utilized by Anderhub et al. [50a], who inject pions of momentum $(40 \pm 3) \text{ MeV}/c$ axially into a magnetic bottle of cylindrical symmetry. Muons, produced by the pion decay, are then trapped in this bottle and are eventually captured by the gas of experimental interest (hydrogen or helium), contained in a target tank inside the bottle. While the muon stopping rate decreases approximately linearly with pressure in a conventional set-up, the magnetic bottle experiment shows a decrease only by a factor of five, as the He pressure drops from 600 to 10 Torr. In fig. 2.7, the normalized delay distributions for the muonic X-rays in He in the energy region 6.5 to 12 keV are shown for various gas pressures. In fig. 2.8, preliminary results in the case of hydrogen show encouraging prospects for using this technique to do nuclear muon capture experiments in low-pressure hydrogen gas target (§3). The success of this technique is also essential for the future measurement of the Lamb shift in muonic hydrogen.

2.6.2. Electroproduction of muons: Dmitriev’s proposal for formation of muonic atoms in very thin targets

Dmitriev has proposed [50b] a new method of producing muonic atoms aimed at studying muon-induced fission of nuclei in very thin targets. The idea is to produce μ^+ , μ^- pairs on nuclei by photons or electrons of ultrarelativistic energies, with μ^- production in an atomic orbit and emission of the μ^+ .

The cross-section for production of muonic atoms by electrons of energy E ($E \gg m_\mu$) in nuclei with $Z\alpha \ll 1$ is [50b]:

$$\sigma \sim \frac{7}{4} r_\mu^2 (Z\alpha)^5 \ln(E/m_e), \quad (2.48)$$

where r_μ is the classical muon radius. For heavy nuclei ($Z\alpha \sim 1$), $Z\alpha$ in the cross-section formula

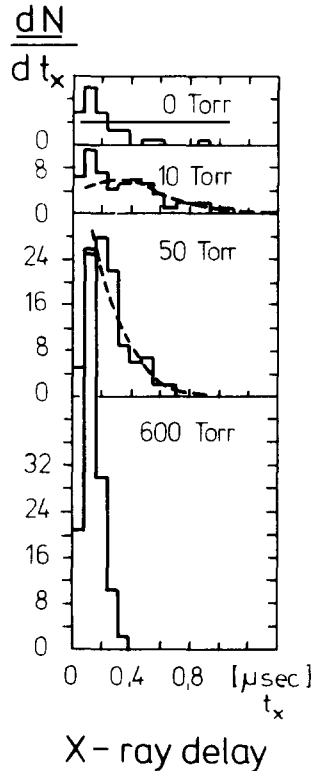


Fig. 2.7. Normalized K X-ray delay distribution in the X-ray energy region 6.5 to 12 keV in muonic He (Anderhub et al. [50a]) for various gas pressures. Dotted lines are Monte Carlo expectations. At 600 Torr, muons are stopped "instantly" in the magnetic bottle.

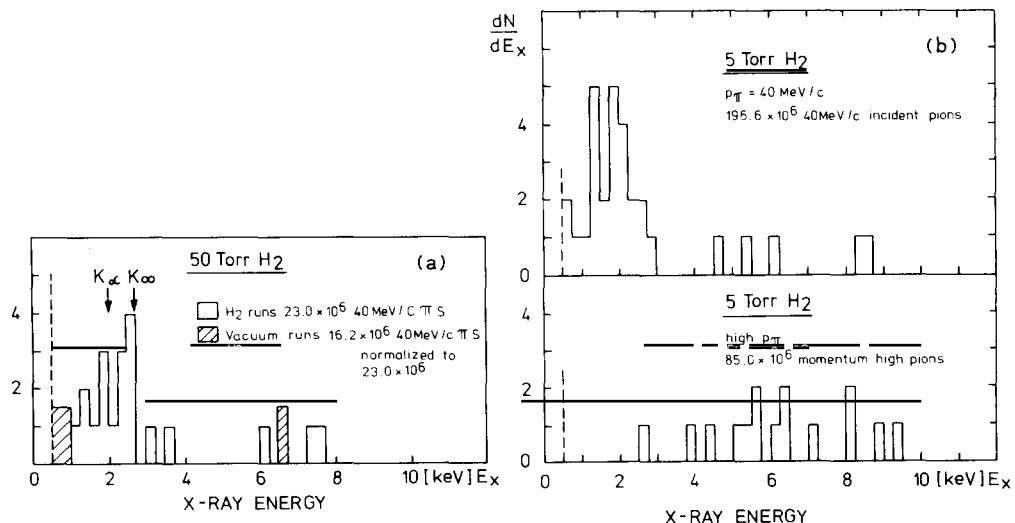


Fig. 2.8. X-ray energy distribution in muonic hydrogen stopped in magnetic bottle for various gas pressures (Anderhub et al., to be published). Notice the importance of the choice of the pion momentum to be 40 MeV/c.

(2.48) appears with a reduced power:

$$(Z\alpha)^5 \rightarrow (Z\alpha)^{2\gamma+1} \sin^2(1+\gamma) \tan^{-1}(2/Z\alpha), \quad (2.49)$$

where $\gamma = \sqrt{1 - Z^2\alpha^2}$. For electron storage rings with 10^{10} electrons injected per second, the estimated number of muonic atoms produced for large Z nuclear targets is $\sim 100 \text{ s}^{-1}$. This is already an interesting number for the study of nuclear fission and the possibility of exciting nuclear fission isomers (§ 8.3).

3. Capture of muons by hydrogen nucleus

3.1. Objective of studying muon capture in hydrogen

The reaction

$$\mu^- + p \rightarrow n + \nu_\mu, \quad (3.1)$$

first experimentally detected by Hildebrand [8]*, is extremely important in understanding the structure of the Lagrangian for the strangeness conserving semileptonic weak interaction involving four fermions. The process (3.1) is analogous to the electron-capture reaction:

$$e^- + [p] \rightarrow [n] + \nu_e, \quad (3.2)$$

the square bracket indicating here that the process can only take place in a nucleus. One can obtain the Lagrangian \mathcal{L}^μ for the process (3.1) from that of (3.2), \mathcal{L}^e , or vice-versa, by invoking the principle of *muon-electron universality* [B16] which relates \mathcal{L}^μ to \mathcal{L}^e in the following way:

$$\mathcal{L}^\mu \not\propto \mathcal{L}^e, \quad \text{as} \quad \begin{pmatrix} \mu^- \\ \nu_\mu \end{pmatrix} \xrightarrow{\quad} \begin{pmatrix} e^- \\ \nu_e \end{pmatrix}. \quad (3.3)$$

The study of the reaction (3.1) thus constitutes an important test for $\mu-e$ universality in weak interaction. It also provides a valuable check on the V-A structure of the Lagrangian.

One of the bonuses provided by the larger mass of the muon, compared to that of the electron, is that the momentum transfer q in the process (3.1) is much larger than that in the process (3.2), or in the related β decay processes

$$n \rightarrow p + e^- + \bar{\nu}_e, \quad [p] \rightarrow [n] + e^+ + \nu_e; \quad (3.4)$$

thus the three-momentum transfer q has the magnitude

$$|q| = m_\mu - \Delta E_B^{1S} - \Delta E, \quad (3.5)$$

ΔE_B^{1S} and ΔE are the muon binding energy and nuclear energy transfer respectively. This can make the contributions of the “induced” weak form factors [eqs. (3.13)–(3.14)] quite important. The reaction

$$\nu_\mu + n \rightarrow p + \mu^-, \quad (3.6)$$

*See plate 3 for one of the bubble chamber events observed by Hildebrand.

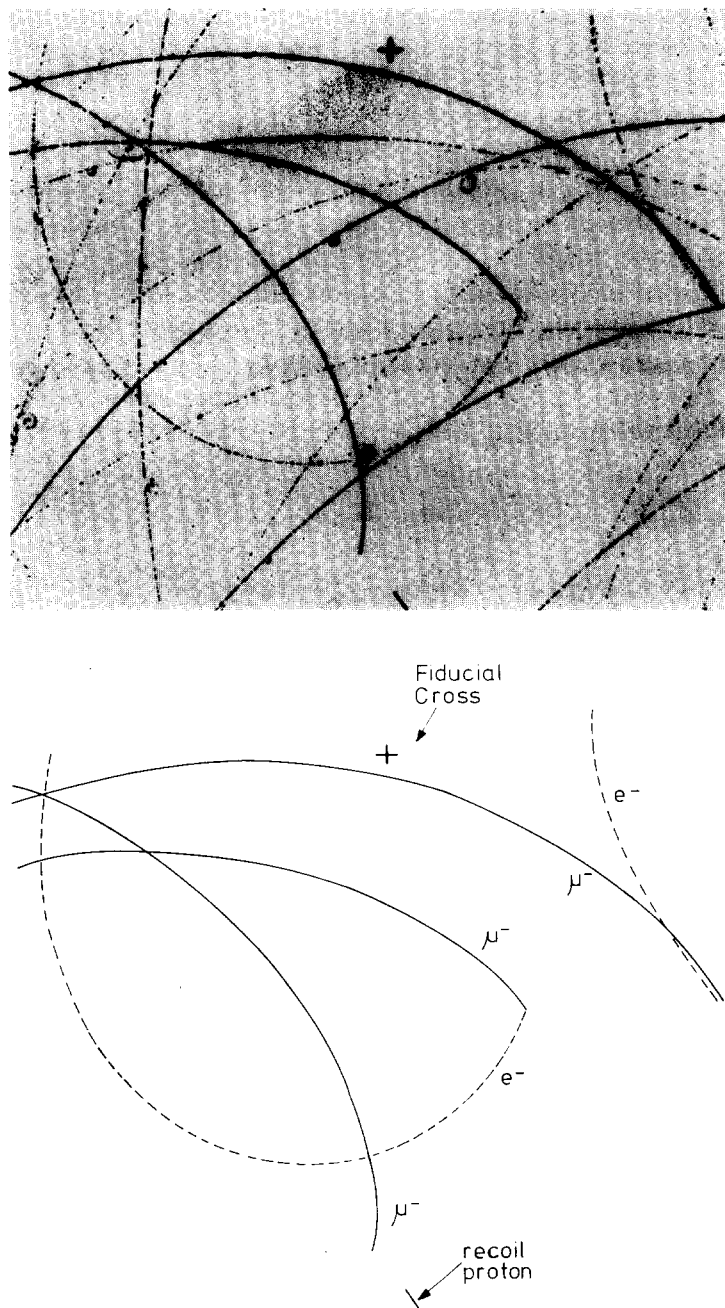


Plate 3. The reaction $\mu^- + p \rightarrow n + \nu_\mu$, first observed in the liquid hydrogen bubble chamber by Hildebrand [8] (courtesy of Professor Roger H. Hildebrand, Enrico Fermi Institute, University of Chicago). The sketch accompanying the plate illustrates the sequence of events: Three negative muons enter from the left and stop in the liquid hydrogen. The two, stopping further to the right, decay and produce visible electron tracks. The third is captured by a proton (hence no electron track visible), producing a neutron and a neutrino. The neutron moves down to the right until it produces a recoil proton a few millimetres from the capture point. From the range the recoil (in this case 2.8 mm) and the angle it makes with the presumed flight path of the neutron, the neutron energy is computed to be 5.2 MeV, in agreement with the kinematics of the capture reaction.

the inverse of (3.1), has also been studied [51] with the objective of learning about the weak form factors.

Importance of muon capture by hydrogen nucleus in the context of capture in more complex nuclei: The study of muon capture in *complex nuclei* involves many uncertainties arising from the approximate treatment of the nuclear many-body problem. This makes the interpretation of the “effective” weak hadron form factors, extracted from these reactions, quite a difficult task. However, the treatment of muon capture by hydrogen does not involve any of these difficulties. Thus the nuclear matrix elements for muon capture by hydrogen are known, and the weak hadron form factors are on-shell quantities. The informations on these form factors, obtained from hydrogen, are of direct relevance to the elementary particle physics. These also provide a convenient reference for comparison, in understanding whether the effective hadron form factors, extracted from muon capture in complex nuclei, reflect effects which are purely nuclear in origin. Thus, hydrogen is here the metaphorical compass in our navigation through the nuclear sea!

3.2. Observables

As discussed earlier (§ 2.5), the experimental informations obtainable from the study of the reaction (3.1) depend crucially on the physical state of hydrogen.

In *gaseous hydrogen* at a given temperature and pressure, the experimental muon capture rate Λ is given by

$$\Lambda = \alpha \Lambda_S + (1 - \alpha) \Lambda_T, \quad (3.7)$$

where α and $(1 - \alpha)$ are the fractional populations of the singlet and triplet hyperfine (HF) states in the $\mu^- p$ system. At very low pressure, the HF populations are statistical and α is $\frac{1}{4}$. At moderate pressures (\sim a few atmospheres), however, α is unity and one is measuring the singlet capture rate only. Thus, by varying the pressure [42], one can, in principle, determine Λ_T , provided that α can be reliably determined. Two observations are important here from the point of view of measuring Λ_T : i) using unpolarized hydrogen, the *richest sample* of triplet population that can be obtained in a $\mu^- p$ system has statistical weight $\frac{3}{4}$. This is possible in a gas target at very low pressure. ii) Further enrichment of the triplet sample may be possible by using a polarized hydrogen target [29].

By doing experiments with gas targets at moderate pressures, the rate Λ_S has been determined by the CERN–Bologna collaboration [19] and the Dubna group [52]. While no precise measurement of Λ_T has been possible as yet, the measured values of Λ_S and Λ_{OM} [eq. (3.8)] can be combined to yield a limit on Λ_T . Obtaining a value of Λ_T at a reasonable accuracy will be an important experimental objective in the future. This may be helped by the technique discussed in § 2.6. A group at Saclay and another at SIN hope to repeat the muon capture experiment in liquid hydrogen, looking particularly for the ratio $\Lambda_{OM}/\Lambda_{PM}$.

In liquid hydrogen, the capture is predominantly from the orthomolecular configuration of the $p\mu^- p$ mesomolecule, and *counter experiments* [44, 53] yield the capture rate Λ_{OM} in the orthomolecular hydrogen. This is given, in terms of Λ_S and Λ_T , as follows:

$$\Lambda_{OM} = 2\gamma_{OM} [\frac{3}{4}\Lambda_S + \frac{1}{4}\Lambda_T], \quad (3.8)$$

where γ_{OM} is the Weinberg parameter [54] that reflects the muon density around the molecule. The Weinberg parameters have been calculated by various authors [55], by solving the three-body

problem of the $p\mu^-p$ molecule:

$$2\gamma_{OM} = 1.01 \pm 0.01. \quad (3.9)$$

Finally, the detection of neutrons in the liquid hydrogen bubble chamber experiments [56] yields a rate [B39]

$$\Lambda_{B.C.} = \Lambda_{OM} + [\Lambda_S - \Lambda_{OM}] \frac{\lambda_0}{\lambda_{pp} + \lambda_0} \exp(-\lambda_{pp}t), \quad (3.10)$$

where t is the time elapsed between the muon stop and the neutron detection. The quantities λ_{pp} and λ_0 are given in table 2.5; these are respectively the rates of the reaction $\mu^-p + p \rightarrow p\mu^-p$ ($L = 1$), and the muon decay.

3.3. The four-fermion interaction Hamiltonian

In order to obtain the theoretical expressions for the capture rates Λ_S and Λ_T , we start here with a discussion of the weak interaction Hamiltonian H_μ in terms of the usual four-fermion coupling (fig. 3.1).

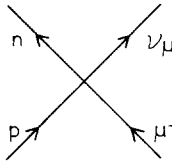


Fig. 3.1. Point interaction of four fermions.

H_μ is given in the current-current form [B16] by the *Gell-Mann–Cabibbo universality* [57]:

$$H_\mu = \frac{G \cos \theta}{\sqrt{2}} (V_\lambda^+ + A_\lambda^+) L_\lambda + \text{h.c.}, \quad (3.11)$$

where G is the Fermi coupling constant and θ is the Cabibbo angle. The hadronic vector and axial vector matrix elements can be obtained phenomenologically [58] in the following form* by invoking Lorentz covariance:

$$V_\lambda^+ = \bar{\psi}_n [g_V \gamma_\lambda - \frac{1}{2}(g_M/M)\sigma_{\lambda\rho}q_\rho - (ig_S/m_\mu)q_\lambda] \psi_p, \quad (3.12)$$

$$A_\lambda^+ = \bar{\psi}_n [g_A \gamma_\lambda \gamma_5 - (ig_P/m_\mu)q_\lambda \gamma_5 - \frac{1}{2}(g_T/M)\sigma_{\lambda\rho}q_\rho \gamma_5] \psi_p. \quad (3.13)$$

The lepton matrix element L_λ has the bare V-A structure [11]

$$L_\lambda = \bar{\psi}_\nu \gamma_\lambda (1 + \gamma_5) \psi_\mu. \quad (3.14)$$

All the hadron form factors are functions of q^2 ($q_\rho \equiv n_\rho - p_\rho$) (the argument q^2 will often be suppressed). The ψ_α 's above are spinor functions for the fermions α . The form factors g_M , g_S , g_P , and g_T are “induced” by the strong interaction of the hadrons. Assuming that the elementary

*We are using the *Pauli metric*. The γ matrices chosen above are hermitian, satisfying the Pauli algebra $[\gamma_\lambda, \gamma_\mu]_+ = 2\delta_{\mu\nu}$. The σ 's above are defined to be $(i/2)(\gamma_\lambda \gamma_\rho - \gamma_\rho \gamma_\lambda)$.

hadronic and leptonic weak currents have the *same* structure, that due to a point particle, we have, in absence of strong interaction, $g_A = g_V = 1$, $g_M = g_P = g_T = g_S = 0$. Thus, in the naive quark model of hadrons, the second-class terms cannot be generated by the strong interaction *ex nihilo**. The deviation of g_A/g_V from unity in the real nucleon world is also due to strong interaction effects [59]. The form factors g_M , g_S , g_P , and g_T do not contribute to the rate in the limit of $q_\lambda \rightarrow 0$, hence they are relatively unimportant in nuclear β decay and electron capture.

3.3.1. Determination of weak hadron form factors

Since the muon capture process involves six independent hadron form factors, it is necessary to determine them by other independent constraints. This has been widely discussed in the literature in the context of the muon capture (see, for example [B16] and [B19]). Here we summarize and update the conclusions. Currently accepted values of the hadron form factors appear in table 3.1.

Table 3.1

Values of weak hadron form factors (coupling constants) *currently recommended* as inputs for muon capture calculation in hydrogen ($q^2 = 0.88 m_\mu^2$). For references and uncertainties on the form factors, see text.

Quantity	Value for muon capture in hydrogen
$G \cos \theta$	1.4122×10^{-49} erg cm ³
g_V	0.978
g_M	3.591
g_S	0
g_A	1.23
g_P	8.4
g_T	0

A study of the superallowed Fermi β decays in nuclei yields the value of the effective Fermi coupling constant [60]**

$$G \cos \theta = (1.41220 \pm 0.00043) \times 10^{-49} \text{ erg cm}^3. \quad (3.15)$$

The constraint of the *time reversal invariance* allows us to take all the form factors to be real***:

$$\text{Im}(g_i) = 0, \quad (3.16)$$

where i represents the subscripts V, M, S, A, P, and T. The *conserved vector current hypothesis* (CVC) [12] gives

$$g_S(q^2) = 0. \quad (3.17)$$

The *isotriplet vector current hypothesis* (IVC) [12] assumes that V_λ , V_λ^+ and the isovector part of the electromagnetic form an isospin 1 triplet, yielding a correspondence between the weak form factors g_V , g_M and the isovector electromagnetic ones:

$$\begin{aligned} g_V(q^2) &= F_1^p(q^2) - F_1^n(q^2), \\ g_M(q^2) &= F_2^p(q^2) - F_2^n(q^2), \end{aligned} \quad (3.18)$$

*See Rho [338] and Wolfenstein (preprint 1976) for further discussions.

**We could have obtained this also by using G deduced from μ -lifetime and the value of $\cos \theta$ explicitly.

***See ref. [61] for a summary of transformation properties of currents under various symmetry operations.

where F_1 and F_2 are the Dirac and Pauli form factors of the superscribed nucleon in the electro-magnetic current. In terms of the Sachs form factors [B13], we can rewrite (3.18) as

$$g_V(q^2) = \frac{1}{(1 + q^2/4M^2)} \left[G_E^p(q^2) - G_E^n(q^2) + \frac{q^2}{4M^2} (G_M^p(q^2) - G_M^n(q^2)) \right], \quad (3.19a)$$

$$g_M(q^2) = \frac{1}{(1 + q^2/4M^2)} [G_M^p(q^2) - G_M^n(q^2) - G_E^p(q^2) + G_E^n(q^2)]. \quad (3.19b)$$

Thus, at $q^2 = 0$,

$$g_V(q^2) = 1, \quad g_M(q^2) = \bar{\mu}_p - \mu_n - 1, \quad (3.20)$$

where $\bar{\mu}_p$ and μ_n are the *total* magnetic moments [62] of the proton and neutron respectively, in nuclear magnetons:

$$\bar{\mu}_p = 2.7928456 \pm 0.0000011, \quad (3.20')$$

$$\mu_n = -1.913146 \pm 0.000066.$$

From the elastic electron–nucleon and electron–deuteron experiments [63, B13], one obtains the following information for the variation of the Sachs form factors with momentum:

$$\begin{aligned} G_E^p(q^2) &\approx G_D(q^2), & G_M^p(q^2) &\approx \bar{\mu}_p G_D(q^2), \\ G_E^n(q^2) &\approx -(q^2/4M^2) \mu_n G_D(q^2), & G_M^n(q^2) &\approx \mu_n G_D(q^2), \end{aligned} \quad (3.21)$$

with

$$G_D(q^2) = \left(1 + \frac{q^2}{0.71 \text{ GeV}^2} \right)^{-2}. \quad (3.22)$$

This yields

$$g_V(q^2) = \frac{G_D(q^2)}{(1 + q^2/4M^2)} \left[1 + \frac{q^2}{4M^2} \bar{\mu}_p \right], \quad (3.22'a)$$

$$g_M(q^2) = \frac{G_D(q^2)}{(1 + q^2/4M^2)} \left[\bar{\mu}_p - \mu_n - 1 + \frac{q^2}{4M^2} \mu_n \right], \quad (3.22'b)$$

giving us*

$$g_V(q^2 = 0.88 m_\mu^2) = 0.978, \quad (3.22'c)$$

$$g_M(q^2 = 0.88 m_\mu^2) = 0.969 (\bar{\mu}_p - \mu_n - 1).$$

The μ –e universality hypothesis [B16] implies that the $(\mu\nu_\mu)$ current couples to the *same* nucleonic current as does the $(e\nu_e)$ -current. Hence the ratio $g_A(0)/g_V(0)$ in the muon capture Hamiltonian can be taken from the neutron β -decay [64]:

$$g_A(0)/g_V(0) = g_A^\beta(0)/g_V^\beta(0) = 1.258 \pm 0.015. \quad (3.23)$$

We now introduce the G transformation [14] defined by the operator $G = C \exp(i\pi T_2)$, where C

*Later on, we will introduce the notation μ_p for the anomalous magnetic moment of the proton, $(\bar{\mu}_p - 1)$, in the expression for g_M .

is the charge conjugation operator $[(\frac{p}{n}) \xrightarrow{C} (\frac{\bar{n}}{\bar{p}})]$, and $U = \exp(i\pi T_2)$ induces rotation by 180° about the second isospin axis $[(\frac{p}{n}) \xrightarrow{U} (-\frac{n}{-p})]$. Thus, under G transformation, the nucleon states transform as follows:

$$\begin{pmatrix} p \\ n \end{pmatrix} \xrightarrow{G} \begin{pmatrix} \bar{n} \\ -\bar{p} \end{pmatrix} \xrightarrow{G} - \begin{pmatrix} p \\ n \end{pmatrix}.$$

If we divide the hadron current into two pieces, regular and irregular under U transformation, indicated by the superscripts R and I respectively,

$$J_\lambda = J_\lambda^R + J_\lambda^I,$$

where $UJ_\lambda^R U^{-1} = -J_\lambda^{R\dagger}$, $UJ_\lambda^I U^{-1} = J_\lambda^{I\dagger}$, then one finds that the V, M, A, P terms are U -regular and S and T terms are U -irregular, where the form factors are all real.

The vector and axial currents having the respective G transformation properties

$$GV_\lambda G^{-1} = V_\lambda, \quad GA_\lambda G^{-1} = -A_\lambda, \quad (3.24)$$

are classified “first class” by Weinberg [14]; scalar and tensor currents are thus “second class” in this classification. Then G invariance of the four-fermion Hamiltonian implies

$$g_S(q^2) = 0, \quad g_T(q^2) = 0. \quad (3.24')$$

Since $g_S(q^2) = 0$ is given by CVC also, a non-vanishing tensor form factor is the sole test of G invariance.

The variation of $g_A(q^2)$ with q^2 is obtained from the study of the reactions (3.6) on deuterium and nuclear targets [51], and by studying the electro-production of the pions [65] and Δ 's [66]. The analyses of these reactions yield [B13]

$$g_A(q^2)/g_A(0) = (1 + q^2/m_A^2)^{-2}, \quad (3.25)$$

where m_A is obtained to be [67]

$$m_A = 0.89^{+0.09}_{-0.08} \text{ GeV}$$

from the analysis of the Argonne experiment [51].

Finally, the *hypothesis of partial conservation of the axial current* (PCAC) [13] gives the pseudo-scalar form factor $g_P(q^2)$. The PCAC hypothesis can be formulated in two equivalent forms [68]: “polological” and field-theoretic versions. In the first version, the matrix element of the divergence of the strangeness conserving axial vector current satisfies an unsubtracted dispersion relation in q^2 , which is dominated by the pion pole in the region $-m_\pi^2 < q^2 < 0$. In the field theoretic form, the divergence of the axial vector current is proportional to the pion field ϕ^π :

$$\partial A_\lambda^+ / \partial x_\lambda \propto \phi^\pi, \quad (3.26)$$

and the matrix element of the corresponding pion current is a slowly varying function of q^2 in the region $-m_\pi^2 < q^2 < 0$. In order to apply PCAC to muon capture, one additionally assumes that it is valid also for positive values of q^2 , in the neighbourhood of m_μ^2 .

Without going through the traditional step of the Goldberger–Treiman relation [15]:

$$2Mg_A(0) = \sqrt{2} g_{\pi NN}(-m_\pi^2) f_\pi, \quad (3.27)$$

we can, following a recent discussion by Wolfenstein [B37], invoke a weaker PCAC, by assuming

that the divergence of the axial-current satisfies a once-subtracted dispersion relation:

$$2Mm_\mu g_A(q^2) - q^2 g_P(q^2) = P + \frac{C}{q^2 + m_\pi^2} + I(q^2), \quad (3.28)$$

where P is a subtraction constant, $I(q^2)$ is the contribution of the 3-pion cut. In eq. (3.27), $g_{\pi NN}$ and f_π are respectively the pion–nucleon coupling constant and pion decay constant [69]:

$$\frac{1}{4\pi} g_{\pi NN}^2(-m_\pi^2) = 14.6, \quad f_\pi = 131.7 \text{ MeV}. \quad (3.29)$$

Then, from analyticity, we can write

$$g_A(q^2) = g_A(0) + g'_A(0) q^2, \quad (3.30)$$

$$g_P(q^2) = \frac{D}{q^2 + m_\pi^2} + E, \quad (3.31)$$

where D and E are constants. From the last three equations we obtain the Wolfenstein estimate (WE) for $g_P(q^2)$:

$$g_P(q^2) = \frac{\sqrt{2}f_\pi g_{\pi NN}(-m_\pi^2) m_\mu}{q^2 + m_\pi^2} - \frac{4Mm_\mu g_A(0)}{m_A^2} - m_\mu I'(0). \quad (3.32)$$

Thus, for muon capture in hydrogen, $g_P(q^2)$ is given by

$$g_P(q^2 = 0.88 m_\mu^2) [\text{WE}] = 9.51 - 0.88 g_A(0) - m_\mu I'(0). \quad (3.32')$$

There are several important points to be noted here: i) the uncertainty of our knowledge of m_A does not significantly affect the estimate for $g_P(q^2)$; ii) the contribution of the cut term is entirely negligible; iii) the subtraction constant P *does not* enter in the estimate for $g_P(q^2)$. Assuming that the cut contribution is completely responsible for the observed 8% discrepancy [70, 380] of the Goldberger–Treiman estimate with the experiment, Wolfenstein has obtained a conservative upper limit for the cut term in eq. (3.32'). This is $0.1 g_A(0)$, and hence unimportant for the determination of $g_P(q^2)$. We thus obtain

$$g_P(q^2 = 0.88 m_\mu^2) [\text{WE}] = 8.4. \quad (3.33)$$

Tests of various hypotheses, by processes other than muon capture, have been recently reviewed by Llewellyn Smith [B17], and give strong confidence in their validity. The only points to add are: i) a recent improvement on the determination of the phase angle ϕ between the coupling constants g_A and g_V in neutron β -decay [71], yielding ϕ equal to $180.14 \pm 0.22^\circ$; ii) renewed suggestions from nuclear physics experiments [72] of a large “second class” form factor $g_T(0)$, of the order of weak magnetism term (§ 9.3.3).

3.3.1.1. Two theorems related to G invariance.

Theorem 1 (Cabibbo [73]): *If the nucleon weak currents are members of a single octet of Hermitian currents, then the regular and irregular parts of the current under CP are also regular and irregular respectively under G . In particular, the currents that have wrong G parity, violate T invariance maximally.*†

The proof will be omitted here. The above theorem is valid for $\Delta S = 0$ transitions *including electromagnetic corrections*; for $\Delta S = 1$ transitions, it is only valid up to SU(3) breaking.

†We should note here that many recent theoretical works on the “second-class” problem (§ 9) deal with currents not satisfying the requirements of the Cabibbo theorem.

Theorem 2: For $\Delta S = 0$ transitions, G invariance is equivalent to charge symmetry U , if T invariance holds to the lowest order in weak coupling constant.

The proof of this is trivial [B17]. It follows immediately by using conditions for CPT and T invariance.

The relevance of Theorem 1 to muon capture in hydrogen has been observed by Cabibbo [73]. A direct consequence of the Cabibbo theorem is that the “second class” terms are out of phase with the “first class” ones and, therefore, no interference is expected in T conserving effects like decay rates, up-down asymmetries, longitudinal polarization etc. For T violation effects one has to look for triple correlation effects appearing in terms like $\sigma \cdot p_1 \times p_2$.

3.3.1.2. Radiative corrections .

In quoting the values of $G \cos \theta$ [eq. (3.15)], $g_A(0)/g_V(0)$ [eq. (3.23)], and f_π [eq. (3.29)], taken from other experiments than muon capture, attention has been paid to the *radiative corrections*.

The effective Fermi constant $\bar{G}_V \equiv G \cos \theta$ is determined from the superallowed decay between $T = 1, J^\pi = 0^+$ states, ft values of which are given by [60]

$$ft(1 + \delta_R) = \frac{K}{\bar{G}_V^2 (1 + \Delta_R) 2 (1 - \delta_C)}, \quad (3.34)$$

where K is a constant, δ_R and Δ_R are the so-called “outer” and “inner” corrections. δ_C is the correction term to the Fermi matrix element due to Coulomb and other charge dependent effects. δ_R varies from nucleus to nucleus, and is about 1.5 to 2%. Δ_R is independent of the nucleus and is given, under suitable approximations, in terms of the Sirlin function $g(W, W_0)$, (W and W_0 are the electron energy and its maximum energy) [74]. Δ_R is about -0.1% [60]. In eq. (3.16), the quoted value of $G \cos \theta$ corresponds to the square root of $\bar{G}_V^2 (1 + \Delta_R)$.

The radiative corrections to f_π have been considered by Sirlin [70]. He has shown that the matrix element of the pion β -decay can be written as

$$M(\pi^- \rightarrow \mu^- + \nu_\mu) = \frac{\bar{G}_V}{\sqrt{2}} (-i f'_\pi P_\nu L^\nu + \alpha N^f),$$

where P_ν is the pion four momentum, f'_π is a coupling constant “renormalized” by the electromagnetic interaction, and αN^f is a known quantity that includes all infrared divergences and is free from ultraviolet divergences; L^ν is the usual lepton current. Sirlin, using the operator product expansion at small distances and Wilson counting fields of low dimensionality, arrives at the result

$$f'_\pi = \frac{1.497 \times 10^{-6}}{\bar{G}_V} (\text{GeV})^{-1} = 131.7 \text{ MeV}. \quad (3.35)$$

Pascual [75] has made an estimate of radiative corrections to muon capture rates Λ_S and Λ_T and has found them to be negligible.

Estimating radiative corrections is not a closed subject, particularly in the context of nuclear β -decay and muon capture (see, for example, ref. [76]). However, the advent of gauge theories, in attempts to unify weak and electromagnetic interactions, has enhanced the prospects of obtaining definite estimates of them. As an example, we note Wilkinson’s recent analysis [76a] of the inner radiative corrections in the superallowed nuclear Fermi β -decay and muon decay. Invoking CVC, $\mu-e$ universality and Sirlin’s gauge-theoretic treatment of the radiative corrections, he finds the

mean quark charge of the nucleon to be 0.20 ± 0.10 , compared with $\frac{1}{6}$ in the Gell-Mann–Zweig model -- an excellent agreement.

3.3.2. Effective Hamiltonian in the muon capture by hydrogen nucleus

One can now carry out a Foldy–Wouthuysen (FW) transformation [77] and obtain an effective Hamiltonian operator acting between non-relativistic nucleon wave functions. Thus, the matrix element $\bar{\psi}_f \Gamma_R \psi_i$ in (3.12) will go to the form $\langle u_f | H_{\text{eff}} | u_i \rangle$, where u 's appear in the Pauli reduction of the relativistic nucleon spinors:

$$\psi = \begin{pmatrix} -\frac{1}{2}M\sigma \cdot p \\ 1 \end{pmatrix} u. \quad (3.36)$$

There is no difficulty in carrying out an FW transformation to any order in (p/M) , since the relativistic nucleon Hamiltonian here is that for the free particle

$$H^D = \beta M + \alpha \cdot p,$$

α and β being the Dirac matrices. Thus, the FW series rapidly converges. The same need not be true for the nucleon *bound* in a nucleus (§9.1).

One particular form of the effective Hamiltonian, used widely in the muon capture literature, is due to Fujii and Primakoff (FP) [78]. The FP Hamiltonian in the coordinate space has the form†

$$H_{\text{eff}} = \frac{\tau^{(+)}}{\sqrt{2}} \left(\frac{1 - \sigma \cdot \nu}{\sqrt{2}} \right) \tau_h^- [G_V 1 \cdot 1_h + G_A \sigma \cdot \sigma_h - G_P \sigma \cdot \nu \sigma_h \cdot \nu + O(p_n/M)] \delta(r - r_h); \quad (3.37)$$

here the subscripted operators are 2×2 matrices acting on the non-relativistic hadron spinors, while the unsubscripted ones are 4×4 matrices acting on the relativistic lepton spinors. The FP effective form factors are, assuming G invariance,

$$\begin{aligned} G_V &= g_V (1 + q/2M), & G_A &= -[g_A + (g_V + g_M)(q/2M)], \\ G_P &= -(g_P - g_A + g_V + g_M)(q/2M). \end{aligned} \quad (3.38)$$

The FP form factors explicitly demonstrate the effect of the large muon mass compared to the electron mass, consequently the importance of the induced form factors in muon capture. Taking the limit $q \rightarrow 0$, we see that the FP form factors go to the familiar vector (Fermi) and axial-vector (Gamow–Teller) coupling constants of nuclear β decay. In the nuclear muon capture problem, we shall use the FP Hamiltonian quite often and neglect the terms of $O(p_n/M)$ in eq. (3.37), to get a feeling for the magnitudes of various effects. For accurate calculations, terms of $O(p_n/M)$, are always included. Ohtsubo [79] and Friar [79] have investigated the effects of terms of $O(p_n/M)^2$ in muon capture processes in complex nuclei and found them to be generally small; anyway, effects of this order cannot be reliably determined in nuclei.

3.4. Singlet and triplet capture rates: Test of $V \pm \lambda A$ hypotheses

It is straightforward to calculate the rates Λ_S and Λ_T starting from the Hamiltonian of section 3.3. Useful but complicated expressions for these are given in Appendix 1 in terms of weak hadron form factors.

To demonstrate the sensitivity of the hyperfine capture rates to the $V \pm \lambda A$ form of the weak

†In eq. (3.37) ν is the unit vector along the direction of the neutrino momentum. τ_h^- is the operator that converts a proton into a neutron. In complex nuclei, we shall call this τ^+ , following the nuclear physics use.

interaction [11, 17], we can ignore the induced form factors and have the following approximate expressions for Λ_S and Λ_T :

$$\Lambda_S \approx 30(1 + 3\lambda)^2, \quad \Lambda_T \approx 30(1 - \lambda)^2, \quad (3.39)$$

where $\lambda = g_A/g_V$. For a $V - \lambda A$ interaction with $\lambda \sim 1.2$, we have

$$\Lambda_S \approx 635 \text{ s}^{-1}, \quad \Lambda_T \approx 1 \text{ s}^{-1}. \quad (3.40a)$$

For a $V + \lambda A$ interactions, we get, setting $\lambda = -1.2$ in eq. (3.39),

$$\Lambda_S \approx 200 \text{ s}^{-1}, \quad \Lambda_T \approx 145 \text{ s}^{-1}. \quad (3.40b)$$

Thus, we have the following dramatic results:

$$\begin{aligned} V - \lambda A: \quad \Lambda_S &\gg \Lambda_T, \quad \Lambda_T \approx 0, \\ V + \lambda A: \quad \Lambda_S &\approx \Lambda_T. \end{aligned} \quad (3.41)$$

The experiments [19, 44, 52, 53] clearly support the $V - \lambda A$ form and completely rule out the $V + \lambda A$ hypothesis. This test of the $V - A$ theory is originally due to Bernstein, Lee, Yang and Primakoff [17]. The huge suppression of Λ_T (a factor of 60 in precise calculations*) compared to Λ_S is a convincing test of the $V - A$ theory.

3.4.2. Comparison of the predicted capture rates with experiments

In table 3.2, we display the experimentally observed rates together with the theoretical predictions using the “canonical” values (table 3.1) of the weak hadron form factors. Notice that, for Λ_S , the agreement between theory and experiment is excellent. This is also true for Λ_{OM} , for which the “world average” of experimental values agrees nicely with the theoretical prediction.

Table 3.2

Summary of experimental determination of nuclear capture rate in hydrogen. BC and C mean respectively bubble chamber and counter experiments.

Method	Measured quantity	Measured value (sec ⁻¹)	Authors	Theoretical estimate (sec ⁻¹)
BC BC	Λ_{BC}	428 ± 85 450 ± 50 443 ± 43	Deode and Hildebrand [56] Bertolini et al. [56] World average	552
C C	Λ_{OM}	515 ± 85 464 ± 42 474 ± 38	Bleser et al. [44a] Rothberg et al. [53] World average	493
C C	Λ_S	651 ± 57 686 ± 88 661 ± 48	Alberigi Quaranta et al. [19] Bystriski et al. [52] World average	650
From Λ_{OM} and Λ_S		< 103	Λ_{OM} and Λ_T used are world average values	14.8

*The role of g_P is crucial for a precise estimate of Λ_T . It is responsible for Λ_T being 15 s^{-1} rather than 1 s^{-1} in eq. (3.40a).

Only the bubble chamber results [56] are somewhat lower than the theoretical prediction. Considering the uncertainties in the analysis of the bubble chamber data, this discrepancy is not serious [B39]. *The excellent agreement of experimental and theoretical values of Λ_S constitutes a clear affirmation of the principle of the $\mu-e$ universality and of the $V-\lambda A$ form of the weak interaction.*

Using eq. (3.9) together with the “world averages” of experimental values of Λ_{OM} and Λ_S , $474 \pm 38 \text{ s}^{-1}$ and $661 \pm 48 \text{ s}^{-1}$ respectively, and the theoretical value of γ_0 equal to 1.005 ± 0.005 , we obtain an experimental upper limit for Λ_T *

$$\Lambda_T < 103 \text{ s}^{-1}, \quad (3.42)$$

which again is in qualitative agreement with the $V-A$ prediction. *The inequality $\Lambda_S \gg \Lambda_T$, a cornerstone of the $V-A$ theory, is tested extremely well*, even by this poor determination of Λ_T from the present experimental values of Λ_{OM} and Λ_S .

3.4.3. Knowledge of weak hadron form factors from Λ_S and Λ_T

As regards to the sensitivity of the capture rates to the weak hadron form factors, several points can be made: i) Λ_S depends overwhelmingly on g_A and g_V , and rather weakly on g_M and g_P . ii) There are cancellations between $g_A g_M$ and $g_A g_P$ interference terms in Λ_S , such that it will not be affected drastically if both g_M and g_P are set to zero. iii) There are dramatic cancellations amongst the contributions of g_A , g_V , and g_M to Λ_T such that only those due to g_P survive. Due to this, Λ_T is effectively determined by g_P .

We can now quote some limits on the weak hadron form factors that one can get by using the

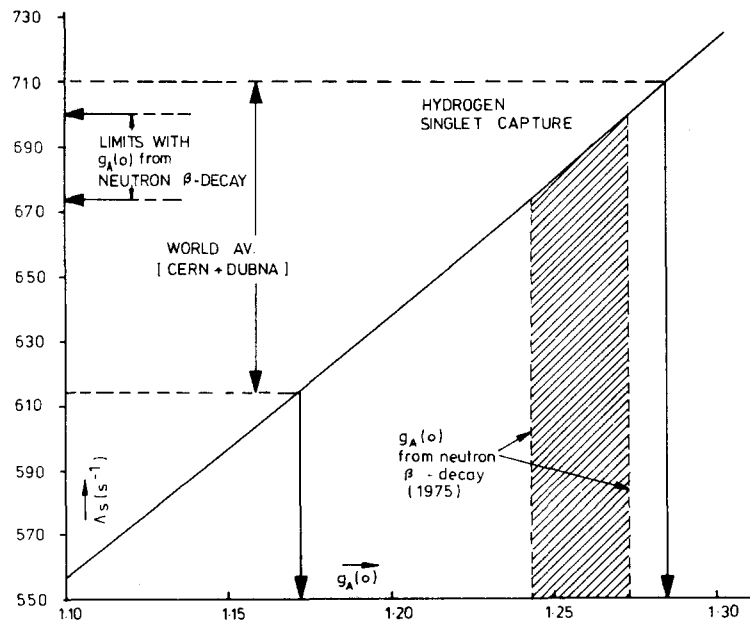


Fig. 3.2. Singlet capture rate Λ_S in hydrogen as a function of the axial-vector form factor $g_A(0)$ and pseudoscalar form factor $g_P(q^2)$, respectively. Horizontal lines show the current experimental accuracy of Λ_S .

*This analysis indicates that Λ_T is most likely close to zero and is very much less than Λ_S and Λ_{OM} .

"world average" values of Λ_S and Λ_{OM} . Assuming g_A to be variable*, we obtain the following limit of $g_A(q^2)$:

$$g_A(q^2) = 1.23 \pm 0.05 \text{ (a),} \quad 1.16 \pm 0.05 \text{ (b),}$$

(a), (b) indicating that these values are obtained from Λ_S and Λ_{OM} [80], respectively. Their average, together with the q^2 dependence of eq. (3.25), yields

$$g_A(0) = 1.23 \pm 0.07, \quad (3.43)$$

using the dipole fit for $g_A(q^2)$ with $m_A = 0.95$ GeV. This is *in excellent agreement* with the prediction of the $\mu-e$ universality [eq. (3.23)].

In order to test the PCAC prediction of the pseudoscalar form factor, we take the standard values of all form factors other than $g_P(q^2)$ [setting $g_T(q^2)$ equal to zero]. Including both counter experiments on Λ_S , we obtain a range of values for $g_P(q^2)$ (see fig. 3.3) given by

$$6 \leq g_P(q^2) \leq 14, \quad (3.44)$$

which is consistent with the Wolfenstein prediction, $g_P(q^2) = 8.4$ [eq. (3.33)]. It is interesting to note that the range of values of $g_P(q^2)$, obtained by *including* the bubble chamber experiments, is slightly inconsistent with the Wolfenstein prediction. In view of the uncertainties of the older bubble chamber experiments, this discrepancy cannot be taken seriously at present.

Finally, we note that while experimental values of Λ_S and Λ_{OM} are consistent with the absence of second-class form factors, their presence cannot be excluded.

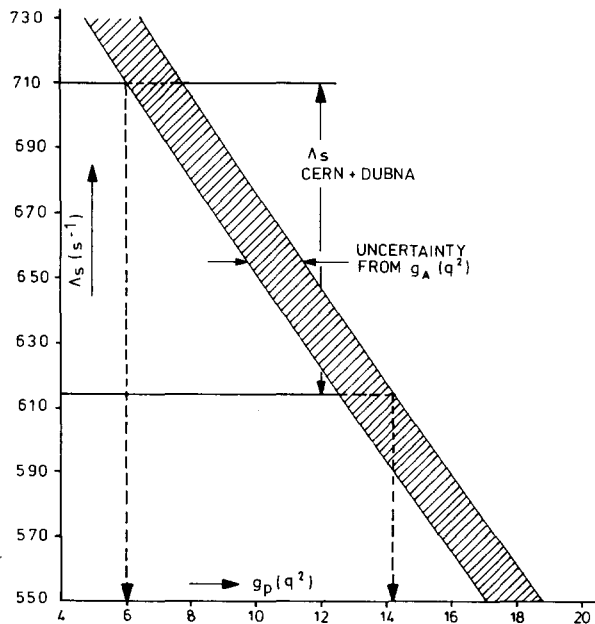


Fig. 3.3. Singlet capture rate Λ_S in hydrogen as a function of the axial-vector form factor $g_A(0)$ and pseudoscalar form factor $g_P(q^2)$, respectively. Horizontal lines show the current experimental accuracy of Λ_S .

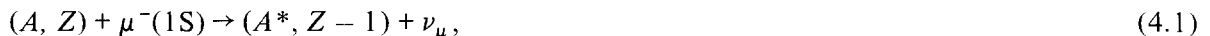
*See fig. 3.2 for a dependence of Λ_S on $g_A(0)$.

Summarizing, the muon capture experiments in hydrogen have already provided convincing tests of the μ -e universality and of the V-A structure of the weak Lagrangian. These tests can (and should) be improved in the near future.

4. Theoretical strategy for treating muon capture in complex nuclei

4.1. Objectives of studying muon capture reactions in complex nuclei

We now consider the reactions



where A is the mass number of the nucleus consisting of Z protons and N neutrons, $A > 1$, $Z \geq 1$. The daughter nucleus (A^* , $Z - 1$) may be in its ground state (g.s.) or in one of its excited states. In the radiative capture, the final state in (4.1) contains a photon as well, the reaction being an analogue of the elementary process $\mu^- + p \rightarrow n + \nu_\mu + \gamma$.

The most important motivation for studying these processes rests on the hope that they may teach us how a nucleon *inside the nucleus* couples weakly to the lepton field. The importance of this problem was posed in the last scientific talk of Amos De Shalit [81]:

“Nuclear physics poses some yet unresolved fundamental problems . . . (one of these can be stated as follows:) When many nucleons are packed together in the nucleus, are the individual properties of each one of the nucleons changed, or do they remain essentially unaffected? Such individual properties include the mass of a nucleon, its charge and magnetization distribution, its *coupling to the leptonic field*, and its interaction with other nucleons.”

In the context of the above problem, we need satisfactory answers to the following questions:

- (1) Are there nuclear transitions for which the nuclear physics inputs are reasonably certain?
- (2) Can the nuclear structure “conspire” to make certain induced form factors, unimportant in hydrogen capture reaction, dominant in the processes (4.1)?

(3) Are there any “exotic” processes [which, for example, will be ruled out by some selection rules (§ 8)] whose existence can be tested by studying muon capture reactions in complex nuclei?

From the *nuclear structure physics point of view*, however, we may start with the assumption that we understand the reaction mechanism underlying (4.1) rather well, and we would like to use these reactions as probes of nuclear structure. To judge the suitability of muon capture processes from this point of view, we have to ask the following:

- (1) In a given class of reactions, are there any dominant multipole excitations? If yes, can any nuclear model predict their strengths accurately? Can such excitations be related to other nuclear excitation mechanisms?
- (2) Are there any nuclear physics grounds for preferential excitations of a set of daughter levels? (This may be related to the question: Are the dominant excitation operators generators of a group representing an approximate symmetry of the nuclear Hamiltonian?)
- (3) Are there any channels (for example, emission of nucleon clusters) reflecting on special inter-nucleon correlations inside the nucleus?

The main objective of this and subsequent sections will be to provide some answers to all of the above questions.

In the nuclear muon capture experiments, the observables may be partial and total capture rates,

polarization and asymmetry of the recoil nucleus, gamma–neutrino correlation and circular polarization of the gamma ray emitted by the daughter nucleus, properties of the fission products, polarization, asymmetry, and energy distribution of the emitted nucleons and so on. In the radiative muon capture experiments, properties of the emitted photons are of primary interest.

4.2. Various approximations and methods of theoretical treatments of nuclear muon capture

The interpretations of nuclear muon capture rates and other experimental observables are done in two different approaches: (i) the impulse approximation approach (IA), and (ii) the “elementary particle” approach (EPA). The former employs methods of classical nuclear physics, for example, by using the nuclear wave functions, sum rules, etc. In the latter approach, nuclei are treated as “elementary particles”, and the muon capture amplitude is given in terms of *nuclear* weak form factors which are determined by theoretical constraints or by appealing to related processes. We postpone the discussion of the EPA until section 9.

4.2.1. The impulse approximation (IA)

The many-body aspect of the nuclear structure enters via the wave functions $\psi_{i,f}$ of the initial and final nuclear states in calculating the amplitude

$$T_{if} = \langle \psi_f | H | \psi_i \rangle, \quad (4.2)$$

where H is the nuclear transition operator, describing the muon capture process in the present case. One proceeds in the IA to replace (4.2) by the approximation [82]

$$T_{if} = \langle \psi_f | \sum_{i=1}^A H_i | \psi_i \rangle, \quad (4.3)$$

thus obtaining the nuclear T matrix from those of the *free nucleons*, and ignoring all the multiple scattering effects. Formally, the latter has been taken into account by Chew and Goldberger [82]. The approximation (4.3) allows us to use the weak hadron form factors of the free nucleons (§ 3) in the nuclear problem.

The nuclear wave functions $\psi_{i,f}$ are obtained in specific models. One thus solves the Schrödinger equation

$$H_N \psi = E\psi, \quad (4.4)$$

where H_N is the model nuclear Hamiltonian

$$H_N = \sum_i H_{1Ni} + \sum_{i < j} V_{ij}, \quad (4.5)$$

V being the two-body potential. In the conventional shell-models, one makes a suitable approximation for the two-body potential and diagonalizes the model Hamiltonian in a reasonably chosen Hilbert space for the nucleons. The model Hamiltonian can be defined, for example, by starting with a general two-body force and fitting the two-body matrix elements to reproduce nuclear excitation energies or other observables. The errors introduced by the truncation of the Hilbert space are quite non-trivial to estimate, and the sheer largeness of the dimension of a realistic model space makes the problem computationally very difficult and, in many cases, even prohibitive [83].

In special cases techniques such as the Tamm-Dancoff and random-phase approximations or their extensions [84] are quite useful in calculating nuclear transition properties.

Below we mention two other variations of the impulse approximation approach used extensively in the muon capture studies.

Sum rule approach: If we are only interested in *total* capture strengths or combined strength to a group of closely spaced levels, sum rule techniques are quite useful. An example is the use of the Foldy–Walecka sum rule [20] to evaluate the giant dipole resonance strengths in nuclei with SU(4) scalar ground states (§ 7). Success of the sum rule approach requires an accurate knowledge of the ground state nuclear wave functions.

Effective operator approach: In this approach, several related processes are analysed together, thereby reducing or eliminating the role of traditional nuclear models. Thus in the “renormalized” jj coupling model, used by Morita and others [85, 86], the rate of the reaction $A(\mu^-, \nu_\mu)B$ is given by

$$\Lambda = \Lambda_{jj}(\mu^-)\Lambda_{\text{exp}}(\beta^-)/\Lambda_{jj}(\beta^-), \quad (4.6)$$

where $\Lambda_{jj}(\mu^-)$ and $\Lambda_{jj}(\beta^-)$ are the calculated rates of the muon capture reaction and the inverse β^- decay, respectively, in the jj coupling model, and $\Lambda_{\text{exp}}(\beta^-)$ is the *experimental* β decay rate. Recently, Donnelly, Walecka and collaborators have revived this approach, treating several related experimental quantities to do the nuclear “configuration analysis” [87]. Überall and collaborators [88] use the so-called “generalized” Helm model, in which the nuclear wave functions are entirely avoided and the muon capture matrix elements are obtained by appealing to other related experiments. These approaches are similar in spirit to the EPA, and their applicability has been appraised by the author elsewhere [89]. Obviously the dominance of a set of processes by one or very few nuclear matrix elements is the key to the success of these methods.

4.3. Classification of transitions

It is customary to classify the muon capture transitions to definite final states of the daughter nuclei in orders of “forbiddenness” [85], in analogy to a similar classification the nuclear β decay and electron capture. Thus a nuclear transition $J_i^\pi \rightarrow J_f^\pi$ is called “ n th forbidden”, if the changes of spin and parity are given as follows:

$$\begin{aligned} \Delta J &\equiv |J_i - J_f| = n \quad \text{or } (n+1), \\ \Delta\pi &\equiv \pi^i\pi^f = (-)^n. \end{aligned} \quad (4.7)$$

The following two special cases should be noted: (i) *allowed* (zeroth forbidden): $\Delta J = 0, 1$, $\Delta\pi = +1$; *first-forbidden*: $\Delta J = 0, 1, 2$, $\Delta\pi = -1$. A transition is *superallowed* if it takes place between members of the same nuclear supermultiplet in the sense of Wigner’s SU(4) symmetry (§ 7). Examples of superallowed muon capture transitions are $p \rightarrow n$, ${}^3\text{He} \rightarrow {}^3\text{H}$, ${}^6\text{Li} \rightarrow {}^6\text{He}_{\text{g.s.}}$. In muon capture by light nuclei, allowed and first-forbidden transitions *almost completely exhaust* the total strength.

There are important distinctions between the classifications of muon capture and β transitions. Thus successive increases of forbiddenness in β decay imply dramatic increase of ft values, i.e. sharp reduction of the nuclear transition rates. This *need not* be the case in the nuclear muon capture. For example, in ${}^{12}\text{C}$, the “allowed” transitions only account for 10% of the *total* capture rate, the remainder going predominantly to the “first-forbidden” group of transitions, exciting the analogue of the giant dipole resonance states. In light nuclei, first-forbidden transitions dominate as a rule; in

heavy nuclei, “higher forbidden transitions” become prominent and the giant dipole analogue excitations decrease in importance.

It should be noted that the contributions of the admissible higher forbidden matrix elements to a transition of a lower order of forbiddenss are not always *a priori* negligible in muon capture [90]. Only in light nuclei, contributions of the second-forbidden matrix elements to allowed transitions are, in general, quite small [91].

4.4. Calculation of observables in the impulse approximation

Steps leading from the Hamiltonian (§ 3.3) to the observables are the following: (i) non-relativistic reduction of the nucleon operators (§ 3); (ii) expressing effective nucleon operators in spherical tensor form, convenient for nuclear structure calculations; and (iii) summing over unobserved quantum numbers and averaging over the initial nuclear magnetic substates. An excellent illustration of these steps can be found in the paper of Morita and Fujii [85], and formulae for various observables (including possible hyperfine effects) are given in the review of Balashov and Eramzhyan [B1]. See Appendix 2 for a few special cases. Appendix 3 contains formulae for the nuclear single particle matrix elements.

4.5. Number of independent observables: constraints of neutrino helicity and time reversal invariance

While it is possible in a transition to have several accessible experimental observables, the number of independent observables [92–94] in a given transition $J_i \xrightarrow{\mu^-} J_f$ is limited by the constraints of rotational invariance and definite helicity of neutrino. Let us consider the following example discussed by Bernabéu [94]*:

$$\mu^- + N_i(J_i = 0) \rightarrow N_f(J_f = j) + \nu_\mu, \quad (4.8)$$

where N_i and N_f are the nuclear states with spins indicated in the parenthesis. The initial state is characterized by the angular momentum $\frac{1}{2}$ and the final state in terms of the helicity λ_f of the nucleus and $-\frac{1}{2}$ of the neutrino. It is thus clear that, independent of the value of j , only $\lambda_f = 0, -1$ are possible, and the process (4.8) can be described by two transition amplitudes $T_\lambda (\lambda = \pm\frac{1}{2})$ in the helicity representation with $\lambda = \lambda_f + \frac{1}{2}$. There are thus *three independent quantities* involved in describing the process (4.8): two absolute magnitudes of the amplitudes and the relative phase between $T_{1/2}$ and $T_{-1/2}$.

We can now write down expressions for various observables in terms of the helicity amplitudes T_λ . These are [94]:

$$\begin{aligned} \Lambda &= \sum_\lambda |T_\lambda|^2, \\ \Lambda(\theta) &= 1 + \alpha(P_\mu \cdot \hat{p}), \quad \alpha = 2(\sum_\lambda \lambda |T_\lambda|^2)/(\sum_\lambda |T_\lambda|^2), \\ P_L &= [\sum_\lambda (\lambda - \frac{1}{2}) |T_\lambda|^2]/[\sum_\lambda |T_\lambda|^2], \end{aligned} \quad (4.9)$$

and so on. Here Λ is the capture rate, $\Lambda(\theta)$ is the angular distribution of the recoil nucleus, α is the asymmetry parameter in the angular distribution, and P_L is the longitudinal polarization of the

*Oziewicz [187] has independently emphasized the model-independent constraints in the muon capture by spin-zero targets. See § 5.8.2.

recoil nucleus. P_μ is the muon residual polarization in the 1S orbit and \hat{p} is the unit vector in the direction of the nuclear recoil momentum. Thus we get the relation [95]

$$\alpha = 1 + 2jP_L, \quad (4.10)$$

obtained by Bernabéu, independent of the dynamics of the problem. Notice that the only assumptions utilized here are the rotational invariance and definite neutrino helicity.

One can now define an average polarization of the residual nucleus P_{av} when the recoil direction is not observed. The quantity is given by

$$P_{av} = P_\mu \times \frac{1}{3} \left\{ \left(\frac{j+1}{j} \right)^{1/2} \times 2 \operatorname{Re}[T_{1/2} T_{-1/2}^*] / [\sum |\lambda| |T_\lambda|^2] - P_L \right\}. \quad (4.11)$$

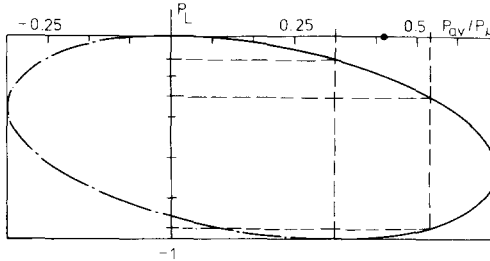


Fig. 4.1. Restriction line between the average polarization P_{av}/P_μ and the longitudinal polarization P_L imposed by the time reversal invariance (after Bernabéu [94]). The full line corresponds to the equal signs for the helicity amplitude and the dash-dotted line to opposite signs. The experimental results of P_{av} (Possoz et al. [168]) are projected to obtain allowed limits for P_L in the case of the $^{12}\text{C} \rightarrow {}^{12}\text{B}_{g.s.}$ transition (§ 5.7).

Now, invoking time-reversal invariance, which makes the amplitudes T_λ *real*, we get a relation between $P_{av}/P_\mu \equiv P$ and P_L , of the form (see fig. 4.1)*:

$$[1 + 4j(j+1)]P_L^2 + 2[3P + 2(j+1)]P_L + 9P^2 = 0, \quad (4.12)$$

by utilizing the identities

$$|T_{1/2}|^2 = \Lambda(1 + jP_L), \quad |T_{-1/2}|^2 = -jP_L \Lambda. \quad (4.13)$$

Thus, for a given value of the quantity P_{av}/P_μ , obtained experimentally, one obtains a prediction for P_L , which becomes a model-independent test for time-reversal invariance.

We shall return to this topic in the section on allowed transitions to discuss an example of current experimental interest (§ 5.7).

4.6. Muon capture in deuteron

4.6.1. Objectives

Muon capture in the deuteron constitutes an important anchor-point in the muon–nuclear weak interaction physics. The deuteron ground state structure is reasonably well known. Muon capture in this system provides us with an opportunity to study the two-neutron interaction in the final state

*In absence of the constraint of T invariance, the factor $(j+1)$ in eq. (4.12) should be replaced by $(j+1) \cos^2 \phi$, ϕ being the relative phase between $T_{1/2}$ and $T_{-1/2}$.

on the one hand, and to learn about corrections to the impulse approximation via meson-exchange effects on the other. The reaction



is one of the closest terrestrial analogues of the solar p–p reaction [96] $p + p \rightarrow d + e^+ + \nu_e$, an important process for the understanding of the solar neutrino puzzle.

4.6.2. Experimental determination of the capture rates

We have already discussed the evolution of muonic deuterium atoms in different physical conditions (§ 2.5). In *gaseous deuterium* (at 4 atm and 293°K), HF conversion rate is very small ($3.5 \times 10^4 \text{ s}^{-1}$) and the μ^-d atom is expected to retain its *statistical* population. The measured capture rate Λ will be

$$\Lambda_{\text{stat}} = \frac{2}{3}\Lambda_Q + \frac{1}{3}\Lambda_D. \quad (4.15)$$

For muon capture in a mixture of hydrogen and deuterium, the transfer process $\mu^-p + d \rightarrow \mu^-d + p$ is exceedingly rapid, and all muons will form μ^-d atoms. Collisions with deuterium and hydrogen will slow down μ^-d atoms rapidly. It is surmised, with some experimental evidence [97], that the hyperfine mixing in the colliding μ^-d and p systems will lead to a substantial conversion of μ^-d atoms to the *doublet* hyperfine state. Still the population of the doublet state may not be 100%, due to possible thermal excitation, since the hyperfine energy interval (0.046 eV) is of the order of magnitude to the thermal energy kT (~ 0.035 eV) at 300°K. Thus, in the experiment by the CERN–Bologna group, which used a gaseous mixture of hydrogen at 7.6 atm and 273°K and a 5% contamination of deuterium, the rate measured is

$$\Lambda' = \alpha\Lambda_Q + (1 - \alpha)\Lambda_D, \quad (4.16)$$

where α is close to, but greater than, zero. Using the theoretical expectation that $\Lambda_Q < \Lambda_D$, we obtain the inequality $\Lambda_D < \Lambda'$, where Λ' is experimentally obtained by the CERN–Bologna group to be

$$\Lambda' = 451 \pm 70 \text{ s}^{-1}. \quad (4.17)$$

The Columbia experiment, done earlier using deuterium contamination in *liquid* hydrogen, observed muon capture in the $p\mu^-d$ molecule at orbital angular momentum $L = 0$. This yields (Wang et al. [44])

$$\Lambda_D = 365 \pm 96 \text{ s}^{-1}. \quad (4.18)$$

The analysis of this experiment needs information on the muon densities at the p and d sites, and an estimation of the neutron background coming from the reaction $\mu^- + {}^3\text{He} \rightarrow \nu + n + d$ and $\nu + 2n + p$, ${}^3\text{He}$ being produced in the muomolecular fusion (§ 2.5).

4.6.3. The distribution of neutrons emitted in muon capture by deuteron, and capture rates

We can easily calculate the probability of a neutron emitted with momentum in the range p_n to $p_n + dp_n$ which is given by [98]

$$d\Lambda = [2(2J_i + 1)(2\pi)^5]^{-1} \times dp_n \int dp_\nu \Sigma_{\lambda\lambda'} |M|^2 \delta(E - E_\nu - E_n - E_f), \quad (4.19)$$

where $E = m_\mu + m_i - m_f - M_n$, $E_n = p_n^2/2M_n$ is the kinetic energy of the emitted neutron, E_f is the

kinetic energy of the residual nucleus, and the subscripts i and f indicate quantities pertaining to the initial and final nuclear states. The sum over indices λ, λ' indicates that over unobserved initial and final magnetic substates. The probabilities for capture from different hyperfine states are given in terms of the Fujii–Primakoff (FP) form factors

$$d\Lambda_D = A \times \{ [(G_V - 2G_A)^2 + \frac{2}{3}G_P(2G_V - 4G_A + G_P)] I_t + \frac{1}{3}(3G_A - G_P)^2 I_S \} dE_n, \quad (4.20a)$$

$$d\Lambda_Q = A \times \{ [(G_V + G_A)^2 - \frac{2}{3}G_P(G_V + G_A - G_P)] I_t + \frac{1}{3}G_P^2 I_S \} dE_n, \quad (4.20b)$$

$$d\Lambda_{\text{stat}} = A \times \{ G_V^2 I_t + [G_A^2 + \frac{1}{3}(G_P^2 - 2G_A G_P)] (2I_t + I_S) \} dE_n, \quad (4.20c)$$

where $A = M_n^2 \gamma_d / (2\pi)^3$, γ_d being the muon density at the position of the deuteron. The FP form factors are averaged over the appropriate values of the neutrino momentum $|\mathbf{p}_\nu|$. The integrals I_α appearing above are defined as follows:

$$I'_\alpha = \int \phi_\mu(r) \phi_d(r) \exp\{i\mathbf{p}_\nu \cdot \mathbf{r}/2\} \phi_\alpha(q, r) d^3r, \quad I_\alpha = \int_{p_{\nu_{\min}}}^{p_{\nu_{\max}}} |I'_\alpha|^2 p_\nu d\nu, \quad (4.21)$$

where $\phi_\alpha(q, r)$ is the two-nucleon scattering state [$\mathbf{q} = (\mathbf{p}_{n1} - \mathbf{p}_{n2})/2$], ϕ_d and ϕ_μ are the deuteron ground state, and muon 1S state wave functions, respectively. Equations (4.20) are obtained by neglecting the terms involving nucleon momentum operators. Integration over neutron energy yields the capture rates Λ_i , where i stands for D, Q or stat. (meaning ‘statistical’).

4.6.4. Sensitivity of the capture rates to various parameters of the problem

We summarize here conclusions obtained by various authors [98–108] on the sensitivity of capture rates to various physical parameters of interest.

- 1) The final-state interaction between the two neutrons is important, and it increases the capture rates Λ_D and Λ_Q by $\sim 15\%$ and $\sim 20\%$, respectively from the plane wave values (Dogotar et al. [106]).
 - 2) The nucleon momentum terms are unimportant for Λ_D and marginally important ($\sim 4\%$) for Λ_Q (Pascual et al. [102]; Dogotar et al. [106]).
 - 3) The deuteron D state contribution reduces* Λ_D by 7% and increases Λ_Q by 4% [106].
 - 4) There is a very strong hyperfine effect in the capture rate, Λ_D being about 35 times Λ_Q . As in hydrogen, the capture from the upper hyperfine state is negligible [98–108].
 - 5) An analysis of the form factor dependence of the rate Λ_D indicates, as expected, a strong dependence on g_A and a rather weak one on g_P and g_M [97].
 - 6) Corrections to the impulse approximation (IA) estimates of Λ_D have been determined to be around 7%, an increase from the IA value (Dautry, Rho and Riska [108]).
- The “best” impulse approximation estimates for the rates are [106–108]

$$\Lambda_D = 372 \text{ s}^{-1}, \quad \Lambda_Q = 11 \text{ s}^{-1}, \quad \Lambda_{\text{stat}} = 131 \text{ s}^{-1}. \quad (4.22)$$

These estimates have been arrived at by using the Reid soft-core potential [110] to describe the two-nucleon system (the hard-core potential gives practically the same result [106]). The deuteron ground state has a D state admixture of 6.5% in this model. Inclusion of meson exchange corrections yields a value of Λ_D equal to 405 s^{-1} [108], to be compared with the experimental lower limit of

*Current estimates on the deuteron D state probability range from about 3% to 7% [109]. The 7% reduction of Λ_D is the upper limit of the D-state effect, proving thereby that muon capture is *not very suitable* to provide precise information on the D state probability.

381 s^{-1} from the CERN–Bologna experiment or with the Columbia result of $365 \pm 95 \text{ s}^{-1}$. Thus the prediction of the V–A theory is in good agreement with experiments in deuteron.

4.6.5. Possibility of an accurate determination of the singlet scattering length a_{nn}

Several authors [104, 106, 108] have theoretically investigated the kinematic region of the neutron spectrum sensitive to the singlet scattering length* a_{nn} . Their conclusion for the muon capture from the hyperfine state $F = \frac{1}{2}$ is that relatively small opening angle between the neutrons (figs. 4.2a, b) and small energy of the detected neutron [$E_n \sim 50$ to 150 keV (fig. 4.2c)] are suitable** for probing a_{nn} . The measurements of the difference in times of flight and the opening angle between the two neutrons of low energy should give adequate kinematic information. Such an experiment appears feasible at SIN [111].

While the experimental informations on the hyperfine capture rates in deuteron remain imprecise, they provide us with added confidence on the soundness of the weak Lagrangian (§3). We are now ready to examine if the impulse approximation is adequate in describing muon capture in more complex nuclei, keeping in mind the fact that our knowledge of the nuclear structure of such systems is often unsatisfactory.

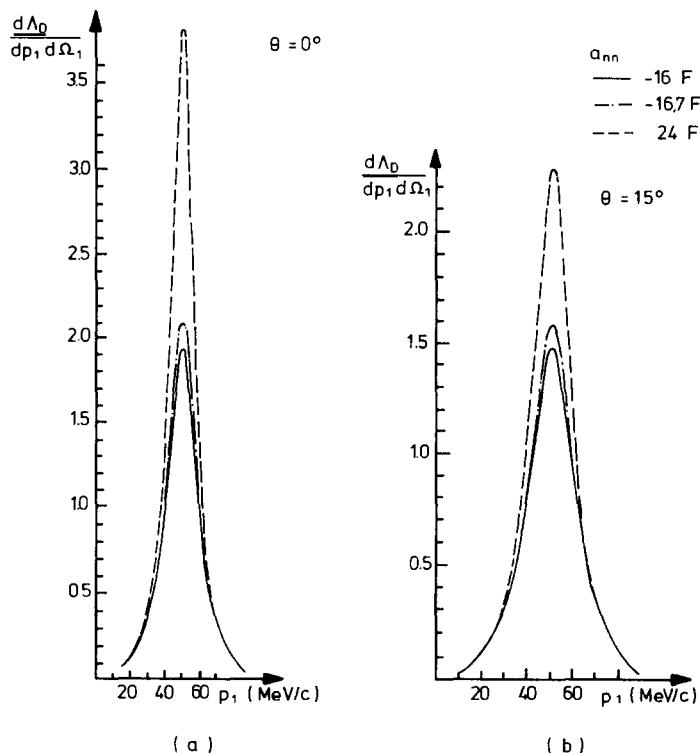


Fig. 4.2(a, b). The differential cross-section $d\Lambda_D/dp_1, d\Omega_1$ for a single neutron in two different opening angles $\theta = 0^\circ$ and $\theta = 15^\circ$ as a function of the neutron momentum p_1 , and as a parametric function of the singlet scattering length a_{nn} (after Dogotar et al. [106]). The greater sensitivity to a_{nn} in low opening angle is apparent.

*See, for a recent review of the experimental knowledge of a_{nn} , B. Kühn, Sov. J. Particles and Nuclei 6 (1975) 139.

**See, however, ref. [107a].

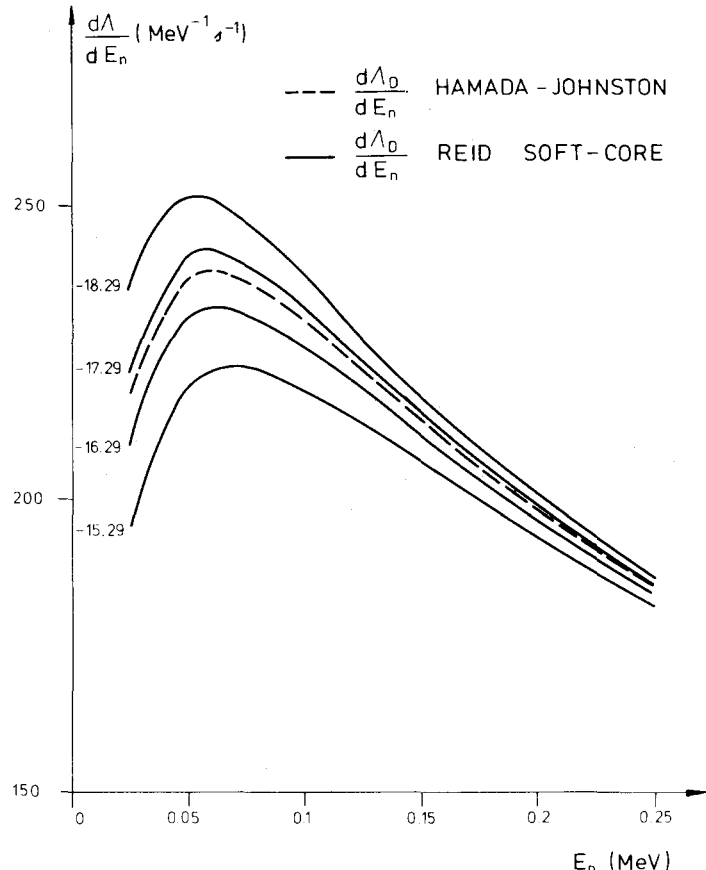


Fig. 4.2c. The differential cross-section $d\Lambda_F/dE_n$ as functions of the neutron energy E_n and of the scattering length a_{nn} , for Hamada–Johnston and Reid soft-core potentials (after Dautry, Rho and Riska [108]). The strong sensitivity to a_{nn} occurs at very low neutron energies.

5. Allowed transitions in complex nuclei

5.1. Objectives of study

Allowed transitions satisfy the Fermi (F) and the Gamow–Teller (GT) selection rules for the nuclear spin, parity and isospin quantum numbers:

$$F: \quad |J_i - J_f| = 0, \quad \pi^i \pi^f = +1, \quad |T_i - T_f| = 0, 1 \quad (5.1)$$

$$GT: \quad |J_i - J_f| = 0, 1 (\text{no } 0 \rightarrow 0), \quad \pi^i \pi^f = +1, \quad |T_i - T_f| = 0, 1. \quad (5.2)$$

The only possible $\Delta T = 0$, F and GT transitions in muon capture are $p \rightarrow n$ and ${}^3\text{He} \rightarrow {}^3\text{H}$.

Allowed transitions in light nuclei, particularly those with $A < 16$, involve states that are generally well-known from the nuclear structure point of view. Hence a test of our knowledge of the weak interaction Hamiltonian *in the nuclear context* is frequently possible. This is usually done within the framework of the impulse approximation.

Light nuclei often exhibit a concentration of allowed strengths in a few low-lying states (giant magnetic dipole analogue resonance), enhancing their value as vehicles for nuclear spectroscopic studies. The asymmetries of the recoiling daughter nuclei with respect to muon polarization axis, and related observables can be described, in the first approximation, independently of the nuclear matrix elements, giving us the possibility of extracting effective weak form factors of the nucleon. Hyperfine capture and gamma-neutrino correlation experiments, in suitable cases, are sensitive to the elusive “second-forbidden” matrix elements.

5.2. Allowed transition rates

Only seven allowed transition rates have been experimentally determined so far (table 5.1) in nuclei heavier than hydrogen. In $^{11}\text{B} \rightarrow ^{11}\text{Be}$ ($1/2^-$:320 keV) transition, an experimental estimate of the ratio of the hyperfine capture rates is also available.

Table 5.1

Experimentally measured allowed transition rates in “complex” ($A > 1$) nuclei. Only the most accurate experimental value is shown here except for ^{14}N . [a] indicates unpublished results (private communications from the authors).

Transition	Capture rate (s^{-1})	Authors
$^3\text{He}(J^\pi T = \frac{1}{2}^+ \frac{1}{2}) \rightarrow ^3\text{H}(J^\pi T = \frac{1}{2}^+ \frac{1}{2})$	1505 ± 46	Auerbach et al. [128]
$^6\text{Li}(1^+ 0) \rightarrow ^6\text{He}(0^+ 1: \text{g.s.})$	1600 ± 330 ~ 129	Deutsch et al. [157]
$^{10}\text{B}(3^+ 0) \rightarrow ^{10}\text{Be}(2^+ 1: 3.37 \text{ MeV})$	~ 1000	Grenacs et al. [a]
$^{10}\text{B}(3^+ 0) \rightarrow ^{10}\text{Be}(2^+ 1: 5.95 \text{ MeV})$	~ 4000	Grenacs et al. [a]
$^{11}\text{B}(\frac{3}{2}^+ \frac{1}{2}) \rightarrow ^{12}\text{Be}(\frac{1}{2}^+ \frac{3}{2}: 0.32 \text{ MeV})$	1000 ± 100	Deutsch et al. [31a]
$^{12}\text{C}(0^+ 0) \rightarrow ^{12}\text{B}(1^+ 1: \text{g.s.})$	6200 ± 300	Budyashov et al. [159] and Miller et al. [373]
$^{14}\text{N}(1^+ 0) \rightarrow ^{14}\text{C}(2^+ 1: 7.01 \text{ MeV})$	$(10 \pm 3) \times 10^3$ ~ 8000	Babaev et al. [158] Grenacs et al. [a]

Theoretically, the capture rate Λ can be calculated in an “exact” manner by including all nuclear transition tensor operators of rank u [$|J_i - J_f| \leq u \leq (J_i + J_f)$] and positive parity; it can be also estimated in the *allowed approximation* (neglecting all tensor operators of ranks two and higher, wherever relevant), or in the *Fujii-Primakoff (FP) approximation*, by retaining only those matrix elements that survive in the $q \rightarrow 0$ limit, viz. the Fermi and Gamow-Teller matrix elements, indicated* by [000] and [101], respectively. In the FP approximation Λ is given by

$$\Lambda^{\text{FP}} = S(\Gamma_F[000]^2 + \frac{1}{3}\Gamma_{\text{GT}}[101]^2), \quad (5.3)$$

where S is the statistical factor, Γ_F and Γ_{GT} are the *effective* Fermi and Gamow-Teller coupling constants expressed in terms of the FP coupling constants:

$$\Gamma_F = G_V^2, \quad \Gamma_{\text{GT}} = [3G_A^2 + (G_P^2 - 2G_P G_A)]. \quad (5.4)$$

Notice that, in the limit $q \rightarrow 0$, $G_V \rightarrow g_V$, $G_A \rightarrow g_A$, $G_P \rightarrow 0$, and we get the electron capture rate. For $\Delta T \neq 0$, $\Delta J \neq 0$ transitions, the matrix element [000] vanishes and Λ^{FP} is given by

$$\Lambda^{\text{FP}}(\Delta T \neq 0, \Delta J \neq 0) = \frac{1}{3}S\Gamma_{\text{GT}}[101]^2. \quad (5.5)$$

*See Appendix 2 for definitions. The notations for matrix elements ([101], etc.) should not be confused with references!

Table 5.2

Hyperfine capture rates Λ_{\pm} in the Fujii–Primakoff (FP) approximation, in terms of the FP form factors, for selected allowed transitions. Over-all phase-space and geometrical factors are suppressed here. The symbols [000] and [101] are Fermi and Gamow–Teller matrix elements, respectively, defined in Appendix 2 (from Balashov and Eramzyan [B1]).

Transition	Λ_+	Λ_-
$1 \rightarrow 0$		$2[101]^2(\frac{1}{3}G_P - G_A)^2$
$\frac{3}{2} \rightarrow \frac{1}{2}$	$\left\{ \frac{2}{9}[101]^2 G_P^2 \right.$	$\frac{2}{9}[101]^2 \{8(\frac{1}{3}G_P - G_A)^2 + \frac{1}{9}G_P^2\}$
$3 \rightarrow 2$		$\frac{2}{9}[101]^2 \{7(\frac{1}{3}G_P - G_A)^2 + \frac{2}{9}G_P^2\}$
$\frac{1}{2} \rightarrow \frac{3}{2}$	$\frac{2}{9}[101]^2 \{4(\frac{1}{3}G_P - G_A)^2 + \frac{5}{9}G_P^2\}$	
$\frac{3}{2} \rightarrow \frac{5}{2}$	$\frac{2}{9}[101]^2 \{8(\frac{1}{3}G_P - G_A)^2 + \frac{7}{9}G_P^2\}$	
$1 \rightarrow 2$	$[101]^2 \{(\frac{1}{3}G_P - G_A)^2 + \frac{1}{9}G_P^2\}$	$\left\{ \frac{2}{9}[101]^2 G_P^2 \right.$
$\frac{1}{2} \rightarrow \frac{1}{2}$	$2\{[000]G_V - \frac{1}{3}[101](\frac{1}{3}G_P - G_A)\}^2 + \frac{16}{81}[101]^2 G_P^2$	$2\{[000]G_V + [101](\frac{1}{3}G_P - G_A)\}^2$

For $\Delta T \neq 0$, $\Delta J = 0$ transitions, [000] need not always vanish, but it can be neglected in light nuclei (§ 7).

Equations (5.3)–(5.5) assume statistical hyperfine populations for non-spin-zero nuclear targets. Expressions for capture rates from individual hyperfine states obtained in the FP approximation are given in table 5.2.

The allowed approximation and the “exact” approach coincide in the transitions $0^+ \rightarrow 0^+$, $1^+ \rightarrow 0^+$ and $0^+ \rightarrow 1^+$. For other transitions, the allowed approximation is usually quite adequate, and the FP approximation gives a good idea of the distribution of the transition strengths. For reliable estimates of the hyperfine capture rates, and observables like the gamma–neutrino correlation functions, admissible second-forbidden matrix elements cannot be ignored [112].

5.3. Allowed transition in ${}^3\text{He}$

The reaction



is the closest *nuclear* analogue of the muon capture by proton and has received very careful theoretical [113–126] and experimental [127–129] attention. The wave function of ${}^3\text{He}$ system is reasonably well known, being of the form [130]:

$$\psi = a {}^2S[3] + b {}^2S[21] + c {}^4D[21], \quad (5.7)$$

in the *LS* representation ${}^{2S+1}L[f]$, $[f]$ being the orbital Young partition. The estimates of b and c are in the range 0.1%–4% and 5%–9%, respectively. A crucial quantity for the determination of the capture rate is the size parameter of the principal S state [130].

5.3.1. Experimental value of the capture rate

Various authors have experimentally determined the rate of the reaction (5.6). They have obtained the values

$$\Lambda^{\text{exp}}({}^3\text{He} \rightarrow {}^3\text{H}) = 1410 \pm 140 \text{ s}^{-1} \quad [127], \quad 1465 \pm 67 \text{ s}^{-1} \quad [129], \quad 1505 \pm 46 \text{ s}^{-1} \quad [128]. \quad (5.8)$$

In comparing the experimentally observed capture rates with theoretical predictions, we have to examine two possible corrections to Λ^{exp} for extracting the statistical capture rate Λ^S : i) correction due to contribution of muon capture from the metastable 2S orbit; and ii) possible non-statistical population due to the hyperfine conversion. The first correction is relevant only for the muon capture in pure ${}^3\text{He}$, as is the case in the experiment of Auerbach et al. [128], since, in the other two experiments, the presence of Xe impurity allows the following prompt electron transfer reaction



followed by the prompt Auger transition to the 1S state of the muonic He atom. As much as 5% of the muons are estimated [131] to be captured from the 2S metastable state of ${}^3\text{He}$ gas at ~ 7 atm. Thus, the observed rate of Auerbach et al. [128], Λ_A^{exp} , is the sum of the 2S and 1S capture rates $\Lambda^{2\text{S}}$ and Λ^S , weighted by the corresponding muon fractions $N_{2\text{S}}$ and $N_{1\text{S}}$:

$$N_{2\text{S}}\Lambda^{2\text{S}} + N_{1\text{S}}\Lambda^S = \Lambda_A^{\text{exp}}. \quad (5.10)$$

With $N_{2\text{S}} = 0.05$, $N_{1\text{S}} = 0.95$, and $\Lambda^{2\text{S}} = \frac{1}{8}\Lambda^S$, we get

$$\Lambda^S = 1572 \pm 46 \text{ s}^{-1}. \quad (5.11)$$

The second correction of possible non-statisticality in the 1S hyperfine states can be ignored, since the conversion of the $F_+ = 1$ (upper) hyperfine state is theoretically estimated to be entirely negligible* [30]. Ignoring this correction, we get an experimental world average value of the rate of the process (5.6) to be

$$\Lambda_{\text{av}}^S = 1529 \pm 37 \text{ s}^{-1}. \quad (5.12)$$

5.3.2. Results of the theoretical analyses

Theoretical studies of the reaction (5.5) yield the following conclusions: a) The capture rate decreases with the increase in the D state probability of the ${}^3\text{He}$ wave function, if we keep the 2S [21] probability fixed around $\sim 1\%$. It is insensitive to the detailed structure of the radial wave function, but strongly sensitive to the size parameter of the 2S [3] state. b) The rate of the reaction (5.6) is strongly dependent on the vector and axial-vector form factors, but rather weakly on the weak magnetism and pseudoscalar terms. The experimental value of rate [eq. (5.12)] yields limits on $g_A(q^2)$ quite close to the value obtained for hydrogen.

Phillips et al. [125] obtain an impulse approximation estimate for the rate to be

$$\Lambda^{\text{th}} = 1433 \pm 60 \text{ s}^{-1}, \quad (5.13)$$

assuming canonical (§ 3) values of the weak form factors, in agreement** with the experimental value [eq. (5.12)]. Uncertainties in eq. (5.13) include those of the nuclear wave functions and weak form factors. These authors also use the elementary particle model approach, and get an estimate of 1425 s^{-1} for the rate. The accuracy of the latter is, however, uncertain because of the unknown q^2 dependence of the *nuclear* axial vector form factor [126] and lack of a proper treatment for the anomalous thresholds [132] affecting the determination of the nuclear pseudoscalar term.

*The experimentally determined upper limit of the conversion rate is $4 \times 10^4 \text{ s}^{-1}$ [B39], which gives at most a 3% uncertainty in rate due to possible non-statisticality. This limit should be improved considerably.

**Note that the impulse approximation estimate (5.13) tends to be slightly *lower* than the experimental value. Within the uncertainty of the theoretical prediction, this is still in agreement with the experiment.

5.4. Allowed transitions in the 1p-shell nuclei*

Allowed transitions in 1p-shell nuclei have been studied extensively in numerous theoretical [B19, B36, 85–91, 133–150] and experimental [31a, 151–159, 168, 373] papers. This author and his collaborators [29, 89, 91, 133–139] have examined these transitions to determine theoretically the distribution of strengths, their usefulness as tools to probe the various weak hadron form factors, and to shed light on the symmetry of the nuclear Hamiltonian. The reaction $^{12}\text{C}(\mu^-, \nu_\mu) ^{12}\text{B}_{\text{g.s.}}$, for example, has been extensively used to test nuclear models and relationships of muon capture to other weak and electromagnetic processes involving the same (or analogous) nuclear states.

Allowed transitions in the 1 p-shell nuclei involve states of normal parity (i.e. with the same parity as that of the ground state of the stable nucleus), that are reasonably well understood in the intermediate coupling [161–162] or many-particle shell-model [163] approaches to the nuclear structure. The muon capture transitions provide a new kinematic domain to test these models, unavailable in the nuclear β spectroscopy.

Since the transitions induced by muon capture in the 1p-shell nuclei involve change of isospin, the Fermi coupling term Γ_F can be ignored in $J_i \rightarrow J_f = J_i$ transitions: the capture rate is proportional to Γ_{GT} and the square of the Gamow–Teller matrix element [101] in the FP approximation [eq. (5.5)]. This approximation is very helpful in understanding many aspects of the allowed transitions discussed below.

5.4.1. Distribution of the allowed transition strength: “giant” allowed excitations

The distribution of the allowed muon capture strength has been studied by the author [135] using Cohen–Kurath wave functions (CKM). The results of the calculation are summarized in table 5.3, where the rates for the prominent allowed transitions in ^6Li , ^9Be , ^{10}B , ^{12}C , ^{13}C , and ^{14}N are displayed. There is negligible strength in ^7Li and none in ^{15}N , so these targets are omitted from the table. The rates are obtained by using the elementary weak form factors (§3) and harmonic oscillator radial functions. Relaxation of these constraints does not alter the distribution of strengths substantially.

Strong concentration of the allowed strength in a few low-lying states of the daughter nuclei is apparent from table 5.3. For example, in ^6Li , ^{12}C , and ^{13}C the ground state (g.s.)-to-g.s. transitions dominate overwhelmingly, while in ^{14}N the calculated rate to the first $2^+(T=1)$ state in ^{14}C accounts for $\sim 92\%$ of the total allowed strength. This sharp concentration of strength is also seen in the isovector M1 electroexcitations [164–165] and in the radiative pion capture [106].

Key to the understanding of these strong excitations is the dominance [89–91] of allowed transitions by the Gamow–Teller matrix element [101], exhibited in fig. 5.1. The same is true for the isovector M1 transition and the radiative pion capture from the 1S orbit. The z component of the isovector M1 operator is given by [161]

$$\mu_z = (\mu_n - \bar{\mu}_p) \sum_{i=1}^A s_z(i) \tau_z(i) - \frac{1}{2} \sum_{i=1}^A l_z(i) \tau_z(i), \quad (5.14)$$

μ_n and μ_p being the magnetic moments of neutron and proton, respectively, \mathbf{l} , \mathbf{s} , and $\boldsymbol{\tau}$ are the single-particle orbital angular momentum spin and isospin operators. Thus the first term on the right-hand

*In §5.4, we discuss only the rates of these transitions. See §5.6 for a discussion of hyperfine effects, and §§5.7–5.8 for other observables.

Table 5.3

Distribution of calculated allowed transition strength in the 1p-shell nuclei in dominant transitions (after Mukhopadhyay [135])

Target (number of possible allowed transitions in the 1p-shell model)	Daughter states dominantly populated	Calculated rate of the dominant excitation $\Lambda(s^{-1})$	Fraction of the total calculated allowed capture rate (%)
⁶ Li(5)	⁶ He(0 ⁺ 1: g.s.)	1270	89.0
⁹ Be(17)	⁹ Li($\frac{3}{2}^-, \frac{3}{2}^+$: g.s.) ⁹ Li($\frac{5}{2}^-, \frac{3}{2}^-$: 4.31 MeV) ⁹ Li($\frac{5}{2}^-, \frac{3}{2}^+$: 5.4 MeV)	193 106 168	38.6 21.2 33.7
¹⁰ B(25)	¹⁰ Be(2 ⁺ 1: 3.37 MeV) ¹⁰ Be(2 ⁺ 1: 5.95 MeV) ¹⁰ Be(3 ⁺ 1: 8.9 MeV) ¹⁰ Be(4 ⁺ 1: 10.8 MeV)	768 5606 1918 372	~8.5 61.9 21.2 ~4.1
¹² C(8)	¹² B(1 ⁺ 1: g.s.)	6200	95.0
¹³ C(4)	¹³ B($\frac{3}{2}^-, \frac{3}{2}^+$: g.s.)	6097	99.0
¹⁴ N(5)	¹⁴ C(2 ⁺ 1: 7.01, 8.34 MeV) ¹⁴ C(1 ⁺ 1: 9.8 MeV)	1.98×10^4 1230	91.6 ~5.7

side of eq. (5.14) dominates. Similarly, the Kroll–Ruderman theorem tells us that the radiative pion capture Hamiltonian is simply [167]

$$H^{\pi,\gamma} \propto \sum_{i=1}^A \tau_i^+ \epsilon \cdot \sigma_i \delta(\mathbf{r} - \mathbf{r}_i) + \text{terms } O(q/M), \quad (5.15)$$

where q is the pion momentum and ϵ is the photon polarization. In the 1S capture, the first term in (5.15) dominates, relating this process to the muon capture.

The dominance of the Gamow–Teller matrix element is muon capture and related processes makes them ideal as analysers of the nuclear supermultiplet symmetry breaking (§ 7).

5.4.2. Roles of the hadronic weak form factors

Absolute contributions of various hadronic weak form factors in allowed transitions are buried in nuclear physics. However, we can estimate their relative roles and find that they are qualitatively independent of nuclear structure. To show this we compare the estimates of the contributions by the form factors obtained in an “exact” calculation with those predicted by the Fujii–Primakoff approximation (FPA) [136].

In the FPA the roles of the weak form factors are independent of the nuclear properties and depend only on the parameter $\beta (= q/2M)$. Thus we can obtain the relative contributions of the weak form factors to the statistical capture rate from the quantity Γ_{GT} [eq. (5.4)]:

$$\begin{aligned} \Gamma_{\text{GT}} = & g_A^2 [\beta^2 + 2\beta + 3 + 2\beta^2(1 + \mu_p - \mu_n)^2 (g_V/g_A)^2 + \beta^2(g_p/g_A)^2 \\ & + 4\beta(1 + \mu_p - \mu_n)(g_V/g_A) - 2(\beta^2 + \beta)(g_p/g_A)] \end{aligned} \quad (5.16)$$

combining the vector and weak magnetism terms and assuming the absence of the tensor form factor g_T . Evaluating the ratios g_V/g_A and g_p/g_A at $q \sim 100$ MeV/c, we see, that, in the FPA, i) the dominant contribution to the rate is due to the axial-vector term (A), which accounts for about 90% of the rate; ii) the contributions due to interference of A with the vector-weak magnetism (VM) and pseudoscalar (PS) terms are nearly equal (~20% of the rate), but opposite in sign; iii) the VM–PS interference term is absent.

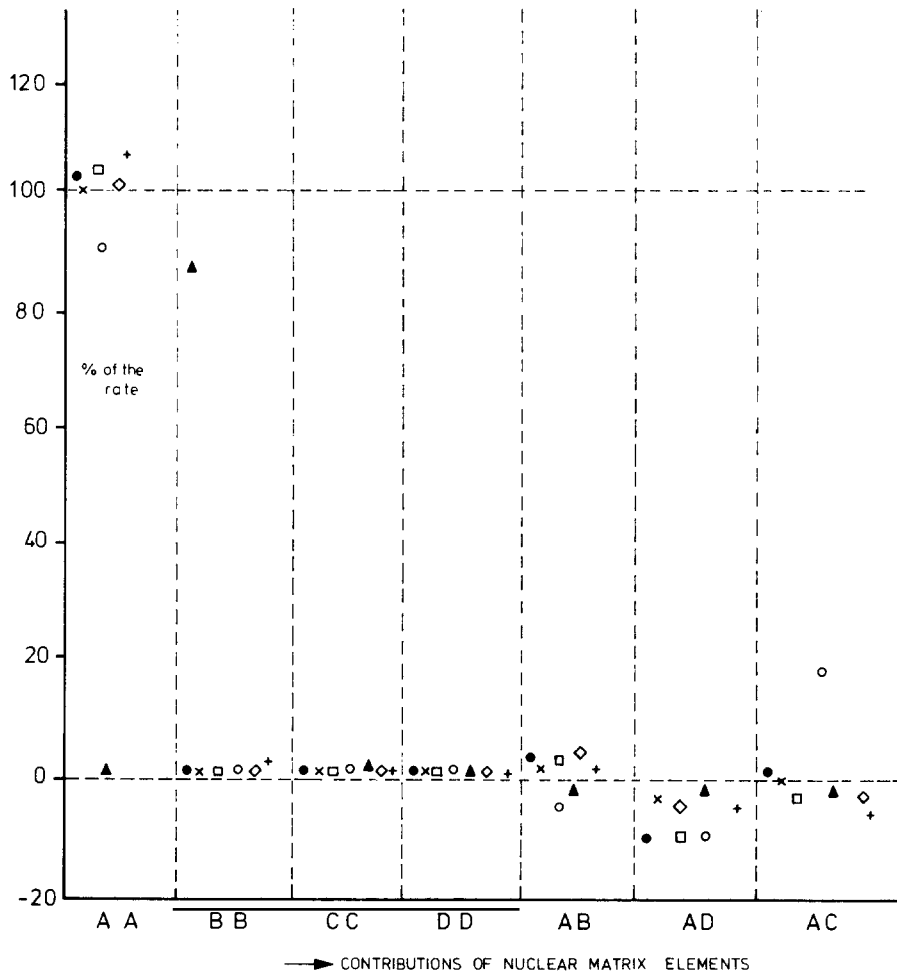


Fig. 5.1. Relative contributions of the various nuclear matrix elements to the rates of the selected allowed transitions in the 1p-shell nuclei (from Mukhopadhyay [C9]). The contributions due to various matrix elements are indicated in the following way: A = [101], B = [121], C = [111p] and D = [011p], in the notation explained in Appendix 2. Notice the dominance of the AA term in all transitions displayed, except in the reaction $^{14}\text{N}(\mu^-, \nu_\mu) ^{14}\text{C}_{\text{g.s.}}$, in which [121] dominates. The reactions shown are: ● $^{12}\text{C} \rightarrow ^{12}\text{B}_{\text{g.s.}}$, × $^6\text{Li} \rightarrow ^6\text{He}_{\text{g.s.}}$, □ $^{13}\text{C} \rightarrow ^{13}\text{B}_{\text{g.s.}}$, ○ $^9\text{Be} \rightarrow ^9\text{Li}_{\text{g.s.}}$, ▲ $^{14}\text{N} \rightarrow ^{14}\text{C}_{\text{g.s.}}$, ◇ $^{14}\text{N} \rightarrow ^{14}\text{C}(2^+: 7.01 \text{ MeV})$, + $^{14}\text{N} \rightarrow ^{14}\text{C}(1^+, T = 1)$.

In table 5.4 we compare the relative contributions of various hadronic weak form factors, as obtained in a precise calculation (retaining all the matrix elements in the allowed approximation), and predicted by the FPA. The agreement between the two is excellent.

These relative contributions in table 5.4 are found to be insensitive to the variation of the oscillator parameter b [136].

We must note, however, that the FPA breaks down completely, as expected, in cases where the Gamow-Teller matrix element itself is small. The $^{14}\text{N}(\mu^-, \nu_\mu) ^{14}\text{G}_{\text{g.s.}}$ transition is such an example [134]*.

*The vanishing of the [101] matrix element makes $^{14}\text{N}(\gamma, \pi^+) ^{14}\text{C}_{\text{g.s.}}$ reaction quite interesting to study various corrections to the Kroll-Ruderman term [139a].

Table 5.4

Relative contributions to the capture rate by various hadronic weak form factors – axial vector (A), vector and weak magnetism (VM), pseudoscalar (PS), and their inferences – in allowed transitions. Rows “a” and “b” indicate “exact” and Fujii–Primakoff approximation estimates (after Mukhopadhyay [136]).

Transition		A	PS	VM	A–PS	A–VM	PS–VM
${}^6\text{Li} \rightarrow {}^6\text{He}(0^+ 1: 0)$	a	89.2	3.56	2.55	-20.2	25.0	-0.01
	b	91.9	3.82	2.47	-22.4	24.2	0
${}^{10}\text{B} \rightarrow {}^{10}\text{Be}(2^+ 1: 5.96)$	a	88.8	3.69	2.40	-20.1	25.3	-0.20
	b	92.3	3.80	2.40	-22.4	23.9	0
${}^{12}\text{C} \rightarrow {}^{12}\text{B}(1^+ 1: 0)$	a	85.1	3.12	2.34	-15.6	25.2	-0.20
	b	94.0	3.64	2.06	-22.0	22.4	0
${}^{13}\text{C} \rightarrow {}^{13}\text{B}(\frac{3}{2}^+ - \frac{1}{2}: 0)$	a	89.2	3.31	1.85	-17.0	22.8	-0.19
	b	94.0	3.63	2.05	-22.0	22.3	0
${}^{14}\text{N} \rightarrow {}^{14}\text{C}(2^+ 1: 7.01)$	a	84.9	2.77	2.35	-14.8	25.1	-0.18
	b	92.6	3.77	2.34	-22.3	23.6	0

Thus the statistical capture rate Λ^S for allowed transitions in 1p-shell nuclei is suitable to probe only the axial-vector form factor $g_A(q^2)$ to a sensitive degree.

5.4.3. Allowed transition in ${}^{12}\text{C}$

As an illustration of the theoretical treatment we discuss here the transition

$${}^{12}\text{C}(J^\pi T = 0^+ 0) + \mu^- \rightarrow {}^{12}\text{B}(J^\pi T = 1^+ 1 : \text{g.s.}) + \nu_\mu, \quad (5.17)$$

on which very extensive theoretical [85–91, 145, 170, 171] and experimental [151–156, 159, 168, 373] literatures exist. Advantages of studying this reaction are many: i) The nuclear wave functions of the states involved in the reaction (5.17) are well-known [138, 163]; these are able to describe the inverse β decay (${}^{12}\text{B}_{\text{g.s.}} \xrightarrow{\beta^{-12}} {}^{12}\text{C}_{\text{g.s.}}$) rate to better than 10%. The properties of the isobaric analogue state of ${}^{12}\text{B}_{\text{g.s.}}$ in ${}^{12}\text{C}$ are also well described by these wave functions. ii) The single-particle nuclear radial functions, which are normally assumed to be harmonic oscillator (HO) functions, can be obtained from more realistic models, so that the Fourier–Bessel transforms of these are very accurately determinable [139]. iii) Both the $p_{3/2}$ and $p_{1/2}$ single-particle orbits, constituting the “valence” states of nucleons in the $A = 12$ system, correspond to bound states; thus we do not have to deal with the problem of unbound single-particle levels (present, for example, in ${}^6\text{Li}$ and ${}^{16}\text{O}$). Therefore, the reaction (5.17) can be studied with reasonably certain nuclear physics inputs, providing us with an important test of the impulse approximation approach. This reaction has an additional advantage: *it is free from the complications of the hyperfine effect*. The best experimental determination of the rate of the process (5.17) has yielded a value [159, 373]

$$\Lambda = (6.2 \pm 0.3) \times 10^3 \text{ s}^{-1}. \quad (5.18)$$

The inverse β decay reaction has an ft value [169]:

$$ft = (1.1789 \pm 0.0051) \times 10^4 \text{ s}. \quad (5.19)$$

The importance of the nuclear structure aspect in the problem is underscored by the failure of a

simple jj model, or Tamm–Dancoff and similar approximations [85–87, 89], to describe weak and electromagnetic transitions in ^{12}C . In these models, the ground state (g.s.) of ^{12}C is a closed ($p_{3/2}$) shell, coupled to $J^\pi T = 0^+ 0$, and $^{12}\text{B}_{\text{g.s.}}$ is a particle–hole (p–h) state with the configuration $[1p_{1/2} \ 1p_{3/2}^{-1}]$, coupled to $J^\pi T = 1^+ 1$. The nuclear matrix element of a tensor operator T^K is simply the single-particle reduced matrix element $\langle p_{1/2} \parallel T^K \parallel p_{3/2} \rangle$, apart from geometrical factors, in these models (Appendix 3). We thus obtain the muon capture rate and βft values as follows:

$$\Lambda(jj) = 35.3 \times 10^3 \text{ s}^{-1}, \quad ft(jj) = 2.3 \times 10^3 \text{ s}, \quad (5.20)$$

assuming for the former, HO radial functions with oscillator parameter $b = 1.64 \text{ fm}$, obtained from the ^{12}C charge radius ($= 2.45 \text{ fm}$). These are off by a factor of ~ 5 and $\sim 5^{-1}$, respectively, compared to the experimental values. This is not surprising, since both Λ and ft are essentially given by the Gamow–Teller matrix element [101] at two different momentum transfers [89, 91]. The discrepancy between (5.20) and the experimental value of Λ is corrected by the scaling recipe of the “renormalized” jj coupling models (RJM):

$$\Lambda_{\text{RJM}} = \xi \Lambda(jj), \quad (5.21)$$

where $\xi = ft(jj)/ft(\text{exp})$. A variation of this approach is to treat both ξ and b as parameters and to determine them from a fit of the inelastic electron scattering form factor in the reaction $^{12}\text{C}(e, e')^{12}\text{C}^*(J^\pi T = 1^+ 1; 15.11 \text{ MeV})$ [145].

In realistic nuclear models, the nuclear matrix elements can be determined without any recourse to scaling. In these models, $^{12}\text{C}_{\text{g.s.}}$ is no longer a “zero-particle zero-hole” (0p–0h) state, but there is a substantial admixture of 2p–2h and 4p–4h configurations; the amplitude $[1p_{1/2} \ 1p_{3/2}^{-1}]$ in the $^{12}\text{B}_{\text{g.s.}}$ is no longer 100%, but only about 60%. With the same oscillator parameter as before, we obtain in a realistic model [138]

$$\Lambda = 6.3 \times 10^3 \text{ s}^{-1}, \quad ft = 1.26 \times 10^4 \text{ s}, \quad (5.22)$$

in substantial agreement with the experiments.

It should be noted, however, that the exact implications of the RJM and realistic nuclear models are not the same in the present context. Thus the four nuclear matrix elements [101], [121], [111p], and [011p], relevant to the muon capture transition in an exact calculation, do not scale in the same way from the jj coupling model to the realistic models, as demonstrated in table 5.5. Thus the RJM is not suitable in estimating effects for which the contributions of the matrix elements other than [101] are important, for example, in determining limits of the hadronic weak form factors. Using the isovector M1 electron scattering form factor as a constraint to fix nuclear wave functions via parameters ξ and b , one cannot take into account differences between the radial wave

Table 5.5

Nuclear matrix elements estimated in the jj -coupling (JJM) and realistic nuclear models (ICM), for the $^{12}\text{C} \xrightarrow{\mu^-} {}^{12}\text{B}_{\text{g.s.}}$ transition. ξ represents the ratio of JJM to ICM estimates which are not equal (from Mukhopadhyay [89]).

	[101]	[121]	[111p]	[011p] _A	[011p] _B
JJM	−0.183 78	0.064 98	−0.037 51	−0.091 89	0
ICM	−0.076 94	0.033 03	2.1546×10^{-4}	−0.065 37	0.024 15
ξ	2.389	1.967	−174.1	1.406	0

functions for $p_{3/2}$ and $p_{1/2}$ orbitals. In this procedure, possible corrections to the impulse approximation in the electron scattering case get absorbed in the wave function. Hence a test of the impulse approximation in *muon capture* becomes uncertain in this approach.

The estimates of eq. (5.22) are good to only about 20%, since the differences between various models, the inaccuracies of the nuclear HO wave functions, and an inexact treatment of the muon wave functions cause substantial errors. In a recent calculation by Martorell and the author [139], attempts have been made to minimize the uncertainties of nuclear and muon radial functions, and to estimate the uncertainties due to different nuclear configuration mixings allowed in reliable models. In this calculation, single-particle wave functions given by Hartree–Fock (H–F) calculations with density-dependent forces [172] have been used to determine the Fourier–Bessel transforms

$$A_l(q) = \int_0^\infty \phi_f(r) \mathcal{O}_L(j_l(qr)G(r)) \mathcal{O}_H \phi_i(r) r^2 dr, \quad (5.23)$$

where ϕ 's are the single-particle nuclear radial functions, \mathcal{O}_L and \mathcal{O}_H are leptonic and hadronic radial operators, j_l and G are neutrino and muon wave functions. The quantities $A_l(q)$ are then used in the configuration mixing calculation to determine the nuclear matrix elements. The same H–F wave functions are able to reproduce the r.m.s. charge radius and the inelastic electron scattering form factor at low momentum transfer. The equivalent HO parameters for the $p_{3/2}$ and $p_{1/2}$ H–F wave functions are found to be different by 10%, explaining the empirical necessity of using two different HO parameters [145] to fit the charge radius and the inelastic form factors.

In the calculation of Martorell and the author, the muon capture rate for the $^{12}\text{C} \rightarrow ^{12}\text{B}_{\text{g.s.}}$ reaction is determined to be*

$$\Lambda = 6.3 \times 10^3 \text{ s}^{-1}, \quad (5.24)$$

within about 10% uncertainty arising from the configuration mixing and hadronic form factor effects. This is within 5 to 10% of the experimental value, providing another important test of the impulse approximation. In the estimate (5.24) realistic muon wave functions have been used, and terms involving the small components of the muon wave function have been retained. It appears that any further improvement of the theoretical accuracy in this case would be very difficult.

Since the rate of the reaction (5.17) is strongly dependent on $g_A(q^2)$, it is perhaps of interest to quote a limit on $g_A(0)$ obtained from our calculation [139] and the present experimental limit on the rate. This is (fig. 5.2) found to be

$$1.21 \leq g_A(0)/g_V(0) \leq 1.30. \quad (5.25)$$

It is important to emphasize that the impulse approximation estimate of the rate is in agreement with the experimental value. This suggests the corrections to the impulse approximation estimates for the rates to be small for allowed transitions in light nuclei.

5.4.4. Other allowed transitions in the 1p-shell nuclei

Below we make some remarks on a few of the allowed transitions in the 1p-shell nuclei in targets other than ^{12}C . Figs. 5.3 illustrate some allowed transitions in ^{10}B and ^{14}N recently studied by the Louvain group.

1) $^6\text{Li}(\mu^-, \nu_\mu)^6\text{He}_{\text{g.s.}}$: This is an almost pure superallowed [133] transition (§ 7) completely dominated by the GT matrix elements which can be determined at $q^2 = 0$ from the inverse β decay.

*This value is obtained in the Cohen–Kurath model (BME) with the SIII Skyrme radial wave functions. The limits in (5.25) are for the Cohen–Kurath models. See [139] for further details.

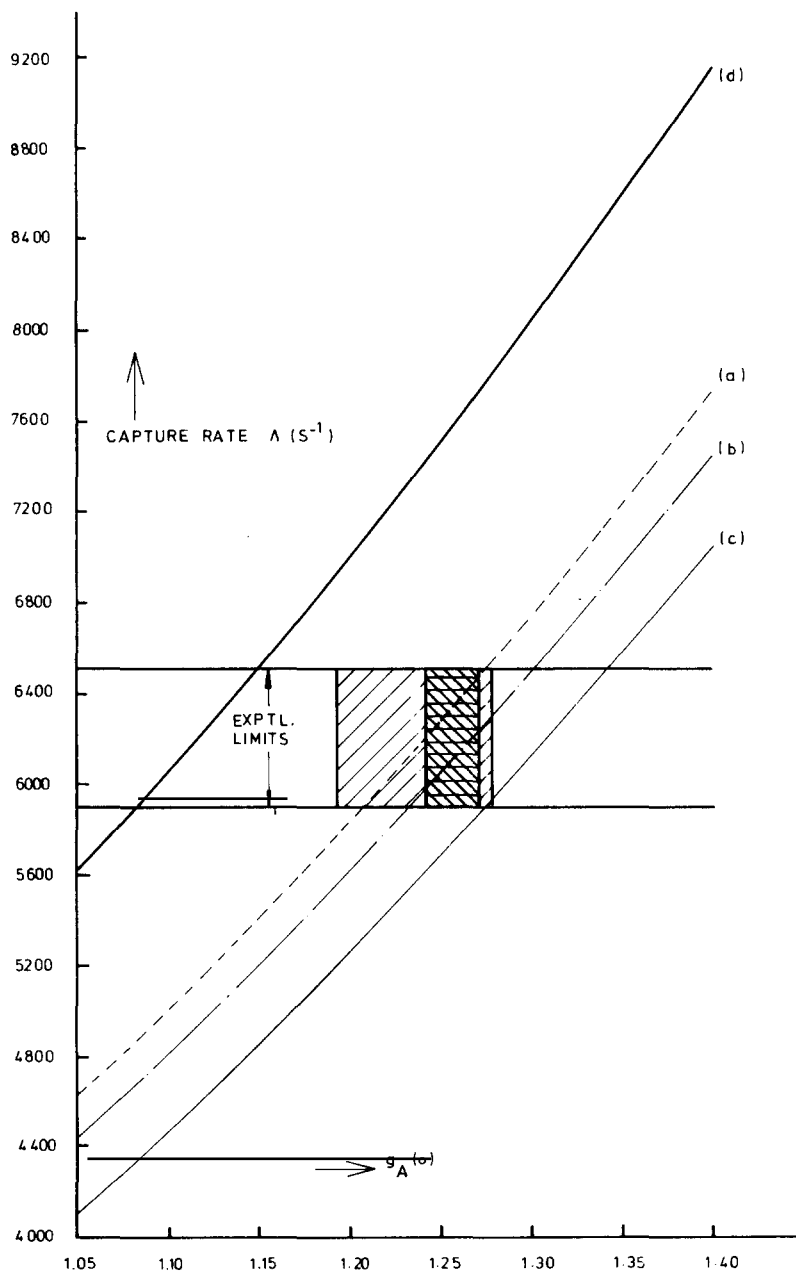


Fig. 5.2. Rate of reaction $^{12}\text{C}(\mu^-, \nu_\mu)^{12}\text{B}_{\text{g.s.}}$ as a function of the axial vector form factor obtained in the impulse approximation estimate using accurate nuclear radial and muon wave functions and nuclear configuration mixings (after Mukhopadhyay and Martorell [139]). The nuclear radial functions are generated by the density-dependent Hartree-Fock approach (model SIII). Theoretical estimates for $g_A(0) = 1.258 \pm 0.015$ are in agreement with the experimental values. Cross-hatched region indicates the limits of $g_A(0)$ from neutron β -decay, while hatched region corresponds to the limits of $g_A(0)$ obtained from muon capture in hydrogen.

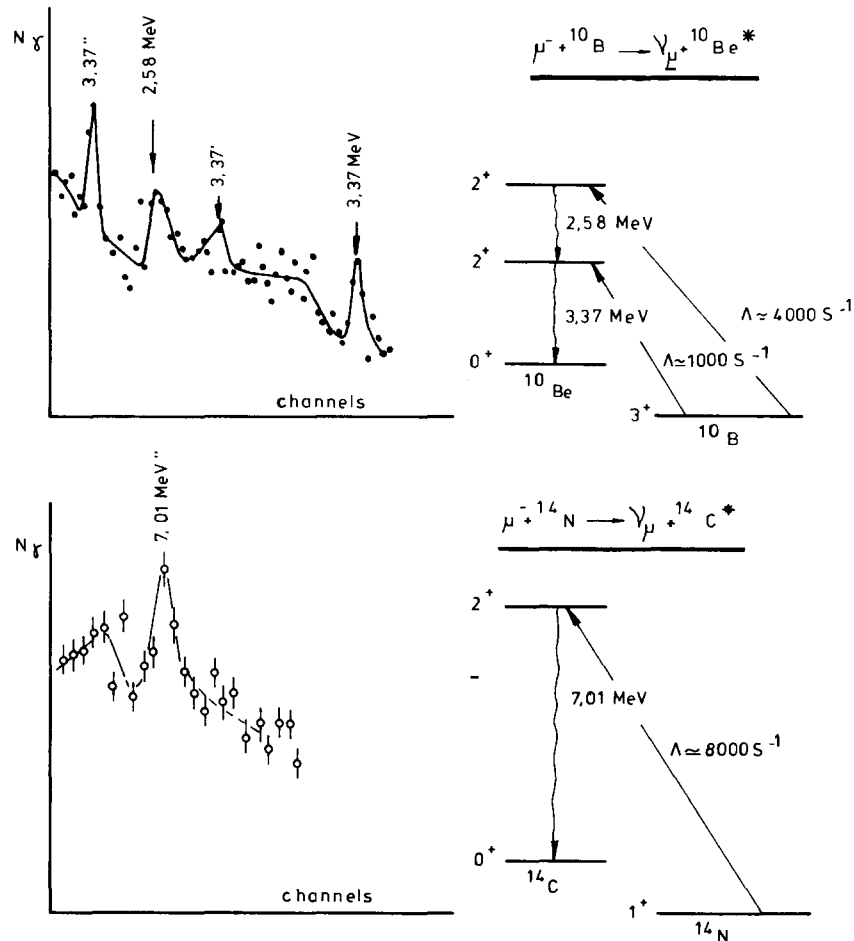


Fig. 5.3. Partial decay schemes of the gamma cascades following muon capture in ${}^{10}\text{B}$ and ${}^{14}\text{N}$, and the experimental delayed gamma spectra, obtained by the CERN–Louvain Collaboration (L. Grenacs, private communications). Experimentally estimated capture rates are also shown. Solid lines in the spectra are guides to the eye.

The experimental rate can be fitted in the harmonic oscillator radial model with an oscillator parameter in the range $1.55 \text{ fm} \leq b \leq 1.92 \text{ fm}$, the upper limit of b being about 5% lower than the value obtained from the inelastic M1 scattering [146, 173]. The radiative pion capture experiments are not yet definitive because of the complication from the 2P capture [166]. Published experimental results on the charged pion photoproduction reaction [174] have yielded a value of b much higher than the range of b in muon capture [175], but currently this discrepancy is suspected to be experimental in origin [176]. An accurate determination of the muon capture rate is desirable to see if the inelastic electron scattering and muon capture experiments are compatible*. While muon capture excites the ${}^6\text{He}_{\text{g.s.}}$, which is 964 keV below the particle emission threshold, the analogue state in ${}^6\text{Li}$, excited by the (e, e') reaction, is only 136 keV lower. This Coulomb energy difference may play a role in distinguishing the (e, e') process from the weak one in ${}^6\text{Li}$.

*The estimated muon capture rate, using the inelastic electron scattering data, ranges from 1187 to 1329 s^{-1} (see Cammarata and Donnelly [146]).

The “elementary particle” approach gives a value $(1.38 \pm 0.16) \times 10^3 \text{ s}^{-1}$ for the rate, in agreement with the experiment [143] (§9).

2) $^{11}\text{B}(\mu^-, \nu_\mu) ^{11}\text{Be}(1/2^-; 320 \text{ keV})$: From the yield of the 320 keV γ -ray, as a function of time (due to hyperfine conversion), the spin of the ^{11}Be state populated in muon capture was uniquely assigned $\frac{1}{2}$ [31a] (§2). The calculated rate of 924 s^{-1} [141] is in excellent agreement with the experiment.

3) $^{14}\text{N}(\mu^-, \nu_\mu) ^{14}\text{C}(2^+; 7.01 \text{ MeV})$: In a $(1\text{p})^{10}$ shell model, the predicted rate for this reaction is about $\sim 2 \times 10^4 \text{ s}^{-1}$ [134, 140], ignoring any hyperfine conversion. Experimentally measured rate is about half of this value [140], confirming a $\sim 50\%$ admixture of $[(1\text{p})^8(2\text{S}-1\text{d})^2]$ configuration in the excited state of ^{14}C , suggested in the electron scattering experiment [177]. The experimental uncertainty in the rate is too large to allow any further quantitative inference at this stage. This transition should show a strong hyperfine conversion effect on the rate (§5.6).

First analysis of a recent SIN–Milano experiment has yielded an experimental value of this muon capture transition rate to be $(6 \pm 1.5) \times 10^3 \text{ s}^{-1}$ (E. Fiorini, private communications). The experimental accuracy will be substantially improved in the near future.

5.5. Allowed transitions in $A \geq 16$ nuclei

The possibility of exciting isovector M1 analogue transitions in nuclei heavier than $A \geq 16$ via muon capture has been suggested [137], but there is only one experiment to date in which this has been achieved. In the $\gamma-\nu$ correlation experiment [160] 1^+ states in ^{28}Al at 2.2 MeV and 1.37 MeV have been populated by muon capture in ^{28}Si . Theoretical calculations are available with realistic models for fluorine [90] and nickel [179] isotopes, and with crude models for the Fermi transition strengths in heavier nuclei [180]. Inelastic electron scattering experiments indicate fairly strong isovector magnetic dipole excitations in ^{19}F , $^{20,22}\text{Ne}$, $^{24,26}\text{Mg}$, ^{28}Si , ^{32}S , ^{36}Ar , $^{58,60}\text{Ni}$, targets (see table 5.6) [165]. These states should be strongly excited by muon capture and related probes. Experimentally determined [181, 182] fractions of the total muon capture strength for *no neutron emission* are fairly substantial in ^{27}Al , ^{28}Si , ^{51}V , and ^{56}Fe . A large part of these strengths should go via allowed transitions [183]. Clearly a lot of experimental work has to be done in this area.

Table 5.6
Isovector M1 analogs of the allowed muon capture transitions excited in electron scattering (after Fagg [165])

Translation $J_f^{\pi} T_i \rightarrow J_f^{\pi} T_f$	Electron scattering target (excitation energy above ground state in MeV)
$0^+ 0 \rightarrow 1^+ 1$	$^{12}\text{C}(15.11)$, $^{20}\text{Ne}(11.24)$, $^{24}\text{Mg}(9.85, 9.97, 10.70)$, $^{28}\text{Si}(10.48, 10.86, 11.41, 12.27, 12.79)$, $^{32}\text{Si}(8.13, 11.14, 11.62)$, $^{38}\text{Ar}(10.05, 11.25)$, $^{40}\text{Ca}(10.34)$
$0^+ 1 \rightarrow 1^+ 2$	$^{58}\text{Ni}(10.15, 10.55, 10.65, 11.05)$
$0^+ 2 \rightarrow 1^+ 3$	$^{60}\text{Ni}(11.89, 12.31)$
$\frac{1}{2}^- \frac{1}{2} \rightarrow \frac{3}{2}^- \frac{3}{2}$	$^{13}\text{C}(15.11)$
$1^+ 0 \rightarrow 0^+ 1$	$^{6}\text{Li}(3.56)$, $^{14}\text{N}(2.31)$
$1^+ 0 \rightarrow 2^+ 1$	$^{14}\text{N}(9.17, 10.43)$
$\frac{3}{2}^- \frac{1}{2} \rightarrow \frac{1}{2}^- \frac{3}{2}$	$^{11}\text{B}(13.0)$
$\frac{3}{2}^- \frac{1}{2} \rightarrow \frac{3}{2}^- \frac{3}{2}$	$^{9}\text{Be}(14.39)$
$\frac{5}{2}^+ \frac{1}{2} \rightarrow (\frac{3}{2}^+ \text{ or } \frac{5}{2}^+) \frac{3}{2}$	$^{25}\text{Mg}(7.81)$
$3^+ 0 \rightarrow 2^+ 1$	$^{10}\text{B}(7.48)$

5.6. Hyperfine effects in the allowed transitions

So far in this section we have assumed that the hyperfine (HF) states of angular momenta F_{\pm} are populated statistically in targets with spin $I(I \neq 0, F_{\pm} = I \pm \frac{1}{2})$. Hence the observed capture rate Λ has been taken to be an incoherent sum of the HF capture rates Λ_{\pm} [eq. (2.13)]. We have already shown that as a consequence of the V–A theory, there is a very large difference between Λ_{\pm} in hydrogen and deuteron (§§3–4). Here we address ourselves to the question of the magnitudes of Λ_{\pm} and ways of determining them in more complex nuclei, specializing to the allowed transitions.

The difference between hyperfine capture rates Λ_{\pm} in allowed transitions is easily demonstrated in the Fujii–Primakoff approximation (see table 5.2). For example, the ratio of HF capture rates for ${}^6\text{Li} \rightarrow {}^6\text{He}_{\text{g.s.}}$ transition is given in this approximation to be*

$$\Lambda_{-}/\Lambda_{+} = (3G_A/G_P - 1)^2 \approx 33. \quad (5.26)$$

In nuclei with mass number $3 \leq A < 10$, the HF interdoublet transition is negligible and the only way to probe the difference between Λ_{\pm} is to use a *polarized nuclear target*, as suggested by Hambro and the author [29] (§ 2). Thus, making two measurements of the capture rate, with and without nuclear polarization, we can determine $(\Lambda_{+} - \Lambda_{-})$ from the following equation

$$\Lambda - \Lambda^S = \frac{I}{I + 1} (\mathbf{a} \cdot \mathbf{b}) (\Lambda_{+} - \Lambda_{-}), \quad (5.27)$$

where \mathbf{a}, \mathbf{b} are muon and nuclear polarizations, Λ and Λ^S are capture rates for targets with and without initial nuclear polarization, respectively. Notice that it is enough to know the sign of $\mathbf{a} \cdot \mathbf{b}$ in order to ascertain the sign of $(\Lambda_{+} - \Lambda_{-})$, once the values of Λ and Λ^S have been determined. To obtain Λ_{+} and Λ_{-} separately, independent knowledge of \mathbf{a} and \mathbf{b} and measurement of Λ for two values of b are necessary [see eq. (2.14)].

In table 5.7 we demonstrate the effect of nuclear polarization on the muon capture rates of prominent allowed transitions. Rather sizable deviations from statistical rates are possible in polarized ${}^6\text{Li}$ and ${}^{10}\text{B}$ targets.

Table 5.7

Effect of nuclear polarization on the allowed muon capture rate. Muon polarization is taken to be $\frac{1}{6}$ of its original value. Λ^S , Λ^A and Λ^B are respectively statistical rate and the rates obtained with nuclei completely polarized || and anti-|| to the muon polarization, all expressed in units of $10^3/\text{s}$. D^{α} 's are deviations of $\Lambda^{\alpha}(\alpha = A, B)$ from Λ^S , expressed in % (after Hambro and Mukhopadhyay [29]).

Transitions	Λ^S	Λ^A	Λ^B	D^A	D^B
${}^6\text{Li}(1^+) \rightarrow {}^6\text{He}(0^+; \text{g.s.})$	1.27	1.08	1.46	-14.7	+14.7
${}^9\text{Be}(\frac{3}{2}^-) \rightarrow {}^9\text{Li}(\frac{3}{2}^-; \text{g.s.})$	0.074	0.068	0.080	-5.6	+8.8
${}^{10}\text{B}(3^+) \rightarrow {}^{10}\text{Be}(2^+; 3.37)$	1.86	1.66	2.05	-10.8	+10.2
${}^{10}\text{B}(3^+) \rightarrow {}^{10}\text{Be}(2^+; 5.96)$	6.55	5.61	7.48	-14.4	+14.2
${}^{11}\text{B}(\frac{3}{2}^-) \rightarrow {}^{11}\text{Be}(\frac{1}{2}^+; 0.32)$	0.924	0.792	1.06	-14.3	+14.7
${}^{13}\text{C}(\frac{1}{2}^-) \rightarrow {}^{13}\text{B}(\frac{3}{2}^-; \text{g.s.})$	6.81	7.18	6.43	+5.4	-5.4
${}^{14}\text{N}(1^+) \rightarrow {}^{14}\text{C}(2^+; 7.01)$	11.09	11.97	10.22	+7.9	-7.8
${}^{19}\text{F}(\frac{1}{2}^+) \rightarrow {}^{19}\text{O}(\frac{3}{2}^+; 0.09)$	0.782	0.819	0.745	+4.7	-4.7

*Walecka [183a] obtains an accurate estimate of this ratio to be ~ 26 .

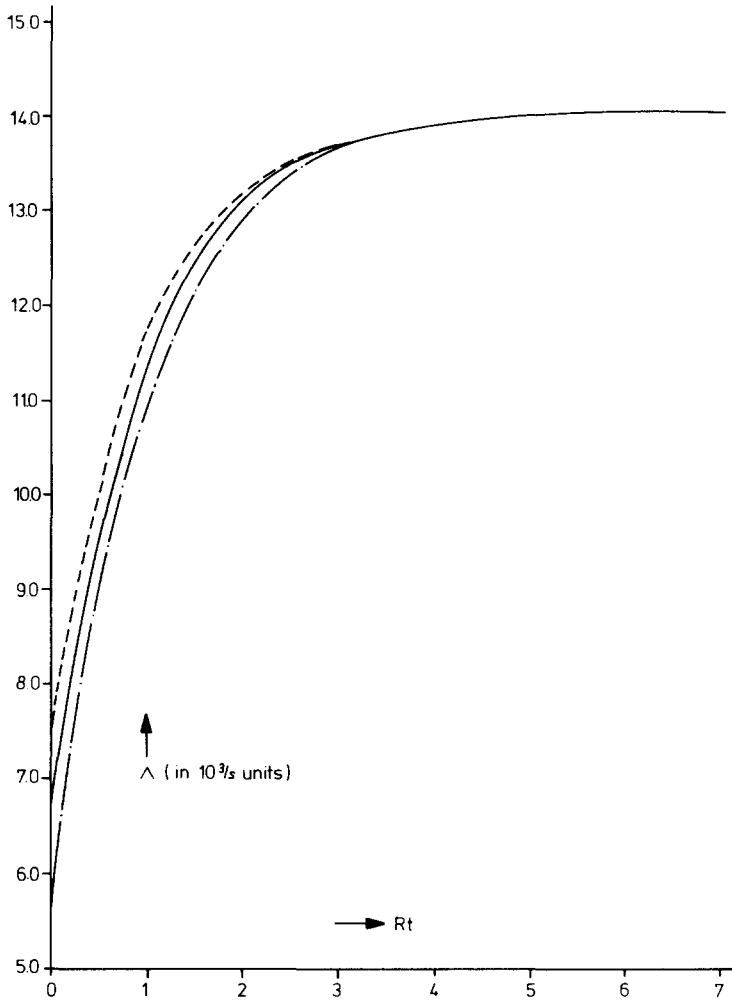


Fig. 5.4. Rate of reaction ${}^{10}\text{B}(\mu^-, \nu_\mu){}^{10}\text{Be}(2^+: 5.96 \text{ MeV})$ as a function of Rt , R being the hyperfine conversion rate, t the time reckoning from the instant of muon's entry in $1S$ orbit. The solid line represents the absence of muon and/or nuclear polarization (a, b respectively); the dashed line and the dash-dotted line respectively represent $a \cdot b$ equal to $-\frac{1}{8}$ and $\frac{1}{8}$ (after Hambro and Mukhopadhyay [29]).

In light-weight nuclei in the mass range $10 \leq A \leq 19$, it is possible to study Λ_+ and Λ_- with the help of the HF interdoublet transitions which occur with a rate comparable to the muon disappearance rate. The interdoublet transitions deplete the HF state lying energetically higher, and enrich the lower one, and a time-dependence of the capture rate (fig. 5.4) and other observables results. Deutsch et al. [31a] have used this method to determine the ratio Λ_+/Λ_- for the ${}^{11}\text{B} \rightarrow {}^{11}\text{Be}(1/2^-: 320 \text{ keV})$ transition, and have obtained the result [374]

$$\Lambda_+/\Lambda_- \leq 0.07. \quad (5.28)$$

Theoretical estimate of Bernabéu [141] for the ratio Λ_+/Λ_- is 0.06, for $g_P/g_A = 8$, and ~ 0.11 , for $g_P/g_A = 12$; these numbers do not substantially change by a variation of the oscillator parameter b

from 1.5 to 1.6 fm, for a given value of g_P/g_A . Fujii–Primakoff approximation gives only about half of the “exact” estimate for Λ_+/Λ_- .

In nuclei with mass number $A > 19$, the capture is always from the energetically lower HF state. No precise theoretical estimates are available for $(\Lambda_+ - \Lambda_-)$ in these nuclei.

5.7. Polarization and asymmetry of the recoiling nuclei

Polarization of the recoil nucleus produced in a muon capture reaction and its asymmetry with respect to the muon polarization axis are two important manifestations of the parity violation in the four-fermion weak interaction [18]. We have already introduced these quantities in section 4. Here we make some further remarks on these observables in the reaction $^{12}\text{C}(\mu^-, \nu_\mu)^{12}\text{B}_{\text{g.s.}}$ for which experimental results are available [168].

In the Fujii–Primakoff approximation, we can derive the following expressions for the recoil asymmetry α and the longitudinal polarization P_L of $^{12}\text{B}_{\text{g.s.}}$ [95]:

$$\alpha = -\frac{G_A^2 - G_P^2 + 2G_A G_P}{3G_A^2 + G_P^2 - 2G_A G_P}, \quad P_L = \frac{-2G_A^2}{3G_A^2 + G_P^2 - 2G_A G_P}, \quad (5.29)$$

yielding the relation $\alpha - 2P_L = 1$ obtained earlier (§4) on general grounds. To a good approximation α and P_L are insensitive to nuclear matrix elements (a result supported by accurate calculations [95] *without* invoking the FPA), and are sensitive to the ratio G_P/G_A . In particular, in the limit $G_P/G_A \rightarrow 0$, $\alpha \rightarrow -\frac{1}{3}$ and $P_L \rightarrow -\frac{2}{3}$. Thus, a measurement of α or P_L constitutes a direct test of the possible presence of the induced form factors in the muon capture. In addition, the test of the relation $\alpha = 1 + 2P_L$ constitutes the test of rotational invariance, neutrino helicity (section 4) and, at the very least, consistency of measurements.

The Louvain–Saclay group have recently measured the average polarization P_{av} in the $^{12}\text{C} \rightarrow ^{12}\text{B}_{\text{g.s.}}$ reaction, obtaining [168] (figs. 5.5)

$$P_{\text{av}}/P_\mu = 0.48^{+0.08}_{-0.10}. \quad (5.30)$$

Using this in Bernabéu’s derived relation between P_{av}/P_μ and P_L [eq. (4.12)], we obtain P_L to be ~ -0.97 or -0.24 . These respectively yield α equal to -0.94 or 0.52 . None of these corresponds to the values obtained in the limit of absence of induced form factors.

In fig. 5.6 we plot as a function of g_P/g_A , the average polarization calculated in the impulse approximation using realistic [163] and jj coupling models. *While the capture rate changes by a factor of five from one model to the other, the average polarization practically remains the same**. The latter is also insensitive to the variations of $g_A(0)$ from 1.23 to 1.26. The Louvain–Saclay results yield the following limits on ratio of g_P/g_A [184]**:

$$g_P/g_A = 10^{-5.5}_{+4.5} \text{ (a)}, \quad 12.5^{-6.5}_{+4.0} \text{ (b)} \quad (5.31)$$

where (a) and (b) refer to the realistic and jj coupling model calculations. This is the best available test of the validity of the PCAC estimate for g_P from the muon capture experiments in complex nuclei.

*This important result is due to Devanathan and collaborators [150].

**Bernabéu (private communications, April 1976) obtains $g_P/g_A = 7.5 \pm 7$. He also discusses further modifications of this experiment to test time-reversal invariance [B1'].

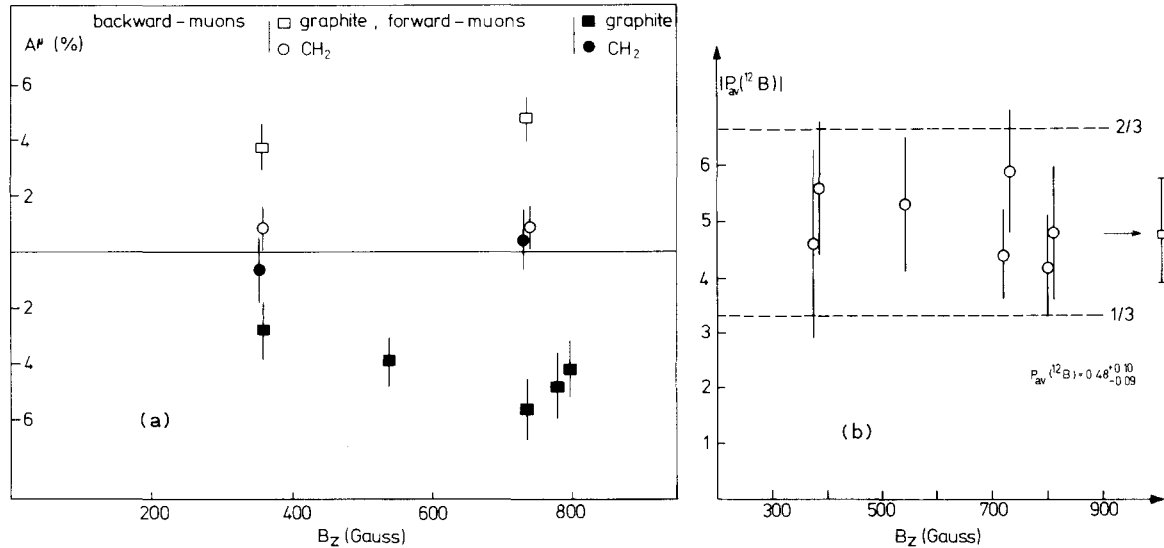


Fig. 5.5. (a) Beta decay asymmetry A^μ of the ^{12}B nuclei (produced by the muon capture in ^{12}C) as a function of the magnetic field B_Z in the direction of the muon beam, measured in graphite and CH_2 . (b) Average polarization of ^{12}B as a function of B_Z (from Possoz et al. [168] and L. Grenacs, private communications).

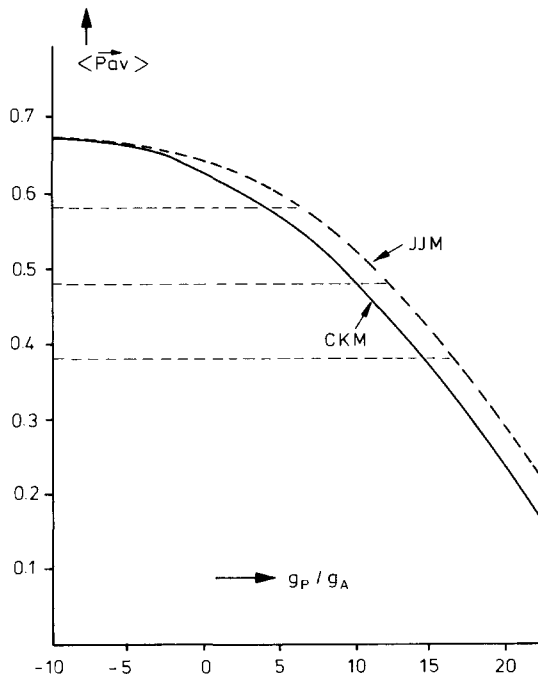


Fig. 5.6. The average polarization $\langle P_{av} \rangle$ of the recoiling ^{12}B nucleus as a function of the pseudoscalar form factor g_P (through the ratio g_P/g_A). Notice the relative insensitivity of this observable to the nuclear models. JJM and CKM are respectively the jj coupling model and the Cohen-Kurath model (from Parthasarathy [private communications]). Horizontal lines represent the measured value of $\langle P_{av} \rangle$.

5.8. Gamma-neutrino correlation

The gamma-neutrino angular distributions in a sequence of reactions

$$\mu^- + (A, Z) \rightarrow (A^*, Z - 1) + \nu_\mu, \quad (5.32a)$$

$$\downarrow (A^{**}, Z - 1) + \gamma, \quad (5.32b)$$

where the daughter nucleus A^* produced in the muon capture reaction decays to another level A^{**} by emitting a photon, has been studied theoretically by Popov, Bukhvostov, Oziewicz and collaborators [185–187] with the primary objective of determining the pseudoscalar form factor $g_p(q^2)$. Experimental possibilities, utilizing the Doppler shift of the emitted photon energy due to the recoil nucleus, were discussed by Grenacs et al. [188]. Only recently such an experiment has been carried out by the William and Mary group [160] in ^{28}Si .

5.8.1. The correlation function

Let us indicate the reaction sequence (5.32) as $J_i \xrightarrow{\mu^-} J_I \xrightarrow{\gamma} J_f$, where J 's indicate the spins of the appropriate nuclear states. From the independent scalars and pseudoscalars constructed out of the available three vector quantities, viz. muon polarization P_μ , neutrino momentum q and photon momentum K , we can write down the $\gamma-\nu$ correlation function W for allowed transitions [185]:

$$\begin{aligned} W = 1 &+ (a_1 + a_2 K^2) \langle P_\mu \rangle \hat{P}_\mu \cdot q + b P_2(K \cdot q) \\ &+ c \langle P_\mu \rangle K \cdot \hat{P}_\mu (K \cdot q) \\ &+ d \langle P_\mu \rangle [(K \cdot q) \cdot \hat{P}_\mu] (K \cdot q), \end{aligned} \quad (5.33)$$

$\langle P_\mu \rangle$ being the degree of longitudinal polarization of muon at the instant of entry to the 1S orbit. The quantities a_i , b , c , d involve nuclear matrix elements and weak coupling constants. *The constraint of T invariance requires the coefficient d to vanish.*

5.8.2. Measurement of the correlation function

The observed energy E of the photon is related to the energy E_0 in the emitting nucleus by the Doppler equation

$$E = E_0(1 - v \cos \theta), \quad (5.34)$$

where v is the velocity of the recoiling nucleus, θ is the angle between the vectors q and k . Equation (5.34) presupposes the emission of photon *before* any significant nuclear recoil, a condition fulfilled in gaseous sources and in some solids [188]. If $N(E)dE$ is the number of photons emitted in the energy interval E and $E + dE$, then

$$N(E) = \sum_i a_i P_i(\cos \theta) \sim W(\theta), \quad (5.35)$$

W being the correlation function.

The William and Mary group have measured the $\gamma-\nu$ correlation functions for the cascades $^{28}\text{Si}(0^+) \xrightarrow{\mu^-} {}^{28}\text{Al}(1^+: 2.2 \text{ MeV}) \xrightarrow{\gamma} {}^{28}\text{Al}(2^+: 31 \text{ keV}), {}^{28}\text{Al}(0^+: 973 \text{ keV})$,

and

$${}^{28}\text{Si}(0^+) \xrightarrow{\mu^-} {}^{28}\text{Al}(1^+: 1.373 \text{ MeV}) \xrightarrow{\gamma} {}^{28}\text{Al}(2^+: 31 \text{ keV}).$$

Table 5.8

Gamma-neutrino correlation coefficients A , B , C (defined in the text) experimentally determined by Miller et al. [160] in $^{28}\text{Si} \xrightarrow{\mu^-} {}^{28}\text{Al}^* \xrightarrow{\gamma} {}^{28}\text{Al}^{**}$ transitions. Below only the gamma sequence is labelled; energies in brackets are in MeV, above the ${}^{28}\text{Al}$ ground state.

	$1^+(2.202) \xrightarrow{\gamma} 2^+(0.031)$	$1^+(2.202) \xrightarrow{\gamma} 0^+(0.973)$	$1^+(1.373) \xrightarrow{\gamma} 2^+(0.031)$
A	-0.37 ± 0.10	0.15 ± 0.25	-0.29 ± 0.15
B	0.54 ± 0.10	1.12 ± 0.10	0.65 ± 0.20
C	0.09 ± 0.01	0.02 ± 0.03	0.06 ± 0.01

The measured correlation coefficients [160] are shown in table 5.8, the coefficients A , B , C being defined as follows:

$$W(\theta) = 1 + AP_2(K \cdot q) + (K \cdot P_\mu)(K \cdot q)[B + CP_2(K \cdot q)]. \quad (5.36)$$

With arguments similar to those of Bernabéu relating α and P_L (rotational invariance, fixed neutrino helicity, T invariance), Oziewicz [187] has shown that the following bounds can be derived in a model-independent fashion for the correlation coefficients A , B , C relevant to the cascade $0 \xrightarrow{\mu^-} 1 \xrightarrow{\gamma} 0$:*

$$-1 \leq A \leq 0.5, \quad |B + C| \leq 1.5,$$

$$[(1 - 2A)^{1/2} - (1 + A)^{1/2}]^2 \leq 3 |C| \leq [(1 - 2A)^{1/2} + (1 + A)^{1/2}]^2. \quad (5.37)$$

The measured values of A , B , C for the cascade $0^+ \xrightarrow{\mu^-} 1^+ \xrightarrow{\gamma} 0^+$ are seen to satisfy these bounds.

Ciechanowicz [186] has calculated the coefficients A , B , and C , using the nuclear wave functions of Wildenthal et al. [189] for the $A = 28$ system, and realistic muon wave functions. With the PCAC estimate of the ratio g_P/g_A , he obtains A , B , and C to be 0.4, 0.53, and 0.88, respectively, in disagreement with the experimental values. The experimental values of these coefficients for the cascade $0^+ \xrightarrow{\mu^-} 1^+ \xrightarrow{\gamma} 2^+$ also disagree with the theoretical estimates [186], and in addition, seem to violate bounds obtained on general grounds [187].

Before we take these discrepancies seriously, the following points remain to be considered. First, the sensitivity of A , B , and C coefficients to the nuclear physics uncertainties remains to be determined. How much are discrepancies due to the inadequacies of the $A = 28$ nuclear wave functions is not known. Second, the alleged violation of general bounds by the coefficients A , B , and C seems to indicate that the assumption of pure M1 multipolarity for the $1^+ \xrightarrow{\gamma} 2^+$ transition, made in extracting the coefficients, may not be correct. Indeed, other experiments suggest that the M1/E2 mixing parameter in the transition $1^+(1.37 \text{ MeV}) \xrightarrow{\gamma} 2^+(0.031 \text{ MeV})$ in ${}^{28}\text{Al}$ can be as high as 0.35 ± 0.10 [190]. Thus, an independent determination of the mixing parameters in the $1^+ \xrightarrow{\gamma} 2^+$ transitions and a refit of the coefficients A , B , and C are in order. More measurements are clearly desirable to improve on the first experiment of Miller et al. [160].

An experiment looking for the Doppler broadening of the 7.01 MeV γ -line, emitted following the muon capture in ${}^{14}\text{N}$ to the ${}^{14}\text{C}$ ($2^+: 7.01 \text{ MeV}$) state, is in progress at SIN [178]. A Doppler shift of $\sim 100 \text{ keV}$ has been observed in this experiment.

We close this section by noting again that the experimental rates agree or come within about 10% of the impulse approximation predictions in two cases where the nuclear physics uncertainties are

*Bernabéu [B1'] obtains the following general relations: $A = -1 - \frac{3}{2}P_L$, $B = 1 + \frac{3}{2}P_L - \frac{3}{2}P$, $C = -1 + \frac{3}{2}P$, where P_L and P are quantities in the notations of §4.5.

minimal (viz. in ${}^3\text{He}$ and ${}^{12}\text{C}$); also, the residual polarization experiments in ${}^{12}\text{C}$, results of which can be predicted in the impulse approximation, with much less sensitivity to the nuclear physics inputs, are in accord with the theoretical estimates using canonical form factors.

6. First- and higher-forbidden transitions, total capture rates

6.1. First-forbidden transitions: Objective of study

These transitions, obeying the selection rules $|\Delta J| = 0, 1, 2$, $\Delta\pi = -1$, are responsible for more than 50% of the total muon capture strength in light and medium-heavy nuclei, with $A < 100$. These include the analogue excitations of the giant dipole resonance (GDR), also an important feature of the photonuclear reaction.

One of the important objectives of studying these transitions, from nuclear physics point of view, is to learn about isospin splitting of the GDR in non-zero isospin targets. For these nuclei, Fallieros et al. [21] have predicted splitting* of the GDR into two isospin components $T_< \equiv T_0$ and $T_0 + 1$, T_0 being the isospin of the target ground state. While the $T_<$ component can be studied by electron scattering or photoreactions, muon capture provides a valuable tool to probe the $T_>$ component, in particular, in nuclei with large neutron excess, where the $T_>$ excitation is strongly suppressed in the electro- and photoreactions. In nuclei with zero isospin, the photoreactions and muon capture cross-sections for the GDR excitation can be related to each other via the Foldy–Walecka sum rules [20]. These sum rules have been extended to other nuclei as well.

In some targets, the first-forbidden transitions populate daughter states that are stable against nucleon emission. In ${}^{16}\text{O}$, for example, these processes give valuable information on the particle–hole excitations of the ground state. In some instances, the reaction rates depend on specific weak form factors in an overwhelming way, giving quantitative information on them. Unfortunately, the nuclear physics inputs are often too uncertain to yield reliable estimates of the weak form factors.

In heavy nuclei, the contributions of the first-forbidden transitions decline in relative importance. This phenomenon is itself a subject of interest in nuclear physics.

Finally, in light nuclei the nuclear supermultiplet symmetry provides an important theoretical framework to understand the nature of these transitions (section 7).

The muon capture cross-sections for the first-forbidden transitions can be obtained from the general expressions given in Appendix 2. Unless stated otherwise, relevant hyperfine effects are neglected below. Nucleon emissions following excitations of the GDR and other particle-unbound states are discussed in section 8.

6.1.1. Excitation of the bound states

Experimental capture cross-sections for the first-forbidden transitions populating specific bound states of the daughter nuclei are very few: they are available in ${}^{11}\text{B}$, ${}^{12}\text{C}$, and ${}^{16}\text{O}$ targets (table 6.1), generally with very poor accuracy. In a variety of nuclei from Al to Pb, a fraction of about 10% of the total capture strength is seen in radiochemical assays [182] to populate bound states, but no detailed spectroscopic studies of this strength are available.

As examples of the first-forbidden transitions to bound states, we take the following reactions in

*See also ref. [212], and Bohr–Mottelson [A6], Vol. II, pp. 497 ff.

Table 6.1

Experimentally obtained rates for the first and higher forbidden transitions to the *bound states* of the daughter nuclei. Excitation energy of the daughter states are in MeV, for states other than ground state (g.s.).

Transition	Experimental rate (10^3 s^{-1})
$^{11}\text{B}(J^\pi T = \frac{3}{2}^+ - \frac{1}{2}) \rightarrow ^{11}\text{Be}(\frac{1}{2}^+ + \frac{3}{2}^-; \text{g.s.})$	$0.01 + 0.13$ $- 0.10$ [31a]
$^{12}\text{C}(0^+ 0) \rightarrow ^{12}\text{B}(2^- 1: 1.67)$	≤ 0.24 [159] 0.37 ± 0.57 [373]
$^{12}\text{C}(0^+ 0) \rightarrow ^{12}\text{B}(1^- 1: 2.62)$	0.72 ± 0.17 [159] 0.73 ± 0.47 [373]
$^{12}\text{C}(0^+ 0) \rightarrow ^{12}\text{B}(2^+ 1: 0.953)$	0.21 ± 0.39 [373]
$^{16}\text{O}(0^+ 0) \rightarrow ^{16}\text{N}(0^- 1: 0.121)$	1.60 ± 0.20 [198] 1.10 ± 0.20 [199] $0.85 + 0.15$ $- 0.06$ [201] 1.56 ± 0.11 [202]
$^{16}\text{O}(0^+ 0) \rightarrow ^{16}\text{N}(1^- 1: 0.397)$	1.40 ± 0.20 [198] 1.88 ± 0.10 [199] $1.85 + 0.36$ $- 0.17$ [201] 1.31 ± 0.11 [202] 1.71 ± 0.15 [379]
$^{16}\text{O}(0^+ 0) \rightarrow ^{16}\text{N}(2^- 1: \text{g.s.})$	6.3 ± 0.7 [199] 8.2 ± 0.7 [200] 8.0 ± 1.2 [202]
$^{16}\text{O}(0^+ 0) \rightarrow ^{16}\text{N}(3^- 1: 0.297)$	0.13 ± 0.08 [379] < 0.09 [202]

the ^{16}O target

$$^{16}\text{O} + \mu^- \rightarrow ^{16}\text{N}(0^-, 1^-, 2^-, T = 1: \text{bound states}) + \nu_\mu; \quad (6.1)$$

these have been studied extensively both theoretically [79, 86, 145, 191–197] and experimentally [198–202], and have been frequently reviewed [B1, B2, B24]. In table 6.1, experimentally obtained values of the capture rates are given, while table 6.2 displays a representative sampling of their theoretical estimates in a variety of models.

The following points summarize the roles of hadronic weak form factors in these reactions:

- (i) The $0^+ \rightarrow 0^-$ transition is independent of the vector form factors and depends strongly on the ratio g_P/g_A [191, 192]. It is also sensitive to a non-zero tensor form factor.
- (ii) The transition $0^+ \rightarrow 1^-$ is independent of g_P , and can give a test of the CVC, through a determination of g_M , the weak magnetism term.
- (iii) The transition $0^+ \rightarrow 2^-$ depends on all the form factors. Besides the muon capture experiments, the β -decay rates of the 2^- and 0^- states [203, 204], the electron scattering form factors of the analog $1^-, 2^-$ states [205–207], the pion photoproduction and radiative pion capture rates [176, 166] are also available experimentally. These quantities are all valuable for testing independently the reliability of the nuclear physics inputs.

Table 6.2

A representative sampling of theoretical estimates for the rates of exciting particle-stable $0^-, 1^-, 2^-, 3^- T = 1$ states in ${}^{16}\text{N}$, by muon capture in ${}^{16}\text{O}$. These estimates have *not* been adjusted for the largest values of the weak hadron form factors.

Authors	Model	Rates in units of 10^3 s^{-1} for exciting $T = 1$ states in ${}^{16}\text{N}$ with J^π			
		0^-	1^-	2^-	3^-
Gillet and Jenkins [86]	Independent particle model	2.19	4.69	25.0	0.187
	Elliot–Flowers wave functions	2.66	4.25	19.8	0.163
	RPA	1.76	2.36	14.1	0.18
Green and Rho [194]	2p–2h correlations in the ground state	1.06	3.18	10.4	0.17
Rho [193]	Migdal wave-functions	1.01	2.16	6.36	0.121
Donnelly and Walecka [195]	TDA wave-functions modified to fit the electron scattering form factors	0.86	1.42	7.54	0.06
Nalcioğlu, Goswami and Graves [196]	Coexistence of spherical and deformed shapes in the ground state	0.94	5.28	4.23	0.29
Rej [197]	0p–0h, 2p–2h and 4p–4h in the ground state and up to 3p–3h in the daughter	1.3	2.1	10.9	—

A look at table 6.2 immediately tells us that, while some theoretical estimates qualitatively agree rather well with the experiment, nuclear physics uncertainties are still too large to yield any reliable quantitative limits on the weak form factors of our interest. The calculations of Rho [193], using the Migdal interaction*, and those of Donnelly and Walecka [195], based on the wave functions obtained by fitting the electron scattering form factors, agree with, or come quite close to the experiment, using canonical values of the weak form factors (for the 0^- transition, the experimental rate is itself uncertain). Unfortunately, these agreements are not definitive. The Migdal wave functions, when used to calculate the photoproduction cross-sections, yield cross-sections which are 40% too low [209], compared to experimental values. Using the electron scattering data to predict the momentum-transfer dependence of the axial vector form factor in the present case has uncertain reliability; in particular, for the $0^+ \rightarrow 0^-$ transition, there is no electron scattering analogue. An indication of the theoretical uncertainty in the Donnelly–Walecka calculation is reflected in the estimate of the β decay rate for the 2^- state of ${}^{16}\text{N}$, which lies in the range of 1.92 to $2.29 \times 10^{-2} \text{ s}^{-1}$, while the experimental value is $(2.53 \pm 0.20) \times 10^{-2} \text{ s}^{-1}$ [203]. The range of values obtained for muon capture rate to the 2^- state is 6.65 to $7.54 \times 10^3 \text{ s}^{-1}$. There is also a change of rate by about 20% in going from the harmonic-oscillator to the Woods–Saxon radial wave functions in the $0^+ \rightarrow 0^-$ transition.

Palfy et al. [204] have recently measured the rate of the β -transition ${}^{16}\text{N}^m(0^-) \xrightarrow{\beta} {}^{16}\text{O}_{\text{g.s.}}$, obtaining a value $0.43 \pm 0.10 \text{ s}^{-1}$. Writing the ${}^{16}\text{N}(0^-)$ wave function in the form

$$|0^-\rangle = (1 - x^2)^{1/2} |1p_{1/2}^{-1} 2s_{1/2}\rangle + x |1p_{3/2}^{-1} 1d_{3/2}\rangle, \quad (6.2)$$

*An unsettled question in the Migdal approaches [138, 183, 193] is the possible variation of Migdal parameters with momentum transfer.

they get $x = -0.07 \pm 0.12$, by using the β decay rate as a constraint to determine x . The muon capture rate can now be written in terms of this parameter x , and the pseudoscalar form factor g_P . This yields the following limit on $g_P(q^2)$:

$$(a) \quad g_P(q^2) = 15 \pm 2, \quad (b) \quad g_P(q^2) = 19.0 \pm 1.5, \quad (6.3)$$

where (a) and (b) refer to the muon capture rate in refs. [198] and [201], respectively. The limits (6.3) are clearly inconsistent with the PCAC estimates for $g_P(q^2)$, but should not be taken too seriously due to nuclear uncertainties.

Two main difficulties in the nuclear physics inputs must be emphasized here: (i) the uncertainty in the configurations of ^{16}O ground state and the ^{16}N states; (ii) the inadequacy of the harmonic oscillator model to describe the radial behaviours of the relevant single-particle functions, particularly for the $1\text{d}_{3/2}$ and $2\text{s}_{1/2}$ states, the first one being unbound and the second one barely bound.

In summary, we can only reiterate the remarks made by Lee and Wu [B16] *more than ten years ago* on this subject:

“It is rather difficult to say anything conclusive on the pseudoscalar coupling based on present experimental results on partial muon capture rates in ^{16}O . The uncertainties in the admixture amplitudes of the nuclear wave functions are (to be) blamed for the inconclusiveness of this investigation. Further clarification of the situation seems to require an extensive programme on the nuclear physics side.”

6.1.2. Self-conjugate nuclei: the Foldy–Welecka sum rule*

Foldy and Welecka (FW) [20] derived, for self-conjugate ($N = Z$) nuclei with scalar ($J = 0$) ground states, a set of elegant sum rules that allow us to calculate the GDR excitation strength induced by muon capture, starting from the experimental cross-sections of the photonuclear reactions. FW assume the effective momentum of the outgoing neutrino to be fixed at the value corresponding to the GDR excitation and neglect all the nucleon velocity terms [of $\mathcal{O}(p/M)$ and higher].

We can define the nuclear matrix elements in the following way:

$$|M_\alpha|^2 = \sum_a \sum_b \left(\frac{\nu_{ab}}{\nu_\mu} \right)^2 \int \frac{d\nu}{4\pi} \left| \left\langle b \left| \sum_{i=1}^A \tau_i^\dagger O_\alpha^{(i)} \exp(-i\nu_{ab} \cdot x_i) \right| a \right\rangle \right|^2, \quad (6.4)$$

where α can be V, A or P, with $O_\alpha^{(i)}$'s given by

$$O_V^{(i)} = 1, \quad O_A^{(i)} = \sigma_i / \sqrt{3}, \quad O_P^{(i)} = \sigma_i \cdot \hat{\nu}. \quad (6.5)$$

The muon capture transition here proceeds from a nuclear state $|a\rangle$ to a state $|b\rangle$. Then the FW sum rules are

$$|M_V|^2 = |M_A|^2 = |M_P|^2. \quad (6.6)$$

The FW procedure of obtaining the dipole part of the muon capture cross-section from the photoreaction data is as follows: (i) Obtain the “unretarded” vector matrix element $|M_V|_{UD}$ from the photoreaction data, using the equation

$$|M_V|_{UD}^2 = \frac{\omega_m^4}{2\pi^2 \alpha} \int_0^{\omega_m} \frac{\sigma_{T+1}(\omega)}{\omega} \left(\frac{\omega_m - \omega}{\omega_m} \right)^4 d\omega, \quad (6.7)$$

*We discuss the group-theoretical basis of these sum rules and their extensions in § 7. These sum rules were derived *earlier* by Luyten et al. [219] under different assumptions and for different nuclei.

where ω_m is the maximum neutrino energy, $\sigma_{T+1}(\omega)$ is the photoabsorption cross-section for the nuclear transition $T \rightarrow T + 1$, with excitation energy ω , T being equal to zero. Thus, $|M_V|_{UD}^2$ is the long wave-length limit of $|M_V|_D^2$. (ii) Use the Goldhaber–Teller model [210] to relate $|M_V|_{UD}^2$ with $|M_U|_D^2$:

$$|M_V|_D^2 = |M_V|_{UD}^2 [F_{el}(\nu_R)]^2, \quad (6.8)$$

where $F_{el}(\nu_R)$ is the elastic form factor for the momentum ν_R , the neutrino momentum for the excitation of the giant dipole resonance. (iii) Assume the equalities (6.6), and determine the dipole contribution to the nuclear muon capture rate by means of the relation:

$$\Lambda_D = \frac{G^2}{2\pi} |\phi_{1S}|_{av}^2 |M_V|_D^2 [G_V^2 + 2G_A^2 + (G_A - G_P)^2], \quad (6.9)$$

where G is the Fermi coupling constant G_A , G_V , G_P are the Primakoff form factors, $|\phi_{1S}|_{av}^2$ is the average value of the probability of finding the muon in the capturing nucleus.

One can add to Λ_D , contributions due to allowed transitions, if any, and contributions due to higher multipoles, the last quantity being estimated in a microscopic model. The sum is the total capture rate Λ . A comparison of the Λ 's, estimated by the above procedure, and experimental rates appears in table 6.3. The agreement is reasonable, confirming the isobaric analogue character of the GDR excitations in photoreactions and muon capture.

Table 6.3

Total muon capture rates Λ_c in $A = 4n$ nuclei. Theoretical estimates are by Walecka [B36] applying the Foldy–Walecka sum rules for the giant dipole excitation. For ^{12}C , allowed contribution has been added to the theoretical estimate.

Target	Λ_c (theory) (s^{-1})	Λ_c (experiment) (s^{-1})	Authors of the experiment
^4He	278	336 ± 75 364 ± 46	Bizzari et al. [242] Block et al. [243]
^{12}C	0.36×10^5	$(0.37 \pm 0.01) \times 10^5$ $(0.36 \pm 0.01) \times 10^5$ $(0.39 \pm 0.01) \times 10^5$	Reiter et al. [244] Lathrop et al. [245] Eckhouse [243a]
^{16}O	1.07×10^5	$(0.97 \pm 0.03) \times 10^5$ $(0.98 \pm 0.05) \times 10^5$	Eckhouse [243a] Barlow et al. [246]
^{40}Ca	31.8×10^5	$(25.5 \pm 0.5) \times 10^5$	Sens [233]

6.1.3. $N > Z$ nuclei: exploration of the $T >$ component of the giant dipole resonance

In nuclei with $N \neq Z$ the ground state isospin of the target is $T_0 = \frac{1}{2}(N - Z)$, and muon capture populates the daughter states with isospin $T_0 + 1$. The final states are the analogues of the parent states lying higher in excitation energy (fig. 6.1), primarily due to the Coulomb shift. These states differ only in the eigenvalue of the third component T_z of the isospin operator.

It is interesting to consider here a “simple” phenomenon – the “blocking” of the $\Delta T_z = 0$ GDR transition strength, observed in electron scattering and photoreaction, compared to the $\Delta T_z = 1$ GDR excitation via muon capture. This phenomenon has geometrical as well as dynamical origins and it underlines the importance of the muon capture processes in studying the $T >$ component of the GDR in a non-isospin-zero target. We discuss here, following Macfarlane [211], the geometrical aspect of the blocking.

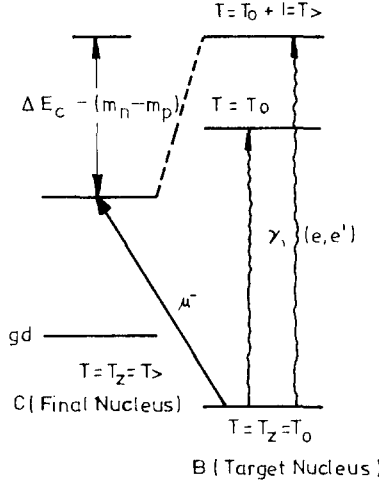


Fig. 6.1. Schematic diagram comparing photoexcitation, inelastic electron scattering and muon capture on $N > Z$ nuclei.

For simplicity, let us consider the excitation by the unretarded dipole operator

$$D_q^1 \sim \sum_i \tau(i) \tau_q^1(i), \quad (6.10)$$

of the target states $|\psi_0\rangle$ with isospin $T_0 = T_{z0} = \frac{1}{2}(N - Z)$. Calling the total “reduced” dipole strength $G_0(T)$, the observed dipole-excitation strength $G(T, q)$ is given by

$$G(T, q) = |\langle T, T_0 + q | D_q^1 | T_0, T_0 \rangle|^2 \equiv |C_{T_0, q}^{T_0, 1} G_0(T)|^2, \quad (6.11)$$

where T is the isospin of the final nuclear state. By applying the Wigner–Eckart theorem, we have extracted the Clebsch–Gordan factor out of the nuclear matrix element in eq. (6.11). Notice that $q = 1$ corresponds to muon capture, and $q = 0$ to the photo- and electro-excitation.

From eq. (6.11) we immediately get

$$G(T_>, 0) = (T_0 + 1)^{-1} G(T_>, 1) = \frac{2}{N - Z + 2} G(T_>, 1). \quad (6.12)$$

This gives the geometrical blocking factor; for ${}^{208}\text{Pb}$, we have

$$G(T_>, 0) = \frac{1}{23} G(T_>, 1). \quad (6.12')$$

Thus, the muon capture process is far superior to probe the $T_>$ component of the GDR compared with photoabsorption of electron scattering.

An example of dramatic suppression of the $T_>$ excitations in photoabsorption, compared with muon capture process, is shown in figs. 6.2. The calculations in the nickel isotopes, used in this figure, are done in the extended RPA approach by Nalcioğlu et al. [179].

6.1.4. Microscopic description of the giant resonance excitations

Many authors have attempted microscopic computations of the GDR excitations rates [B2, B36]. Some of the more recent calculations are in the following targets: ${}^6, {}^7\text{Li}$ [213, 214], ${}^{12}\text{C}$ [166, 214], ${}^{14}\text{N}$ [215], ${}^{15}\text{N}$ and ${}^{32}\text{S}$ [216], ${}^{16}\text{O}$ [217], Ca [218], Ni [179], ${}^{88}\text{Sr}$, ${}^{114}\text{Sn}$, ${}^{140}\text{Ce}$ and ${}^{208}\text{Pb}$

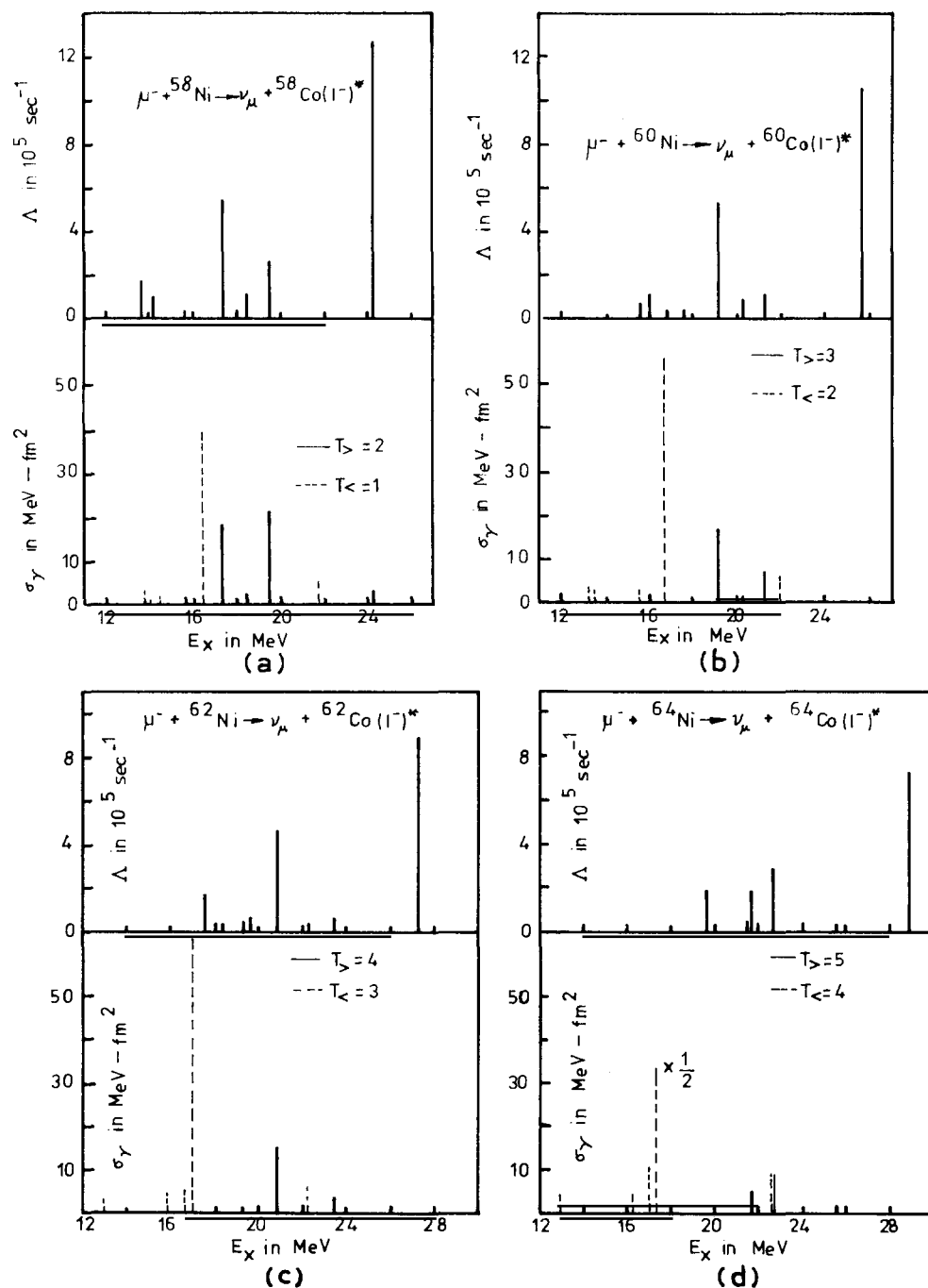


Fig. 6.2. Calculated photoreaction cross-sections σ_γ and partial muon capture rates Λ for the 1^- states in $^{58,60,62,64}\text{Ni}$. Notice the suppression of the $T_{>}$ strengths in photoreaction compared to muon capture (after Nalcioğlu et al. [179]).

[218]. Earlier, extensive applications of the Migdal approach have been made [182–183] with impressive successes in reproducing the experimentally observed total capture rates.

The basic objective of the microscopic models describing giant resonances is to take the nucleon–nucleon correlations properly into account. This results in the mixing of various particle–hole excitations that can be built from a general open-shell description of the target ground state, leading to the so-called configuration splitting of the GDR. Recent extensions of the RPA approach to handle the open-shell ground states have been achieved both via the equations-of-motion approach [179] and the Migdal Green’s function framework [138]. Experiments in Ni isotopes should provide a crucial test of the extended RPA theories.

Simple shell-model descriptions, used extensively by Luyten et al. [219] in the early sixties, have been recently utilized in many $N > Z$ nuclei by Goulard and collaborators [180, 218, 220]. The result is: while they sustain, to a good approximation, the FW relations, these calculations yield values of total capture rates not in agreement with the experiment.

Überall [B34] has cited numerous examples of neutron spectra obtained experimentally [221–222] after muon capture in ^{12}C , ^{16}O , ^{32}S , and ^{40}Ca , comparing them with microscopic expectations in the giant dipole resonance excitation. These spectra have a characteristic evaporation background on top of which giant resonance peaks ride. Typical examples are given in figs. 6.3.

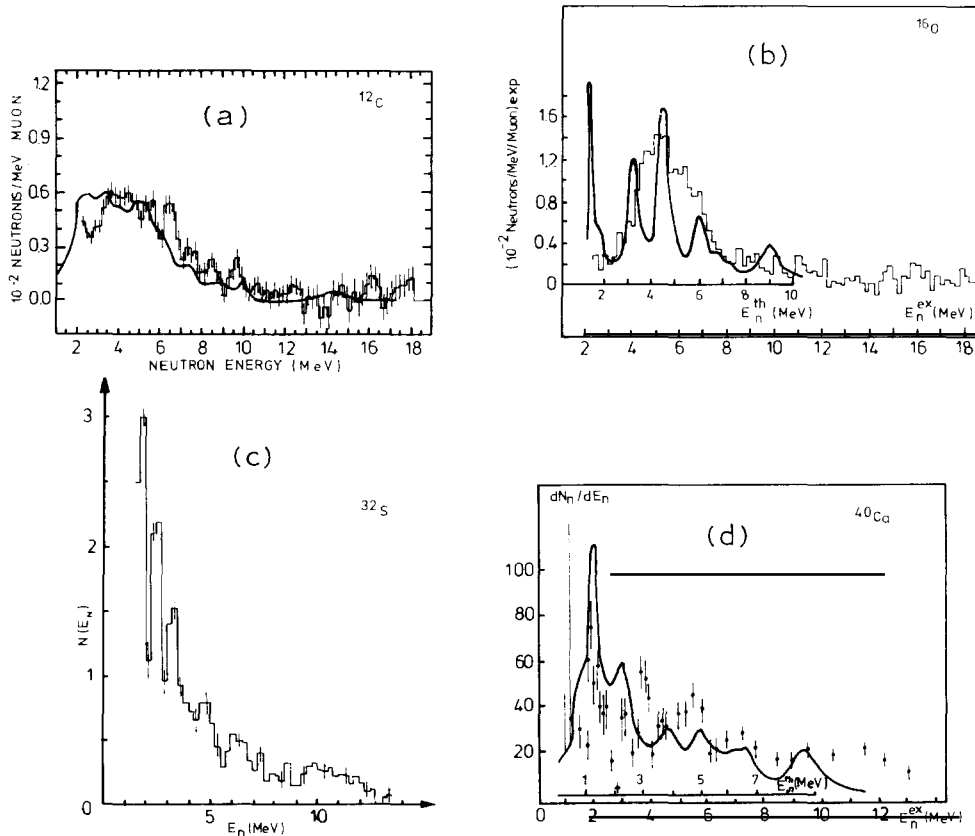


Fig. 6.3. Experimental low energy ($E_n < 20$ MeV) neutron spectra in several light nuclear targets, showing low-lying resonance states. ^{12}C and ^{16}O data are from Plett and Sobottka [222], ^{32}S data are due to Evseev et al. [221], ^{40}Ca data are from Schröder [C17]. Theoretical predictions in ^{12}C , ^{16}O and ^{40}Ca are due to Überall and collaborators [B34].

Reactions of the type

$$\mu^- + (A, Z) \rightarrow (A - 1, Z - 1)^* + n + \nu_\mu, \quad (6.13)$$

where $(A - 1, Z - 1)^*$ are bound states, have been studied with a view of understanding the nature of the possible intermediate states populated in the daughter $(A, Z - 1)^*$. Experiments studying these reactions in ^{16}O , S and ^{40}Ca and heavier elements are now available [223–228]. Theoretical estimates, assuming the mechanism of a GDR doorway, account for the reaction rates at the qualitative level. Thus, the rate of the reaction $^{16}\text{O}(\mu^-, n\nu_\mu) ^{15}\text{N}(\frac{3}{2}^-; 6.32 \text{ MeV})$ is experimentally known to be $(2.50 \pm 0.23) \times 10^4 \text{ s}^{-1}$ [223] and $(2.0 \pm 0.5) \times 10^4 \text{ s}^{-1}$ [159], compared with the theoretical estimates of $\sim 3 \times 10^4 \text{ s}^{-1}$ [229]. Uncertainties associated with the description of the nuclear continuum states make a reliable theoretical estimate difficult to achieve. Recently, Balashov, Eranzhyan [B1], Goulard and collaborators [230] have discussed the reactions (6.13) from a unified perspective of incorporating direct and resonance processes. It would be interesting to make some careful applications of this approach to test its merit.

6.2. Second and higher forbidden transitions

These transitions obey the selection rules

$$|\Delta J| = n, n + 1, \quad \Delta \pi = (-)^n, \quad (6.14)$$

where n is the order of forbiddenness ($n \geq 2$). Not much is known about them either experimentally or theoretically. Two examples of these transitions appear in table 6.1.

Model estimates indicate that the second forbidden transitions play only a minor role in light nuclei around a mass number $A \sim 16$, but in heavier nuclei, they become increasingly important. Thus, in a simple shell-model approach [218], the 2^+ states take an estimated $\sim 15\%$ of the total strength in ^{40}Ca , while this percentage rises to $\sim 50\%$ in ^{208}Pb . The open-shell RPA calculations of Nalcioğlu et al. [179], which reproduce the observed total muon capture rates in nickel isotopes, predict a 14% of the total strength going to the 2^+ states in Ni (table 6.4). No precise experimental information on these transitions is available: the $^{12}\text{B}(2^+, T = 1)$ state has been excited with a very low transition rate (table 6.1), and the $\gamma-\nu$ correlation experiment in ^{28}Si has yielded [160] the spin of the 2.139 MeV state in ^{28}Al to be 2 ($J^\pi = 2^+$).

Table 6.4

Allowed and forbidden transition rates (in units of 10^5 s^{-1}) for the nickel isotopes, as estimated in the open-shell RPA model of Nalcioğlu et al. [179]. Quantities in brackets indicate percentage of the calculated *total* rate. Experimental rates are due to Bobrov et al. [247].

Transition	^{58}Ni	^{60}Ni	^{62}Ni	^{64}Ni
$0^+ \rightarrow 0^+$	1.11 (1.70)	0.99 (1.78)	0.88 (1.89)	0.78 (2.01)
$0^+ \rightarrow 1^+$	11.62 (17.85)	9.52 (17.16)	7.50 (16.07)	5.66 (14.59)
$0^+ \rightarrow 0^-$	5.54 (8.51)	4.90 (8.83)	4.23 (9.06)	3.60 (9.28)
$0^+ \rightarrow 1^-$	25.09 (38.54)	21.66 (39.05)	18.41 (39.44)	15.42 (39.74)
$0^+ \rightarrow 2^-$	11.78 (18.09)	9.98 (17.99)	8.58 (18.38)	7.46 (19.23)
$0^+ \rightarrow 2^+$	8.97 (13.78)	7.62 (13.75)	6.45 (13.81)	5.39 (13.89)
$0^+ \rightarrow 3^-$	1.00 (1.53)	0.80 (1.44)	0.63 (1.35)	0.49 (1.26)
Total rate: calculated	65.11	55.47	46.68	38.80
experiment	61.10 ± 1.05	55.62 ± 0.97	47.16 ± 0.95	—

The third-forbidden transitions are expected to play a marginal role in light nuclei, carrying less than 2% of the estimated total strength in Ni. This may rise to about 6% in Pb. Forbidden transitions of order $n \geq 4$ are entirely negligible (in ^{208}Pb , 4^+ states are estimated to have a strength of 2% of the total [218]).

It would be interesting to study *experimentally* the strength distributions in heavy nuclei to see if there are giant resonances in the second-forbidden multipole excitations. Radiative pion capture experiments in ^{209}Bi indicate a suggestion of an isovector quadrupole resonance [231]. Searches for these resonances by the study of secondary particles (for example, neutrons) are desirable to shed further light on the structure of the unbound analog states. Experiments of Evseev et al. [221] and Plett and Sobottka [222] already give some indication for the resonance structure of the unbound states.

6.3. Total capture rates

The total muon capture rate Λ_c is simply the difference in the reciprocals of the total and decay life times of a muon in the 1S atomic orbit. This is clearly a very complex quantity to interpret for nuclei with mass number greater than three. There has been an impressive accumulation of experimental data for the total rates in a variety of nuclei throughout the periodic table [B10, 183, 228, 232].

The original motivation of studying the total capture rates was to test the idea of the *universal Fermi interaction* (UFI) in the nuclear context [233]. It has, however, now become clear that this objective can be fulfilled only in a very qualitative sense; quantitative tests of the UFI must be made in selected partial transitions and observables, for which nuclear physics uncertainties are not serious.

Total capture rates Λ_c , in the simplest term, obey the Wheeler law [9]

$$\Lambda_c \propto Z_{\text{eff}}^4. \quad (6.15)$$

For low Z , $Z_{\text{eff}} \sim Z$ and Z_{eff} for uranium is ~ 35 [234]. The physics of this proportionality relation is trivial: Λ_c is proportional to the muon probability density for the 1S orbit (which varies as Z^3) and the number of protons in the nucleus. The effect of the finite nuclear charge distribution is absorbed in the Z_{eff} parameter [234].

A quantitative understanding of the total rates can be made in two ways: (i) using realistic microscopic models to determine the partial transition strengths and hence the total strength; (ii) making use of sum rules.

The simplest example of determining the total capture rates by summing various channels is the case of ^3He , where three possible channels, with hadronic final states ^3H , (dn) and (2np), yield the total capture strength. Theoretical estimates [125] of the breakup channels are 414 and 209 s^{-1} , yielding an excellent agreement with the experimental breakup rate of $600 \pm 160 \text{ s}^{-1}$ [375]. The approach of summing allowed, first and higher forbidden contributions, work quite well in nuclei up to mass number 64 [see, for example, the agreement in the case of nickel isotopes (table 6.4)]. Bunyatyan [183] claims agreement in heavier nuclei as well by following the Migdal quasi-particle approach.

The most successful sum rule approach is that of Foldy and Walecka, discussed earlier (§ 6.1.2) and its extensions (§ 7.7). However, the semi-empirical work of Primakoff [18] has been the inspiration for many latter attempts to improve the sum rule approach, which are continuing even now [235–237].

6.3.1. The Primakoff formula

Primakoff, using closure and the assumption of an effective neutrino momentum, derived a semi-empirical formula for the total capture rate Λ_c [18] :

$$\Lambda_c(A, Z) = Z_{\text{eff}}^4 \Lambda(^1 \text{H}) \gamma \left(1 - \frac{\delta(A - Z)}{2A} \right). \quad (6.16)$$

The significance of the parameters in (6.16) are as follows: $\Lambda(^1 \text{H})$ represents the basic weak interaction effects, γ is the change of the phase space in the *nuclear* muon capture compared to that by a nucleon, the term involving δ embodies the effect of the Pauli principle. This formula has been widely criticized on theoretical grounds. In particular, the choice of an effective neutrino momentum becomes problematic for a process in which several regimes of nuclear levels, well-separated in energy, are excited. There is a lot of discussion in the recent literature [214, 235–237] as to what the effective neutrino momentum really means, in the context of a realistic calculation. Taken in a semi-empirical spirit, this formula has yielded a good fit to the over-all trend of the capture rate throughout the periodic table [B10]. Typical parameters obtained in these fits are [233]

$$\delta \sim 3.15, \quad \gamma \Lambda(^1 \text{H}) \sim 188 \text{ s}^{-1}. \quad (6.17)$$

The Primakoff formula predicts a simple relation for the isotope shift of the muon capture rates:

$$\Lambda_c(A, Z)/\Lambda_c(A', Z) \simeq [1 - \delta(A - Z)/2A]/[1 - \delta(A' - Z)/2A']. \quad (6.18)$$

Table 6.5 summarizes the experimental data. Again the agreement between the Primakoff prediction and the experiment is at least qualitatively quite reasonable, particularly in heavier nuclei.

6.3.1.1. Deviations from the Primakoff formula.

It is important to note that, while the Primakoff formula does not have a high absolute accuracy, systematic deviations from it can be interesting. Equation (6.16) clearly breaks down, if the neutron

Table 6.5

Measured isotope effect expressed as a ratio of the total muon capture rates. For comparison, the Primakoff prediction is included, assuming $\delta = 3.14$, and neglecting the variation of Z_{eff} , from one isotope to the other, in a pair (strictly, the variation of Z_{eff} is not negligible, resulting in a $\sim 3\%$ increase of the calculated effect for Eu). Notice that the agreement with the prediction is better in heavier ($A > 40$) nuclei. Experimental references quoted are mostly secondary sources.

Isotope pair	Isotope effect			Isotope pair	Isotope effect		
	Calc.	Measured	Ref.		Calc.	Measured	Ref.
² D/ ¹ H	—	0.69 ± 0.16(a)	[B39]	⁵⁴ Cr/ ⁵² Cr	0.83	0.89 ± 0.02	[183]
⁴ He/ ³ He	—	0.17 ± 0.03	[128, B36]	⁵⁴ Cr/ ⁵³ Cr	0.91	0.93 ± 0.02	[183]
⁷ Li/ ⁶ Li	0.48	0.30 ± 0.19	[B10]	⁶⁰ Ni/ ⁵⁸ Ni	0.87	0.91 ± 0.02	[183]
¹¹ B/ ¹⁰ B	0.67	0.83 ± 0.07	[B10]	⁶² Ni/ ⁵⁸ Ni	0.74	0.77 ± 0.02	[183]
³⁷ Cl/ ³⁵ Cl	0.79	0.69 ± 0.03	[A5]	⁶² Ni/ ⁶⁰ Ni	0.85	0.85 ± 0.02	[183]
⁴⁴ Ca/ ⁴⁰ Ca	0.67	0.71 ± 0.02	[183]	⁸¹ Br/ ⁷⁹ Br	0.86	1.08 ± 0.08	[228]
⁵² Cr/ ⁵⁰ Cr	0.84	0.92 ± 0.02	[183]	¹⁵³ Eu/ ¹⁵¹ Eu	0.95	0.919 ± 0.036	[248]
⁵³ Cr/ ⁵⁰ Cr	0.77	0.86 ± 0.02	[183]	²⁰⁵ Tl/ ²⁰³ Tl	0.89	0.943 ± 0.023	[252]
⁵⁴ Cr/ ⁵⁰ Cr	0.70	0.80 ± 0.02	[183]	²³⁸ U/ ²³⁵ U	0.83	{ 0.88 ± 0.07 0.96 ± 0.05 }	[A5] [250]
⁵³ Cr/ ⁵² Cr	0.91	0.96 ± 0.02	[183]	²⁴² Pu/ ²³⁹ Pu	0.84	0.89 ± 0.08	[250a]

(a)Using experimental values of the capture rates from the *lower* hyperfine state, in absence of experimental statistical rates.

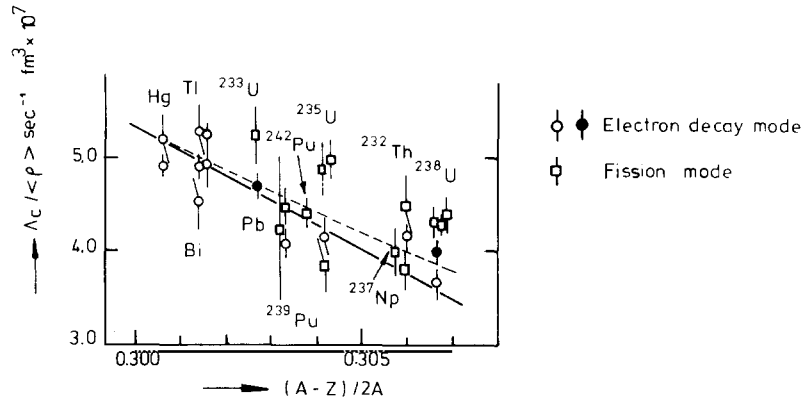


Fig. 6.4. Reduced total muon capture rates $\Lambda_c / \langle \rho \rangle$ for heavy nuclei plotted against $(A - Z)/ZA$, where $\langle \rho \rangle$ is the overlap of muon and nuclear charge densities. Experimental data are obtained by using the $\mu^- \rightarrow e^-$ decay (Sens [C18] and Hashimoto et al. [250]), the fission data lying substantially above. The straight line is the Primakoff plot extrapolated from the fit of the lighter nuclei, the dotted line is the fit to the Goulard–Primakoff formula [eq. (6.19a)].

excess satisfies the condition

$$2A/(A - Z) = \delta, \quad (6.19)$$

implying $Z/A = 1 - 2/\delta \approx 0.36$. For ^{238}U , Z/A is about 0.39; thus higher order Pauli corrections to the Primakoff formula (6.16) would become important in this mass region. Figure 6.4 shows the Primakoff fit to the capture rates in the actinide region; the experimental point seems to indicate a slightly reduced dependence on $(A - Z)/A$ than demanded by the Primakoff formula. This trend is fitted better with a three-parameter formula, obtained recently by Goulard and Primakoff [237]:

$$\Lambda_c \sim \text{kinematic factors} \times Z_{\text{eff}}^4 \times \left\{ 1 + \frac{A}{2Z} \beta_1 - \frac{(A - 2Z)}{2Z} \beta_2 - \left(\frac{A - Z}{2A} + \frac{|A - 2Z|}{8ZA} \right) \beta_3 \right\}. \quad (6.19a)$$

The better fit of the actinide data with eq. (6.19a) is shown by the dashed line in fig. 6.4 [300].

The Primakoff formula assumes implicitly that, for non-spin-zero targets, either the hyperfine states are statistically populated, or there is no sizable difference between the hyperfine capture rates in the case of an appreciable hyperfine conversion. Since we know that, for $A \geq 19$, the capture is from the lower hyperfine state, large deviations from the Primakoff formula *selectively* in the non-spin-zero targets would signal a significant difference between the capture rates from the two hyperfine states [30]. Nuclei such as ^{19}F , ^{23}Na , ^{27}Al , ^{31}P seem to show this phenomenon [fig. 6.5*].

In the case of ^{19}F , the large hyperfine effect in the *total capture rate* has been explicitly demonstrated in an experiment by Telegdi and collaborators [30]. These authors use LiF and LiOH targets, and study the time distribution of neutrons and γ -rays emitted following muon capture in ^{19}F and ^{16}O , respectively, after correcting for the exponential decay (figs. 6.6a, b). The spinless ^{16}O target shows no variation with time (fig. 6.6b), while ^{19}F shows a distribution of the form $1 - Ae^{-Rt}$, where A and R are obtained to be 0.31 ± 0.02 and $(5.9 \pm 0.8) \times 10^6 \text{ s}^{-1}$, respectively.

*Notice that some spin-zero nuclei like ^{16}O are also showing big deviations from the Primakoff plot.

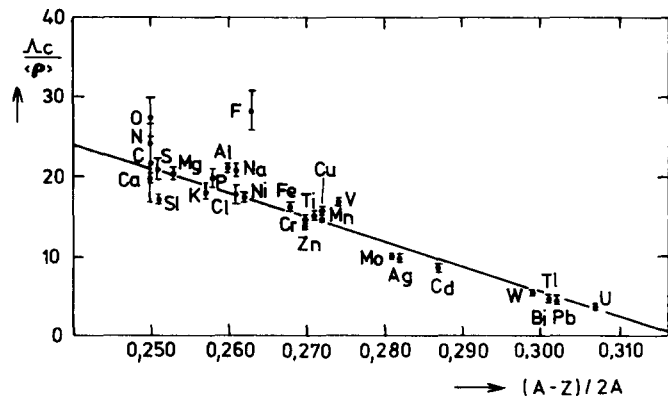


Fig 6.5. Primakoff plot of the total capture rates over the periodic table. Notice a strong deviation from the fitted line in ^{19}F due to hyperfine effects (after Eckhause et al. [249]).

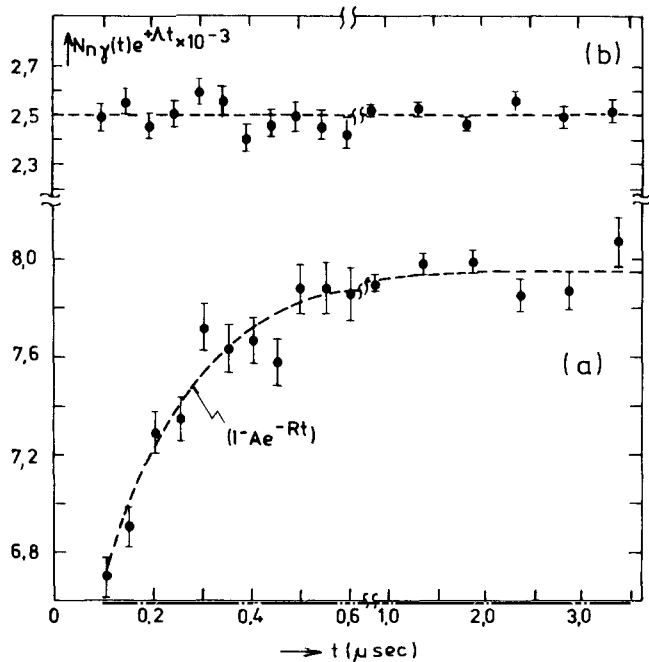


Fig. 6.6. (a) Time dependence of neutrals (neutrons and gamma rays) $N_{n\gamma}(t)$, from $(\text{Li})^{19}\text{F}$, after correction for the asymptotic exponential dependence, $\exp(-\Lambda t)$, with $\Lambda = 6.9 \times 10^5 \text{ s}^{-1}$. Dashed curve corresponds to $A = 0.31 \pm 0.02$, $R = (5.9 \pm 0.8) \times 10^6 \text{ s}^{-1}$.
 (b) Same for ^{16}O (in LiOH), corrected for asymptotic time dependence $\exp(-\Delta t)$, with $\Lambda = 6.1 \times 10^5 \text{ s}^{-1}$ (after Culligan et al. [30]).

The curvature A can be shown to be equal to

$$A = N_+(0) \left(\frac{\Lambda_- - \Lambda_+}{\Lambda_S} \right) [1 + N_+(0)(\Lambda_- - \Lambda_+)/\Lambda_S]^{-1}, \quad (6.19')$$

where Λ_+ , Λ_- , and Λ_S are *total* hyperfine and statistical capture rates. From eq. (6.19') and the experimental value of R , these authors obtain

$$(\Lambda_- - \Lambda_+)/\Lambda_S \approx 0.6. \quad (6.19'a)$$

This is again strongly in accord with the $V - \lambda A$ theory ($\lambda \sim 1.25$), and in complete disagreement with the $V + \lambda A$ theory, which would predict a value of A to be about 4 to 7%.

Accurate theoretical predictions for the quantity $(\Lambda_- - \Lambda_+)/\Lambda_S$ are not available in the literature. Bernstein et al. [17] obtained, for a nucleus having a proton coupled to a zero spin core of charge ($Z - 1$), the equation

$$(\Lambda_- - \Lambda_+)/\Lambda_S = \frac{1}{4Z} \delta_P \times \begin{cases} (2I+1)/I, & \text{for } I = l + \frac{1}{2}, \\ -(2I+1)/(I+1), & \text{for } I = l - \frac{1}{2}, \end{cases} \quad (6.19'b)$$

where δ_P is the left-hand side of (6.19'b) evaluated for proton, \tilde{Z} is the effective charge equal to $[(Z-1)\xi + 1]$, ξ being a parameter reflecting the effect of Pauli principle on the core ($\xi \leq 1$), I is the orbital angular momentum of the “lone” proton. Überall [38] has made more realistic calculations on the basis of the shell-model, and has estimated the ratio $(\Lambda_- - \Lambda_+)/\Lambda_S$ to be 0.50 and 0.45 for ^{27}Al and ^{31}P , respectively. In view of the conjectured long refilling time of the Auger holes in red ^{31}P , it is important to see if this large HF effect in phosphorus can be experimentally determined. Positive results would signal applicability of nuclear muon capture in studying atomic effects determining the filling time of Auger holes.

If the quantity $(\Lambda_- - \Lambda_+)/\Lambda_S$ goes as $(Z)^{-1}$, it should be negligible in heavy nuclei. It would be interesting to see if there is any *special deviation* from the Primakoff prediction for the isotope effect in the case of two targets with and without spin (for example, ^{24}Mg and ^{25}Mg), or those with magnetic moments of *opposite* signs (^{161}Dy and ^{163}Dy) compared with the spin zero isotopes in the same mass region [238].

Watson [239] has raised the possibility of a more exotic deviation from the Primakoff formula: that due to a quenching of the Cabibbo angle caused by intense magnetic fields in some nuclear interiors, as expected in a class of gauge theories [240]. Watson's specific example is the case of ^{93}Nb nucleus, which can be thought of as an $l = 4$ proton coupled to the spin-zero ^{92}Zr core, with a high magnetic field in the innermost 0.1 fm of the niobium nucleus. Thus, the signature for the Cabibbo angle quenching is a deviation of the observed muon capture rate in ^{93}Nb from the Primakoff formula by $1/\cos^2 \theta_c$. However, the intrinsic inaccuracy of the Primakoff formula, together with the additional uncertainty of the hyperfine effect, is likely to obscure this exotic scenario, if it takes place at all [238]!

6.3.2. Improvements on the Primakoff formula

This is a subject of considerable topical interest [214, 235–237]. For illustration we choose here the approach of Do Dang [241], and Bernabéu [241]. The muon capture rate for the nuclear transition $a \rightarrow b$ can be written as

$$\Lambda(a \rightarrow b) = \Gamma Z_{\text{eff}}^4 \Lambda_r(a \rightarrow b), \quad (6.20)$$

where the factor Γ can be assumed here to be a constant. The reduced capture rate Λ_r is given by

$$Z\Lambda_r(a \rightarrow b) = \left(\frac{\nu_{ab}}{m_\mu} \right)^2 \sum_{\alpha=1}^3 (A_\alpha | \langle b | \sum_j \tau_j^+ \exp \{ i\nu_{ab} \cdot x_j \} | O_\alpha | a \rangle |^2), \quad (6.21)$$

A_α 's are combinations of weak form factors, $O_1 = 1$, $O_2 = \sigma_{x_j}$, $O_3 = \sigma_{z_j}$. ν_{ab} is the neutrino momentum. Then, from the identity $\nu_{ab} \equiv \nu [1 + (\nu_{ab} - \nu)/\nu]$, we can develop an expansion for the n th power of ν_{ab} :

$$\nu_{ab}^n \approx \nu^n \left[1 + \frac{n}{\nu} (\nu_{ab} - \nu) \right], \quad (6.22)$$

yielding an equivalent approximation for $\Lambda_r(a \rightarrow b)$:

$$\Lambda_r(a \rightarrow b) \approx \Lambda_r(a \rightarrow b) |_{\nu_{ab}=\nu} + \frac{d\Lambda_r(a \rightarrow b)}{d\nu_{ab}} \Big|_{\nu_{ab}=\nu} (\nu_{ab} - \nu). \quad (6.23)$$

The Primakoff result is recovered by ignoring the second term in the right-hand side of eq. (6.23) and taking the sum over b . We get, after summing over b ,

$$\Lambda_r \equiv \left[1 - (m_\mu - \nu) \frac{d}{d\nu} \right] \Lambda_r(\nu) - \frac{d}{d\nu} \left[\sum_b (E_b - E_a) \Lambda_r(a \rightarrow b) |_{\nu_{ab}=\nu} \right], \quad (6.24)$$

$\Lambda_r(\nu)$ being the quantity $\sum_b \Lambda_r(a \rightarrow b)$ evaluated at $\nu_{ab} = \nu$. The energy-weighted sum rule can be evaluated in the usual way by taking the expectation value of the appropriate operator in the ground state.

Barnabéu and Cannata [214] have evaluated Λ_r in light nuclei, finding that the reduced capture rate is not very sensitive to the choice of the parameter ν , but is strongly dependent on the choice of the target ground state wave function. This is demonstrated in table 6.6, where their study of ^{12}C nucleus is excerpted. The calculated reduced capture rate, for the reliable Cohen-Kurath ^{12}C ground state and ν around 75 MeV, is 0.124, compared with the experimental value of 0.125 ± 0.005 .

In view of the rather large correction introduced by the first-order energy weighted sum rule in eq. (6.23), it is clearly important to consider higher order terms and examine the convergence of the expansion, truncated in eq. (6.23).

Realistic treatment of the total capture rate in heavier nuclei via sum rules is the concern of several recent works [235–237].

Total capture rates have also been estimated in the Fermi gas model by many authors [237a, 235]. Bell and Løvseth [237a] show that the Primakoff formula can be recovered in the lowest

Table 6.6

Total (reduced) capture rate Λ_r obtained with various model wave functions for the ^{12}C ground state. Models used are: jj , LS , and Cohen-Kurath [163]. Notice the relative insensitivity of Λ_r to the parameter ν , used in the first-order energy weighted sum rule for the capture rate (after Barnabéu and Cannata [214]). The experimental reduced rate is $\Lambda_r = 0.125 \pm 0.005$.

ν (MeV)	61	66	71	77	82	87
Model						
jj	0.220	0.227	0.229	0.226	0.217	0.200
LS	0.080	0.087	0.091	0.089	0.082	0.068
CKM	0.116	0.122	0.125	0.123	0.114	0.098

order of neutron excess by making the assumption of a fixed average neutrino momentum $\langle v \rangle$. Christillin et al. [235], using a value of $\langle v \rangle$, determined in the model itself, reproduce the trend of the total capture rate and predict isotope shifts for the capture rate, which can be quantitatively different from those obtained by the Primakoff formula. This approach, however, contains a number of assumptions needing further scrutiny: in particular, the exact value of the effective nucleon mass, introduced to simulate ignored exchange effects, and its possible constancy in a given isotope chain are open questions.

7. Muon capture and symmetry of the nuclear Hamiltonian

In this section we study the relevance of the approximate symmetries of the nuclear Hamiltonian to the nuclear capture processes. The focus of our discussion will be the nuclear supermultiplet [$SU(4)$] symmetry.

7.1. The isospin $[SU(2)]$ symmetry

A fundamental feature of the nuclear forces is the basic symmetry of nuclear interactions between neutrons and protons. For a system of A nucleons, we can define an isospin operator $T = \sum_{i=1}^A t_i$. The rotational invariance of nuclear Hamiltonian H in the *isospin space* implies

$$[H, T] = 0. \quad (7.1)$$

Thus the nuclear states can be labelled by the isospin quantum number T . The isospin symmetry in nuclei is broken only by the electromagnetic interactions of the nucleons.

One of the important tests of the isospin symmetry is provided by the rates of the Fermi β decays. The Fermi operators $T^\pm = \sum_i \tau_i^\pm$ are generators of the $SU(2)$ group underlying the isospin symmetry; they can only induce transitions *within* the same isospin multiplet [see (§ 7.4) for a generalization of this result]. Therefore, *the Fermi β transitions between states of different isospins are forbidden*. Experimentally, the isospin changing Fermi β transitions are found to have very long lifetimes compared to superallowed transitions, providing an excellent test for the isospin selection rule [A6].

Only two examples of muon capture transition, superallowed in the sense of the $SU(2)$ symmetry discussed here, are $p \rightarrow n$ and ${}^3\text{He} \rightarrow {}^3\text{H}$, belonging to the $T = \frac{1}{2}$ isomultiplet.

7.1.2. Isospin-hindered Fermi transitions in muon capture

The allowed Fermi operator for non-zero three-momentum transfer q is

$$O_F = \sum_{i=1}^A j_0(qr_i) \tau_i^+, \quad (7.2)$$

which reduces to T^+ in the limit $q \rightarrow 0$. Therefore, the operator O_F is a generator of the $SU(2)$ group only in the limit $q \rightarrow 0$ and not otherwise. Thus, the Fermi superselection rule is not *a fortiori* applicable in muon capture, q being $\sim 0.5 \text{ fm}^{-1}$ and the Fermi transition between different nuclear isospin states is not automatically forbidden. Hence an examination of the persistence of the Fermi selection rule is in order here.

To choose an example, let us suppose we are dealing with the following transitions in the “1p-shell”

nuclei": $J_i T_i \xrightarrow{\mu^-} J_f = J_i$, $T_f = T_i + 1$. If the radial form factor

$$R_{fi} = \int_0^\infty \phi_f j_0(qr) \phi_i r^2 dr \quad (7.2a)$$

for any two initial and final single-particle state involved in the nuclear transition is the same, then clearly it factorizes out of the nuclear matrix element and the Fermi superselection rule is *a fortiori* applicable for the operator O_F . Thus the Fermi matrix element will be non-zero only when the R_{fi} 's are not the same for any pair of relevant single-particle states. Therefore, in general, the mixing of two oscillator shells with the same orbital angular momentum (1p with 2p, for example), the mixing of states of different orbital angular momenta with the same oscillator shell, Coulomb and spin-orbit effects may give rise to non-zero strengths in isospin-hindered muon capture transitions of the Fermi type.

Table 7.1

Rates Λ_F , of isospin-changing Fermi transitions induced by nuclear muon capture, expressed as % of the total muon capture rates Λ in the target (after Goulard et al. [180]).

Target nucleus	$T_i \rightarrow T_f$	$\Lambda_F/\Lambda\%$
^{40}Ca	$0 \rightarrow 1$	7.00
^{48}Ca	$4 \rightarrow 5$	9.00
^{88}Sr	$6 \rightarrow 7$	15.00
^{140}Ce	$12 \rightarrow 13$	18.00
^{208}Pb	$22 \rightarrow 23$	29.00

In table 7.1 we display the contributions of isospin-hindered Fermi transitions to the total muon capture rate in heavier ($A \geq 40$) nuclei obtained* by Goulard et al. [180] in pure shell model. Notice the near monotonic increase of the role of these transitions with mass number until, in ^{208}Pb , these account for an estimated 30% of the total rate. This should be compared with the isospin-hindered Fermi β transitions, which show a retardation of 10^4 to 10^8 compared with superallowed ones.

7.2. The Wigner supermultiplet ($SU(4)$) symmetry

This symmetry, proposed by Wigner in the thirties [253], is realized if the nuclear forces are independent of spin and isospin of the nucleons. Its early successes included a natural explanation of the very fast allowed β transitions between members of the same supermultiplet and considerably slower transitions between members of the *different* supermultiplets. More recent applications of the symmetry, besides those in the muon capture, are: i) the Franzini–Radicati mass formulae for the nuclear ground states [254]; and ii) the explanations of the missing strengths of the allowed hindered β transitions [255].

*The estimates of Goulard et al. [180] should be taken only as qualitative indications. Their calculated total capture rates fail to reproduce the experimental rates by a factor of 2 to 2.5. Their estimates in ^{60}Ni for the 0^+ contribution is 6% of the total rate, to be contrasted with 2% obtained by Nalcioğlu et al. [179], who reproduce the observed total capture rates.

The Wigner supermultiplet symmetry is known to be approximate since, besides the SU(4)-invariant Wigner and Majorana interactions, nuclear forces involve SU(4) breaking exchange forces, the spin-orbit force, the tensor force and the Coulomb force. Nevertheless, in light nuclei, the SU(4) breaking, while severe, still only mixes a few of the low-lying supermultiplets. Hence some exact SU(4) results can still be useful even in the case of realistic breaking of the symmetry [137].

The relevance of the nuclear supermultiplet symmetry to the muon capture phenomena was first emphasized by Foldy and Walecka [20] in connection with the excitation of the giant electric dipole (GD) analogue resonances. The Foldy–Walecka relations [eq. (7.21)], derived for the scalar supermultiplet ground-state, have been extended to other SU(4) ground states by Goulard and Primakoff [256] and by Hraskó [257], who show that they fail only for the $N > Z$ odd–odd nuclei. Checking the validities of these relations for realistic nuclear descriptions has been a major research direction in the recent years in the theory of muon capture [214, 217–220].

Recently this author has shown [135] that in light nuclei the allowed transition strength is saturated by a few low-lying daughter states, exhibiting the analogue of giant magnetic dipole (GMD) excitation. This observation, together with the dominance of the Gamow–Teller operator in these processes (§5), has found a satisfactory explanation [137] in terms of the excitations of the SU(4) doorway states. In light nuclei, the exact SU(4) allowed selection rules have been shown to persist. In nuclei such as ^6Li and ^{14}N , SU(4) relations have been successfully used to relate elastic magnetic form factors with muon capture amplitude and the total allowed capture strengths in different nuclei [258, 259].

7.2.1. The supermultiplet group $SU(4)$ and its relevance to nuclear structure

The fifteen (4×4) Hermitian traceless matrices

$$T_\alpha = \frac{1}{2} \mathbf{1} \otimes \tau_\alpha, \quad S_\lambda = \frac{1}{2} \sigma_\lambda \otimes \mathbf{1}, \quad (7.3)$$

$$Y_{\lambda\alpha} = \frac{1}{2} \sigma_\lambda \otimes \tau_\alpha, \quad (\alpha, \lambda = 1, 2, 3)$$

constitute the generators \mathcal{G} of the supermultiplet symmetry group $SU(4)$. The operators T_α and S_λ each are generators of the $SU(2)$ group. The symmetry group $SU(4)$ thus contains the subgroup $SU(2)_T \otimes SU(2)_S$.

The $SU(4)$ generators satisfy the Lie algebra

$$[\mathcal{G}_\alpha, \mathcal{G}_\beta] = C_{\alpha\beta}^\gamma \mathcal{G}_\gamma, \quad (7.4)$$

where $C_{\alpha\beta}^\gamma$'s are the structure constants of the algebra. If the nuclear wave functions ψ_i are written in the spin–isospin basis as

$$\psi_i = \varphi_{m_s} \chi_{m_t}, \quad i = 1, \dots, 4; \quad m_s = \pm\frac{1}{2}, \quad m_t = \pm\frac{1}{2}, \quad (7.4'a)$$

then the transformations

$$R(\omega) \psi_i = [\exp(i\omega_\alpha \mathcal{G}_\alpha)]_{ji} \psi_j \equiv a(\omega)_{ij} \psi_j, \quad (7.4'b)$$

where $\omega_\alpha (\alpha = 1, \dots, 15)$ are real parameters, give a representation $a(\omega)_{ij}$ of the group. Clearly $a(\omega)$ is a unitary unimodular 4×4 matrix.

The $SU(4)$ states are classified by the three quantum numbers $(PP'P'')$ or, equivalently, by the orbital symmetry quantum number $[f]$ of the Young tableaux. The ground state assignments for $(PP'P'')$ are determined by assuming $P = |T_3| = \frac{1}{2}|Z - N|$, and using for P' and P'' minimum values

Table 7.2

Ground state SU(4) quantum numbers for $A = 2n + 1$, $A = 4n$ and $A = 4n + 2$ nuclei ($n \equiv \text{integer}$). T_3 is $\frac{1}{2} |N - Z|$, where Z and N are proton and neutron numbers respectively (after Franzini and Radicati [254]).

$A = 2n + 1$	$A = 4n$	$A = 4n + 2$
$T_3 (P' P'' P''')$	$T_3 (P' P'' P''')$	$T_3 (P' P'' P''')$
$\frac{1}{2} (\frac{1}{2} \frac{1}{2} \frac{1}{2})$	0 (0 0 0)	0,1 (1 0 0)
$\frac{3}{2} (\frac{3}{2} \frac{1}{2} \frac{1}{2})$	1 (1 1 0)	2 (2 1 0)
$\frac{5}{2} (\frac{5}{2} \frac{1}{2} \frac{1}{2})$	2 (2 0 0)	3 (3 0 0)
$\frac{7}{2} (\frac{7}{2} \frac{1}{2} \frac{1}{2})$	3 (3 1 0)	4 (4 1 0)
$\frac{9}{2} (\frac{9}{2} \frac{1}{2} \frac{1}{2})$	4 (4 0 0)	5 (5 0 0)

compatible with P and A [254]. Table 7.2 shows the ground state assignments for some $A = 2n + 1$, $4n$ and $4n + 2$ nuclei ($n = \text{integer}$), used by Franzini and Radicati in their mass formulae [254].

7.3. Two theorems

Theorem 1: Wigner's theorem (the Wigner superselection rule). If \mathcal{G} is a generator of the symmetry group, it can connect states within the same multiplet only.

We thus have

$$\langle PP'P'' | \mathcal{G} | P_1P'_1P''_1 \rangle \propto \delta_{PP_1} \delta_{P'P'_1} \delta_{P''P''_1}, \quad (7.5)$$

or equivalently

$$\langle [f] | \mathcal{G} | [f'] \rangle \propto \delta_{[f][f']} . \quad (7.6)$$

Theorem 2: The Ademollo–Gatto theorem [260].

Let the nuclear Hamiltonian H consist of two terms

$$H = H_0 + \eta B, \quad (7.7)$$

where H_0 is SU(4) invariant and ηB is the term breaking the SU(4) symmetry. Then the Ademollo–Gatto theorem can be stated as follows:

In the sum rule involving the strength of the matrix element of the symmetry generators, the symmetry-breaking parameter enters quadratically.

This theorem was postulated in a different context by the original authors. In the present context, the theorem can be stated as follows [260]:

$$\sum_n |\langle n | Y^+ | 0 \rangle|^2 = T_3 + \sum_{n_0} |\langle n_0 | Y^- | 0 \rangle|^2 + \eta^2 \sum_{n'} \frac{\langle 0 | [Y^+, B] | n' \rangle \langle n' | [B, Y^-] | 0 \rangle}{(E_{n'} - E_0)^2} . \quad (7.8)$$

We have specialized here to the strength of the Gamow–Teller operator Y^\pm ; $|0\rangle$ is the nuclear ground state with isospin quantum numbers (T , T_3), $|n\rangle$ is a complete set of nuclear states containing a subset $|n_0\rangle$ with the same SU(4) structure as $|0\rangle$, $|n'\rangle$ being the complementary subset; E_n and E_0 are the eigenvalues for the states $|0\rangle$, respectively.

It is easy to derive eq. (7.7). We can write the left-hand side as

$$\sum_n |\langle 0 | Y^+ | n \rangle|^2 = \langle 0 | [Y^-, Y^+] | 0 \rangle + \sum_{n_0} \langle 0 | Y^+ | n_0 \rangle \langle n_0 | Y^- | 0 \rangle + \sum_{n'} \langle 0 | Y^+ | n' \rangle \langle n' | Y^- | 0 \rangle. \quad (7.9)$$

We can now use the commutation relations

$$[H_0, Y^\pm] = 0, \quad [Y^-, Y^+] = -T_3, \quad (7.10)$$

and the relation

$$\langle a | Y^\pm | b \rangle = \frac{\eta}{(E_b - E_a)} \langle a | [Y^\pm, B] | b \rangle, \quad (7.11)$$

in eq. (7.9) and obtain the desired sum rule [eq. (7.8)].

Implications of eq. (7.8) in the allowed muon capture are the following: i) the symmetry breaking effects enter the sum rule at $O(\eta^2)$; and ii) in the symmetry limit ($\eta \rightarrow 0$) the “direct” (e.g. ${}^6\text{Li} \rightarrow {}^6\text{He}$) and the “broken” channel (${}^6\text{Li} \rightarrow {}^6\text{Be}$) strengths of the Gamow–Teller excitation are related in a simple way; in particular, for a self-conjugate ($T = 0$) parent ground state, they are equal.

7.4. Allowed transitions and $SU(4)$ symmetry: 1p-shell nuclei

The scale of these transitions is set by the Gamow–Teller (GT) matrix element (§ 5); the GT operator has the structure

$$Y' \sim \frac{1}{2} \sum_{i=1}^A \mathbf{\sigma}^i \tau_\pm^i f(r_i), \quad (7.12)$$

where $f(r_i)$ involve radial functions of lepton and hadron variables. Ignoring minor differences among different single-particle configurations, the extra term $f(r_i)$ factorizes out of the sum in the 1p-shell and the operator Y' obeys the same $SU(4)$ selection rule as Y .

7.4.1. An exact $SU(4)$ selection rule

From the structure of the ground state supermultiplet (table 7.3), it is easy to obtain the following selection rule by invoking Wigner’s theorem [eqs. (7.5)–(7.6)] [137]:

In the $SU(4)$ limit, the $| \Delta T | = 1$ Gamow–Teller transitions in the ground state supermultiplet of the 1p-shell nuclei are allowed in $A = 4n + 2$ nuclei only ($n = 1, 2, 3$) and forbidden in others.

Table 7.3

Structure of the ground state (g.s.) $SU(4)$ multiplet in the $(1p)^n$ configuration, n being given in the first column. The second column indicates orbital partition $[f]$ characterizing the g.s. multiplet, the first one corresponding to the first value of n and so on. The third column gives the allowed $[TS]$ values in the g.s. multiplet. The last column follows the spectroscopic notation $2T+1 \ 2S+1 L$.

n	$[f]$	$[TS]$	LS coupling configuration for the ground state
0, 12	[0], [444]	(00)	1S
1, 11	[1], [443]	$(\frac{1}{2}, \frac{1}{2})$	2P
2, 10	[2], [442]	(01), (10)	1S
3, 9	[3], [441]	$(\frac{1}{2}, \frac{1}{2})$	2P
4, 8	[4], [44]	(00)	1S
5, 7	[41], [43]	$(\frac{1}{2}, \frac{1}{2})$	2P
6	[42]	(01), (10)	1S

This selection rule can be readily understood: For allowed $|\Delta T| = 1$ transitions to be possible in the ground state multiplet, the latter must have *more than one (TS) values possible*. Thus in the SU(4) limit, allowed muon capture and related transitions are forbidden in ${}^7\text{Li}$, ${}^9\text{Be}$, ${}^{11}\text{B}$, ${}^{12,13}\text{C}$, and ${}^{15}\text{N}$ targets.

Let us now consider two cases of SU(4) breaking: i) a “*mild*” *breaking*, for example, when the two-body interaction is of Inglis or Rosenfeld type [161, 162], with a small spin-orbit force; ii) the “*realistic*” *breaking*, as in the case of the intermediate coupling calculations reproducing the spectra of the low-lying states of the nucleus [161–163].

7.4.2. “Mild” SU(4) breaking: SU(4) doorways

In the “mild” SU(4) breaking, the spin-orbit force is weak and can be treated perturbatively. In this situation, the degeneracies of the SU(4) multiplet are removed, but there is no significant mixing of different L values in a given multiplet, or of configurations of different multiplets, so that the nuclear states are given in the LS coupling, L and S being nuclear orbital and spin quantum numbers (see table 7.3 for the ground state configurations in this scheme). *In this case the SU(4) selection rule obtained above remains in force*. For nuclei with $A = 4n + 2$, the entire allowed strength is concentrated in the *spin-flip doorway state* ${}^{31}\text{S}_0$, since the ground state is ${}^{13}\text{S}_1$ in each case. Thus *there is occurrence of the spin-flip giant magnetic dipole resonance (GMDR) in 4n + 2 nuclei*.

7.4.3. “Realistic” breaking of the SU(4) symmetry

In the realistic breaking of SU(4) symmetry, the nuclear ground states have a large mixing of configurations of different permutation symmetries in the mass region $A = 11–13$, but have marginal impurity towards the beginning and end of the shell (see table 7.4). Realistic calculations [161–163] lead to the following conclusions: i) the absence of allowed transition strength remains a useful selection rule in ${}^7\text{Li}$ and to a lesser extent in ${}^9\text{Be}$; ii) in ${}^6\text{Li}$ and ${}^{14}\text{N}$ the doorways ${}^{13}\text{S}_1 \rightarrow {}^{31}\text{S}_0$ and ${}^{13}\text{D}_1 \rightarrow {}^{31}\text{D}_2$, respectively, provide avenues for the GMDR excitation; iii) in ${}^{10}\text{B}$ there is considerable fragmentation in the GMDR because of the large number of doorways available to the ground state; and iv) ${}^{11}\text{B}$, ${}^{12}\text{C}$, and ${}^{13}\text{C}$ acquire some allowed strength, ${}^{12}\text{C}$ and ${}^{13}\text{C}$ having GMDR’s due to doorways in [431] and [432] configurations, respectively. Notice that, in the realistic calculation,

Table 7.4

Approximate intensities in the ground state of 1p-shell nuclei in percentage of the space symmetry [f], obtained by using Rosenfeld interaction and the intermediate coupling parameters of Boyarkina [162].

Nuclear mass number	Symmetry chain	Ground state intensities
6	[2]–[11]	99–1
7	[3]–[21]	97–3
8	[4]–[31]	97–3
9	[41]–[32]–[311]	96–3–1
10	[42]–[411]–[33]–[321]	91–0–3–6
11	[43]–[421]–[331]–[322]	73–22–4–1
12	[44]–[431]–[422]	81–17–2
13	[441]–[432]	65–35
14	[442]–[433]	96–4

${}^6\text{Li} \xrightarrow{\mu^-} {}^6\text{He}_{g.s.}$ and ${}^{14}\text{N} \xrightarrow{\mu^-} {}^{14}\text{C}$ (2^+ : 7.01 MeV) transitions are practically “superallowed” (the latter in the ${}^{13}\text{D}_1 \rightarrow {}^{31}\text{D}_2$ channel).

7.4.4. Persistence of the $SU(4)$ selection rule for allowed transitions

The persistence of the supermultiplet selection rule can be tested in the realistic treatments of nuclear structure. In table 7.5, we display the total allowed Gamow–Teller strength

$$A_0 = \sum_n |\langle n | Y^+ | 0 \rangle|^2,$$

the centroid energy $\langle E^1 \rangle$ and the width Γ of the GMDR’s, as obtained in the Cohen–Kurath shell model. The quantities Γ and $\langle E^1 \rangle$ are defined as follows:

$$\Gamma = [\langle E^2 \rangle - \langle E^1 \rangle^2]^{1/2}, \quad (7.13)$$

$$\langle E^q \rangle = \left[\sum_n E_n^q |\langle n | Y^+ | 0 \rangle|^2 \right] / A_0. \quad (7.14)$$

From table 7.5 it is obvious that the total Gamow–Teller strengths in $A \neq 4n + 2$ nuclei are considerably less than those in $A = 4n + 2$ nuclei, thereby proving that *while the $SU(4)$ symmetry itself is badly broken, the effect of the $SU(4)$ selection rule persists* [137].

Table 7.5

Total Gamow–Teller strength (A_0), the giant magnetic dipole resonance centroid energy ($\langle E^1 \rangle$) and the resonance width Γ for selected 1p-shell nuclei, obtained from the Cohen–Kurath model (after Mukhopadhyay and Cannata [137]).

Nucleus	A_0 (in 10^{-4} units)	$\langle E^1 \rangle$ (MeV)	Γ (MeV)
${}^6\text{Li}$	1069	3.67	0.78
${}^9\text{Be}$	49	17.49	3.97
${}^{10}\text{B}$	547	7.83	2.49
${}^{11}\text{B}$	155	14.39	2.70
${}^{12}\text{C}$	65	13.95	2.23
${}^{13}\text{C}$	91	15.13	0.75
${}^{14}\text{N}$	301	9.10	1.12

7.4.5. Relevance of $SU(4)$ symmetry to related processes and for nuclei with $A \geq 16$

The processes that are dominated by the GT matrix element, as the allowed muon capture in the 1p-shell nuclei, will likewise reflect the $SU(4)$ selection rule discussed above. Examples are inelastic electron scattering, 1S orbital radiative π capture, charged pion photoproduction, and inelastic neutrino scattering.

From the Franzini–Radicati assignments (table 7.2) of the $SU(4)$ ground states, it is clear that the $A = 4n + 2$ nuclei with $N = Z$ are the only ones having allowed strength, according to the $SU(4)$ superselection rule. Since no $4n + 2$ nucleus with $N = Z$ beyond ${}^{16}\text{O}$ is stable, this implies absence of allowed strength in any target beyond ${}^{16}\text{O}$. However, the allowed selection rules, discussed above for the 1p-shell, are to be invoked with caution in heavier nuclei. Even if the GT matrix element continues to dominate the allowed transitions, the single-particle radial form factors $R_{if} = \langle \phi_f | f(r_i) | \phi_i \rangle$ are no longer equal for any pair of single-particle configurations i and f ; hence the operator Y'

[eq. (7.12)] ceases to be a generator of the SU(4) group. Thus, in the (s–d) shell, the SU(4) selection rules for the Gamow–Teller transitions are *less likely* to be valid even for pure SU(4) ground states.

The SU(4) contents of ground states of the (s–d) shell nuclei have been determined by French and Parikh [261]. The nuclei in the beginning of the shell are found to be purer in configurations [*f*]’s compared to those occurring in the middle of the shell. In view of the strong GMDR excitations observed [165] by electron scattering in the (s–d) shell nuclei, the interpretation of these excitations in terms of the broken SU(4) symmetry will be quite interesting.

7.4.6. *SU(4) relations between elastic magnetic scattering and muon capture*

Krüger and van Leuven [258] have exploited the SU(4) relation between the transverse magnetic form factor for ${}^6\text{Li}$ and the dominant muon capture matrix element for the reaction ${}^6\text{Li} \xrightarrow{\mu^-} {}^6\text{He}_{\text{g.s.}}$, assuming that both the nuclear states belong to the supermultiplet [100]:

$$2|\langle f | \sum_i j_0(qr_i) \sigma_i \tau_i^+ | i \rangle|^2 = |\langle i | \sum_i j_0(qr_i) \sigma_i | i \rangle|^2. \quad (7.15)$$

Here $|i\rangle$ is the ${}^6\text{Li}_{\text{g.s.}}$ and $|f\rangle$ is the ${}^6\text{He}_{\text{g.s.}}$. Then they express the muon capture rate as

$$\Lambda({}^6\text{Li} \rightarrow {}^6\text{He}_{\text{g.s.}}) = \frac{Rq^2 \Gamma_A}{\pi a_\mu^3} F(q), \quad (7.16)$$

where R is the nuclear finite-size correction factor, a_μ is the Bohr radius of the muonic atom with nucleus A, $F(q)$ is the magnetic form factor and Γ_A is the FP effective coupling constant. Using $R = 0.92$, and calculating $F(q)$ with the projected Hartree–Fock wave functions for ${}^6\text{Li}$, Krüger and van Leuven obtain $\Lambda = 1500 \text{ s}^{-1}$, in fair agreement with experiment [258].

An equation similar to eq. (7.16) should be also valid for ${}^{14}\text{N} \xrightarrow{\mu^-} {}^{14}\text{C}$ allowed transitions, due to the fact that ${}^{14}\text{N}_{\text{g.s.}}$ has a 96% [100] component in its wave function. Thus the total allowed strengths in ${}^6\text{Li}$ and ${}^{14}\text{N}$ are related by the equation

$$\Lambda_a / \Lambda_b = (R_a q_a^2 \Gamma_a (q_a) / a_\mu^3 [a]) / (R_b q_b^2 \Gamma_b (q_b) / a_\mu^3 [b]), \quad (7.17)$$

where $a \equiv {}^6\text{Li}$, $b \equiv {}^{14}\text{N}$. Assuming, for simplicity, all other quantities except a_μ and $R_{a,b}$ to be the same in both targets, we get a rough estimate of $\Lambda_{{}^{14}\text{N}}$, knowing $\Lambda_{{}^6\text{Li}}$. This gives $\Lambda_{{}^{14}\text{N}}$ to be about $2 \times 10^4 \text{ s}^{-1}$, in excellent agreement with more sophisticated shell model estimates (§5). Similar agreements are also obtained for ${}^{10}\text{B}$ [259].

7.5. *Isovector giant dipole resonance in the SU(4) scheme*

In $A = 4n$ nuclei, the ground state [000] belongs to the identity (1) representation in the direct product scheme $\underline{4} \otimes \underline{4} = \underline{1} \oplus \underline{15}$. The $S = 0, L = 1, T = 1$ and $S = 1, L = 1, T = 1, J = 1^-$ states of the $\underline{15}$ representation constitute the E1 resonance, and are degenerate in the symmetry limit.

7.6. *The Foldy–Walecka theorem* [20]

Let the ground state of the $A = 4n$ (n integer) nucleus belong to the identity representation of SU(4) indicated by $|0\rangle$. Then the following relationships constitute the Foldy–Walecka theorem*:

*See Walecka’s Varenna lectures [262] for a simple derivation, and Hraskó [257] for its possible extension to other SU(4) ground states.

$$\sum_m |\langle m | \sum_i \tau_{\pm}^i \omega^i | 0 \rangle|^2 = \frac{1}{2} \sum_m |\langle m | \sum_i \tau_3^i \omega^i | 0 \rangle|^2, \quad (7.18a)$$

$$= \frac{1}{3} \sum_{m,\lambda} |\langle m | \sum_i \tau_{\pm}^i \sigma_{\lambda}^i \omega^i | 0 \rangle|^2, \quad (7.18b)$$

$$= \frac{1}{6} \sum_{m,\lambda} |\langle m | \sum_i \tau_3^i \sigma_{\lambda}^i \omega^i | 0 \rangle|^2, \quad (7.18c)$$

where ω^i is an arbitrary function of x_i and $|m\rangle$ are the nuclear excited states with energies E_m above the g.s.

7.6.1. Implications

Specializing to $\omega = \exp[-i\boldsymbol{\nu} \cdot \boldsymbol{x}^j]$, doing an integration over $\boldsymbol{\nu}$, and averaging over the initially unobserved nuclear magnetic substates, one obtains the well-known relations

$$M_V^2 = M_A^2 = M_P^2, \quad (7.19)$$

from eqs. (7.18a–c), utilized in section 6 to discuss the first-forbidden transitions.

7.6.2. Extensions of the Foldy–Walecka theorem (Goulard–Primakoff [256], Hraskó [257])

The relations $M_V^2 = M_A^2 = M_P^2$ have been shown to be true for the Franzini–Radicati assignment of the SU(4) ground state and with the assumption of the same average neutrino energy for all the three matrix elements, for all nuclei *except odd–odd ones with $N > Z$* .

7.6.3. Test of the equalities $M_V^2 = M_A^2 = M_P^2$ beyond the SU(4) approximation

Various authors have examined the validity of the FW equalities beyond the assumption of the supermultiplet symmetry, and found them to be valid in a surprisingly large number of situations. Joseph et al. [218] provide a concise summary of these. We mention here some important results.

- i) The equalities are valid in the *jj coupling scheme* in the muon capture transition $p(n_p, l_p, j_p) \rightarrow n(n_n, l_n, j_n)$, provided a) either the proton leaves a doubly closed shell *or* the neutron comes to a doubly empty shell, b) spin–orbit splitting is neglected (Luyten et al. [219]).
- ii) The equalities are badly violated in ${}^4\text{He}$ and ${}^{16}\text{O}$ in closure approximation, with target ground state wave functions including the effect of short-range nucleon–nucleon correlations (McCarthy and Walker [217]).
- iii) For $N > Z$ nuclei, simple shell model wave functions give near equality of $|M_{A,V,P}|^2$. These models, however, fail to reproduce the experimentally desired value of M_V^2 (Joseph et al. [218]).
- iv) Cannata et al. [263] have shown that the effect of SU(4) breaking for the (15) giant resonance states is reflected in the relationship $M_A/M_V \sim (1 - 2\Delta\omega/(E_m - \omega_F))$, where E_m is of the order of 100 MeV, ω_F is the peak energy for the E1 photoabsorption, $\Delta\omega$ is the separation between the two $T = 1$ levels with $S = 1$ and $S = 0$.

Thus the nuclear isospin and supermultiplet symmetries provide valuable theoretical frameworks of understanding the distribution of the nuclear muon capture strengths, particularly in the light nuclei. The SU(4) symmetry explains in a natural way the occurrence of the “giant” excitations.

8. Nucleon emissions following muon capture, fission and rarer reaction modes

In this section we consider the emissions of neutrons and charged particles following muon capture, muon-induced fission in heavy nuclei, and the rarer reaction modes such as the radiative muon capture and possible muon–electron conversion.

The “mean” excitation energy in the nuclear muon capture is around 15 to 20 MeV. This is well above the nucleon emission threshold in all complex nuclei. Thus, the daughter nucleus ($A^*, Z - 1$) can de-excite by emitting one or more neutrons, or charged particle, besides via the ordinary electromagnetic mode. In some heavy nuclei, the mean excitation energy is above the fission threshold, and the daughter nucleus can also undergo fission.

The radiative muon capture is a rarer process in which a photon is emitted along with a neutrino in the final state, the “elementary” reaction being $p + \mu^- \rightarrow n + \nu_\mu + \gamma$. This process is believed to populate predominantly the nucleon-unstable region of the daughter nucleus.

The muon–electron (positron) conversion is of fundamental importance in our understanding of lepton selection rules. An unequivocal proof of its laboratory detection is, however, still lacking.

8.1. Neutron emission*

The neutron emission is the preferential channel of nuclear muon capture reactions. The observables studied most frequently are the neutron multiplicity, energy spectra, and asymmetry.

The problem of neutron emission is very complex because of the interplay of several dynamical mechanisms. It is convenient to group the emitted neutrons in three separate regimes of energy to focus on these different aspects of nuclear dynamics, according to their individual prominence in a particular regime.

Low-energy neutrons ($E_n \lesssim 10$ MeV) show characteristic evaporation background, on the top of which lines may appear indicating the prominence of giant resonance excitations. The low-energy neutron spectra are sensitive to the final-state interactions. The neutron asymmetry is negligible for such energies.

The intermediate energy neutrons ($10 \text{ MeV} \lesssim E_n \lesssim 25 \text{ MeV}$) are well-described in terms of the muon absorption on single protons, though the final-state interaction of the neutrons with the remaining nucleus can be quite important, particularly in nuclei with $A \leq 40$. We can get some information on the proton momentum distribution inside nuclear matter from the properties of the intermediate energy neutrons. The neutron asymmetry is a complicated function of energy in this region.

The high-energy neutron emission ($E_n \gg 25$ MeV) is increasingly rarer due to a decrease of phase space with increasing neutron energy. In this region, muon capture process begins to resemble, at least kinematically, the absorption of pions at rest, with negligible momentum transfer and large energy transfer to the nucleus. Internucleon correlation effects become quite important. The emission of high-energy *protons* definitely establishes the role of cluster absorption of muons.

One must emphasize that the above-mentioned division of neutrons into three energy regimes is not very clear-cut.

8.1.1. Neutron multiplicity

Experimentally neutron multiplicity m can be determined by gamma-ray spectroscopy [227, 228, 251, 252, 265] or by activation techniques [182, 264]. The average multiplicity $\langle m \rangle$ shows

*See also section 4 for a discussion of the neutron spectra following muon capture in deuteron, and sections 6 and 7 for a review of giant dipole and other nuclear resonances. See Überall [B34] and Singer [B30] for further experimental details.

Table 8.1

Average neutron multiplicity $\langle m \rangle$ per muon capture determined experimentally in naturally occurring elements (after Singer [B30]).

Element	$\langle m \rangle$	Element	$\langle m \rangle$
Al	1.26 ± 0.06	Ag	1.61 ± 0.06
Si	0.86 ± 0.07	I	1.44 ± 0.06
Ca	0.75 ± 0.03	Au	1.66 ± 0.04
Fe	1.12 ± 0.04	Pb	1.71 ± 0.07

considerable sensitivity to the nuclear structure (table 8.1), but has the following rough trend [266]:

$$\langle m \rangle \sim 0.3 A^{1/3}. \quad (8.1)$$

The neutron multiplicities are sensitive to the momentum distribution in the nucleus and some aspects of internucleon correlations.

The Singer model [267]: This is a simple approach to understand properties of neutrons emitted following the muon capture. It has the following basic assumptions: i) compound nucleus formation by the muon absorption; ii) only neutron emission whenever energetically possible; iii) successive evaporation of neutrons characterized by a single mean nuclear temperature θ . Assumptions (i) and (ii) are reasonable, but (iii) underestimates high neutron multiplicities, which are found to be also sensitive to nuclear correlations.

The basic steps in the Singer model are the following. The capture rate Λ is given, in terms of an effective coupling constant $\langle G \rangle$, by the relation*:

$$\Lambda \sim \langle G \rangle^2 |\psi_\mu|_{av}^2 \int d^3 K d^3 p d^3 q g(p)(1 - h(q)) \delta(p - K - q) \delta(E_0 - T_p - T_n - E_\nu), \quad (8.2)$$

where K, p and q are momenta of neutrino, proton and neutron respectively, $g(p)$ and $[1 - h(q)]$ are the nuclear proton and neutron hole momentum distributions, T_p and T_n are proton and neutron kinetic energies; E_0 is $(M_i - M_f + m_\mu - B_\mu)$, where M_i and M_f are the initial and final nuclear masses, B_μ is the muon binding energy. The nuclear excitation energy Q is $E_0 - K$. Singer assumes g and h to be Gaussian:

$$g(p) \sim \exp(-p^2/\alpha^2), \quad h(q) \sim \exp(-q^2/\alpha^2), \quad (8.3)$$

with $\alpha^2/2M \sim 16-20$ MeV. We can now define a nuclear excitation function $I(Q)$:

$$\Lambda \sim \int_0^{E_0} I(Q) dQ, \quad (8.4)$$

and calculate the neutron multiplicity m_i , the probability for emission of i neutrons:

$$m_i = \int_{B_i}^{E_0} dQ N_i(Q) I(Q) - \int_{B_{i+1}}^{E_0} dQ N_{i+1}(Q) I(Q), \quad (8.5)$$

where $N_i(Q)$ is the probability for emission of *at least* i neutrons, B_i is the binding energy of i neutrons in the compound nucleus. Clearly $N_0(Q) = 1$, and for $Q \geq B_1$, $N_1(Q) = 1$. For $i \geq 2$, N_i is a function of Q , B_i and nuclear temperature θ [C17]. The nuclear excitation function $I(Q)$ is given in terms of the kinematic variables E_0 and Q , and the nucleon effective mass m^* [C17].

*We shall use the symbol \sim in this subsection to indicate dropping of uninteresting normalization factors.

MacDonald et al. [267a] have obtained reasonable agreements with experimentally observed multiplicity distributions by assuming a nuclear temperature between 0.65 to 0.75 MeV and an effective nucleon mass about 0.5 times the nucleon mass. This agreement, while qualitatively good, is not satisfactory, since the Brueckner theories yield effective nucleon masses around 0.7 M [268], and the nuclear temperatures extracted from the neutron energy distributions are higher by a factor of two (see §8.1.2).

Hadermann [269] has improved the Singer procedure by generating the nucleon momentum distributions from a Woods–Saxon potential, and taking a better account of the Pauli principle. For proton momenta above 250 MeV/c, correlation effects are also taken into consideration in a phenomenological way. The result is a much better agreement with the experimental multiplicity distribution with reasonable values of the effective nucleon mass, and nuclear temperature (table 8.2).

Table 8.2

Neutron multiplicity distributions for natural Pb target, corrected for counter efficiency. Calculated values are from Hadermann and Junker [269], for two choices of effective mass m^* , and from the older calculations [267a] using $m^* = 0.41 M$, M being the nucleon mass.

Multiplicities	Experiment [267a, 376]		Calculated values		
	Kaplan et al.	MacDonald et al.	Hadermann and Junker [269] $m^* = 0.68 m$	$m^* = 0.60 m$	Singer model [267a]
0	0.348 ± 0.100	0.324 ± 0.022	0.362	0.366	0.387
1	0.479 ± 0.057	0.483 ± 0.025	0.470	0.459	0.377
2	0.137 ± 0.027	0.137 ± 0.018	0.154	0.155	0.167
3	0.018 ± 0.012	0.045 ± 0.010	0.014	0.019	0.057
4	0.010 ± 0.005	0.011 ± 0.006	2×10^{-4}	2×10^{-4}	0.011
5	0.005 ± 0.004	—	~0	~0	0.001

8.1.2. Neutron spectra

Low energy spectra ($E_n \leq 10$ MeV): Experiments in light ($A \leq 40$) nuclei at good resolution indicate the importance of the giant dipole resonance excitations (§6, figs. 6.3). The particle–hole models give a reasonable description of the observed spectra (e.g., see Überall et al. [229]), while more ambitious shell- and continuum-model calculation [B1, 230] are expected to do better.

Low-energy neutron spectra observed *in heavier nuclei*, with good resolution (~ 200 keV), appear structureless. A reasonable fit is obtained by using the evaporation formula [270]

$$dN(E)/dE \sim E^{5/11} e^{-E/\theta}, \quad (8.6)$$

where θ varies between 1.0 to 1.5 MeV for nuclei between Ag to Th. It is interesting to note that there is a discrepancy between values of θ obtained here and those by (n, n') experiments in nuclei other than those around $A = 208$ [270] (fig. 8.1).

Intermediate energy ($10 \leq E_n \leq 25$ MeV) spectra are well explained by the distorted wave impulse approximation calculations. In ^{40}Ca , the neutron energy distribution is found to be sensitive to the real part of the neutron optical potential [271].

High energy ($E_n > 24$ MeV) part of the neutron spectra is sensitive to internucleon correlations (fig. 8.2). Bernabéu, Ericson and Jarlskog [272] have pointed out that the slope of the spectral “tail” can be predicted, on general grounds, to have a lower bound which can be related to the

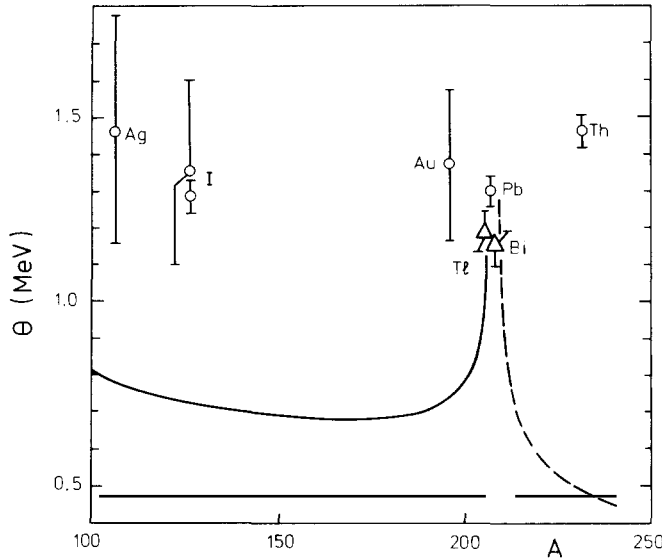


Fig. 8.1. Nuclear temperature θ as a function of the mass number A , obtained from the spectra of the low-energy neutrons emitted after muon capture. Solid line is the trend of θ extracted from the (n, n') reaction, showing a clear shell effect (after private communications from Evseev).

properties of pionic atoms. Thus, the muon capture probability Γ can be written as

$$\Gamma \sim V^2 + A^2 + A_0^2, \quad (8.7)$$

where V_μ and A_μ are the hadronic vector and axial vector currents. In the limit $q \rightarrow 0$, we have, from the PCAC hypothesis,

$$q_0 A_0 \sim \langle X | \phi_\pi | N \rangle, \quad (8.8)$$

for the nuclear transition $N \rightarrow X$, ϕ_π being the pion field. Hence the term A_0 can be obtained by the extrapolation of the S-wave pion absorption amplitude from the physical pion mass m_π to the mass m_μ . This will provide a lower limit for the quantity $d\Gamma_{N \rightarrow X} / dq^2$ at $q = 0$. The vector contribution may be obtained similarly from the process $\gamma + N \rightarrow X$.

8.1.3. Neutron asymmetry

In the elementary reaction $\mu^- + p \rightarrow n + \nu_\mu$, parity violation in the weak interaction will manifest itself in the asymmetry of the neutron distribution about the muon polarization axis. In the nuclear reaction going through an intermediate *compound nuclear state*, this asymmetry is lost, since the decay of the compound nucleus is not governed by the history of the process producing it. Thus, the low-energy neutrons are not expected to show asymmetries. The intermediate and high-energy neutrons contain to some degree the information of the weak interaction itself, and can exhibit sizable asymmetry.

Let us consider the process*

$$\mu^- + (A, Z) \rightarrow (A - 1, Z - 1)^* + n + \nu_\mu. \quad (8.8')$$

*We are assuming that this process is direct (i.e. not compound-nuclear) for the purpose of the theoretical discussion below.

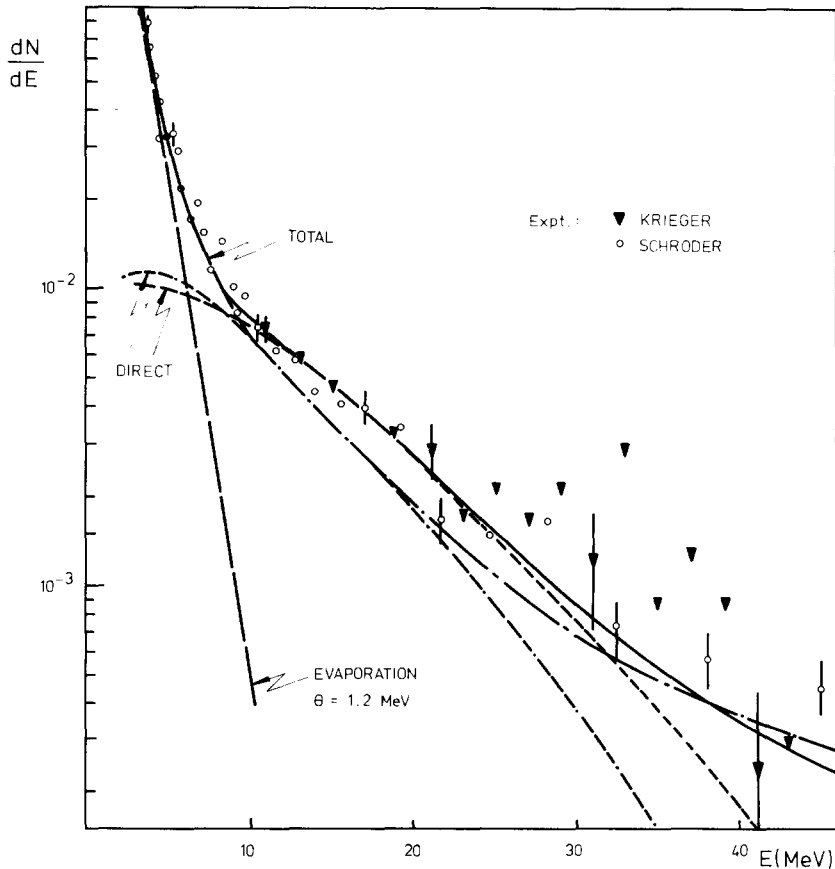


Fig. 8.2. Experimental spectra of neutrons at low and intermediate energies (Krieger [thesis] and Schröder [C17]). The peak-like structure around 35 MeV is statistically insignificant. Theoretical curves are due to Hadermann and Junker (private communications), demonstrating dominance of the evaporation mechanism at low energies and direct emission above 15 MeV of neutron energy.

The differential neutron spectrum for this process is given by

$$\frac{d\Lambda}{dE_n d\Omega_n} = A(E_n) [1 + \alpha(E_n) P_\mu \cdot \hat{n}], \quad (8.9)$$

where P_μ is the muon polarization vector and \hat{n} is the unit vector in the direction of the neutron momentum. The quantities $A(E_n)$ and $\alpha(E_n)$ are, in general, complicated functions of weak interaction form factors and nuclear matrix elements [C1]. The number of emitted neutrons $N(E_n)$ is simply $4\pi A(E_n)$.

Experimental situation: The experimental determination of the energy dependence of the asymmetry coefficient has a long and confusing history [273]. Experiments determining the asymmetry, *as a function of neutron registration threshold*, generally found negative coefficients with values close to -1 at large energies [274–275]. However, experiments in ^{40}Ca [273], determining the asymmetry coefficient directly *as a function of emitted neutron energy*, found a near zero asymmetry in the energy region 10–15 MeV, then a positive peak around 18–20 MeV,

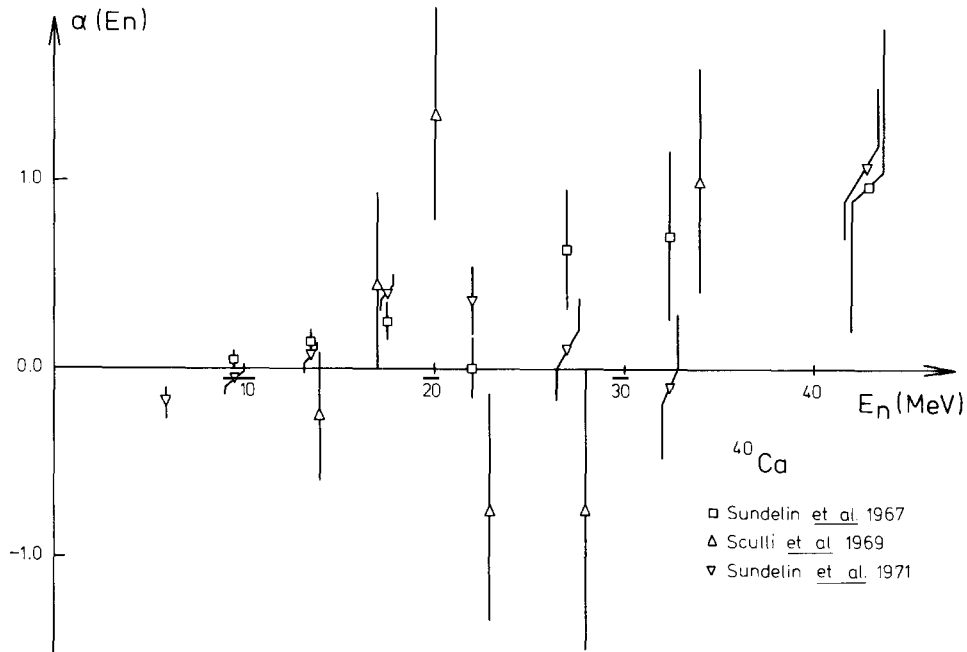


Fig. 8.3. Experimental results of the neutron asymmetry $\alpha(E_n)$ as a function of neutron energy E_n in ^{40}Ca (after Bouyssy [C1]).

followed by a dip at ~ 27 MeV and a rise to positive values after ~ 35 MeV (fig. 8.3). Evseev [276] has shown that the two sets of experiments can be reconciled, if one assumes that $\alpha(E_n)$ is close to zero in the range $10 \text{ MeV} \leq E_n \leq 40 \text{ MeV}$, with a possible positive regime around $E_n \sim 20$ MeV, tending to -1 at high energies. However, the Carnegie–Mellon experiment [273] does not indicate the tendency of α_n going to -1 at high energies. The experiments of Sculli [277] and Sundelin and Edelstein [273] are currently taken as more definitive than other experiments for theoretical comparison.

Theoretical predictions: Primakoff [18], neglecting nucleon recoil terms and final interactions, has obtained the following expression for $\alpha(E_n)$ in the case of spin-zero targets:

$$\alpha(E_n) \equiv \beta \alpha_p = \beta(G_V^2 - G_A^2 - G_P^2 - 2G_A G_P)/(G_V^2 + 3G_A^2 + G_P^2 - 2G_A G_P), \quad (8.10)$$

where α_p (≈ -0.4) represents the neutron asymmetry in the muon capture by protons. Thus, β contains all the effects of nuclear physics.

Theoretical improvements from the Primakoff estimate consist of the following: (i) inclusion of nucleon velocity terms (Klein et al. [278], Devanathan and Rose [279], Bogan [280], Piketty et al. [281], Eramzhyan et al. [282]); (ii) taking account of the final state interaction between the outgoing neutron and the residual nucleus by means of an optical potential with surface and volume absorption terms (Bouyssy and Vinh-Mau [271]); (iii) use of realistic (Brueckner–Hartree–Fock) wave functions for bound protons (Bouyssy et al. [271]); (iv) inclusion of terms involving small components of the lepton wave functions and a coupled-channel treatment for the outgoing neutron wave (Kume et al. [283]).

The main conclusions emerging from these studies are: (i) The energy dependences of the asymmetry coefficient $\alpha(E_n)$ and the neutron intensity are sensitive to the final-state interaction of the outgoing neutron with the residual nucleus. In particular, as pointed out first by Bouyssy and Vinh-Mau [271], the positive peak in the asymmetry at about 20 MeV can be reproduced by the consideration of the neutron optical potential having surface and volume absorptive terms. (ii) The first-order nucleon velocity terms in the muon capture Hamiltonian are very important and are responsible for the sensitivity to the surface absorption aspect of the neutron wave functions. (iii) Coupled-channel calculations do not reproduce the neutron spectra very well, but are able to account for the fine structure (peaks and dips) of the $\alpha(E_n)$ better. (iv) Refined calculations all predict *positive* asymmetries for neutron energies of about 50 MeV.

Some calculations of the asymmetry are illustrated in figs. 8.4.

Thus, the asymmetry and spectra of neutrons following muon capture do not reveal much about weak interaction from factors *even at high energies*, contrary to our naive expectations. Complicated nuclear physics aspects enter in the interpretation of these observables. It would be experimentally interesting, nevertheless, to determine at least the sign of the asymmetry above 50 MeV neutron energy with sufficient reliability. The asymmetry parameter, at these energies, is also of basic interest to the radiative muon capture experiment (see § 8.4.3).

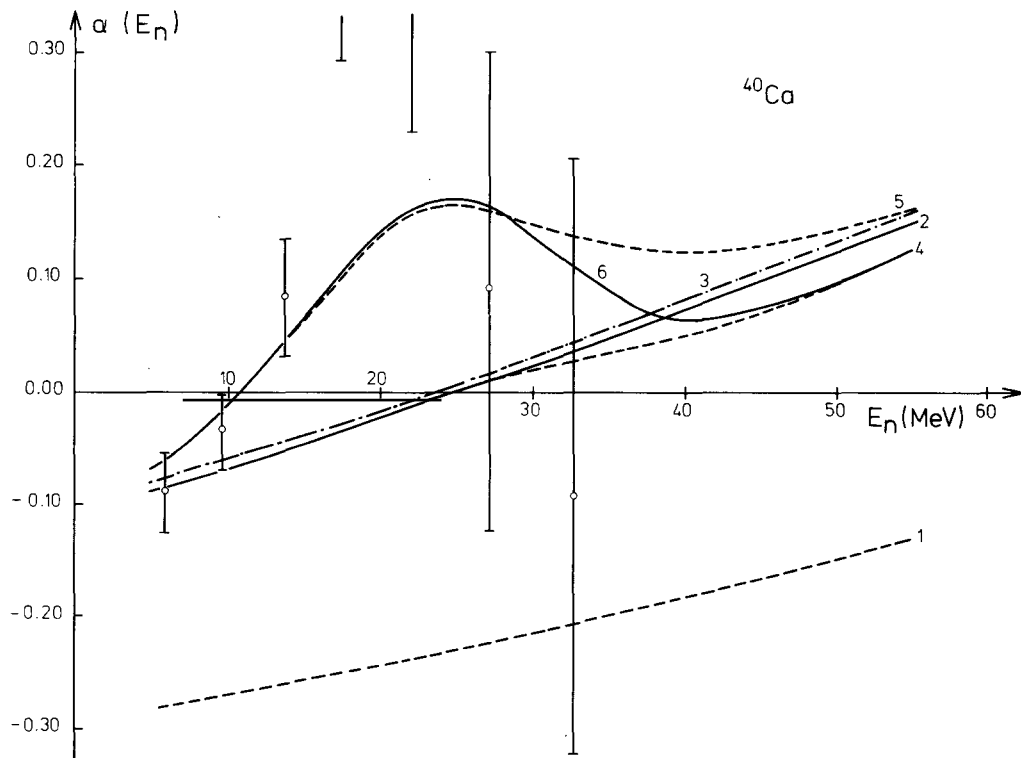


Fig. 8.4. Calculated neutron asymmetry $\alpha(E_n)$ as a function of neutron energy E_n obtained in a hierarchy of approximations (Bouyssy and Vinh-Mau [271]). 1: shell-model, no nucleon velocity terms and no final-state interactions (FSI); 2: shell-model with nucleon velocity terms and real part of the optical potential for FSI; 3: Same as #2, with configuration mixing; 4: same as #3, with volume absorption; 5: #3 with surface absorption; 6: #3 with surface and volume absorption. Experimental results are of Sundelin et al. [273].

8.1.4. Helicity of neutrons

Several authors [284, 285] have looked into the theoretical significance of studying the longitudinal polarizations of neutrons emitted in the muon capture. Bouyssy and Vinh-Mau [284] have found that the neutron longitudinal polarization for muon capture in ^{40}Ca is more sensitive to the final state interaction than to the details of the nuclear density; thus its measurement complements that of the asymmetry coefficient, since these two observables do not depend on the same combination of nuclear matrix elements and weak form factors.

8.2. Emission of charged particles

Since the pioneering experimental work of Morinaga and Fry [286] studying emission of charged particles following muon capture in nuclear emulsions, there have been several experiments studying this phenomenon [287–291]. Singer [B30] has recently reviewed these in depth*. One new experiment, done at SIN using radio-chemical techniques [292], is now available, giving the yield of $(\mu^-, \nu_\mu \text{pxn})$ reaction products ($x = 0–4$) in several targets. All experiments point to the relative rarity of the charged particle emission following muon capture in medium and heavy nuclei. We summarize below some interesting experimental results.

(1) Charged particle emission is more probable for light nuclei than for heavy nuclei (fig. 8.5). Neon, for example, has a large percentage of charged particle emission, $20 \pm 4\%$ per muon stop [289], while heavy nuclei have a very small probability. Emulsion experiments show that the elements C, N, O have a probability of $\sim 15\%$, of which 9.5% are protons and 3.4% are α -particles [286]. The ratio of deuteron to proton emission declines rapidly from Si to Cu, from about 37% to about 16% [291].

(2) Experimental α and proton energy distributions for muon capture in AgBr emulsion cannot be simultaneously reproduced in the compound nucleus picture of the reaction (fig. 8.6). Models reproducing α particle distributions do not yield correct distributions of the protons. Some direct proton emission is clearly implicated, for example, via the reaction [267]



where (p, p) is a two-proton cluster in the nucleus. It would be obviously interesting to measure the proton asymmetry with respect to muon polarization axis, to see if the correlated proton pair model has any bearing on the proton emission.

(3) The proton spectra, obtained by Budyashov et al. [291], in ^{28}Si , ^{32}S , ^{40}Ca , and Cu can be reproduced in a qualitative way by the precompound model calculations of Kozlowski and Zglinski [293], who assume nuclear doorway excitations of monopole, dipole and quadrupole collective states.

(4) Weissenberg et al. [288], in an emulsion experiment, find 13 proton events with energies extending up to ~ 80 MeV. This experiment gives a probability of $(4.7 \pm 1.1) \times 10^{-5}$ protons per muon stop, for protons above 40 MeV energy. No explanation of this observation is currently available.

(5) The Dubna group [294] have investigated in photoemulsions the reactions:



*See also the review of Yu.A. Batusov and R.A. Eramzhyan, Dubna preprint E1–9457 (January, 1976), to be published.

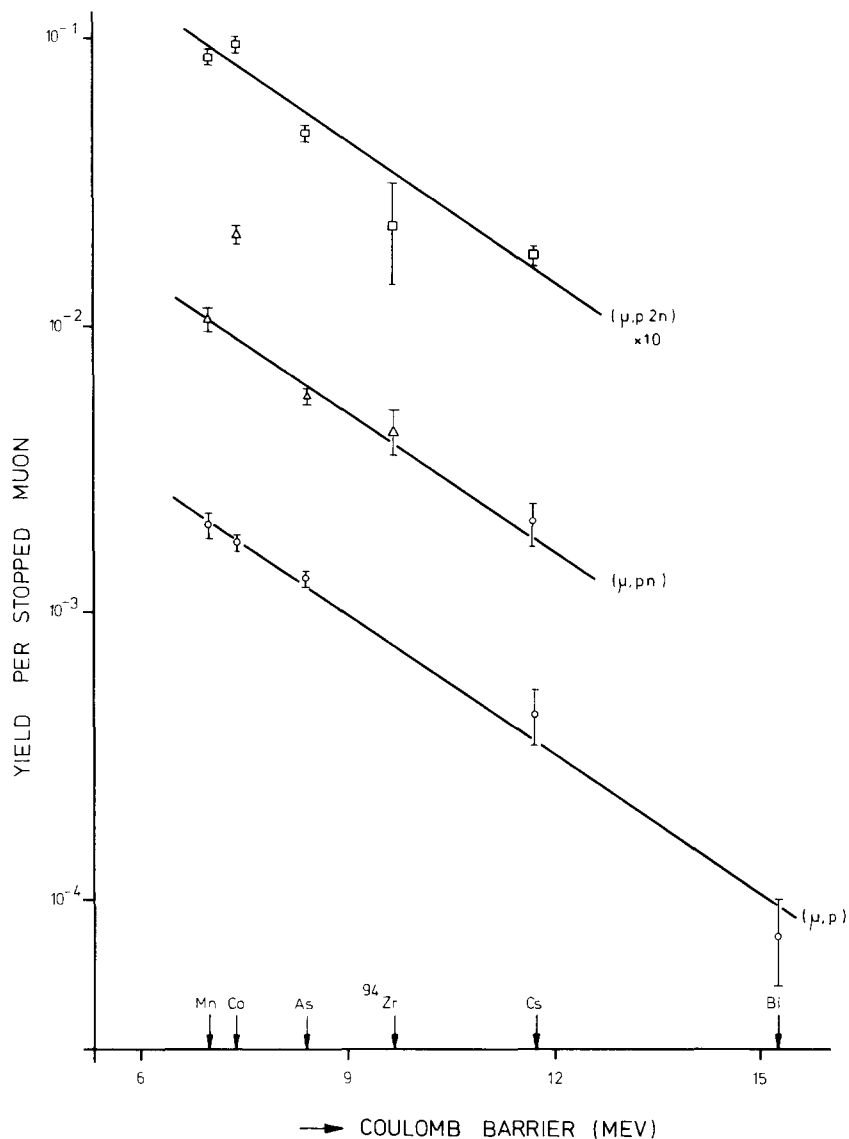


Fig. 8.5. Yields of (μ^-, p) , (μ^-, pn) , (μ^-, p_{2n}) reactions per stopped muon as functions of the Coulomb barrier, in various targets from Mn to Bi: (Wyttanbach et al. [292]). Solid lines are guides to the eye.

and found their branching ratios to be $<2.6 \times 10^{-4}$, $\sim 1.4 \times 10^{-3}$ and $<2 \times 10^{-2}$, respectively. Capture reactions in ^{14}N and ^{16}O leading to ^8Li in the final state have also been observed. It is interesting to note that the reaction $\pi^- {}^{12}\text{C} \rightarrow {}^8\text{Li} {}^3\text{He} n$ occurs due to direct absorption on ${}^4\text{Li}$ cluster and this mechanism for (8.12b) cannot be excluded. A resonance excitation to an intermediate ${}^{12}\text{B}^*$ state, followed by its decay, appears to be a more likely sequence for the reaction (8.12c).

(6) Wyttanbach et al. [292] have studied recently at SIN the reactions $(\mu^-, pxn\nu_\mu)$ in a variety of targets. Their observed yields (fig. 8.5) show roughly an exponential dependence on the Coulomb

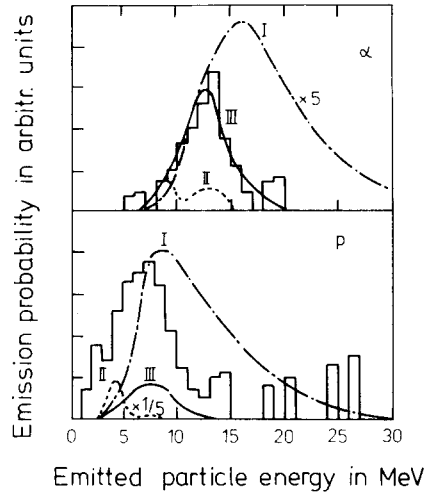


Fig. 8.6. Energy distributions of emitted α particles and protons following muon capture in the AgBr emulsion (Morinaga and Fry [286]). Theoretical estimates (solid broken curves) are by Ishii [285a]: I: Chew-Goldberger distribution $\rho(p) \sim A(B^2 + p^2)^{-2}$; II: Fermi gas at zero temperature; III: Fermi gas at finite temperature ($kT = 9$ MeV).

barrier, as is expected from the penetration of the proton through the barrier. For varying multiplicities x , the yields exhibit roughly the same trend as the cross-section for the (μ^-, xnv_μ) reaction, provided the direct emission of one neutron is subtracted in the latter case; thus, the reaction mechanism seems to be a direct proton emission followed by the evaporation of several neutrons.

8.2.1. Possible determination of the neutrino mass

The reaction $\mu^- + {}^6\text{Li} \rightarrow {}^3\text{H} + {}^3\text{H} + \nu_\mu$ has been theoretically studied by Wienke and Meyer [295], who have pointed out its usefulness in determining the muon neutrino mass from the *kinematics alone*. Thus, the square of the neutrino mass m_ν is given by

$$m_\nu = [m_\mu + m_{\text{Li}} - 2m_T]^2 - 2(m_\mu + m_{\text{Li}} - m_T)(T_1 + T_2) + 2T_1 T_2 - 2P_1 P_2 \cos \theta, \quad (8.13)$$

where T_i is the energy of the i th triton, θ is the angle between the tritons and $P_1 P_2 \approx 2m_T \sqrt{T_1 T_2}$: m_α 's are the masses of the particles α .

The important advantages of the reaction (8.13) have been noted by Wienke and Meyer [295]; these are: (i) the ready accessibility of the two charged particles in the final state for identification and accurate energy measurement (± 40 keV); (ii) no significant mass uncertainties contributing to the error of the neutrino mass (m_μ is known to ± 0.35 keV).

Until recently, the best available upper limit of the muon neutrino mass was 650 keV, obtained by Clark et al. [296] from the $K_{\mu 3}$ decay. A recent measurement of $m_{\nu_\mu}^2$ from the decay $\pi^+ \rightarrow \mu^+ \nu_\mu$ has yielded the value -0.10 ± 0.19 MeV² [296a]. The accuracy of the last experiment is limited by that of the pion mass. Proposed "velodrom" experiment of Seiler et al. at SIN is expected to achieve an accuracy of ± 0.04 MeV² [296a]. The muon capture breakup of ${}^6\text{Li}$ to two tritons has an estimated rate of 140 s^{-1} ; hence a comparatively accurate neutrino mass measurement by this reaction looks very difficult.

8.3. Muon-induced fission

Muons can induce nuclear fission in two ways – by electromagnetic 2P–1S radiationless transition (prompt fission), or by weak capture reaction (delayed fission). The promptness of the former is due to the electromagnetic lifetimes. The possibility of the muon induced fission was discussed originally by Wheeler [9]. Zaretsky and Novikov [297] have made thorough investigations of the prompt fission.

8.3.1. Prompt fission*

The prompt fission occurs in the actinides, for which the 2P–1S transition energies (~ 6 MeV) are the order of the fission barrier. It is a few per cent of the total fission probability in thorium, and about a third in plutonium**.

The advantages of the prompt fission are its known electromagnetic nature and the definiteness of the energy transfer to the nucleus, which permits a focus on the nuclear fission dynamics itself.

An important effect of the muon–nuclear Coulomb interaction is to change the muon binding energy with nuclear deformation [298] (fig. 8.7). This results in an increase in the fission barrier, and hence in a *decreased prompt fission probability*. As the second barrier may be increased by as much as an MeV relative to the second minimum, *the shape isomer states excited by the radiationless muon transition may become more stable*.

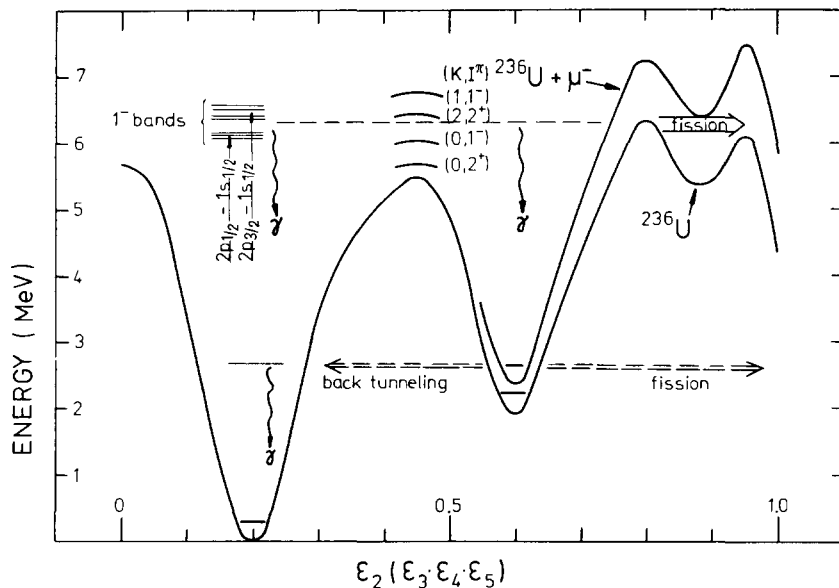


Fig. 8.7. Deformation energy for the nucleus ^{236}U (lower curve) and the muonic atom $^{236}\text{U} + \mu^-$ as a function of the prolate deformation parameter ϵ_2 , minimized with respect to higher multipoles (Leander and Möller [298]).

*Strictly this subsection belongs to § 2. However, for its closeness to the contents of § 8.3.2, we keep it here.

**All experiments, however, do not agree on these magnitudes (see table 8.3).

8.3.1.1. Shape isomers excited in muon capture?

Bloom [299] has recently made an interesting suggestion to explain an apparent discrepancy between the muon lifetimes obtained by the electron and fission measurements (fig. 6.4). He has considered two possible lifetimes, τ_μ and τ_i , for the μ^- (1S) – ^{238}U systems*:

$$\begin{aligned} (\tau_\mu)^{-1} &= \Lambda_e + \Lambda_{cf} + \Lambda_{cn}, \\ (\tau_i)^{-1} &= \Lambda_{if} + \Lambda_{ic} + \Lambda_{i\gamma}; \end{aligned} \quad (8.14)$$

τ_μ is the lifetime of the μ^- -U system with μ^- in the 1S state and U in the ground state and τ_i is the lifetime of the isomeric state of U excited by the 2P–1S transition; Λ_e is the $\mu \rightarrow e$ decay rate, Λ_{cn} and Λ_{ic} are the non-fission capture rates for ordinary and isomeric U, Λ_{cf} and Λ_{if} are their respective fission rates, Λ_i is the electromagnetic decay rate of the isomeric state of U. Reckoning $\Lambda_e \ll \Lambda_{i\gamma}$, $\Lambda_{cf} \ll (\tau_\mu)^{-1}$, $\Lambda_{if} \ll (\tau_i)^{-1}$, and assuming $\Lambda_{cn} \approx \Lambda_{ic}$, we note that

$$\tau_\mu > \tau_i. \quad (8.15)$$

The electron production and the fission rates are

$$\dot{n}_e = \Lambda_e \exp(-t/\tau_\mu), \quad (8.16a)$$

$$\dot{n}_f = \Lambda_{cf} \exp(-t/\tau_\mu) + \epsilon \Lambda_{if} \exp(-t/\tau_i), \quad (8.16b)$$

where ϵ is the fraction of isomer production. By virtue of the inequality (8.15), it is clear that the apparent lifetimes measured by the fission experiment will be shorter than that obtained in the electron experiment, since the right-hand side of eq. (8.16b) will be dominated by the second exponential. This is Bloom's explanation of the possible lifetime discrepancy in the ^{238}U system.

A direct attempt to measure $(\Lambda_{i\gamma})^{-1}$ by Kaplan et al. [300] has been inconclusive due to the poor γ -ray intensities, but the Bloom hypothesis has been supported qualitatively.

8.3.2. Delayed fission

Delayed fission is intrinsically a complex phenomenon because of the distribution of energies given to the nucleus. The large energy transfer (of the order of the mean excitation energy) makes second and even higher chance fissions possible. Measurable parameters are the daughter mass distributions, delayed fission probabilities and the ratios of prompt to delayed probabilities.

In table 8.3, we display the experimental results on the total fission probability following muon capture, and prompt to delayed fission probability ratio. Notice that the delayed fission probabilities, determined by the Polikanov group [301] disagree strongly with the theoretical predictions [302] and with the other experiments [303] wherever available. This group also finds the puzzling result that with the increase of Z^2/A , the fission probability does not always increase monotonically. Baertschi et al. [304] have completed the first fission experiment at SIN, obtaining the yields of some product chains in the muon-induced fission in ^{208}U (table 8.4). In this experiment, unfortunately, no separation is possible between the prompt and delayed events, but since only about 10% is the contribution of the prompt fraction, we can assume that the relative mass yield is primarily due to the delayed events. This fission mode is clearly asymmetric (see table 8.4), with a peak to valley ratio smaller than the corresponding value in the 14 MeV neutron-induced fission in ^{238}U .

Theoretical interpretations of the delayed fission are not plentiful. Chultem et al. [301] and

*We have somewhat simplified Bloom's treatment [299] in the present discussion.

Table 8.3

Experimental results for the prompt/delayed fission probability ratio and total fission probability following muon capture. All numbers except [a-d] are from the tabulation of Hadermann and Junker [302]; [a] are from Aleksandrov et al. [250a]; [b], [c] and [d] are from Rushton [377], Diaz et al. [378] and Baertschi et al. [304] respectively.

Nucleus	Fission probability	
	Prompt/delayed	Total
^{232}Th	0.130 ± 0.012 0.064 ± 0.022 [c] 0.073 ± 0.031 [b]	0.018 ± 0.012 0.0043 ± 0.0010
^{233}U	~ 0.17 0.094 ± 0.027 [b] 0.111 ± 0.021 [c]	~ 0.035 [a]
^{238}U	0.072 ± 0.022 [c] 0.080 ± 0.024 [b] 0.071 ± 0.003	0.15 ± 0.06 0.07 ± 0.03 0.070 ± 0.008 0.031 ± 0.007 0.13 ± 0.05 [d]

Nucleus	Fission probability	
	Prompt/delayed	Total
^{237}Np	~ 0.32	~ 0.098 [a]
^{239}Pu	0.43 ± 0.09 0.28 ± 0.04 0.41 ± 0.10	$\begin{cases} 0.74 \pm 0.18, \dots, \\ 0.94 \pm 0.23 \end{cases}$ 0.045 ± 0.006 $\begin{cases} 0.49 \pm 0.12, \dots, \\ 0.70 \pm 0.23 \end{cases}$
^{242}Pu	~ 0.42	~ 0.099 [a]

Table 8.4

Relative mass yields in the muon and 14 MeV neutron induced fission of ^{238}U (after Baertschi et al. [304]).

Product nuclide	Relative mass yield		
	Muon induced fission		14 MeV neutron induced fission
	Run #1	Run #2	
^{91}Sr	1.0	1.0	1.0
^{93}Y		1.2	1.19
^{99}Mo		1.3	1.42
^{111}Ag	0.4	0.4	0.25
^{113}Ag	0.5	0.4	0.28
^{115}Cd	0.3	0.5	0.25
^{143}Ce	0.9	0.9	1.03

Hadermann and Junker [302] have estimated the delayed fission yield assuming that the μ -capture process excites the nucleus to about 15–20 MeV, which then attains an equilibrium state and undergoes fission. The delayed fission rate is then determined by the excitation function $I(Q)$ and the fractional probability for the fission $R(Q)$:

$$\Lambda_f = C \int I(Q)R(Q) dQ, \quad (8.17)$$

Q being the nuclear excitation energy, C is a normalization constant ($= 0.85$). $R(Q)$ equals Γ_f/Γ , where Γ_f and Γ are the fission and total widths.

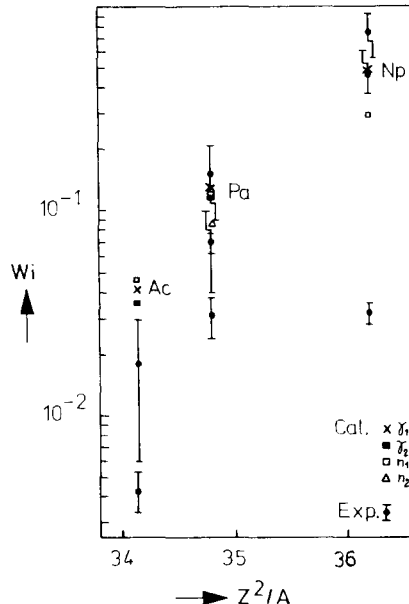


Fig. 8.8. A comparison between experimental and calculated fission probabilities following muon capture in ^{232}Th , ^{238}U , and ^{239}Pu targets, plotted against the fissility parameter Z^2/A . Calculated values are for delayed fission, while, for all targets except ^{239}Pu , the experimental values are total fission probabilities. Legends n_1 , n_2 , γ_1 , γ_2 correspond to different assumptions for neutron and photoreaction cross-section (after Hadermann and Junker [302]).

Hadermann and Junker [302] have used an improved version of the Singer model [269] (§ 8.1.1) to calculate $I(Q)$. They have considered ^{232}Th , ^{238}U and ^{239}Pu targets. Thus, they need the experimental data for $R(Q)$ for the reactions $n + (A - 1, Z - 1)$ and $\gamma + (A, Z - 1)$ in the energy regime $Q \leq 30$ MeV, which are unavailable. Hence they have used the available data from the neighbouring nuclei and made suitable extrapolations [302]. Their calculated delayed fission probabilities are presented in fig. 8.8, where these are plotted against the fissility parameter Z^2/A . The calculated delayed fission probabilities show expected monotonic increase with Z^2/A , and are in reasonable agreement with experiments other than those by Polikanov et al. In general, the photo-reaction data yield better agreement than the neutron data.

8.3.3. Future fission research with muons

Prompt fission looks more promising in understanding fission dynamics due to its relative simplicity. The possibility of determining nuclear isomeric lifetimes reflecting the effects of the augmentation of the fission barrier in presence of the muon, and the fate of the muon *after* the prompt fission should be challenging to investigate. The systematic low value of the fission probability obtained by Polikanov et al. [301] merits a careful experimental scrutiny. Comparison of the non-induced fission with photo- and neutron-fission is now only at a qualitative stage. This hopefully would reach a level of quantitative understanding*.

*Relationship of muon-induced fission to other mechanisms of inducing fission at similar excitation energies is under investigation by Mukhopadhyay et al. [302].

8.4. Radiative muon capture

The reaction

$$\mu^- + p \rightarrow n + \nu_\mu + \gamma, \quad (8.18)$$

and its analogs in nuclei are rarer, compared to the ordinary (photonless) capture reaction, and very little is experimentally known about these processes because of their low rates. Many exciting developments are expected in their studies at the meson factories with presently available high muon intensities.

The radiative lepton capture reaction was first studied theoretically for electrons by Oppenheimer, Morrison and Schiff [305]. Huang, Lee and Yang [306] discussed the process, pointing out important manifestations of parity violation in the weak interaction. Manacher and Wolfenstein [307] emphasized the importance of induced form factors entering through various contributions that arise as a consequence of the gauge invariance. Alder and Dothan [308] used the Low procedure [309] to relate the radiative muon capture matrix elements to pion photo-production amplitudes and elastic weak form factors.

While early theoretical attentions [310] were focused on the radiative muon capture in proton, it was obvious that the extremely low branching ratio ($\sim 10^{-4}$ of the non-radiate strength) and absolute yield would make proton an unlikely target for experiments. Thus, the theoretical efforts naturally shifted to heavier nuclei [311–313]. Rood, Tolhoek and collaborators [311] have made an extensive study of $A = 4n$ (n integer) nuclei. For experimental reasons, most calculations have been done by summing over final nuclear states. Beder [314] has examined recently the partial radiative transition ${}^3\text{He} \rightarrow {}^3\text{H}$ and found its study experimentally feasible at meson factories.

Experimentally, the process (8.18) was first detected at CERN by Conforto et al. in the iron target [315]. This experiment established the expected branching ratio of $\sim 10^{-4}$ to the radiative channel compared with the normal capture, confirmed later by Chu et al. [316] in copper. Subsequently, the radiative muon capture experiments were done by Conversi et al. [317] at CERN, and later by Di Lella, Hammerman and Rosenstein [318] at Nevis, using ${}^{40}\text{Ca}$ nucleus as a target*. A variety of experiments are under way at meson factories, with the hope of studying experimentally the partial radiative transitions such as ${}^3\text{He} \rightarrow {}^3\text{H}$, ${}^{12}\text{C} \rightarrow {}^{12}\text{B}_{\text{g.s.}}$ for the first time, and looking at the radiative processes in nuclear targets throughout the periodic table [319].

8.4.1. Observables in the radiative muon capture**

Denoting the probability of a radiative muon capture transition from an initial nuclear state $| a \rangle$ to a final nuclear state $| b \rangle$ by $P_{ab}(K, \nu, \lambda, P_\mu)$, K, ν being photon and neutrino momenta, λ the circular polarization of the photon, P_μ muon polarization, we have

$$P_{ab}(K, \nu, \lambda, P_\mu) dK d\Omega_K d\Omega_\nu = \frac{e^2}{4(2\pi)^4} |\phi_\mu|_{av}^2 \sum_{\text{spin}} K(K_m - K)^2 |M_{ba}|^2 dK d\Omega_K d\Omega_\nu, \quad (8.19)$$

where

$$K_m = m_\mu - (E_b - E_a), \quad M_{ba} = \langle b, \nu, K | H^r | a, \mu \rangle. \quad (8.20)$$

*A remeasurement by the William and Mary group of the photon asymmetry, in the radiative muon capture by ${}^{40}\text{Ca}$, is nearing completion at SREL (March 1976).

**This discussion is after Rood [C15].

K_m is the maximum photon energy in the transition $a \rightarrow b$, M_{ba} is the matrix element of the radiative muon capture Hamiltonian H^r .

If the final nuclear states are summed over, we can introduce a function $W(x, \hat{K}, \hat{\nu}, \lambda, P_\mu)$ defined by

$$W(x, \hat{K}, \hat{\nu}, \lambda, P_\mu) dx d\Omega_K d\Omega_\nu = \sum_b P_{ab}(K, \nu, \lambda, P_\mu) dK d\Omega_K d\Omega_\nu, \quad (8.21)$$

where $x = K/K_m$; $K_m = m_\mu - \langle E_b - E_a \rangle_{av}$, the subscript av indicating average over all b's. Below we indicate the arguments of W in eq. (8.21) by β .

Some interesting observables can now be written in terms of the function $W(\alpha)$. Thus, the *shape of the photon spectrum* is given by:

$$N(x) dx = \sum_\lambda \int d\Omega_K d\Omega_\nu W(\beta) dx. \quad (8.22)$$

Integration over x yields the *total rate for radiative muon capture* Λ_c^r :

$$\Lambda_c^r = \int_0^1 N(x) dx. \quad (8.23)$$

The *photon-neutrino directional correlation* is

$$W(x, \theta_{\nu\gamma}) = \sum_\lambda \int d\Omega_{P_\mu} W(\beta). \quad (8.24)$$

The *angular distribution of the photons with respect to the muon polarization axis* is similarly

$$W(x, \theta_{\mu\gamma}) = \sum_\lambda \int d\Omega_\nu W(\beta) \sim 1 + \alpha P_\mu \cos \theta. \quad (8.25)$$

The *circular polarization* of the photons is given by

$$P_\gamma(x) = \frac{\int \int d\Omega_K d\Omega_\nu (W_+ - W_-)}{\int \int d\Omega_K d\Omega_\nu (W_+ + W_-)}, \quad (8.26)$$

where W_\pm are the values of $W(\beta)$ for $\lambda = \pm 1$. In eqs. (8.24) and (8.25), $\theta_{\nu\gamma}$ and $\theta_{\mu\gamma}$ are $\not{\epsilon}(\nu, K)$ and $\not{\epsilon}(P_\mu, K)$, respectively. Notice that, for a partial transition $a \rightarrow b$, there is no sum over b in eq. (8.21), x is defined as K/K_m , and all the definitions (8.22)–(8.26) are valid: Λ_c^r then indicates the *partial radiative capture rate* $\Lambda^r(a \rightarrow b)$. In the earlier works, the studies of angular correlations and circular polarization were emphasized for manifesting parity violation in the weak interaction. Currently, the importance of radiative muon capture is to shed light on induced form factors, particularly pseudoscalar (and possibly tensor) terms, on which many of these observables are strongly dependent.

The Hamiltonian H^r in eq. (8.20) is obtained by considering the relevant Feynman diagrams for the radiative process and doing a Foldy–Wouthuysen transformation, as in the case of ordinary muon capture. This is a straightforward, but tedious procedure leading to a very complicated expression for H^r which would be omitted here*.

*The FW transformation procedure and much of the subsequent algebra can be handled via computer, using algorithms such as Schoonschip [321] developed by Veltman and collaborators [322]. See Rood [C15] for algebraic forms of H^r and Rood et al. [311] for unimportance of certain terms for consideration of the high-energy side of the photon spectrum.

8.4.2. Some theorems

For radiative muon capture in proton, we state two theorems without proof.

Theorem 1 (Cutkosky [320], Huang, Lee and Yang [306]): *For pure V–A interaction the photon spectrum, circular polarization and angular correlation, with respect to neutrino, are the same as for the non-radiative emission of a positive lepton in the ultra relativistic limit ($v \rightarrow c$).*

In particular, it can be shown that

$$\alpha_\gamma = P_\gamma(x) = 1 \quad (8.27)$$

for pure V–A interaction.

As pointed out by Manacher and Wolfenstein [307], the Cutkosky theorem is violated by the induced form factors and hence is not very useful, except to demonstrate the presence of these terms.

Theorem 2 (Adler and Dothan [308])*: *Radiative muon capture amplitudes, up to contributions linear in the leptonic four-momentum transfers and photon four-momentum, can be given in terms of the pion photoproduction amplitudes and elastic weak form factors.*

The contributions to the radiative muon capture in the Adler–Dothan procedure are the radiation by the muon itself (fig. 8.9a), and the radiations from the hadrons (figs. 8.9b–j). The latter consist of the following: the nucleon Born graphs (figs. 8.9b–e); radiative virtual pion decay (figs. 8.9f–h); the “sea-gull” graph (fig. 8.9i); and remaining terms (represented by fig. 8.9j) linear in pion or photon four-momenta, needed to satisfy the vector and axial-vector divergence conditions. The structure term in fig. 8.9h cannot be determined in the Adler–Dothan procedure.

8.4.3. Comparison of theory and experiment

Basic theoretical conclusions for the inclusive (total) radiative capture processes are the following: i) The ratio of radiative to non-radiative capture rates is $\sim 2.3 \times 10^{-4}$ for ^{16}O and ^{40}Ca , and $\sim 4 \times 10^{-4}$ for proton assuming the PCAC estimate of g_P/g_A [311]. ii) The high energy ($E_\gamma > 50$ MeV) part of the photon spectrum, the $\gamma-\nu$ correlation, asymmetry and circular polarization of the photons are all sensitive to the pseudoscalar (and tensor) form factors. iii) Theoretical results, taken relative to the non-radiative capture, seem to be insensitive to nuclear structure effects. iv) The closure approximation involves the unknown parameter K_m ; the spectrum is sensitive to it (shape is proportional to K_m^6), while the angular correlation is essentially independent of K_m .

Earlier experiment in ^{40}Ca by Conversi et al. [317] has been vitiated by a large neutron contamination; it will not be discussed here any further. Di Lella et al. [318] have redone the experiment in ^{40}Ca and have found the best fit to the experimental data with the theoretical spectrum of Rood and Tolhoek by using $K_m = 89.4$ MeV and $g_P = -5.9 g_A$, in serious disagreement with the PCAC prediction for g_P (fig. 8.10). The experimentally obtained radiative branching ratio is $(1.14 \pm 0.09) \times 10^{-4}$, about 50% of the theoretical value.

The photon asymmetry parameter α_γ has been measured by Di Lella et al. [318] for photon energies between 57 MeV and 75 MeV:

*Application of the Low procedure to the complex nuclei needs a careful treatment of the variation of nuclear form factors with momentum transfer, which is non-trivial [321].

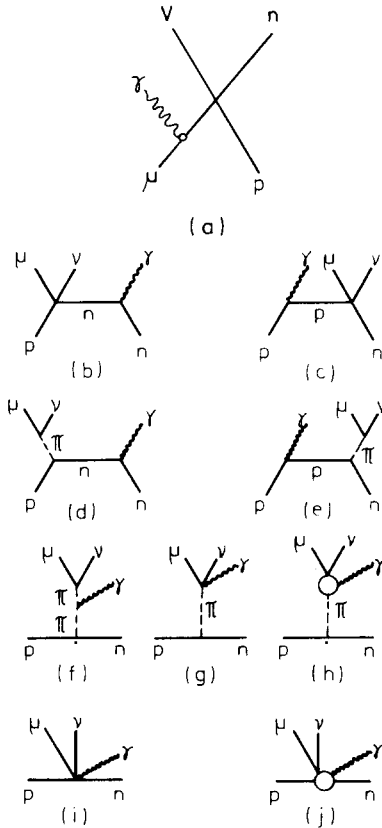


Fig. 8.9. Contributions considered by Adler and Dothan [308] for radiative muon capture by protons. (a) represents the radiation by the muon, and (b–j) are the radiations by the hadrons. (b–e) are the nuclear Born contributions; (f–h) represent radiative decay of the virtual pion; (i) and (j) respectively describe the “seagull” term and the remaining effects needed for satisfying CVC and PCAC constraints.

$$\alpha_\gamma = (-0.32 \pm 0.48) - (0.82 \pm 0.12) \alpha_n, \quad (8.28)$$

where α_n is the asymmetry due to possible neutron contamination. As pointed out in §8.1.3, α_n is not experimentally known above ~ 50 MeV. If we take the trend of Sundelin and Edelstein [237] and theoretical predictions that $\alpha_n \geq 0$, we then have

$$\alpha_\gamma \leq -0.32 \pm 0.48, \quad (8.29)$$

compared with the Rood–Tolhoek value of +0.75 [311] (averaged over the desired photon energy range). The improved calculation of Rood et al. [311] gives values *higher* than +0.75 in this photon energy range. It is clear that the standard theory is in serious trouble here.

There are many speculations as to the nature of the trouble [314, 323, 324] including possible limitations of the impulse approximation procedure itself. Ohta claims to obtain a desirable reduction of the theoretically obtained radiative branching ratio, and a correct photon spectrum by considering $N^*(1236)$ excitations [324]. However, the accuracy of this claim has been disputed [347]. If the role of $N^*(1236)$ turns out to be as big as this, this will be indeed spectacular. According to Fearing [323], α_γ is difficult to estimate theoretically, since the contributions of $O(M^{-2})$ to α_γ would have to be taken into account.

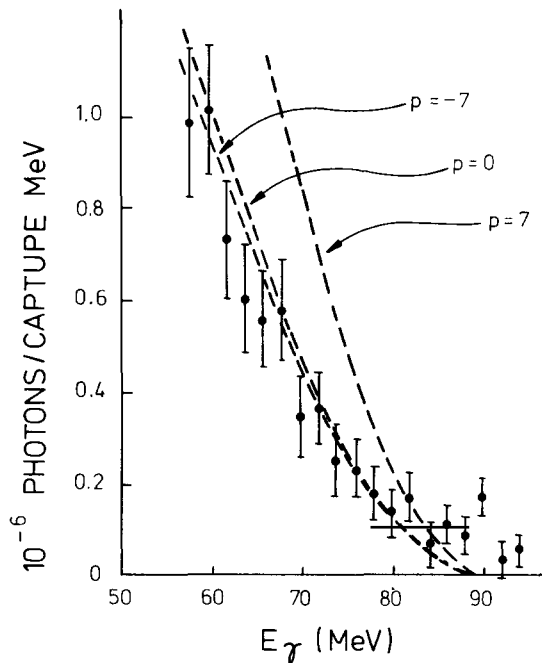


Fig. 8.10. Experimental photon spectrum for the radiative muon capture in ^{40}Ca (Hamerman and Rosenstein [318]) and the Rood-Tolhoek fit to the experiment. Notice that $\rho = 7$ corresponds to the PCAC estimate of the pseudoscalar term.

8.4.4. New theoretical and experimental horizons for radiative muon capture studies

It is clear from the above discussion that fresh angles are necessary to understand the reasons behind the present discrepancy between theory and experiment. Two ideal experiments *from the theoretical point of view* are to investigate the reactions



Here the theoretical advantages are obvious: closure approximation is not needed and nuclear physics uncertainties are minimal; uncertainties due to the hyperfine effects are unimportant in ^3He (§5) and absent in ^{12}C . Finally, in ^{12}C , the widely-believed hypothesis that the interesting observables in radiative capture are largely insensitive to uncertainties in nuclear wave functions can be tested very easily, by using the jj -coupling model and realistic models (§5). Thus any disagreement of the experiments *with the standard theory* will be significant.

These two experiments appear feasible [319]. The UBC-TRIUMF group plans to study the reaction in ^3He using lead-glass Čerenkov detectors and large NaI counters [319]. The Čerenkov detectors will not register neutrons and hence a comparison of the spectra obtained by the two detectors will yield a good idea of the neutron contamination.

The role of isobars in the radiative muon capture, advocated by Ohta [324] and Beder [314] in somewhat different circumstances, deserves a careful theoretical scrutiny. In particular, Ohta's treatment does not discuss possible nuclear modification of the time component of the axial vector current.

8.5. Exotic muon capture reactions

In this subsection, we discuss the possibility of two exotic muon capture reactions:

$$\mu^- + (Z, A) \rightarrow e^- + (Z, A), \quad (8.31)$$

$$\mu^- + (Z, A) \rightarrow e^+ + (Z - 2, A). \quad (8.32)$$

These two reactions give us crucial tests of the assignment of leptonic quantum numbers \mathcal{L}_i , defined below.

If we assign $\mathcal{L}_\mu = +1$ to μ^- and ν_μ , -1 to μ^+ and $\bar{\nu}_\mu$, $\mathcal{L}_e = +1$ to e^- and ν_e , -1 to e^+ and $\bar{\nu}_e$, and $\mathcal{L}_e = \mathcal{L}_\mu = 0$ to the rest of the elementary particles, we can devise the following lepton conservation laws [325]: i) $\sum \mathcal{L}_e$, $\sum \mathcal{L}_\mu$ separately conserved (*additive law*); ii) $\sum (\mathcal{L}_e + \mathcal{L}_\mu)$, $(-)^\Sigma \mathcal{L}_e$, $(-)^\Sigma \mathcal{L}_\mu$ separately conserved (*multiplicative law*)*; iii) $\sum (\mathcal{L}_e + 2 \mathcal{L}_\mu)$ conserved; iv) $\sum (\mathcal{L}_e - \mathcal{L}_\mu)$ conserved (Konopinski-Mahmoud (KM) scheme [326]). The reaction (8.31) is forbidden by all of the conservation laws (i) to (iv), while the reaction (8.32) is *only* allowed in the scheme (iv) – the KM scheme. Notice that while the process (8.31) is a “first-forbidden” one in scheme (iii) [viz., $|\Delta \mathcal{L}| = 1$, where $\mathcal{L} = \sum (\mathcal{L}_e + 2 \mathcal{L}_\mu)$], the process (8.32) is “third-forbidden” ($|\Delta \mathcal{L}| = 3$). The KM scheme is the most economical since it requires only one effective lepton charge (+1 for e^- , ν_e , μ^+ , $\bar{\nu}_\mu$, -1 for e^+ , $\bar{\nu}_e$, μ^- , ν_μ) and the multiplicative scheme is the least restrictive.

The reaction (8.31) has been searched by Conversi et al. [327] in a spark chamber experiment at CERN. The branching ratio in Cu has recently been reinvestigated by the VPI group [330], who obtain the following limit [B11a]:

$$R(\mu^- + Cu \rightarrow e^- + Cu)/R(\mu^- + Cu \rightarrow \nu_\mu + Ni) < 1.9 \times 10^{-8}. \quad (8.33)$$

This tests the absence of $\mu \rightarrow e$ transition at about the same level as $\mu^+ \rightarrow 2e^+ + e^-$, but worse than the test in the $\mu \rightarrow e + \gamma$ decay. The limit (8.33) can be substantially improved. The basic background to the reaction (8.31) is the radiative muon capture reaction $\mu^- + Z \rightarrow \nu_\mu + [Z - 1] + \gamma$, the photon converting to an (e^+e^-) pair. The maximum electron energy in the radiative conversion process is lower than the electron energy in the reaction (8.31) by an amount $(m_{Z-1} + 2m_e - m_Z)$. This quantity is maximum in the carbon region (for ^{12}C , it is 14.39 MeV). Using the Feinberg-Weinberg [325a] estimate for the (Z, A) dependence of the cross-section for the reaction (8.31), it appears that ^{12}C is only half as effective as Cu, which has the maximum cross-section. Other favourable targets are Ne, Mg, Al, Mn, and I, on the basis of energy separation between background and “interesting” electrons.

The reaction (8.32), discussed theoretically first by Okun' and collaborators [325] and more recently by Kisslinger [328], Shuster and Rho [329], resembles neutrinoless double- β decay, except for the fact that it is a (μe) process contrasted with the latter, which is an (ee) process.

Bryman et al. [330] have studied the reaction (8.32) in copper and determined the following branching ratio:

$$R(\mu^- + Cu \rightarrow e^+ + Co)/R(\mu^- + Cu \rightarrow \nu_\mu + Ni) < 2.6 \times 10^{-8}. \quad (8.34)$$

These authors have observed one event at momentum 89.9 ± 3.5 MeV/c (fig. 8.11), which is consistent with the process (8.32), the radiative muon capture background being expected to

*The detection of the decay $\mu^+ \rightarrow e^+ + \bar{\nu}_e + \nu_\mu$ (together with the “normal” one to $e^+ + \nu_e + \bar{\nu}_\mu$) will signal a preference for the multiplicative law. See, for an excellent discussion of the topics in §8.5, the contribution of Frankel in [A13]. See the article of Baltay in [A13] for the tests of lepton number selection rules via the neutrino reactions.

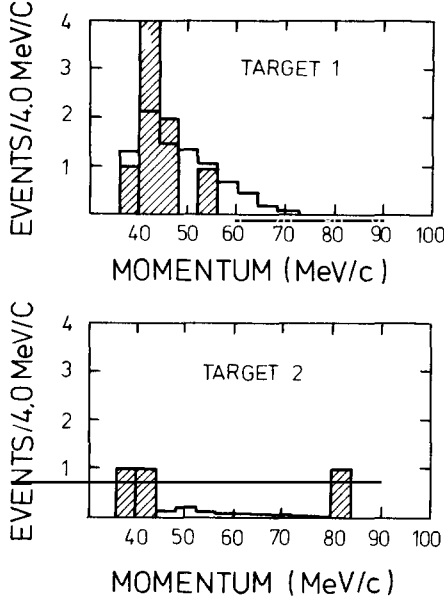


Fig. 8.11. Search for the reaction $\mu^+ + \text{Cu} \rightarrow e^+ + \text{Co}$ by Bryman et al. [330]. Observed positron spectra for two target runs are shown hatched, and the calculated spectra for positrons due to conversion of radiative muon capture photons in the energy regime $50 < E_\gamma < 91$ MeV are shown in the solid lines. Notice the discrepancy with background in target 2, for one event at momentum ~ 84 MeV/c.

contribute at a level of 10^{-2} event in the Rood-Tolhoek theory. The biggest uncertainty in this experiment for a positive identification of an event is associated with the subtraction of the radiative capture background. If the reaction rate is as large as the positive identification of the event of Bryman et al. would indicate, a proposed experiment at SIN [330a] might be expected to see many of them. Notice that the positron end point of the radiative background is lower than the energy of the positron in the reaction (8.32) by the amount $(m_{Z-1} - m_{Z-2})$. One should, therefore, choose isotopes with largest $m_{Z-1} - m_{Z-2}$ difference. If separated isotopes are not available, ^{58}Ni appears to be the best candidate (see Frankel in [A13]).

Assuming with Kisslinger [328] that, in absence of strong interaction effects, there is only a pion-lepton isotensor Lagrangian of the form

$$\mathcal{L}_\pi^{\Delta T=2} = \frac{-if}{m_\pi} \phi^- \partial_\mu \phi^+ L_\mu^+, \quad (8.35)$$

Rho and Shuster [329] obtain the following Lagrangian for the reaction $p + p + \mu^- \rightarrow n + n + e^+$:

$$\begin{aligned} \mathcal{L}^{\Delta T=2} \sim & \frac{-iG_1}{\sqrt{2}m_\pi} (\bar{\psi}_\mu \gamma_\nu \gamma_5 T_{-2}^2 \psi_N + \bar{\psi}_N \gamma_\nu \gamma_5 T_{-2}^2 \psi_\mu) F_{\mu\nu}^+ - \frac{iG_2}{\sqrt{2}m_\pi} \bar{\psi}_\mu T_{-2}^2 \psi_\nu F_{\mu\nu}^+ \\ & - \frac{iG_3}{\sqrt{2}} \bar{\psi}_\mu \gamma_\nu T_{-2}^2 \psi_\mu L_\nu^+ + \text{h.c.}, \end{aligned} \quad (8.36)$$

where $F_{\mu\nu} = \partial_\mu L_\nu - \partial_\nu L_\mu$, $L_\mu = \bar{\psi}(e^-)\gamma_\mu(1 + \gamma_5)\psi(\mu^+)$, T_{-2}^2 is the appropriate charge-changing operator, G_i 's are suitable coupling constants. The relevant Feynman diagrams for the process are

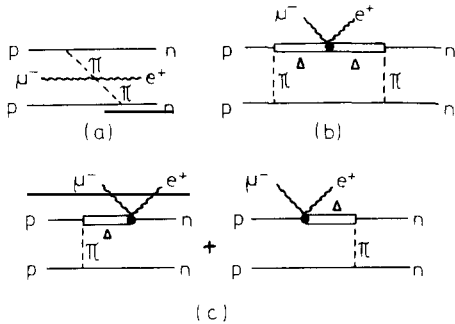


Fig. 8.12. Mechanisms for the reaction $\mu^- + p + p \rightarrow e^+ + n + n$, considered by Shuster and Rho [329].

given in figs. 8.12a–c. Of these, the amplitude corresponding to fig. 8.12a vanishes in nuclei due to the antisymmetry of the nuclear wave functions and the matrix elements for figs. 8.12b and c are roughly

$$M_b \approx |\alpha_\Delta|^2 G', \quad M_c \approx 2 |\alpha_\Delta| G_i, \quad (8.37)$$

where $|\alpha_\Delta|^2$ is the probability of exciting a virtual $\Delta(1236)$ resonance in nuclei, a model-dependent quantity, roughly of the order of a few per cent [328], G' is a combination of G_2 and G_3 .

Assuming the mean momentum transfers for the "exotic" and normal channels to be 60 and 80 MeV/c, respectively, Rho and Shuster [329] obtain, for ^{65}Cu the following branching ratio*

$$R = 3.5 \times 10^{-2} (G_1/G)^2. \quad (8.38)$$

Using the experimental branching ratio of (8.34), we infer:

$$G_1 \leq 9 \times 10^{-4} G, \quad (8.39)$$

indicating that the isotensor weak interaction is not favourable. The limit on the isotensor electromagnetic coupling constant G_T , obtained from $\gamma p \rightarrow \Delta^+$ and $\gamma n \rightarrow \Delta^0$ reactions [329], is $G_T \leq 7 \times 10^{-3}$, the upper limit being about an order of magnitude larger than that suggested by (8.39). Thus, a positive experimental identification of the reaction (8.32) will signal the discovery of a new type of weak interaction, with a coupling constant at least three orders of magnitude lower than the Fermi constant.

9. Beyond the impulse approximation

So far we have only emphasized the framework of the naive impulse approximation [IA] (§ 4) in discussing nuclear muon capture processes and have generally found reasonable agreement between theory and experiment in light nuclei, where the nuclear physics inputs are fairly certain. Naturally attempts have been made to go beyond the IA, or at least to estimate the corrections to it.

*Rho and Shuster use closure and the Fermi gas model, neglecting terms of $O[(N - Z)/A]$, in evaluating the rate of $\mu^- \rightarrow e^+$ reaction. Note that the factor multiplying $(G_1/G)^2$ in eq. (8.38) differs from Kisslinger's corresponding term by *four orders* of magnitude, two of which are due to difference in scalar and vector couplings and other two due to Kisslinger's neglect of additional Δ contributions, considered by Rho and Shuster.

The efforts to go beyond the IA are roughly the following: i) calculating explicitly meson exchange corrections; ii) retaining the framework of the impulse approximation but using effective hadron form factors, different from those for the free hadrons, to be determined in some “renormalization” models; iii) using directly the *nuclear* form factors in the framework of the so-called “elementary particle” model of the nucleus. Approaches (i) and (ii) are obviously interrelated. Our knowledge in this domain is not yet definitive and we make no attempt to make an exhaustive survey of the efforts. Only some basic ideas are indicated here.

9.1. From relativistic to non-relativistic matrix elements

As an example of the difficulties that one encounters in describing the interaction of a nucleon *inside* a nucleus with a lepton, we consider the problem of the Foldy–Wouthuysen (FW) reduction of the weak Lagrangian. For a free nucleon, the canonical FW transformation [77] is straightforward and the resultant FW series converges rapidly. However, for a nucleon Hamiltonian H_D with interaction terms:

$$H_D \sim \alpha \cdot p + \beta M + \sum_a \mathcal{V}_a \mathcal{C}_a, \quad (9.1)$$

where α and β are Dirac matrices and the last term in eq. (9.1) is a combination of interaction coefficients \mathcal{V}_a and γ matrices \mathcal{C}_a [331], the convergence of the FW series is no longer guaranteed to be rapid, and is, in general, dependent on the magnitudes of interaction terms in H_D . Thus the construction of an effective Hamiltonian H_{eff} , to be used in the IA for nuclei, becomes a non-trivial task*. Hence the use of an H_{eff} , obtained by the FW transformation for free nucleons, as we have done before, involves unknown corrections (“relativistic” corrections).

There are some matrix elements that do not involve uncontrolled relativistic uncertainties. Miller and the author [331] have discussed some examples of this type. Thus the Fermi (F) and the Gamow–Teller (GT) matrix elements at zero momentum transfer, in the relativistic and non-relativistic representations, indicated respectively by the subscripts R and NR, are given by:

$$I_R^\delta = \int \bar{\psi}_{jm}^\omega(r) A^\delta \psi_{jm'}^\omega(r) d^3r, \quad (9.2a)$$

$$I_{NR}^F = \delta_{mm'}, \quad I_{NR}^{GT} = C_m^{j-1} \bar{m}' - m' \langle j\omega \parallel \sigma \parallel j\omega \rangle, \quad (9.2b)$$

where $A^F = \gamma^0$, $A^{GT} = \gamma\gamma^5$, ψ_{jm}^ω are the eigenfunctions of the Dirac Hamiltonian H_D , j and m are the total single-nucleon angular momentum and its z-projection; the quantum number ω is related to parity π by the equation $\pi = (-)^{j+\omega/2}$; σ is the two-dimensional Pauli operator. We have suppressed in eqs. (9.2a, b) the trivial isospin factors. It is easy to evaluate I_R^δ explicitly [331]:

$$I_R^F = \delta_{mm'}, \quad I_R^{GT} = I_{NR}^{GT}(1 - N_S D_{j\omega}), \quad (9.3)$$

where N_S is the normalization factor for the small radial component of the nucleon four-spinors and $D_{j\omega}$ equals $[1 + \{j/(j+1)\}^{-\omega}]$, N_S and $D_{j\omega}$ being both positive quantities. Thus *the relativistic correction to the Fermi matrix element I_{NR}^F is zero, and the Gamow–Teller matrix element*

*Problems of analogous type arise if one tries to make an FW reduction of the γ_5 Lagrangian for the pion–nucleus interaction (see, for example, Barnhill [332]). See also a discussion by Krajcik and Foldy [333] on the electromagnetic interaction with an arbitrary loosely bound system, particularly in the context of the low-energy theorem for Compton scattering and the Drell–Hearn–Gerasimov sum rule.

is always reduced with respect to its non-relativistic value I_{NR}^{GT} . The quantity N_S is insensitive [331] to the details of the interaction terms in eq. (9.1); hence the relativistic corrections to the GT matrix element are largely model-independent and are of the order of a few per cent.

Unfortunately the same need not be true for any operator in place of A^6 in eq. (9.2a). Operators that connect nucleon–antinucleon spinors [331] have relativistic corrections sensitive to the interaction terms in H_D . In some models for ψ_a that cannot be ruled out currently, these corrections may become quite large. These difficulties also affect attempts to determine the effective axial vector form factor in mirror β decays in a model-independent way, by using the magnetic moments of mirror nuclei as determinants of the GT matrix element [334].

As reflected in the discussions above, the determination of the relativistic corrections to the free FW series is uncertain at present in the context of the muon capture. There is, at present, no clear-cut way of isolating these corrections from so-called “meson exchange” corrections discussed below.

9.2. Explicit calculation of meson exchange corrections

The calculation of meson exchange corrections* to the weak and electromagnetic processes at low momentum transfer has become quite a standard procedure [335]. Thus the discrepancy between the experimental ft value of the β decay of 3H and its theoretical estimate in the impulse approximation, has been explained by the meson exchange corrections [336]. Similarly these corrections play an important role in the reaction $p + p \rightarrow d + e^+ + \nu_e$, relevant for the production of solar neutrinos [337].

Dautry, Rho and Riska [108] have extended the Chemtob–Rho procedure [335] to estimate the meson exchange corrections for the reaction $d + \mu^- \rightarrow 2n + \nu_\mu$, considering the contributions of the graphs of pionic range (figs. 9.1a–c). They estimate the doublet capture rate Λ_D to be 400 s^{-1} with exchange corrections, and 383 s^{-1} without them, a 4% contribution of the meson exchange effects. They show that the extraction of the singlet scattering length a_{nn} is sensitively dependent on the proper treatment of exchange corrections (fig. 9.1d).

Ohta and Wakamatsu [339] conclude that the one-pion exchange current effectively “renormalizes” the axial vector and induced pseudoscalar form factors, with the effect of decreasing the total muon capture rate and the radiative to ordinary muon capture branching ratio by about 15%. Their renormalization effects are similar to the results of Ericson et al. [340], obtained earlier in a different way (see below).

9.3. Nuclear renormalization of the hadronic weak form factors

Despite possible nuclear structure sensitivity of the meson exchange corrections [341], attempts have been made to absorb these corrections by replacing the free weak hadron form factors with effective ones and to retain the framework of the impulse approximation, in describing the lepton–nuclear interaction. The approaches proposed are mostly in the domain of nuclear matter, and definitive answers in the context of specific transitions in the finite nuclei are still to come. Form factors generally examined are the axial vector ones.

*See §9.3.3 for possible “second-class” meson exchange effects.

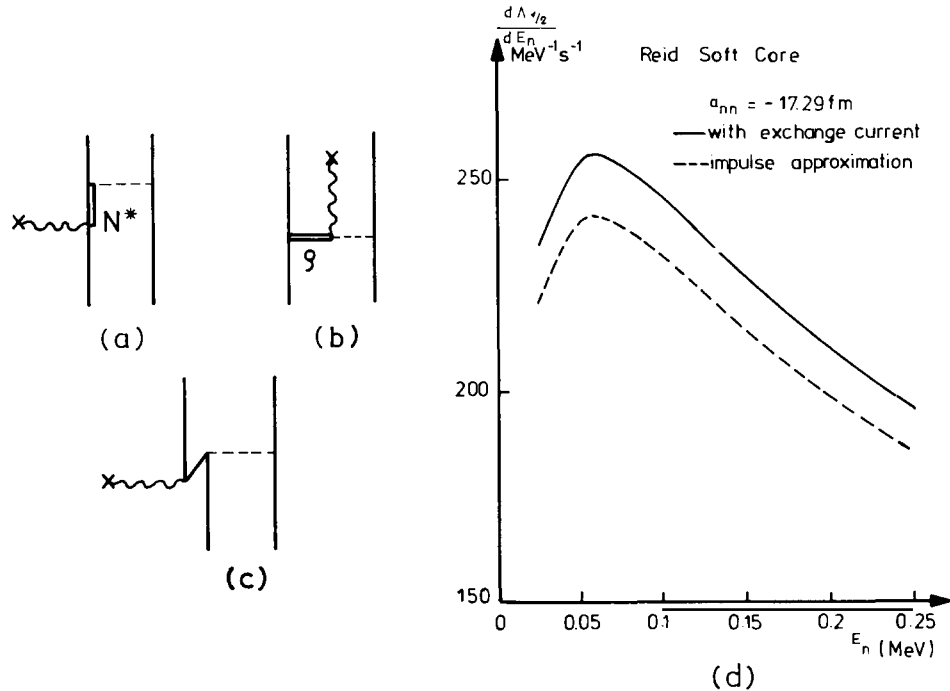


Fig. 9.1. (a–c) Meson exchange contributions of pionic range considered by Dautry, Rho and Riska [108]. (d) The effect of meson exchange correction on the extraction of the singlet scattering length a_{nn} from the muon capture in deuteron (Dautry et al. [108]).

9.3.1. Effective axial vector form factor

Ericson [342] first discussed the possibility of obtaining an effective axial vector form factor g_A^{eff} at zero momentum transfer, by considering the nuclear modification of the Adler–Weissberger sum rule (AWSR) [59]. In the nucleon case, we recall, the AWSR provides a dramatic test for the chiral current algebra approach and successfully accounts for the observed renormalization of the g_A/g_V at zero momentum transfer. For nuclei, the important step consists in writing a dispersion relation for the isospin antisymmetric *pion–nucleus* scattering amplitude, in which the effects of the various nuclear excited states in the unphysical region are simulated by an effective pole [342a]. One then obtains a relation connecting the effective pion–nucleon coupling $g_{\pi NN}^{\text{eff}}$, the pion decay constant f_π , and the dispersion integral over the π -nuclear cross-section – the nuclear analogue of the Weinberg–Tomozawa dispersion relation in the pion–nucleon case [343]. This approach finally yields [342]:

$$g_A^{\text{eff}}(0)/g_A(0) = g_{\pi NN}^{\text{eff}}/g_{\pi NN} \approx 0.92, \quad (9.4)$$

for nuclei around $A \sim 17$, thus predicting a quenching of the effective axial vector coupling constant $g_A^{\text{eff}}(0)$, compared to the free nucleon value $g_A(0)$. The estimate (9.4) is an average over many nuclear states, and does not imply a strict value of g_A^{eff} for a given nuclear transition.

The quantity $g_A^{\text{eff}}(0)$ has also been calculated in the pion–nuclear optical potential framework by Ericson and collaborators [340], Rho [344], Ohta and Okamatsu [339]. Ericson et al. emphasize that a pion source inside a nuclear medium has its “strength” appreciably altered in much

the same way, as the strength of an electric dipole located in a hollow cavity within a dielectric medium gets “renormalized” in the electrostatics (the Lorentz–Lorenz effect [345]).

The arguments of Ericson et al. can be summarized as follows: In absence of any interaction, the free pion field in the coordinate space is given in the usual Yukawa form:

$$\phi_0(x) = \sqrt{2} \frac{g_{\pi NN}}{2M} \sigma \cdot \nabla \frac{\exp(-m_\pi x)}{x}. \quad (9.5)$$

This is characterized by the free π –N coupling constant $g_{\pi NN}$ and the range of the interaction (via the free pion mass m_π). Considering a p-wave pion interaction with the “spectator” nucleons in infinite nuclear matter, the pion field $\phi(x)$ gets a modified coupling constant $g_{\pi NN}^{\text{eff}}$ and a modified pion mass m'_π :

$$\phi(x) = \sqrt{2} \frac{g_{\pi NN}^{\text{eff}}}{2M} \sigma \cdot \nabla \frac{\exp(-m'_\pi x)}{x} \quad (9.6)$$

where

$$g_{\pi NN}^{\text{eff}} = g_{\pi NN}(1 + \alpha_0)^{-1}, \quad m'^2_\pi = m_\pi^2(1 + |\alpha_0|)^{-1}. \quad (9.7)$$

The parameter α_0 is given in terms of the p-wave π –N scattering volume c_0 and the nuclear matter density ρ_0 :*

$$\alpha_0 = -4\pi c_0 \rho_0. \quad (9.8)$$

One can then use an analog of the Goldberger–Treiman relation to obtain an effective value of $g_A^{(0)}$.

Equations (9.7), however, are not final. Inclusion [345] of short-range corrections leads to a quenching of the $g_{\pi NN}$ and $g_A(0)$ in the nuclear medium (Lorentz–Lorenz effect):

$$g_A^{\text{eff}}(0) = g_A(0) \left[1 + \frac{\frac{1}{3}\alpha_0}{1 - \frac{1}{3}\alpha_0} \right] = 0.76g_A(0), \quad (9.9)$$

putting the numerical value of $\alpha_0 \approx -0.9$ [347]. Rho and others [344, 339] use the Δ (isobar)-hole model of the pion-nuclear optical potential, developed by Barshay et al. [346], in which the optical potential is represented by a sum of the Δ -hole bubble diagrams, with the one-pion exchange contribution subtracted out. They obtain the same result as eq. (9.9).

Notice that the result (9.9) is applicable only for infinite nuclear matter. Rho [344] has given a rough estimate as to how the quenching will go as a function of A . He replaces the parameter α_0 by the quantity α given by

$$\alpha = \alpha_0 \rho / \rho_0 \quad (9.10)$$

where $\rho = 2K_F^3/3\pi^2$, K_F the Fermi momentum, being measured by quasi-elastic electron scattering. This gives, for ^{12}C , a quenching of 15% from the elementary particle value of $g_A(0)$, and a quenching of 22% in $A \sim 60$. Rho expects this procedure to be reasonable only for $A \gtrsim 100$. For light nuclei, there may be additional surface corrections [344] and this approach is not reliable. Eq. (9.10) is rigorously also a nuclear matter recipe.

*The value of c_0 , extrapolated to zero pion energy, is $\sim 0.15 m_\pi^{-3}$, ρ_0 is $\sim 0.48 m_\pi^3$. Thus α_0 is -0.9 .

Ericson et al. [347] have also examined the renormalization for finite nuclei using a simple model, having one active nucleon in an infinitely thin spherical shell. The core nucleons, in such a model, are uniformly distributed in a sphere of radius R . The renormalized values of g_A and g_P , the former at momentum transfers $q = 0$ and $100 \text{ MeV}/c$, are depicted in figs. 9.2a–c. In heavy nuclei, $g_A(0)$ is quenched from the elementary particle value. In light nuclei, surface effects are important and no clear-cut statements can be made on the magnitude and sign of the effect.

We should note here that the Lorentz–Lorenz effect, which is playing a crucial role in the quenching of $g_A(0)$, is not an established phenomenon in the pion–nuclear interaction. Its existence and magnitude both are open questions (see, for example, Hüfner [349] and Brown et al. [349]). However, even if the Lorentz–Lorenz correlations are healed, longer-range Pauli correlations could give rise to a quenching of g_A by a magnitude similar to the former effect [347].

Experimental information: Wilkinson, in a series of papers [334], has examined the mirror β decays and has concluded that the “effective” axial vector coupling constant for these decays is about 10% smaller { his latest figures [334]: $g_A^{\text{eff}}(0) = (0.899 \pm 0.035) g_A(0)$ } than $g_A(0)$ for a free nucleon. However, this quenching is not attributable to one single mechanism, but can be due to a wide variety of physical effects. The reader is referred to Blin-Stoyle [348] for a catalogue of possible mechanisms.

From muon capture reactions discussed earlier in §§4–5, the impulse approximation analyses of the transitions ${}^2\text{D} \rightarrow \text{nn}$, ${}^3\text{He} \rightarrow {}^3\text{H}$, ${}^6\text{Li} \rightarrow {}^6\text{Li}_{\text{g.s.}}$ (all, particularly the last one, dominated by axial-vector form factor) yield capture rates, which tend to be slightly smaller than the experimental values. This could be optimistically interpreted as being suggestive of g_A^{eff} *larger* than the elementary value of g_A ; these reactions, for which nuclear physics inputs are reasonably certain, tend to rule out a decrease of g_A by the magnitude indicated in the Wilkinson analysis of β -decays. The ${}^{12}\text{C} \rightarrow {}^{12}\text{B}_{\text{g.s.}}$ muon capture transition rate, however, yields a range of g_A^{eff} *consistent* with the ‘elementary’ value of g_A . An urgent theoretical task is to examine these reactions in realistic “renormalization” models and estimate the corrections to the impulse approximation. Experimentally, it would be interesting to measure these and other similar muon capture reaction rates and related observables with higher precision. Partial transitions in the lead region will be also interesting to study to learn about the renormalization effects.

It is believed that the nuclear transitions involving peripheral nucleons are not favourable to study the Lorentz–Lorenz quenching [347]. This is rather unfortunate, as most precise impulse approximation estimates can only be made for partial transitions, which generally involve valence nucleons. Total capture rates (§6) are not predictable with great precision to check renormalization effects. Nevertheless, hyperfine *total* capture rates, in light and medium nuclei, could be useful observables to shed light on these questions.

9.3.2. Effective pseudoscalar form factor

The pseudoscalar form factor of a nucleon in a nucleus can be effectively modified in two ways – a vertex modification, and a modification of the virtual pion propagator. The vertex modification reflects the change of the pion–nucleon coupling constant. The propagator modification can be due to the Coulomb interaction as well as the strong interaction of the propagating virtual pion with the “spectator” nucleons.

The *Coulomb modification* of the pion propagator, in absence of the strong interaction effects, has been considered by Baba [350], Fulcher and the author [351], and Yano et al. [352]. Consideration of the Coulomb effects due to a point nuclear charge leads to unphysical results with

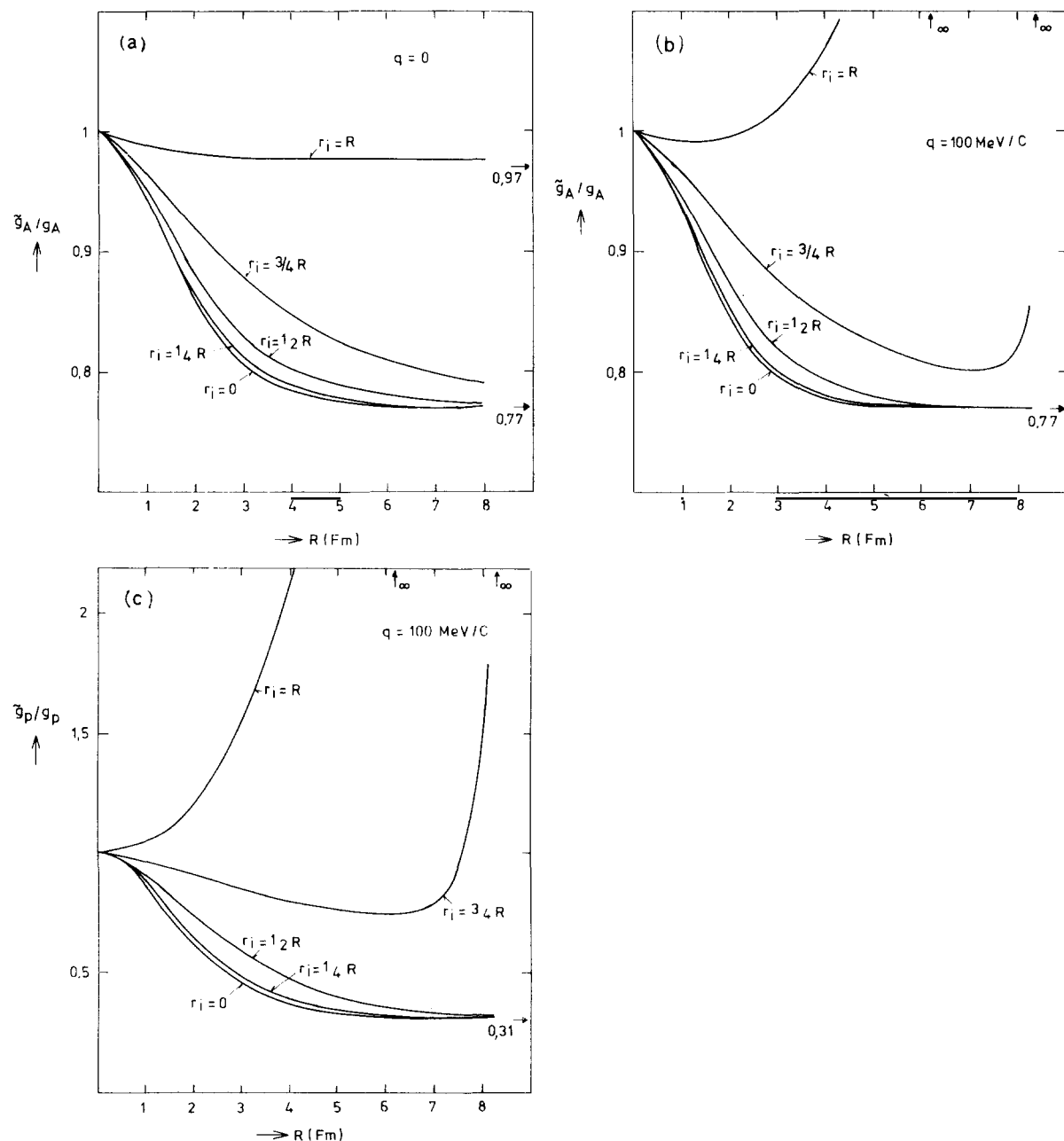


Fig. 9.2. Model estimates of renormalization of the axial vector form factor at (a) $q = 0$, and (b) $q = 100 \text{ MeV}/c$; the same for (c) pseudoscalar form factor at $q = 100 \text{ MeV}/c$ (Delorme et al. [347]).

the Case singularity at $\alpha Z = \frac{1}{2}$ [353] (see fig. 9.3a, b). Thus finite size of the nuclear charge distribution is an essential consideration in the problem [351]. The Coulomb Green's function satisfies the equation

$$[\nabla^2 + (\omega - V_c)^2 - m_\pi^2] G_\omega(x, x') = \delta(x - x'), \quad (9.11)$$

where ω is the pion energy and V_c is the static nuclear potential. $G_\omega(x, x')$ can be decomposed in partial waves:

$$G_\omega(x, x') = \sum_{l, m} Y_{lm}^*(\hat{x}') Y_{lm}(\hat{x}) g_l(x, x') \quad (9.12)$$

and the resultant differential equation for $g_l(x, x')$ is then solved numerically [351]. For momentum transfer above $20 \text{ MeV}/c$, approximate analytical solutions have been given for the problem [351].

Results for the numerical calculation indicate that the pure Coulomb corrections are small and can be neglected [351]. Thus for the muon capture reaction $^{16}\text{O}(\mu^-, \nu_\mu) ^{16}\text{N}(0^-)$, the Coulomb effect reduces the induced pseudoscalar coupling constant by 1%, and for the radiative muon capture in ^{40}Ca there is a reduction by 2% for the neutrino momentum $80 \text{ MeV}/c$, and an increase of the pseudoscalar coupling constant by 2% for the neutrino momentum of $20 \text{ MeV}/c$ (figs. 9.3c, d).

The *strong interaction* distortion* of the pion propagator is more difficult to estimate since not much is known about the propagation of the off-shell pions in the nuclear interior. Some estimates can be obtained in the optical potential picture [354–356, 339, 347].

The pion propagator $D(q, \omega)$ can be written in the momentum space as

$$D(q, \omega) = [|\mathbf{q}|^2 + m_\pi^2 - \omega^2 - \pi(q, \omega)]^{-1}, \quad (9.13)$$

where $\pi(q, \omega)$ is the self-energy of the off-shell pion due to the strong interaction effects. Notice that, even in absence of the pion self-energy term, $D(q, \omega)$ is strongly sensitive to (q, ω) . Thus, values of the free propagator $D_0(q, \omega)$ for two extreme four-momenta $(0, m_\mu)$ and $(m_\mu, 0)$ have the following ratio:

$$D_0(0, m_\mu)/D_0(m_\mu, 0) = (m_\pi^2 + m_\mu^2)/(m_\pi^2 - m_\mu^2) \approx 3.7. \quad (9.14)$$

Assuming the pion propagation in nuclear matter, and considering the Kisslinger form [357] of the pion–nuclear optical potential, we have

$$D(q, \omega) = [m_\pi^2 - \omega^2 + (1 + \alpha_0) |\mathbf{q}|^2]^{-1} \quad (9.15)$$

neglecting the s-wave pion–nuclear interaction**.

Combining the effects of vertex renormalization and pion propagator modification due to strong interaction effects, the following expression for $g_p^{\text{eff}}(q^2)/g_p(q^2)$ is obtained for zero energy pions ($|\mathbf{q}| \sim m_\mu$), in nuclear matter [347]:

$$g_p^{\text{eff}}(q^2)/g_p(q^2) = \left(1 + \frac{\frac{1}{3}\alpha_0}{1 - \frac{1}{3}\alpha_0} \right) (1 + \alpha_0) \frac{q^2 + m_\pi^2}{(1 + \alpha_0)q^2 + m_\pi^2}. \quad (9.16)$$

*In the context of muon capture, this was first considered by Green and Rho [354], following a discussion of three-body forces in nuclear matter by Brown and Green [354].

**The s-wave interaction is repulsive and is, of course, crucial in determining the pole of the propagator, as in the pion-condensate problem.

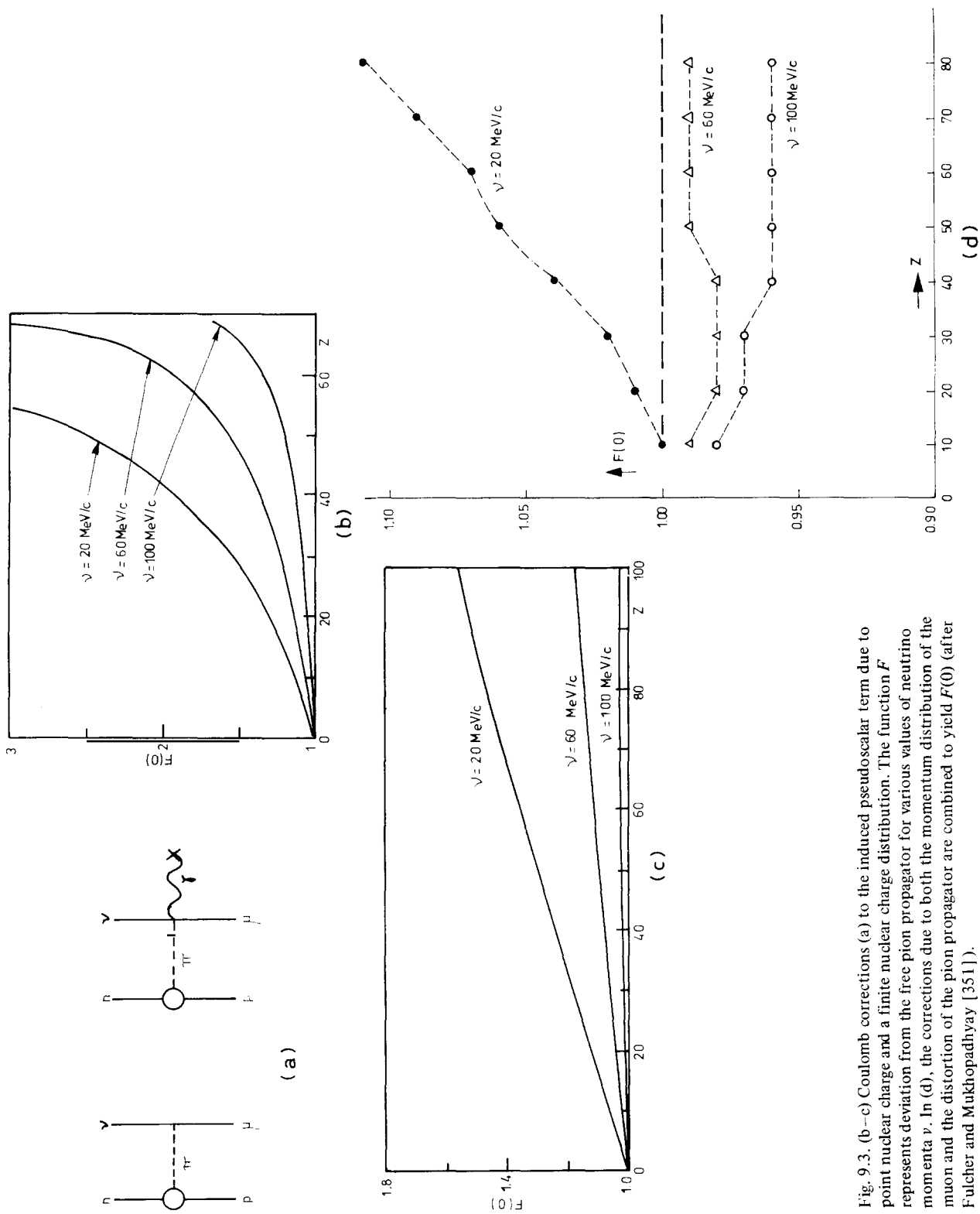


Fig. 9.3. (b–c) Coulomb corrections (a) to the induced pseudoscalar term due to point nuclear charge and a finite nuclear charge distribution. The function F represents deviation from the free pion propagator for various values of neutrino momenta v . In (d), the corrections due to both the momentum distribution of the muon and the distortion of the pion propagator are combined to yield $F(0)$ (after Fischer and Mukhopadhyay [351]).

Thus, there is a dramatic quenching of the pseudoscalar form factor: for zero range π -N interaction, g_p^{eff}/g_p equals 0.35 (with finite range, this quenching is even bigger [347]).

Experimental indications. At the moment, there exist a few cases of muon capture reactions [for example, $^{16}\text{O} \rightarrow ^{16}\text{N}(0^-)$], for which the impulse approximation estimates fail to account for the experimental results. Naively, these discrepancies are often expressed in terms of a g_p^{eff}/g_p which is drastically different from unity, g_p being the PCAC estimate for the nucleon case. However, as discussed in § 6, canonical nuclear physics uncertainties still are too large to allow any attribution of these discrepancies to the nuclear renormalization effects, in the sense of discussions in this subsection.

For consideration of effects in radiative muon capture, the analysis presented above must be suitably extended to the appropriate kinematic regime for the axial-vector current.

9.3.3. Effective tensor form factor

There are various ways in which an apparent “induced tensor form factor” can arise in the lepton–nucleon interaction [358–359]. We refer to the work of Kubodera, Delorme and Rho [359] for a more complete theoretical discussion of the problem.

The nucleon in the nucleus is off its mass shell and it can, for example, couple to the second-class current in the following way [359]:

$$\Gamma_\lambda(p', p) = i[g_T \sigma_{\lambda\rho} q_\rho \gamma_5 + g'_T i P_\lambda \gamma_5] \tau_-, \quad (9.17)$$

where $P = p + p'$, $q = p - p'$, p and p' are the four-momenta of the incoming and outgoing nucleon states. For a nucleon on its mass shell, there is only one tensor coupling constant ($g_T + g'_T$). Meson exchange corrections can also generate second-class contributions [358–359]. For instance, the exchange of an ω -meson, whose β decay $\omega \rightarrow \pi e \nu$ is second-class, can give rise to such contributions. Thus, the search for “second-class” form factors in nuclei necessarily involves ambiguities and inspiring assumptions, which are often motivated by grounds of simplicity. Presence of such form factors potentially complicates also the task of determining effective pseudo-scalar form factor, because these are often important in the same observable in nuclear muon capture experiments.

Experimental evidence? Experimental evidences for second-class effects in the last few years have fluctuated in conclusions considerably. Calaprice [72] has recently summarized the situation of nuclear β -decay experiments as follows:

“On the negative side, there seems to be no evidence for second-class effects in the ft asymmetries of the mirror Gamow–Teller decays (investigated very carefully over the last few years by Wilkinson [360]). Angular correlation measurements (inspired theoretically mainly by the work of Holstein and Treiman [361]) on the $A = 12$ [72] and $A = 19$ [362] systems, on the other hand, favour relatively large second-class effects (of the order of the weak magnetism term), while in the measurement on the $A = 8$ nuclei [363], no second-class effects are seen

Existing data on the electron neutrino correlation for ${}^6\text{He}$ β decay is found to be consistent with absence of second-class term [72], but the conclusion is somewhat model-dependent”.

To the above, we must add a new [363a] experiment, now in progress at Louvain, which seems to indicate, in the $A = 12$ systems, effects due to an apparent g_T having about the same magnitude as that estimated by Sugimoto et al. [72], but with *opposite sign*!

On the theoretical side, Rho, in his Saclay lecture, has shown how to accommodate at least some of the above seemingly conflicting experiments in terms of second-class effects [338]*. The trick is to introduce two parameters, one for the second-class meson exchange effects, and the other characteristic of the fundamental second-class coupling constant, which has a value of $(g_T + g'_T)$ on shell for the nucleon current. From the experimental results of Calaprice [362] and Sugimoto [72], Rho, obtains an effective tensor coupling constant, *of the order of weak magnetism term*.

The “second-class” question clearly remains open both on experimental and theoretical fronts. The experiments of the Osaka and Louvain groups in the $A = 12$ system are in conflict with each other. On the theoretical side, the adequacy and fundamental significance of the derived coupling constants in the current analyses are open problems. What their implications are for nuclear muon capture processes is also unclear at present.

9.4. Nuclei as “elementary particles”**

In the so-called “elementary particle model” (EPM) of the nucleus, first suggested by Fujii and Yamaguchi [117] and by Kim and Primakoff [365], nuclear wave functions are avoided and the muon capture rates (and other observables) are written in terms of nuclear form factors, to be determined by invoking general principles like CVC and PCAC (§3), and appealing to related experiments involving weak and electromagnetic interactions. While the objective of the model is to avoid making the assumption of the impulse approximation, it becomes often necessary to invoke this assumption. However, even in that case, absence of nuclear model complications makes this approach particularly simple to work with.

Numerous applications of the EPM have been made by many authors [365, 366] for allowed transitions in ${}^3\text{He}$, ${}^6\text{Li}$, and ${}^{12}\text{C}$, discussed earlier in the framework of the impulse approximation (§5), and reasonable agreements with experiment have been obtained. We refer to the paper of Galindo and Pascual [366] for the formulation of the EPM for nuclear targets of arbitrary spin. Dalorme [C3] discusses the relationship of the EPM with the ordinary impulse approximation approach. Jarlskog and Yndurain [132], and Kopeliovich [367] tackle the problem of handling anomalous cuts in the form factors relevant for muon capture by ${}^3\text{He}$.

9.4.1. An example: the reaction ${}^6\text{Li}(\mu^-, \nu_\mu){}^6\text{He}_{\text{g.s.}}$

We take this example, discussed earlier (§5), to illustrate the EPM approach and its limitation. We follow the treatment given by Delorme [C3].

The muon capture transition amplitude T is given by

$$T = \frac{G \cos \theta}{\sqrt{2}} \langle N_f | (A_\lambda + V_\lambda) | N_i \rangle L_\lambda, \quad (9.18)$$

where N_i and N_f are the initial and final nuclear states, respectively, V_λ and A_λ are the *nuclear* weak vector and axial vector currents, L_λ is the lepton current. The matrix element of A_λ and V_λ

*Readers are referred to Rho’s lecture for a thorough discussion on the physics (and other aspects) of the second-class problem. One moral for the item in parenthesis: Do not be “misguided by the Elementary Particle enthusiasts”, in sorting out your class conscience!

**This concept is originally due to Chew, used in his discussion on the S matrix theory of strong interaction [364].

can be given using the Lorentz covariance [C3, 366]:

$$\langle J_f^{\pi f} = 0^+ | V_\lambda | J_i^{\pi i} = 1^+, M_i \rangle = (4E_i E_f)^{-1/2} i\epsilon_{\lambda\mu\nu\rho} p_\mu q_\nu S_\rho^{(M_i)} F_M(t)/2m_i m_\pi, \quad (9.19a)$$

$$\begin{aligned} \langle J_f^{\pi f} = 0^+ | A_\lambda | J_i^{\pi i} = 1^+, M_i \rangle &= 4(E_i E_f)^{-1/2} [iS_\lambda^{(M_i)} F_A(t) + iq_\lambda S^{(M_i)} \cdot q F_P(t)/m_\pi^2 \\ &\quad + ip_\lambda S^{(M_i)} \cdot q F_R(t)/2m_i m_\pi], \end{aligned} \quad (9.19b)$$

where we have used the following notation: $J_{i,f}$, $\pi_{i,f}$, $M_{i,f}$, $m_{i,f}$, $E_{i,f}$, $(p_{i,f})_\lambda$ are respectively, spins, parities, spin projections, masses, energies, and four-momenta of the initial and final states; $\epsilon_{\lambda\mu\nu\rho}$ is the completely antisymmetric Levi–Civita tensor in four dimensions. We additionally have $p_\lambda = (p_f + p_i)_\lambda$, $q_\lambda = (p_f - p_i)_\lambda$, $\Delta = m_f - m_i$, and $S_\lambda^{(M_i)}$ is the polarization vector for the spin 1 initial nucleus. Our task is now to determine four form factors of the nucleus $F_M(t)$, $F_A(t)$, $F_P(t)$, and $F_R(t)$, where $t = |\mathbf{q}|^2 + q_4^2 \approx q^2$, for $q^2 \gg \Delta^2$.

$F_M(t)$ can be determined by appealing to the inelastic electron scattering process ${}^6\text{Li}(e, e') {}^6\text{Li}^*$ (1^+ , $T = 1$), exciting the isobaric analogue of ${}^6\text{He}_{\text{g.s.}}$ in ${}^6\text{Li}$. The differential cross-section of this process is [C3]

$$\left(\frac{d\sigma}{d\Omega} \right)_{ee'} = \frac{1}{3} \frac{\alpha^2}{4E_e^2} \left(1 + \frac{2E_e}{m_i} \sin^2 \frac{\theta}{2} \right)^{-1} \times \left(\frac{1 + \sin^{-2}(\theta/2)}{2 \sin^2(\theta/2)} \right) \times \left(\frac{q}{m_\pi} \right)^2 \frac{F_M^2(t)}{4m_i^2}; \quad (9.20)$$

E_e is the incoming electron energy related to t by the equation $t \simeq 2E_e(E_e - \Delta^*) (1 - \cos \theta)$, where Δ^* is the excitation energy of ${}^6\text{Li}^*$ state (3.56 MeV). In identifying the form factor in eq. (9.20) as $F_M(t)$, we are ignoring the effect of the Coulomb energy difference between ${}^6\text{He}_{\text{g.s.}}$ and ${}^6\text{Li}^*$ states, and are using the isotriplet vector current hypothesis (§ 3).

The form factor $F_A(t)$ can be determined in two steps. $F_A(0)$ is given by the ft value of the ${}^6\text{He}_{\text{g.s.}} \xrightarrow{\beta^-} {}^6\text{Li}_{\text{g.s.}}$ transition:

$$F_A^2(0) = \frac{1}{3} \frac{8\pi^3 m_i^2 \ln 2}{G^2 \cos^2 \theta ft}. \quad (9.21)$$

One can then use the approximate relation

$$\frac{F_A(t)}{F_A(0)} \approx \frac{F_M(t)}{F_M(0)}, \quad (9.22)$$

where $F_M(t)$ is obtained from eq. (9.20) and $F_M(0)$ can be extracted from the γ decay width Γ of the ${}^6\text{Li}^*$ state:

$$\Gamma_{{}^6\text{Li}^*} = 2\alpha m_\pi (\Delta^*/m_\pi)^3 F_M^2(0)/4m_i^2. \quad (9.23)$$

Application of the PCAC hypothesis in the form $\langle {}^6\text{He} | \partial_\lambda A_\lambda | {}^6\text{Li} \rangle = m_\pi^2 f_\pi \langle {}^6\text{He} | \phi_\pi | {}^6\text{Li} \rangle$ yields the Ward identity:

$$F_A(t) + \frac{t}{m_\pi^2} F_P(t) - \frac{\Delta}{m_\pi} F_R(t) = g_{\pi N_i N_f} f_\pi m_\pi^2 / (t + m_\pi^2). \quad (9.24)$$

Using the “generalized” Goldberger–Treiman relation [obtained by setting $t = 0$ in eq. (9.24)], neglecting the contributions of $F_R(t)$ and assuming $F_A(t)/F_A(0) \approx g_{\pi N_i N_f}(t)/g_{\pi N_i N_f}(0)$, we arrive at the result

$$F_P(t) \approx -F_A(t) m_\pi^2 / (t + m_\pi^2). \quad (9.25)$$

The limitation of the EPM is clear at this stage. In absence of direct knowledge of the quantities $F_A(t)$, $g_{\pi N_i N_f}(t)$, and $F_R(t)$ as functions of t , we have to introduce additional assumptions such as eq. (9.22) and those that are needed to derive eq. (9.25) from eq. (9.24). These are *ad hoc* and can be justified, in the ${}^6\text{Li}$ case, only by appealing to the impulse approximation. It has been shown by Delorme [C3] that, in this case, eq. (9.25) is satisfied to better than 10%, when $F_P(t)$ and $F_A(t)$ are expressed in the impulse approximation in terms of nuclear matrix elements and evaluated explicitly.

The muon capture rate for ${}^6\text{Li}(\mu^-, \nu_\mu){}^6\text{He}_{\text{g.s.}}$, obtained by the above procedure, is $\sim 1.4 \times 10^3 \text{ s}^{-1}$, in good agreement with the experiment. Notice that, by the Kroll-Ruderman theorem, the muon capture process is also related to the 1S radiative pion capture process (or pion photoproduction process at threshold), the rates of which are proportional to $F_A^2(t')$, where t' corresponds to the four-momentum transfer of the latter processes.

In order to make further progress in the EPM approach, new ideas are needed in determining nuclear form factors [such as $F_A(t)$ in the above analysis] and pion–nuclear coupling “constants”. Suitable extrapolation schemes for these quantities as functions of t are essential before additional success can be achieved with the EPM, and with such powerful procedures as those of Low, Adler and Dothan (§ 8).

10. Résumé and outlook

After this extensive *tour d'horizon*, we review here what we have learnt thus far from the study of the *nuclear* muon capture, summarizing the conclusions from the respective angles of the lepton–hadron interaction and nuclear physics. We also reiterate current “discrepancies”. We end this survey by suggesting some experimental and theoretical investigations, aiming at clarifying old problems and opening new areas of research in the “meson factories”.

10.1. What have we learnt about the muon–nucleon interaction?

Let us examine separately the conclusions obtained from the muon capture by hydrogen, and by more complex nuclei.

Muon capture in hydrogen has given a strong endorsement of the V–A theory for the charged weak current. Experiments overwhelmingly favour a large hyperfine effect ($\Lambda_S \gg \Lambda_T$), predicted by the V – A theory, over the approximate equality of the hyperfine capture rates ($\Lambda_S \approx \Lambda_T$), anticipated in the V + A theory. The μ –e universality for the axial vector coupling constant is strongly supported by the measured values of Λ_S . These yield the ratio

$$|g_A(0)/g_V(0)|_\mu = 1.23 \pm 0.05, \quad (10.1)$$

compared with the value $|g_A(0)/g_V(0)|_e = 1.258 \pm 0.015$, obtained from the neutron β decay. The test of the PCAC in hydrogen is rather weak: the limits on $g_P(q^2)$ from Λ_S is

$$6 \leq g_P(q^2) \leq 14, \quad (10.2)$$

compared with the Wolfenstein estimate of 8.4 with about 5% theoretical uncertainty. Thus, the experimental verification of the Goldberger–Treiman relation at about 10% level remains the best test of the PCAC. Λ_S provides a poor test for the hypotheses of isotriplet vector current and G invariance, as the former is not very sensitive selectively to weak-magnetism or tensor form factors.

Muon capture experiments in nuclei provide additional support for the V–A theory via several observables: absolute capture rates in light nuclei (e.g. ^{12}C), and large hyperfine rates (D , ^{19}F). Measured values of the capture rate in deuteron, and those for the allowed transitions $^3\text{He} \rightarrow ^3\text{H}$ and $^{12}\text{C} \rightarrow ^1\text{B}_{\text{g.s.}}$, all of which can be theoretically interpreted in terms of reasonably solid nuclear physics inputs, come quite close to (for $A = 12$ agree with) the predictions involving impulse approximation and the V–A theory, within the theoretical uncertainties of about 10% in the latter two cases. This shows that *all* corrections to the impulse approximation, *taken together*, must be small in light nuclei.

To get an idea* about the *deviation* of the hadronic weak form factors in light nuclei *from the elementary value*, we quote the following limit for $g_A^{\text{eff}}(0)/g_V^{\text{eff}}(0)$, obtained from the reaction $^{12}\text{C} \rightarrow ^1\text{B}_{\text{g.s.}}$ dominated by the axial-vector form factor:

$$1.21 \leq g_A^{\text{eff}}(0)/g_V^{\text{eff}}(0) \leq 1.30. \quad (10.3)$$

This suggests small corrections to the impulse approximation estimate for the rate of this transition. Interestingly, impulse approximation estimates for the rates of capture in deuteron and those of allowed transitions in ^3He and ^6Li seem to be slightly *lower* than the experimental values. Explicit computation of the corrections to the impulse estimate is found to yield a positive value for the doublet capture rate in deuteron. These all contrast with the observation by Wilkinson of a slight quenching in the ratio (g_A/g_V) in the mirror β -decays of light nuclei. Theoretical models on “renormalization” of axial vector form factors do not help here, as the delicate role of the nuclear surface effects makes the predicted outcome rather uncertain. Calculations of these effects in many cases of interest above are still to be made in realistic renormalization models.

The presence of the so-called *induced form factors* (at least the “first-class” ones) have been inferred in a model-independent way from the residual polarization and recoil experiments involving ^{12}B nuclei. Limits on their values, however, are not precise. Polarization measurements of the recoiling ^{12}B nuclei after muon capture in ^{12}C yield the following limit on $g_P(q^2)$:

$$5 \leq g_P(q^2) \leq 15. \quad (10.4)$$

In the near future, both theoretical and experimental uncertainties in extracting this limit will be improved.

The informations on the *rare and ultra-rare processes* involving muon capture have come only from complex nuclei. The measured radiative branching ratio in medium nuclei such as calcium or copper is about 10^{-4} of the ordinary capture, as expected theoretically. Searches for the $\mu^- \rightarrow e^-$ and $\mu^- \rightarrow e^+$ conversions in muon capture have put the following limits on their branching ratios:

$$R(\mu^- + \text{Cu} \rightarrow e^- + \text{Cu})/R(\mu^- + \text{Cu} \rightarrow \nu_\mu + \text{Ni}) < 1.9 \times 10^{-8}, \quad (10.5a)$$

$$R(\mu^- + \text{Cu} \rightarrow e^+ + \text{Cu})/R(\mu^- + \text{Cu} \rightarrow \nu_\mu + \text{Ni}) < 2.6 \times 10^{-8}. \quad (10.5b)$$

The first reaction tests the validity of muon lepton number conservation at about the level achieved in the decay $\mu^+ \rightarrow 2e^+ + e^-$. The unequivocal detection of the second reaction will select the Konopinski-Mahmoud scheme of lepton classification; the current upper limit of its branching ratio yields an isotensor ($\Delta T = 2$) weak coupling constant which is at most a thousandth of the Fermi coupling constant.

*See also § 10.3, where we group experiments for which nuclear physics inputs are less certain. These do not agree with the theoretical predictions using canonical form factors.

10.2. What have we learnt about nuclear physics?

From the point of view of nuclear spectroscopy, the advantage of muon capture is in the expected stratification of the capture strength to various isolated groups of final states. The dominant role of the giant (electric) dipole resonance excitation in light and medium nuclei, long anticipated on theoretical grounds, is now well-established experimentally. The less-known, but recently predicted, giant magnetic dipole resonance analog excitations in light nuclei have also been experimentally studied in the 1p-shell targets. Useful spectroscopic informations have been obtained from the use of the hyperfine conversion (in $^{11}\text{B} \rightarrow ^{11}\text{Be}^*$) and from the $\gamma-\nu$ correlations (in $^{28}\text{Si} \xrightarrow{\mu^-} ^{28}\text{Al}^*$).

Emissions of neutrons and charged particles at low energies show characteristic evaporation spectra, with giant resonance peaks superimposed on them. Observation of nucleons at relatively high energies (above, say, 50 MeV) indicates the possible roles of muon capture mechanisms involving more than one nucleon. Neutron spectra and asymmetries, even at relatively high (~ 40 MeV) energy, seem to be greatly influenced by the final-state interactions.

Calculated muon capture rates for a variety of target nuclei show very strong sensitivity to the quality of the nuclear wave functions used. Thus, muon capture, together with the related processes at low and intermediate momentum transfers (β -decay, radiative pion capture, photoproduction of pions, electron scattering, etc.), provides a powerful testing ground for various nuclear models. Reliable predictions for the observed excitation strengths to the nucleon-unbound daughter states will be an important task of the future.

Both prompt and delayed fission experiments are beginning to yield results. The former should carry significant information on the nuclear deformation, and the latter depends on the mean nuclear excitation energy and integrated strength above the fission barrier. There are suggestions of excitations of fission isomers in the actinides.

10.3. Discrepancies

Some of the older experiments in liquid hydrogen are in mild disagreement with the theoretical predictions; this discrepancy is believed to be experimental in origin. There are, however, many experiments in complex nuclei which strongly disagree with the conventional theory -- muon capture rates in ^{16}O , gamma-neutrino correlations in ^{28}Si , photon asymmetry and spectra in the radiative muon capture in ^{40}Ca , to cite a few examples. While many "exotic" explanations for these have been suggested, canonical nuclear physics uncertainties are still too high to be forgotten. In some cases [for example, $^{16}\text{O}(0^+) \rightarrow ^{16}\text{N}(0^-)$ transition], different experiments are not in mutual agreement. The customary way of expressing these discrepancies is to extract a range of effective values of g_P/g_A from the impulse approximation analysis, and show that this range is completely outside the PCAC expectation for the *free nucleon case**. *We caution the reader against taking these ranges as serious indications for "renormalization" of the elementary axial-vector coupling constants in nuclei.* An interesting parallel to keep in mind is the set of effective g_V and g_A , obtained from the experimental βft values in heavy nuclei, cited by Bohr and Mottelson**: the large "renormalizations" of both g_V and g_A are here primarily due to polarizations of the closed nucleon shells, a "classical" nuclear physics effect.

Sample values for g_P/g_A are in the range 13 to 20 from the $^{16}\text{O} \rightarrow ^{16}\text{N}(0^-)$ transition rate, -6 to 1 from the $\gamma-\nu$ correlation experiment in $^{28}\text{Si} \rightarrow ^{28}\text{Al}^$ and ~ -7 from the radiative muon capture experiments in ^{40}Ca , while the PCAC expectation is about 7.

**See Bohr and Mottelson [A6] Vol. I, Chapter 3, p. 353.

10.4. Outlook

In view of the heightened muon intensities currently available in the meson factories, we may now ask the question: *What are the experiments that deserve priority in the new facilities?* From the elementary muon–nucleon interaction angle, the first goal is obviously to measure the singlet capture rate Λ_S in hydrogen with a much higher precision than currently available, perhaps improving the accuracy by a factor of five. This would allow a sharpened test of the muon–electron universality in the axial vector current. This seems feasible in the near future. Present upper limit on the triplet capture Λ_T in hydrogen is extremely poor – efforts should be made to improve this by doing experiment in gaseous hydrogen at *low* pressure. This also appears possible by the use of the magnetic bottle technique.

Searches for the $\mu^- \rightarrow e^\pm$ conversion in nuclear muon capture should now be intensified. Improvements on the current upper limits of the branching ratios by several orders of magnitude are now possible, by better discrimination of the radiative background contributions. This would lead to a better test of the assignments and conservation laws of the lepton numbers.

Interpretation of partial radiative muon capture transitions in ${}^3\text{He}$, ${}^{12}\text{C}$, and possibly in several other targets, via the well-known allowed channels, ought to involve less of the conventional nuclear physics difficulties and should be given priority in experimental investigation. The same is true for the recoil polarization experiments in ordinary muon capture. These experiments should further our insights on the adequacy of the elementary muon–nucleon interaction in nuclei.

Very little experimental work has been done so far on the hyperfine effects. Thus the dramatic manifestation of hyperfine conversions, expected in various observables for muon capture in light nuclei, are practically unexplored. Use of the polarized nuclear targets remains likewise a technique of the future. This may allow us to probe the differences in the hyperfine capture rates in light nuclei. The “repolarization” of muon, by the hyperfine interaction with polarized light nuclear targets, will make studies of parity-violating effects much easier.

In the area of “classical” nuclear physics, giant resonance spectroscopy is still an open problem. While qualitative studies of the giant resonance excitations are available, systematic investigations along the periodic table to probe the isospin splitting of the giant dipole resonance in $N \neq Z$ nuclei (in conjunction with electromagnetic probes), remain largely unaccomplished. We do not know experimentally if excitations of quadrupole resonances in heavier nuclei manifest a strong concentration of strengths in muon capture reactions. Large muon intensities in the meson factories, coupled with the new advances in neutron and charged particle detection techniques, should make this an exciting nuclear physics enterprise. Emission of protons at high energies also is not understood, and we are just beginning to learn to use muons as probes in fission physics. We will hear more about these in the near future, beyond doubt. The singlet neutron–neutron scattering length is also expected to be determined experimentally from the muon capture in deuteron, hopefully at an accuracy that improves the test of the charge symmetry of the nuclear forces via the possible equality of a_{pp} and a_{nn} .

On the theoretical side, there are many problems in the “classical” nuclear physics that remain to be tackled. To take some examples, the descriptions of the $0^-, 1^-, 2^-, T=1$ bound states in ${}^{16}\text{N}$, excited in the muon capture by ${}^{16}\text{O}$, continue to be controversial. We do not know how to treat the excitation of states in the continuum in an adequate way – hence our understanding of the dominant excitation modes is only very approximate. The exact interplay between direct, pre-compound and other supposed mechanisms of nucleon emission is not clearly known.

However, above these, remains one question, which, to me, is the most fundamental of all: *Does a nucleon inside a nucleus couple weakly to a lepton in exactly the same way as it does as a free particle?* If the answer is *no*, the deviations from the free values do not appear to be big, at least in light nuclei. Current theoretical conjectures mostly deal with the ideal world of “nuclear matter” in discussing this question. But in the real world of finite nuclei, theoretical answers are uncertain, experimental answers are largely unknown. It is not clear if the “classical” nuclear structure effects can be completely separated from an observable to allow us a handle on this question. Further theoretical insights will depend, at the minimum, on our better grasp of the description of a nucleon in the nucleus and a more fundamental understanding of the pion–nuclear interaction than what is now available.

All in all, it still looks like an exciting enterprise ahead of us!

Acknowledgements

Little did I think when I started writing this review more than two years ago that it would take so long! But this period of travail has been educationally most rewarding.

This report owes its existence primarily to three people: Torleif Ericson, who conceived its boundaries, urged me to write it up, and guided me throughout the course of its preparation; Maurice Jacob, the editor for this report, who gave me valuable suggestions; Florian Scheck, who, at SIN, was constantly available with his helpful criticisms, and who supported most generously my numerous excursions to other institutions. I am also privileged to use here three historic photographs, kindly sent by L.W. Alvarez, V.P. Dzhelepov and R.H. Hildebrand.

The materials covered here have been used by me in a series of lectures given at Los Alamos (Summer, 1973), Villars (Winter, 1974) and Amsterdam (Autumn, 1974); these have been most extensively developed at the Université Catholique de Louvain (Spring, 1975) during my pleasant tenure there as an Invited Professor. I thank L. Rosen and P. Thomson, T. Ericson, A.H. Wapstra and P. Goudsmit, and J. Deutsch for their kind hospitalities.

Many colleagues have helped me through numerous discussions on various aspects of this report: I thank particularly M.K. Banerjee, J. Bernabéu, V. Devanathan, T.W. Donnelly, C. Dover, M. and T. Ericson, L. Fulcher, B. Goulard, V. Gupta, J. Hüfner, D. Kurath, M. Macfarlane, H. Rood, M. Rosa-Clot, N. Straumann, R. Tarrach, W. Weise, C. Wilkin, Sir Denys Wilkinson and L. Wolfenstein for theoretical comments; I am grateful to G. Backenstoss, J. Deutsch, D. Englehardt, R. Engfer, V.S. Evseev, D. Favart, E. Fiorini, L. Grenacs, B. Hahn, H. Hofer, H.J. Leisi, S. Mango, C. Petitjean, C. Samour, W. Sapp, P. Truöl, R. van Dantzig, H.K. Walter, A. Wyttenbach and E. Zavattini, for discussions on the experimental aspects. M.H. Macfarlane, at Chicago, introduced me to the subject of this report.

I thank all the authors who have written to me about their projects and clarified many points of their published works. I am particularly indebted to J. Delorme, M. Eckhause, L.L. Foldy, A. Fujii, M. Hasinoff, C. Jarlskog, L.S. Kisslinger, M. Leon, J.A. Monard, H. Ohtsubo, Z. Oziewicz, A.M. Rushton and R.E. Welsh for their correspondences. F. Cannata, R. Eramzhyan, H. Primakoff, H. Überall and J.D. Walecka have kindly made *their* reviews available to me prior to publication.

Pepe Bernabéu, Joan Martorell and Florian Scheck have taken great pains to read the entire manuscript, some sections in several versions. Their patience and insistence on accuracy and readability have undoubtedly contributed to a vastly improved manuscript. My special gratitude is due to them.

The text has been also read in part by E. Borie, M. Camani, P. Christillin, A. Figureau, J. Hadermann, K. Junker, F. Lenz, M. Locher, T. Mizutani, H.J. Pfeiffer and A. Wullschleger. I thank all of them for their help. I have tried my best to eliminate the errors spotted by these alert colleagues.

Responsibilities for all the remaining mistakes and subjective judgments remain solely mine.

Last, but not the least, I must thank J. Ulrich, M. Dubs and their colleagues at SIN for their excellent drawings. Mrs. Ingrid Makowiecki and Mrs. Erika Harbort bravely typed constantly changing earlier drafts; the final manuscript has been beautifully set to type by Miss I. Henderson and Mrs. Y. Piemontese at CERN, under the direction of Mrs. K. Wakley and Mrs. S. Vascotto. For them, I leave a special word of thanks.

Appendix 1. Hyperfine capture rates* Λ_S and Λ_T for hydrogen nucleus in terms of the hadronic weak form factors and kinematic variables, assuming the absence of second-class form factors (after Pascual [75])

Λ_S and Λ_T are given by

$$\Lambda_F = \frac{G^2 \cos^2 \theta}{64\pi^2} \frac{1}{(2F+1)} \frac{s - M_n^2}{M_p m_\mu s} (m'_\mu \alpha)^3 C_\mu R_F, \quad (\text{A1.1})$$

where

$$R_0 = z \left[(1 + 3x)g_V + (3 + x)g_A - (x + y) \frac{\nu}{m_\mu} g_P + (2 - x - 3y) \frac{\nu}{2M_p} g_M \right]^2 \quad (\text{A1.2})$$

$$\begin{aligned} R_1 = z & \left[(3 + 2x + 3x^2)(g_V - g_A)^2 - (4 + 2x + 2y + 2x^2 + 6xy) \frac{\nu}{2M_p} (g_V - g_A)g_M + 3(x + y)^2 \frac{\nu^2}{m_\mu^2} g_P^2 \right. \\ & + (2x + 2y + 6x^2 + 6xy)(g_V - g_A) \frac{\nu}{m_\mu} g_P + (4 + 4x - 4y + 2xy + 3x^2 + 3y^2) \frac{\nu^2}{4M_p^2} g_M^2 \\ & \left. - (2x^2 + 6y^2 - 4x - 4y + 8xy) \frac{\nu}{2M_p} \frac{\nu}{m_\mu} g_P g_M \right], \end{aligned} \quad (\text{A1.3})$$

C_μ being $1 - 2m_\mu \alpha R_p$, with $s = (M_p + m_\mu)^2$, $\nu \equiv$ neutrino momentum $= (s - M_n^2)/2\sqrt{s}$, $E \equiv$ neutron energy $= \sqrt{M_n^2 + \nu^2}$, $x = \nu/(E + M_n)$, $y = (E + M_p)/(E + M_n)$, $z = 8M_p(E + M_n)m_\mu\nu$, M_n , M_p being neutron and proton masses, $\Lambda_0 \equiv \Lambda_S$, $\Lambda_1 \equiv \Lambda_T$; m'_μ is the muon reduced mass. R_p is ~ 1.02 fm.

The second-class terms can be easily included in the above expressions for rates (see [126]).

Appendix 2. Nuclear transition amplitudes

For a nuclear muon capture transition $J_i^{\pi_i} \rightarrow J_f^{\pi_f}$, all nuclear transition operators of rank J and parity π , satisfying the constraints

$$|J_i - J_f| \leq J \leq [J_i + J_f], \quad \pi = \pi_i^\dagger \pi_f, \quad (\text{A2.1})$$

will contribute. Restricting ourselves to the contributions of a given “forbiddenness”, say, of order n , J and π have the following values:

$$J = n, n + 1, \quad \pi = (-)^n. \quad (\text{A2.2})$$

Various observables can now be written in terms of the transition amplitudes $T_J(\kappa)$, where κ is the neutrino wave number, related to parity π by the equation

$$\pi = (-)^{|\kappa| + \frac{1}{2}(S_\kappa - 1)}, \quad (\text{A2.3})$$

*Note the change of signs in some terms in eqs. (A1.2) and (A1.3), compared with ref. [75]. These arise due to our choice of form factors, in which the ratios g_V/g_A and g_P/g_A are both positive.

S_κ being the sign of κ . Thus, for the n th forbidden transition, there are *four* amplitudes that are going to contribute: $T_n(-n-1)$, $T_n(n)$, $T_{n+1}(-n-1)$, $T_{n+1}(n+2)$. These can be obtained from the following equations*:

$$T_n(-n-1) = \sqrt{\frac{2}{2n+1}} \left\{ g_V \sqrt{n+1} [0nn] - g_A \sqrt{\frac{n}{3}} [1nn] + g_V \frac{q}{2M} \sqrt{n+1} [0nn] - g_V \frac{q}{2M} (1 + \mu_p - \mu_n) \sqrt{\frac{n}{3}} [1nn-] \right. \\ \left. - \frac{g_V}{M} \sqrt{\frac{2n+1}{3}} [1n+1np] \right\}, \quad (\text{A2.4a})$$

$$T_n(n) = \sqrt{\frac{2}{2n+1}} \left\{ g_V \sqrt{n} [0nn] + g_V \frac{q}{2M} \sqrt{n} [0nn+] + g_A \sqrt{\frac{n+1}{3}} [1nn] + g_V \frac{q}{2M} (1 + \mu_p - \mu_n) \sqrt{\frac{n+1}{3}} [1nn+] \right. \\ \left. - \frac{g_V}{M} \sqrt{\frac{2n+1}{3}} [1n-1np] \right\}, \quad (\text{A2.4b})$$

$$T_{n+1}(-n-1) = \sqrt{\frac{2}{2n+3}} \left\{ + g_A \sqrt{\frac{2n+3}{3}} [1nn+1] + \frac{g_A}{M} \sqrt{n+1} [0n+1n+1p] + \frac{g_V}{M} \sqrt{\frac{n+2}{3}} [1n+1n+1p] \right. \\ \left. - g_V \frac{q}{2M} (1 + \mu_p - \mu_n) \sqrt{\frac{n+2}{3}} \left(\sqrt{\frac{n+1}{2n+3}} [1n+2n+1+] - \sqrt{\frac{n+2}{2n+3}} [1nn+1-] \right) \right. \\ \left. + (g_A - g_P) \frac{q}{2M} \sqrt{\frac{n+1}{3}} \left(\sqrt{\frac{n+2}{2n+3}} [1n+2n+1+] + \sqrt{\frac{n+1}{2n+3}} [1nn+1-] \right) \right\}, \quad (\text{A2.4c})$$

$$T_{n+1}(n+2) = \sqrt{\frac{2}{2n+3}} \left\{ - g_A \sqrt{\frac{2n+3}{3}} [1n+2n+1] - \frac{g_A}{M} \sqrt{n+2} [0n+1n+1p] + \frac{g_V}{M} \sqrt{\frac{n+1}{3}} [1n+1n+1p] \right. \\ \left. - g_V \frac{q}{2M} (1 + \mu_p - \mu_n) \sqrt{\frac{n+1}{3}} \left(\sqrt{\frac{n+1}{2n+3}} [1n+2n+1+] - \sqrt{\frac{n+2}{2n+3}} [1nn+1-] \right) \right. \\ \left. - (g_A - g_P) \frac{q}{2M} \sqrt{\frac{n+2}{3}} \left(\sqrt{\frac{n+2}{2n+3}} [1n+2n+1+] + \sqrt{\frac{n+1}{2n+3}} [1nn+1-] \right) \right\}, \quad (\text{A2.4d})$$

where we have substituted $g_M = g_V(\mu_p - \mu_n)$. The operators, used above, are defined in table A2.1. $\mathcal{Y}_{0wu}^M(\mathbf{f}), \mathcal{Y}_{1wu}^M(\mathbf{f}, \mathbf{a})$ are defined as

$$\mathcal{Y}_{0wu}^M(\mathbf{f}) = (4\pi)^{-1/2} \mathcal{Y}_w^M(\mathbf{f}), \mathcal{Y}_{1wu}^M(\hat{\mathbf{f}}, \mathbf{a}) = \sum_m C_{-m}^1 \mathcal{Y}_{M+m}^M(\mathbf{a}) \mathcal{Y}_w^{M+m}(\mathbf{f}), \quad (\text{A2.5})$$

$\mathcal{Y}_w^M(\mathbf{f})$ and $\mathcal{Y}_{-1}^{-m}(\mathbf{a})$ being spherical and solid harmonics [85]. The parity for the operators $[kwu]$, $[kwu^\pm]$ is $(-)^w$ and that for the operators $[kwup]$ is $(-)^{w+1}$.

Following special cases should be noted: *allowed* transitions ($\Delta J = 0, 1, \Delta\pi = +1$) involve transition amplitudes $T_0(-1), T_1(-1), T_1(2)$, and *first-forbidden* transitions ($\Delta J = 0, 1, 2, \Delta\pi = -1$) involve amplitudes $T_0(1), T_1(1), T_1(-2), T_2(-2), T_2(3)$, in the above approximation. For allowed transitions, [000] and [101] are the ordinary Fermi and Gamow-Teller matrix elements, respectively, at the momentum transfer corresponding to the muon capture reaction. In a particular reaction, the contributions of higher-forbidden amplitudes to the observables calculated in a given order of forbiddeness can be ascertained only by actual computation of such amplitudes explicitly. In general, the former need not be negligible [B3].

Relationships of the amplitudes defined in eqs. (A2.4) to those given in other representations (e.g. helicity amplitudes) are discussed in the work of Chiechanowicz and Oziewicz [B3].

The statistical capture rate Λ for the transition $J_i^{\pi i} \rightarrow J_f^{\pi f}$ is given, in the lowest-forbidden approximation (of order n), to be

$$\Lambda = 2q^2 \frac{2J_f + 1}{2J_i + 1} [T_n^2(-n-1) + T_n^2(n) + T_{n+1}^2(-n-1) + T_{n+1}^2(n+2)]. \quad (\text{A2.6})$$

*The expressions for $T_J(\kappa)$, quoted here, are obtained by Balashov and Eramzhyan [B1], following the procedure of Morita and Fujii [85]. These ignore the contributions of the small components of lepton wave functions; the inclusion of the latter would complicate these expressions immensely; Mukhopadhyay and Martorell [139] have found their contributions negligible (<1%), to the rate of the reaction ${}^{12}\text{C} \xrightarrow{\mu} {}^{12}\text{B}_{\text{g.s.}}$; Kume et al. [283] have, however, emphasized their importance in certain observables in the neutron emission.

Table A2.1

Nuclear single-particle transition operators $F_{k\omega u}(i)$, tabulated below in the second column, and the corresponding nuclear matrix elements, given in the first column. The latter are defined as follows: $[k\omega u] = \langle J_f M_f | \sum_{i=1}^A (\tau_i^\dagger / \sqrt{2}) F_{k\omega u}^M(i) | J_i M_i \rangle / C_{M_f M_M}^{j_f u j_i}$, and so on. $j_i(qr)$ and $G(r)$ are respectively neutrino and muon radial functions. The operators $D_\pm(w)$ are: $D_+(w) = [(d/dr) - (w/r)]$ and $D_-(w) = [(d/dr) + (w+1)/r]$.

$\{0wu\}$	$j_w(qr) G(r) \mathcal{Y}_{0wu}(\hat{r}) \delta_{wu}$
$\{0wu+\}$	$\{D_+(w-1) j_{w-1}(qr) G(r)\} \mathcal{Y}_{0wu}(\hat{r}) \delta_{wu}$
$\{0wu-\}$	$\{D_-(w+1) j_{w+1}(qr) G(r)\} \mathcal{Y}_{0wu}(\hat{r}) \delta_{wu}$
$\{1wu\}$	$j_w(qr) G(r) \mathcal{Y}_{1wu}(\hat{r}, \sigma)$
$\{1wu+\}$	$\{D_+(w-1) j_{w-1}(qr) G(r)\} \mathcal{Y}_{1wu}(\hat{r}, \sigma)$
$\{1wu-\}$	$\{D_-(w+1) j_{w+1}(qr) G(r)\} \mathcal{Y}_{1wu}(\hat{r}, \sigma)$
$\{0wup\}$	$i j_w(qr) G(r) \mathcal{Y}_{0wu}(\hat{r}) \delta_{wu} \sigma \cdot p$
$\{1wup\}$	$i j_w(qr) G(r) \mathcal{Y}_{1wu}(\hat{r}, p)$

Formulae for other observables, such as angular asymmetry and average polarization of the recoil nuclei, gamma-neutrino correlation coefficients, etc., are given in refs. [B1, B3].

In Appendix 3, we give the nuclear reduced matrix elements for single-particle transitions.

A systematic theoretical treatment of the observables in the *radiative* muon capture is lacking in the published literature. Rood's thesis [C15], however, forms a good basis for such a treatment.

Appendix 3. Expressions for single-particle reduced matrix elements of nuclear transition operators

In this section, we shall give expressions for the reduced matrix elements for the single-particle transition $j_p \xrightarrow{\mu} j_n$:

$$\langle j_n \frac{1}{2} \| T^{u1} \| j_p \frac{1}{2} \rangle, \quad (A3.1)$$

which can be broken into

$$\langle j_n \| T_u \| j_p \rangle \langle \frac{1}{2} \| \tau^+ / \sqrt{2} \| \frac{1}{2} \rangle, \quad (A3.2)$$

where j_n and j_p are single-particle states; we have, thus,

$$j_n = l_n + \frac{1}{2}; \quad j_p = l_p + \frac{1}{2}. \quad (A3.3)$$

We have

$$\langle \frac{1}{2} \| \tau^+ / \sqrt{2} \| \frac{1}{2} \rangle = \sqrt{\frac{3}{2}}. \quad (A3.4)$$

We use the Wigner-Eckart theorem: $\langle j_2 m_2 \| T_q^k \| j_1 m_1 \rangle = \langle j_2 \| T_q^k \| j_1 \rangle C_{m_1 q m_2}^{j_1 k j_2}$.

The expressions for $A = \langle j_n \| T_u \| j_p \rangle$ for various T_u are given below

1. $T_u = \mathcal{Y}_{k\omega u}(\hat{r}, \sigma)$

$$A = (-)^{j_p - j_n} \frac{(2k+1)}{4\pi} C_0^{l_n w} {}_0^l p [2(2l_n+1)(2j_p+1)(2w+1)(2u+1)]^{1/2} \begin{Bmatrix} l_n & l_p & w \\ j_n & j_p & u \\ \frac{1}{2} & \frac{1}{2} & k \end{Bmatrix}. \quad (A3.5)$$

2. $T_u = i \mathcal{Y}_{1wu}(\hat{r}, p)$

$$A = [3(2j_p+1)(2w+1)(2u+1)]^{1/2} \{ W(j_p \frac{1}{2} u l_n; l_p j_n) / 4\pi \} \times \left\{ C_0^{l_p+1 w} {}_0^l n W(l_p 1 l_n w; l_p + 1 u) [(2l_p + 3)(l_p + 1)]^{1/2} \left(\frac{d}{dr} - \frac{l_p}{r} \right) - C_0^{l_p-1 w} {}_0^l n W(l_p 1 l_n w; l_p - 1, u) [l_p (2l_p - 1)]^{1/2} \left(\frac{d}{dr} + \frac{l_p + 1}{r} \right) \right\}. \quad (A3.6)$$

3. $T_u = i \mathcal{Y}_{0uu}(\theta) \sigma \cdot p$

$$A = \{ [6(2j_p + 1)(2U + 1)]^{1/2}/4\pi \} \\ \times \left\{ -C_0^{l_p+1} {}_0^u l_n W(l_p j_p 1_{1/2}; {}_1^1 l_p + 1) W(j_p u {}_1^1 l_n; j_n l_p + 1) [(2l_p + 3)(l_p + 1)]^{1/2} \left(\frac{d}{dr} - \frac{l_p}{r} \right) \right. \\ \left. + C_0^{l_p-1} {}_0^u l_n W(l_p j_p 1_{1/2}; {}_1^1 l_p - 1) W(j_p u {}_1^1 l_n; j_n l_p - 1) [l_p(2l_p - 1)]^{1/2} \left(\frac{d}{dr} + \frac{l_p + 1}{r} \right) \right\}. \quad (\text{A3.7})$$

In the expressions above, the symbols

$$W(a, b, c, d; ef), \quad \begin{Bmatrix} abc \\ def \\ ghi \end{Bmatrix} \quad \text{and} \quad C_{def}^{abc}$$

stand for Racah, Fano (9j) and Clebsch–Gordan coefficients, respectively.

The single-particle radial integrals are of the form

$$\int_0^\infty \phi_n \mathcal{O}_L [\mathcal{O}_H \phi_p] r^2 dr,$$

where \mathcal{O}_L and \mathcal{O}_H are lepton and hadron radial functions. These can be explicitly evaluated; ϕ_n and ϕ_p are single-particle radial wave functions (harmonic oscillator, Woods–Saxon, Hartree–Fock, etc.). See ref. [139] for details.

By using standard fractional parentage techniques, one can obtain nuclear matrix elements of more complicated configurations. A special case for the particle–hole configuration will be noted here [A6]:

$$\langle (j_1^{-1} j_2) J \parallel T_u \parallel 0 \rangle = (-)^{j_1 + j_2 - u} \frac{[j_a]}{[J]} \langle j_2 \parallel T_u \parallel j_1 \rangle \delta(J, u), \quad (\text{A3.8})$$

where $[j_a] = (2j_a + 1)^{1/2}$. Equation (A3.8) can thus be used directly to calculate the ${}^{12}\text{C} \rightarrow {}^{12}\text{B}_{\text{g.s.}}$ transition matrix elements in the jj coupling model, with $j_1 = p_{3/2}, j_2 = p_{1/2}$.

Notes added in proof*

1. (See §§1 and 8.5.) The branching ratio R

$$R = (\mu^+ \rightarrow e^+ + \gamma) / (\mu^+ \rightarrow e^+ + \nu_e + \bar{\nu}_\mu)$$

is being remeasured by a group (W. Dey, R. Engfer, W. Eichenberger, C. Petitjean, H.P. Povel, A. van der Schaaf and H.K. Walter) at SIN. A very preliminary analysis of data suggests a positive indication of the radiative decay, $\mu^+ \rightarrow e^+ + \gamma$, at a level of R which is about a quarter of the best published upper limit [62] (H.P. Povel, private communication, Nov. 1976). If this result holds, it will add a new chapter to the muon mystery.

2. (See §2.1.) The Munich group have studied the muonic X-ray cascade in Fe, with Ge detectors, in order to determine the best initial orbital angular momentum (l) distribution, assuming a fixed principal quantum number n from which the X-ray cascade begins [F.J. Hartmann et al., Phys. Rev. Lett. 37 (1976) 331]. They find a rather flat initial l distribution, in agreement with the expectations of the “fuzzy Fermi-Teller model” of Leon and Miller [to be published].

3. (See §2.4.2.) The asymmetries δ of the emitted photons in the muonic transitions $2P_{3/2} \rightarrow 1S_{1/2}$ and $2P_{1/2} \rightarrow 1S_{1/2}$ have been measured in a circular polarization experiment in the natural Se, by the Basel–Karlsruhe group. The values obtained are (L. Simmons, private communications, Nov. 1976):

$$\delta(2P_{3/2} \rightarrow 1S_{1/2}) = -(3.8 \pm 1.2) \times 10^{-3}, \quad \delta(2P_{1/2} \rightarrow 1S_{1/2}) = -(1.5 \pm 1.7) \times 10^{-3}.$$

The latter would be zero, if the muons were completely depolarized in the $2P_{1/2} \rightarrow 1S_{1/2}$ cascade.

4. (See §2.5.2.) W.P.S. Tan [Nature 263 (1976) 656] has examined the muon-catalysed fusion reactions $\mu t + d^+$ (or $\mu d + t^+$) $\rightarrow \alpha$ (3.6 MeV) + n (14 MeV) + μ . He finds these reactions to have a better energy output to input ratio than the corresponding ones for the laser-driven fusion!

5. (See §§2.6.1 and 3.2.) The pressure dependence of the nuclear muon capture rate in gaseous hydrogen is currently under investigation by an ETH–SIN group (authors of ref. [50a] and C. Tschalär, D. Taquq, V.L. Telegdi and A. Zehnder). Fig. N1 represents preliminary results obtained in a parasitic run in August 1976. The solid curve is derived from a simplified model where

*This section will refer to important works appearing in the literature after the completion of the present report.

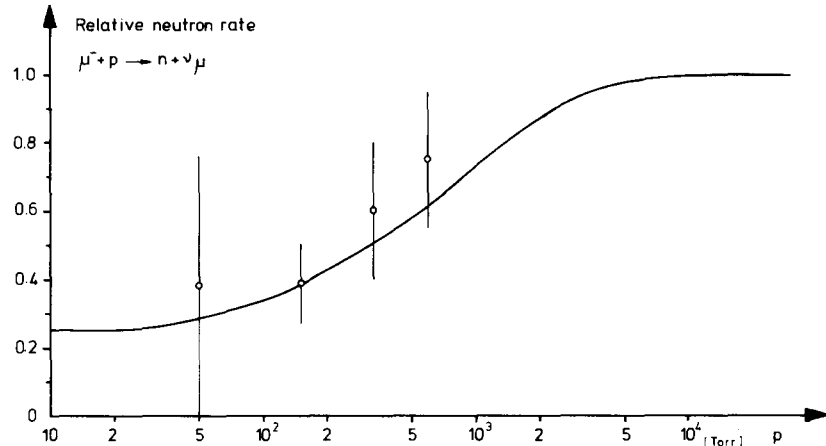


Fig. N1. Relative neutron rate in the reaction $\mu^- + p \rightarrow n + \nu_\mu$ as a function of hydrogen pressure (H. Anderhub et al., private communications).

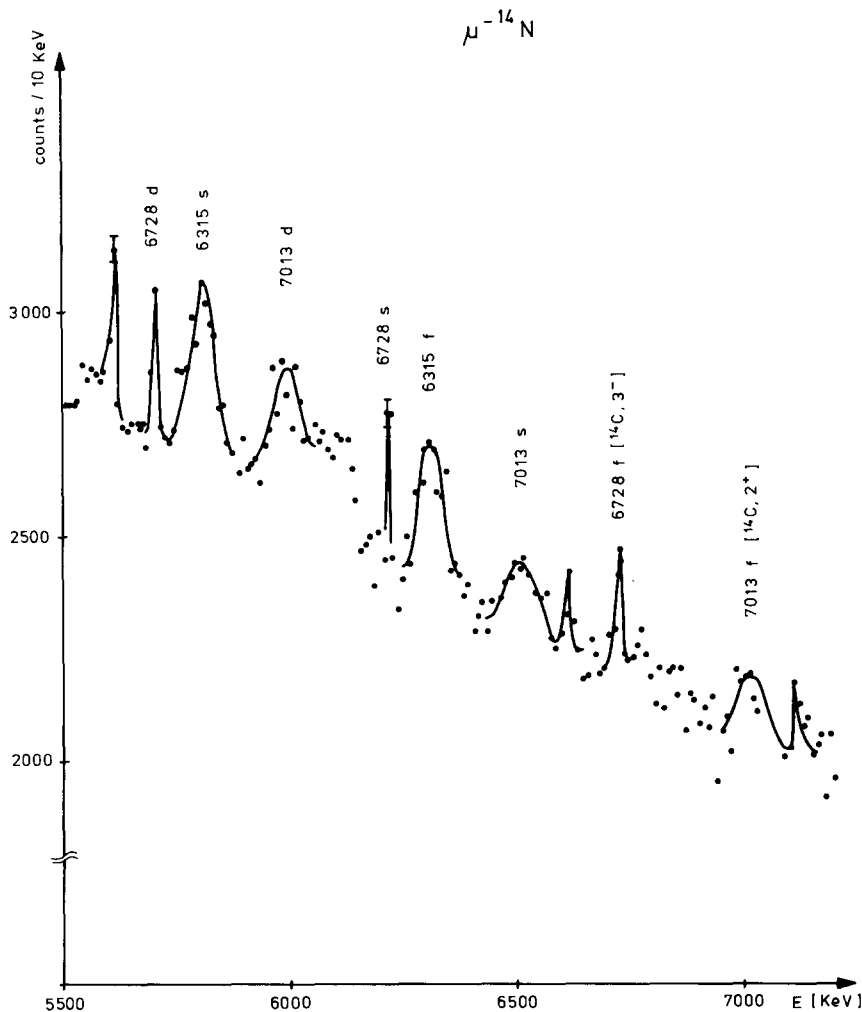


Fig. N2. The gamma spectrum following muon capture in ^{14}N in the region of ^{14}C excitation of 7.01 MeV. s and d in the figure represent single- and double-escape peaks respectively, f being the full energy peak. The 6315 keV line is not identified (E. Bellotti et al., private communications).

the initial statistical populations of the triplet and singlet states change due to a hyperfine conversion rate $\lambda(p)$, linearly dependent on pressure p ; the singlet population is then assumed to be of the form

$$1 - \frac{3}{4} \exp [-\lambda(p)t].$$

Due to experimental reasons, only neutrons delayed by more than 700 ns from the time of the formation of the μp system are taken into account (P. LeCoultre, private communications, Nov. 1976).

6. (See §§5.4.1 and 5.6.) Differences in numerical values for the statistical rate of a given muon capture transition, occurring in several instances in tables 5.3 and 5.7, are due to different nuclear model inputs used in the two calculations. See references [135] and [90], respectively, for further details.

7. (See §5.4.3.) Mukhopadhyay and Martorell [139] have studied the weak and electromagnetic transitions between the ^{12}C ground state and the 1^+ members of the $T = 1$ isomultiplet. Uncertainties due to the nuclear configuration mixing and radial effects have been examined, former in the frameworks of the Cohen-Kurath and Migdal models, and latter in the density-dependent Hartree-Fock approach. Within the uncertainties of the nuclear models, the weak interaction properties are well-reproduced, but the electromagnetic ones are not. An attempt to reproduce the results of the weak and electromagnetic transitions simultaneously at different momentum transfers is unsuccessful. This work brings into sharper focus the limitations of the "effective operator approach" discussed in §4.2.1.

8. (See §5.4.4.) The ETH-SIN-Milan group have studied the reaction $\mu^{-1}\text{N} \rightarrow ^{14}\text{C}^*\nu_\mu$ in the region of the ^{14}C excitation energy of 7.01 MeV. The spectrum obtained by them is reproduced in fig. N2 (E. Bellotti, E. Fiorini and H.K. Walter, private communications, Nov. 1976).

9. (See §§5.5 and 6.1.1.) A. Wyttenbach et al. (private communications, Nov. 1976) have measured, by radiochemical methods, the branching ratio $P = \Lambda_0/\Lambda_c$, where Λ_0 is the rate of muon capture leading to no nucleon emission, and Λ_c is the total capture rate. Targets, with measured values of P in % given in parentheses, are: ^{23}Na (10.7 ± 0.4), ^{27}Al (11.5 ± 0.3), ^{51}V (10.6 ± 0.9), ^{56}Fe (16.5 ± 1.9), ^{59}Co (9.6 ± 0.2), ^{65}Cu (5.8 ± 0.3), ^{75}As (5.4 ± 0.2), ^{104}Ru (16.0 ± 1.6), ^{123}Sb (5.8 ± 0.2), ^{133}Cs (2.4 ± 0.1), ^{165}Ho (9.6 ± 0.2), ^{181}Ta (8.9 ± 1.6), ^{208}Pb (10.5 ± 1.2). Earlier, G.H. Miller (Thesis, College of William and Mary, 1972, unpublished) obtained total ^{28}Al gamma yield of 0.26 ± 0.03 per muon capture in ^{28}Si ; his measured number of ^{24}Na photons is 0.228 ± 0.022 per muon capture in ^{24}Mg .

10. (See §6.3.1.1 [fig. 6.4] and §8.3.1.1.) M.W. Johnson et al. [Bull. Am. Phys. Soc. 21 (1976) 983] have determined the muon capture lifetimes τ_e by decay electrons in the following targets: ^{232}Th , ^{235}U , ^{238}U and ^{239}Pu . Their measured values of τ_e in ns are: 79.2 ± 2.0 , 75.4 ± 1.9 , 73.5 ± 2.0 and 73.4 ± 2.8 respectively, in good agreement with the measurements by the fission method. These values do not show anomalies due to the population of the fission isomers (see also note 13).

11. (See §6.3.1.1.) A. Mekjian [Phys. Rev. Letters 36 (1976) 1242] has examined the three parameter formula of Gouland and Primakoff [eq. (6.19a)] via a microscopic analysis. He finds that the inclusion of long-range correlations in the shell model improves the agreement between the fitted and estimated parameters, though incompatibilities still remain in individual ones.

12. (See §8.3.1.1.) W.D. Fromm et al. have recently reported gamma decays with lifetimes 75 ns and 13 ns, which may be an evidence of the decay of shape-isomers excited in the muonic ^{238}U (see the contribution VII. 20 in the June 1976 Dubna Conference on Nuclear Structure) [I thank Dr. J. Meyer-ter-Vehn for bringing this work to my attention]. See, however, note 13.

13. (See §8.3.1.1.) S.N. Kaplan et al. [Phys. Letters 64B (1976) 217] have found the probability of the fission isomer excitation by muons in ^{238}U to be less than 3%. J. Hadermann (private communications, Nov. 1976) has reinvestigated the possible difference of the electronic and fission muon capture life times of ^{238}U , taking into account the prompt and isomeric decay channels. He finds no essential difference in these life-times, if the muon stays with the fission fragment. Thus, a significant difference in these life times could shed light on the fate of the muon after prompt fission.

14. (See §8.3.3.) I.M. Band et al. [JETP Letters 22 (1975) 236] theoretically examine the fate of the muon after prompt fission (the muon usually remains in the K-shell of the larger fragment). They emphasize the importance of the muonic internal conversion as a way of deexcitation of the fission fragment and estimate the internal conversion coefficients in realistic models.

15. (See §8.4.) A preliminary analysis of the radiative muon capture experiment in ^{40}Ca done by the William and Mary group (M. Eckhouse, private communications, October 1976) based on approximately one thousand radiative muon capture events indicates that the photon asymmetry relative to the muon polarization is opposite to that of the decay electrons, in agreement with theoretical expectations and in disagreement with the earlier experiment of DiLella, Hammerman and Rosenstein [318].

References

A. Selected books and monographs dealing with nuclear muon capture and related topics

- [A1] G. Källén, Elementary particle physics (Addison-Wesley, Reading, Palo Alto, London, 1964) Ch. 14.
- [A2] L. B. Okun', Weak interaction of elementary particles, translators S. and M. Nikolić (Pergamon Press, Oxford and London, 1965) Ch. 8.

- [A3] E. J. Konopinski, The theory of beta radioactivity (Oxford Univ. Press, Oxford and London, 1966) Ch. XIII.
- [A4] C. S. Wu and S. A. Moszkowski, Beta decay (Interscience, New York, 1966) Ch. 6.
- [A5] A. O. Weissenberg, Muons, translator S. Chomet (North-Holland, Amsterdam, 1967) Chs. 3 and 6.
- [A6] A. Bohr and B. R. Mottelson, Nuclear structure (Benjamin, New York, Amsterdam, 1969) Vol. I, Ch. 3; Vol. II (1975) Ch. 6.
- [A7] R. E. Marshak, Riazuddin and C. P. Ryan, Theory of weak interactions (Wiley-Interscience, New York, London, 1969) Ch. 4.
- [A8] J. M. Eisenberg and W. Greiner, Nuclear theory (North-Holland, Amsterdam, London, New York, 1970) Vol. 2, Chs. 10 and 11.
- [A9] Y. N. Kim, Mesic atoms and nuclear structure (North-Holland, Amsterdam, 1971).
- [A10] R. J. Blin-Stoyle, Fundamental interactions and the nucleus (North-Holland, Amsterdam, 1973) Ch. VII.
- [A11] M. Morita, Beta decay and muon capture (Benjamin, Reading, 1973) Chs. 8 and 9.
- [A12] A. de Shalit and H. Feshbach, Theoretical nuclear physics (Wiley, New York, London, 1974) Ch. IX.
- [A13] C. S. Wu and V. Hughes (eds.), Muon physics (Academic Press, New York, London, 1975) 3 volumes.
- [A14] F. Scheck, Les interactions faibles (Université de Neuchâtel) Ch. VIII.

B. Review articles on muon capture and related topics

- [B0] D. Bailin, Rep. Prog. Phys. 34 (1971) 491.
- [B1] V. V. Balashov and R. A. Eramzhyan, Atomic energy review (Vienna) 5 (1967) 3.
- [B1'] J. Bernabéu, in: Zuoz (1976) Lectures, to be published.
- [B1a] A. Bertin, A. Vitale and A. Placci, Riv. Nuovo Cimento 5 (1975) 423.
- [B1b] G. E. Brown and W. Weise, Phys. Reports 22C (1975) 279, and in press.
- [B2] F. Cannata, R. Graves and H. Überall, The capture of muons by complex nuclei, Riv. Nuovo Cimento, to be published.
- [B3] C. Chiechanowicz and Z. Oziewicz, Kinematics of muon capture, Dubna preprint JINR- E4-6138 (1971).
- [B3a] R. H. Dalitz, Proc. Roy. Soc. A285 (1965) 229.
- [B4] J. Deutsch, Nuclear structure information from particle-emission in muon capture, in: Zuoz (1973) Lectures, CERN report 74-8 (1974).
- [B5] V. Devanathan, in: Lectures on theoretical physics, eds. A. O. Barut and W. E. Britten (Gordon and Breach, 1968).
- [B6] R. Engfer, in: Informal report on the IKO low-energy pion/muon physics study week (hereafter called IKO lectures), eds. R. van Dantzig et al. (IKO, Amsterdam, 1975) Vol. I, p. 33.
- [B7] M. Ericson and M. Rho, Phys. Reports 5C (1972) 57.
- [B8] T. E. O. Ericson, in: Proc. 12th Internat. Conf. on High-Energy Physics, Dubna (1966) Vol. 2, p. 204.
- [B9] V. S. Evseev, Depolarization of negative muons and interactions of mesonic atoms with the medium, in: Wu-Hughes [A13].
- [B10] G. Feinberg and L. M. Lederman, Ann. Rev. Nuclear Sci. 13 (1963) 43.
- [B11] E. Fiorini, Riv. Nuovo Cimento 4 (1975) 401.
- [B11a] S. Frankel, Rare and ultra-rare μ -decays, in: Wu-Hughes [A13].
- [B12] S. S. Gershtein and L. I. Ponomarev, Mesonuclear processes induced by μ^- mesons, in: Wu-Hughes [A13].
- [B13] M. Gourdin, Phys. Reports 11C (1974) 29.
- [B13a] J. Hüfner, Phys. Reports 21C (1975) 1.
- [B14] J. Hüfner, F. Scheck and C. S. Wu, Muonic atoms, in: Wu-Hughes [A13].
- [B14a'] C. Jarlskog, Nuclear Phys., to be published.
- [B14a] G. Källén, Radiative corrections to weak interactions, in: Nuclear and particle physics, eds. B. Margolis et al. (Benjamin, Amsterdam, 1968) p. 123.
- [B15] C. W. Kim, Riv. Nuovo Cimento 4 (1974) 189.
- [B16] T. D. Lee and C. S. Wu, Ann. Rev. Nuclear Sci. 15 (1965) 381.
- [B17] C. H. Llewellyn Smith, Phys. Reports 3C (1972) 264.
- [B17a] M. Locher (ed.), Proc. 1976 Zuoz topical meeting on the Intermediate Energy Physics, to be published.
- [B18] M. Morita, A. Fujii and H. Ohtsubo, Suppl. Progr. Theoret. Phys. Extra Number (1968) 303;;
M. Morita et al., Suppl. Progr. Theoret. Phys. 41 (1971) 41.
- [B19] N. C. Mukhopadhyay, Remarks on the muon-nucleon weak interaction, CERN-TH 1959 (1974), and in: IKO Lectures, eds. R. van Dantzig et al. (IKO, Amsterdam, 1975) Vol. I, p. 49 and Vol. II, p. 315; Zuoz (1976) Lectures, to be published.
- [B20] L. I. Ponomarev, Ann. Rev. Nuclear Sci. 23 (1973) 395.
- [B21] H. Primakoff, Springer Tracts 53 (1970) 6.
- [B22] H. Primakoff, Elementary particle aspects of muon decay and muon capture, in: Wu-Hughes [A13].

- [B23] M. Rho, Muon capture in nuclei and Migdal theory, in: Nuclear and particle physics, eds. B. Margolis et al. (Benjamin, Amsterdam, 1968) p. 343.
- [B24] M. Rho, in: Les Houches lectures (1968), eds. C. De Witt and V. Gillet (Gordon and Breach, London, 1969) p. 669.
- [B25] H. P. C. Rood, Suppl. Nuovo Cimento 4 (1966) 185.
- [B26] J. E. Rothberg, Lectures on muon physics, in: Proc. Banff Summer School (1970), eds G. C. Neilson et al. (Univ. of Alberta) p. 43.
- [B27] F. Scheck, in: Zuoz (1972) Lectures (SIN, Villigen, 1972) p. 1.
- [B27a] N. Straumann, in: Zuoz (1972) lectures (SIN, Villigen, 1972) p. 91.
- [B28] L. Schellenberg, Chemical effects in the capture of negative muons, in: IKO Lectures, eds. R. van Dantzig et al. (IKO, Amsterdam, 1975) Vol. I, p. 61.
- [B29] J. C. Sens, in: Proc. Internat. Conf. on High-Energy Physics and Nuclear Structure (1963) p. 143.
- [B30] P. Singer, Springer Tracts 71 (1974) 39.
- [B31] R. M. Sundelin and R. M. Edelstein, in: High-Energy Physics and Nuclear Structure, ed. S. Devons (Plenum Press, New York, 1970) p. 150.
- [B32] V. L. Telegdi, in: Weak interactions and topics in dispersion physics (Benjamin, New York, 1962) p. 16.
- [B33] H. A. Tolhoek, in: Selected topics in nuclear theory (IAEA, Vienna, 1963) p. 343.
- [B34] H. Überall, Springer Tracts 71 (1974) 1.
- [B35] P. Vogel, P. K. Haff, V. Akylas and A. Winther, Nuclear Phys. A254 (1975) 445.
- [B36] J. D. Walecka, Semi-leptonic weak interactions in nuclei, in: Wu-Hughes [A13].
- [B37] L. Wolfenstein, in: High-energy Physics and Nuclear Structure, ed. S. Devons (Plenum, New York, 1970) p. 661.
- [B38] C. S. Wu and L. Wilets, Ann. Rev. Nuclear Sci. 19 (1969) 527.
- [B39] E. Zavattini, Muon capture, in: Wu-Hughes [A13].

C. Selected doctoral dissertations utilized in this review*

- [C1] A. Bouyssy, Etude de l'émission de neutrons après capture de muons par les noyaux, Orsay and Paris-Sud (1974).
- [C2] D. A. Bryman, A search for the reaction $\mu^- + \text{Cu} \rightarrow e^+ + \text{Co}$, Virginia Polytechnic Institute (1972).
- [C3] J. Delorme, Sur une méthode globale de traitement des courants nucléaires, Lyon (1972).
- [C4] D. Favart, Depolarisation des muons négatifs par l'interaction hyperfine, Louvain (1970).
- [C5] M. Hiro-Oka, Muon capture in ^{12}C and ^{16}O , Osaka (1969).
- [C6] J. Joseph, L'absorption des muons par les noyaux, Lyon (1973).
- [C7] J. R. Luyten, Calculation of total muon capture rates in nuclei, Groningen (1968).
- [C8] G. K. Manacher, Contributions of pion and nucleon currents to radiative μ -meson capture by a proton, Carnegie Tech. (1961).
- [C9] N. C. Mukhopadhyay, Allowed muon capture in light nuclei, Chicago (1972).
- [C10] H. Ohtsubo, Muon capture (in Japanese), Tokyo Inst. of Technology (1967).
- [C11] Z. Oziewicz, Partial muon capture, Wrocław (1970).
- [C12] L. Palfy, Mesure du taux de désintégration de $^{16}\text{N}^m$ en vue de préciser la constante pseudoscalaire induite, Louvain (1974).
- [C13] R. Parthasarathy, Asymmetry and polarization of the recoil nucleus in the muon capture in ^{12}C , Madras (1974).
- [C14] H.-J. Pfeiffer, Messung mesischer Röntgenstrahlen mit einem Hochdruck-Gastarget, Technische Universität München (1974).
- [C15] H. P. C. Rood, On the theory of muon capture in nuclei, Groningen (1964).
- [C16] L. M. Rosenstein, Radiative muon capture in ^{40}Ca , Columbia (1972).
- [C17] W.-U. Schröder, Spectroscopy of neutrons from μ -capture in Ca, Tl, Pb, and Bi, Darmstadt (1973).
- [C18] J. C. Sens, Capture of negative muons by nuclei, Chicago (1958).
- [C19] R. Winston, Observable hyperfine effects in muon capture, Chicago (1962).

D. References (mostly) to the journal articles

- [1] E. Fermi, Z. Physik 88 (1934) 161.
- [2] S. Tomonaga and G. Araki, Phys. Rev. 58 (1940) 90.

*See also the dissertations of J.S. Baijal (Berkeley 1962), J. Bernabéu (Valencia 1970), W.J. Bertram (Carnegie 1960), B. Block (Carnegie 1960), R.M. Cantwell (Washington 1956), R.C. Cohen (Columbia 1965), J. Doede (Chicago 1963), W. Eisenstein (Columbia 1964), R.J. Esterling (Berkeley 1964), T.N.K. Godfrey (Princeton 1954) D.E. Hagge (Berkeley 1963), D.A. Jenkins (Berkeley 1964), J. Kane (Carnegie 1964), N.H. Lipman (Liverpool 1959), E. Lubkin (Columbia 1960), B. MacDonald (Berkeley 1964), E.T.R. Maier (Carnegie 1962), R.A. Mann (Oak Ridge 1960), G.H. Miller (William and Mary 1972), A.M. Rushton (Columbia 1972), R.M. Sundelin (Carnegie 1967), J.D. Teja (Genève 1959).

- [3] M. Conversi, E. Pancini and O. Piccioni, Phys. Rev. 68 (1945) 232; 71 (1947) 209.
- [4] E. Fermi and E. Teller, Phys. Rev. 72 (1947) 399.
- [5] J. Tiomno and J. A. Wheeler, Rev. Mod. Phys. 21 (1949) 153.
- [6] U. Camerini, H. Muirhead, C. F. Powell and D. H. Rison, Nature 162 (1948) 433; E. P. Gorge and J. Evans, Proc. Phys. Soc. 63A (1950) 124; H. Morinaga and W. F. Fry, Nuovo Cimento 10 (1953) 308.
- [7] T. N. K. Godfrey, Phys. Rev. 92 (1953) 512.
- [8] R. H. Hildebrand, Phys. Rev. Letters 8 (1962) 34.
- [9] J. A. Wheeler, Rev. Mod. Phys. 21 (1949) 133.
- [10] T. D. Lee and C. N. Yang, Phys. Rev. 104 (1956) 254.
- [11] R. Marshak and E. C. G. Sudarshan, Proc. Internat. Conf. Elem. Particles, Padua--Venice (1957); R. P. Feynman and M. Gell-Mann, Phys. Rev. 109 (1958) 193; J. J. Sakurai, Nuovo Cimento 7 (1958) 649.
- [12] Ya. B. Zel'dovich and S. S. Gershtein, Sov. Phys. JETP 2 (1957) 576; Feynman and Gell-Mann [11].
- [13] Y. Nambu, Phys. Rev. Letters 4 (1960) 380; M. Gell-Mann M. Lévy, Nuovo Cimento 16 (1960) 705.
- [14] S. Weinberg, Phys. Rev. 112 (1958) 1375.
- [15] M. L. Goldberger and S. B. Treiman, Phys. Rev. 111 (1958) 354.
- [16] L. Wolfenstein, Nuovo Cimento 8 (1958) 882.
- [17] J. Bernstein, T. D. Lee, C. N. Yang and H. Primakoff, Phys. Rev. 111 (1958) 313.
- [18] H. Primakoff, Rev. Mod. Phys. 31 (1959) 802. See also C. S. Wu and M. L. Goldberger, *ibid.*, pp. 783 and 797 resp.
- [19] A. A. Quaranta, A. Bertin, G. Matone, F. Palmonari, G. Torelli, P. Dalpiaz, A. Placci and E. Zavattini, Phys. Rev. 177 (1969) 2118.
- [20] L. L. Foldy and J. D. Walecka, Nuovo Cimento 34 (1964) 1026.
- [21] S. Fallieros, B. Goulard and R. H. Venter, Phys. Letters 19 (1965) 398; B. Goulard and S. Fallieros, Can. J. Phys. 45 (1967) 3221; S. Fallieros and B. Goulard, Nuclear Phys. A147 (1970) 593.
- [22] See K. P. Lohs, G. W. Wolschin and J. Hüfner, Nuclear Phys. A236 (1974) 457 and references therein; W. Kaufmann and H. Pilkuhn, to be published.
- [23] D. F. Zaretskii and V. M. Novikov, Nuclear Phys. 14 (1960) 540; V. S. Evseev and T. N. Mamedov, Sov. J. Nuclear Phys. 19 (1974) 624.
- [24] See, for example, P. Vogel, P. K. Haff, V. Akylas and A. Winther, Nuclear Phys. A254 (1975) 445 and references therein; M. Leon and R. Seki, Phys. Rev. Letters 32 (1974) 132, and private communications (1975); R. Kuselman, J. Law, M. Leon and J. Miller, Phys. Rev. Letters 36 (1976) 446; H. Daniel, Phys. Rev. Letters 35 (1975) 1649.
- [24a] V. G. Zinov, A. D. Konin and A. I. Mukhin, Sov. J. Nuclear Phys. 2 (1966) 613. A recent experiment at LAMPF has given qualitatively similar results.
- [25] S. Nagamiya et al., contributions II. 15–17 at the Santa Fe meeting (June 1975).
- [26] L. F. Mausner, R. A. Naumann, J. A. Monard and S. N. Kaplan, Contribution II. 24 at the Santa Fe meeting (June 1975); J. A. Monard, private communications (June 1975).
- [27] C. E. Porter and H. Primakoff, Phys. Rev. 83 (1951) 849; V. Gilinski and J. Mathews, Phys. Rev. 120 (1960) 1450; R. W. Huff, Ann. Phys. 16 (1961) 288; P. Hänggi, R. D. Violler, V. Raff and K. Alder, Phys. Letters 51B (1974) 119; P. Hänggi, private communications (January 1976).
- [28] See, for example, H. A. Bethe and E. F. Salpeter, Quantum mechanics of one and two-electron systems, in: Handbuch der Physik, ed. S. Flügge (Springer-Verlag, Berlin, 1957) Vol. XXXV, pp. 193 ff.
- [29] L. Hambro and N. C. Mukhopadhyay, Lett. Nuovo Cimento 14 (1975) 53, and to be published.
- [30] V. L. Telegdi, Phys. Rev. Letters 3 (1959) 59; R. Winston and V. L. Telegdi, Phys. Rev. Letters 7 (1961) 104; R. Winston, Phys. Rev. 129 (1961) 2766; G. Culligan, J. F. Lathrop, V. L. Telegdi, R. Winston and R. A. Lundy, Phys. Rev. Letters 7 (1961) 458.
- [31a] J. P. Deutsch, L. Grenacs, J. Lehmann, P. Lipnik and P. C. Macq, Phys. Letters 28B (1968) 178.
- [31b] D. Favart, F. Brouillard, L. Grenacs, P. Igo-Kemenes, P. Lipnik and P. C. Macq, Phys. Rev. Letters 25 (1970) 1348.
- [32] G. Breit, Nature 122 (1928) 649; T. Yamazaki, S. Nagamiya, O. Hashimoto, K. Nagamine, K. Nakai, K. Sugimoto and K. M. Crowe, Phys. Letters 53B (1974) 117, and references therein.
- [33] See, for example, G. Wentzel, Phys. Rev. 75 (1949) 1810. In section IV of this paper, replace π by μ !

- [34] I.M. Shmushkevich, Nuclear Phys. 11 (1959) 419;
V.A. Dzhrbashyan, ZETF 36 (1959) 277;
R.A. Mann and M.E. Rose, Phys. Rev. 121 (1961) 293;
A.P. Bukhvostov, Sov. J. Nuclear Phys. 9 (1969) 65; see also Evseev [B9].
- [35] P.A. Souder, D.E. Casperson, T.W. Crane, V.W. Hughes, D.C. Lu, H. Orth, H.W. Reist, M.H. Yam and G. zu Putlitz, Phys. Rev. Letters 34 (1975) 1417.
- [36] A.A. Dzhuravc, V.S. Evseev, G.G. Myasischcheva, Yu.V. Obukhov and V.S. Roganov, Sov. Phys. JETP 35 (1972) 748.
- [37] R.K. Wangness and F. Bloch, Phys. Rev. 89 (1953) 728.
- [38] H. Überall, Phys. Rev. 114 (1959) 1640; 121 (1961) 1219.
- [38a] L. Simons, private communications (May 1976).
- [39] G. Holzwarth and H.-J. Pfeiffer, Z. Physik A272 (1975) 311;
H.-J. Pfeiffer, K. Springer and H. Daniel, Nuclear Phys. A254 (1975) 533.
For a discussion of the high-pressure hydrogen target, see K. Springer, Nuclear Instrum. Methods 106 (1973) 65.
- [40a] Y.B. Zel'dovich and S.S. Gershtein, Sov. Phys. Usp. 3 (1961) 593;
- [40b] S. Cohen, D.L. Judd and R.J. Riddel, Phys. Rev. 119 (1960) 397.
- [41] A. Alberigi Quaranta, A. Bertin, G. Matone, F. Palmonari, A. Placci, P. Dalpiaz, G. Torelli and E. Zavattini, Nuovo Cimento 47B (1967) 72.
- [42] G. Matone, Lett. Nuovo Cimento 2 (1971) 151.
- [43a] E.J. Bleser, E.W. Anderson, L.M. Lederman, S.L. Meyer, J.L. Rosen, J.E. Rothberg and I.-T. Wang, Phys. Rev. 132 (1963) 2679
- [43b] G. Conforto, C. Rubbia, E. Zavattini and S. Focardi, Nuovo Cimento 33 (1964) 1001.
- [44a] E.J. Bleser, L.M. Lederman, J.L. Rosen, J.E. Rothberg and E. Zavattini, Phys. Rev. Letters 8 (1962) 288.
- [44b] I.-T. Wang, E.W. Anderson, E.J. Bleser, L.M. Lederman, S.L. Meyer, J.L. Rosen and J.E. Rothberg, Phys. Rev. 139 (1965) B1528.
- [45] See V.M. Bystritskii, V.P. Dzhelepov, K.O. Oganesyan, N.N. Omel'yanenko, S.Yu. Porokhovoi, A.I. Rudenko and V.V. Fil'chenkov, Sov. Phys. JETP 39 (1974) 27, and references therein.
- [46] E.A. Vesman, JETP Letters 5 (1967) 91.
- [47] L.W. Alvarez, H. Bradner, F.S. Crawford, P. Falk-Vairant, M.L. Good, J.D. Gow, A.H. Rosenfeld, F.T. Solmitz, M.L. Stevenson, H.K. Ticho and R.D. Tripp, Phys. Rev. 105 (1957) 1127;
See L.W. Alvarez, in: Adventures in physics, Vol. a, ed. B. Maglić (1974).
- [48] L.W. Alvarez, Nobel lecture, reproduced in: Evolution of particle physics, ed. M. Conversi (Academic, New York, 1970).
- [49] V.P. Dzhelepov, M. Frimi, S.S. Gershtein, Yu.V. Katyshev, V.I. Moskalev and P.F. Ermolov, Proc. Internat. Conf. on High-Energy Physics, CERN, Geneva (1962) p. 484;
G. Conforto, C. Rubbia, E. Zavattini and S. Focardi, Nuovo Cimento 33 (1964) 1001;
Yu. Budyashov, I.F. Ermolov, V.G. Zinov, A.D. Konin and A.I. Mukhin, Sov. J. Nuclear Phys. 5 (1967) 426.
- [50] A. Placci, E. Zavattini, A. Bertin and A. Vitale, Nuovo Cimento 52A (1967) 1274; 64A (1969) 1053.
- [50a] H. Anderhub, F. Kottmann, H. Hofer, P. Le Coultre, D. Makowiecki, O. Pitzurra, B. Sapp, P.G. Seiler, P. Shrager, M. Wälchi and P. Wolff, Phys. Letters 60B (1976) 273.
- [50b] V.F. Dmitriev, Sov. J. Nuclear Phys. 20 (1975) 215.
- [51] W.A. Mann, V. Mehtani, B. Musgrave, Y. Oren, P.A. Schreiner, R. Singer, H. Yuta, R. Ammar, S. Barish, Y. Cho, M. Derrick, R. Engelman and L.G. Hyman, Phys. Rev. Letters 31 (1973) 844;
See D.H. Perkins, Review of neutrino experiments, in: Proc. of 1975 Stanford Symposium on Lepton and Photon Interactions at High Energies, p. 571.
- [52] V.M. Byskitskii, V.P. Dzhelepov, P.F. Ermolov, K.O. Oganesyan, M.N. Omel'yanenko, S.Yu. Porokhovoi, V.S. Roganov, A.I. Rudenko and V.V. Fil'chenkov, Sov. Phys. JETP 39 (1974) 19.
- [53] J.E. Rothberg, E.W. Anderson, E.J. Bleser, L.M. Lederman, S.L. Meyer, J.L. Rosen and I.-T. Wang, Phys. Rev. 132 (1963) 2664.
- [54] S. Weinberg, Phys. Rev. Letters 4 (1960) 575.
- [55] W.R. Wessel and P. Philipson, Phys. Rev. Letters 13 (1964) 23;
A. Halpern, Phys. Rev. Letters 13 (1964) 660.
- [56] J.H. Doede and R. Hildebrand, Proc. Internat. Conf. on High-Energy physics, CERN, Geneva (1962) p. 418;
E. Bertolini, A. Citron, G. Gialamella, S. Focardi, A. Mukhin, C. Rubbia and F. Saporetti, ibid. p. 421;
See also the report by C. Rubbia in: Proc. Internat. Conf. on Fundamental Aspects of Weak Interactions, Brookhaven (1963) p. 277;
J.H. Doede, Phys. Rev. 132 (1963) 1782.
- [57] M. Gell-Mann, Phys. Rev. 125 (1962) 1067;
N. Cabibbo, Phys. Rev. Letters 10 (1963) 531.

- [58] See, for an excellent introduction, J. Bernstein, Elementary particles and their currents (Freeman, San Francisco, London) 1968;
- J.J. Sakurai, Currents and mesons (Chicago University Press, Chicago and London, 1969).
- [59] S.L. Adler, Phys. Rev. Letters 14 (1965) 1051;
W.T. Weisberger, Phys. Rev. Letters 14 (1965) 1047.
- [60] J.C. Hardy, G.C. Ball, J.S. Geiger, R.L. Graham, J.A. MacDonald and H. Schmeing, Phys. Rev. Letters 33 (1974) 320.
See also I.S. Towner and J.C. Hardy, Nuclear Phys. A205 (1973) 33;
Wilkinson [76a];
D.H. Wilkinson and D.E. Alburger, Phys. Rev. C13 (1976) 2517.
- [61] J. Delorme and M. Rho, Nuclear Phys. B34 (1971) 317.
- [62] Particle Data Group, Rev. Mod. Phys. 48 (1976) S1.
- [63] B. Bartoli, F. Felicetti and V. Silvestrini, Riv. Nuovo Cimento 2 (1972) 241.
- [64] V.E. Krohn and G.R. Ringo, Phys. Letters 55B (1975) 175. Their value should be compared with the value quoted in ref. [62]: 1.25 ± 0.0094 .
- [65] See, for example, G. Furlan, N. Paver and C. Verzegnassi, Springer Tracts 62 (1972) 118.
- [66] E.D. Bloom, R.L.A. Cottrell, H. de Staebler, C.L. Jordan, H.G. Piel, C.Y. Prescott, R. Siemann, S. Stein and R.E. Taylor, Phys. Rev. Letters 30 (1973) 1186.
- [67] C. Jarlskog, private communications (1976), and to be published;
see also D.H. Perkins [51].
- [68] S.L. Adler and R.F. Dashen, Current algebras (Benjamin, New York, Amsterdam, 1968) pp. 46 ff.
- [69] H. Pilkuhn, W. Schmidt, A.D. Martin, C. Michael, F. Steiner, B.R. Martin, M.M. Nagels and J.J. De Swart, Nuclear Phys. B65 (1973) 460, and to be published.
- [70] A. Sirlin, Phys. Rev. D5 (1972) 436;
H. Pagels and A. Zepeda, Phys. Rev. D5 (1972) 3262.
- [71] R.I. Steinberg, P. Liaud, B. Vignon and V.W. Hughes, Phys. Rev. Letters 33 (1974) 41.
- [72] K. Sugimoto, I. Tanihata and J. Göring, Phys. Rev. Letters 34 (1975) 1533;
M. Morita and I. Tanahata, Phys. Rev. Letters 35 (1975) 26;
F. Calaprice, Phys. Rev. C12 (1975) 2016, and Bull. Am. Phys. Soc. 21 (1976) 507.
- [73] N. Cabibbo, Phys. Letters 12 (1964) 137.
- [74] A. Sirlin, Phys. Rev. 164 (1967) 1767;
G. Källén, Nuclear Phys. B1 (1967) 225;
D.H. Wilkinson and B.E.F. Macefield, Nuclear Phys. A158 (1970) 110.
- [75] P. Pascual, An. Fís. 67 (1971) 197;
see also P. Kabir, Z. Physik 197 (1966) 447;
H. Ohtsubo and A. Fujii, Nuovo Cimento 42 (1966) 109;
J. Frazier and C.W. Kim, Phys. Rev. 177 (1969) 2568, and ref. [126].
- [76] R.J. Blin-Stoyle and J.M. Freeman, Nuclear Phys. A150 (1970) 369;
R.T. Shann, Nuovo Cimento 5A (1971) 591;
Y. Yokoo, S. Suzuki and M. Morita, Progr. Theoret. Phys. (Kyoto) 50 (1973) 1894.
- [76a] D.H. Wilkinson, Nature 257 (1975) 189.
- [77] L.L. Foldy and S.A. Wouthuysen, Phys. Rev. 78 (1950) 29.
- [78] A. Fujii and H. Primakoff, Nuovo Cimento 12 (1959) 327.
- [79] H. Ohtsubo, Phys. Letters 22 (1966) 480;
J.L. Friar, Nuclear Phys. 87 (1966) 407.
- [80] A. Vitale, A. Bertin and G. Carboni, Phys. Rev. D11 (1975) 2441.
- [81] A. de Shalit, Summary talk at the International Conf. on Nuclear Reactions induced by heavy ions, Heidelberg, 1969, eds. R. Bock and W.R. Hering (North-Holland, Amsterdam, 1970) pp. 807.
- [82] E. Fermi, Ric. Sci. V11-11 (1936) 13;
G.F. Chew and M.L. Goldberger, Phys. Rev. 87 (1952) 778.
- [83] M.H. MacFarlane, in: Proc. Intern. School of Physics "Enrico Fermi", Course XL, ed. M. Jean (Academic Press, New York, 1969);
G.F. Bertsch, The practitioner's shell model (North-Holland, Amsterdam, London, 1972).
- [84] G.E. Brown, Unified theory of nuclear models (North-Holland, Amsterdam, 1964);
D.J. Rowe and C. Ngo-Trong, Rev. Mod. Phys. 47 (1975) 331, and references therein.
- [85] M. Morita and A. Fujii, Phys. Rev. 118 (1960) 606.
- [86] V. Gillet and D.A. Jenkins, Phys. Rev. 140 (1965) B32.
- [87] T.W. Donnelly, in: Zuoz School (1975) proceedings, ed. F. Scheck (SIN, Villigen, 1975).

- [88] V. Devanathan, P.R. Subramanian, R.D. Graves and H. Überall, Phys. Letters 57B (1975) 241.
- [89] N.C. Mukhopadhyay, Phys. Rev. C7 (1973) 1720.
- [90] A.P. Bukhvostov, A.M. Chatrchan, G.E. Dogotar, R.A. Eramzhyan, N.P. Popov and V.A. Vartanjan, Acta Phys. Polon. B3 (1972) 375.
- [91] N.C. Mukhopadhyay and M.H. Macfarlane, Phys. Rev. Letters 27 (1971) 1823; 28 (1972) 1545E.
- [92] N.P. Popov, Thesis, A.I.F. Ioffe Technical Inst., Leningrad (1965) (unpublished).
- [93] Z. Oziewicz, Acta Phys. Polon. 31 (1967) 501.
- [94] J. Bernabéu, Phys. Letters 55B (1975) 313.
- [95] This relation was obtained earlier by explicit calculation in the impulse approximation. See L. Wolfenstein, Nuovo Cimento 13 (1959) 319; P.R. Subramanian and V. Devanathan, Phys. Rev. C11 (1975) 520.
- [96] V. Trimble and F. Reines, Rev. Mod. Phys. 45 (1973) 1;
T.E.O. Ericson, Summary talk at the 6th Internat. Conf. on High-Energy Physics and Nuclear structure (1975), (A.I.P., New York, 1975) p. 702.
- [97] A. Placci, E. Zavattini, A. Bertin and A. Vitale, Phys. Rev. Letters 25 (1970) 475; Phys. Rev. D8 (1973) 3774.
- [98] I.-T. Wang, Phys. Rev. 139 (1965) B1539.
- [99] H. Überall and L. Wolfenstein, Nuovo Cimento 10 (1958) 136.
- [100] E. Cremmer, Nuclear Phys. B2 (1967) 409.
- [101] E. Truhlik, Nuclear Phys. B45 (1972) 303.
- [102] P. Pascual, R. Tarrach and F. Vidal, Nuovo Cimento 12A (1972) 241.
- [103] S.L. Mintz, Phys. Rev. D8 (1973) 2946.
- [104] B.F. Gibson and G.J. Stephenson, Los Alamos informal report LA-5424 MS (November 1973), unpublished, and private communications to C. Petitjean (February 1976).
- [105] M. Sotona and E. Truhlik, Phys. Letters 43B (1973) 362; Nuclear Phys. A229 (1974) 471.
- [106] G.E. Dogotar, R.A. Eramzhyan and Yu.A. Salganik, Dubna preprint E4-8263 (September 1974); Dubna preprint P2-9469 (1976).
- [107] N.T. Nguyen, Nuclear Phys. A254 (1975) 485.
- [107a] H. Picker, J. Levin and Q. Ho-Kim, Phys. Rev. C13 (1976) 1966.
- [108] F. Dautry, M. Rho and D.O. Riska, Nucl. Phys. A264 (1976) 507.
- [109] W. Gibbs, Invited talk in the 4th Internat. Symposium of Polarization Phenomena in Nuclear Reactions, Zürich (August, 1975), to be published;
L.D. Knutson and W. Haeberli, Phys. Rev. Letters 35 (1975) 558.
- [110] R.V. Reid, Ann. of Phys. (N.Y.) 50 (1968) 411.
- [111] W.H. Breunlich, W.J. Kossler, L.A. Schaller, C. Petitjean and R. van Dantzig, private communications (March, 1976).
- [112] T.A. Dmitrieva, Z. Oziewicz and A. Pikulski, Nuclear Phys. A155 (1970) 205.
- [113] A. Fujii, Phys. Rev. 118 (1960) 870.
- [114] C. Werntz, Nuclear Phys. 16 (1960) 59.
- [115] H.G. Wahsweiler, Z. Phys. 172 (1963) 375.
- [116] G.Ya. Korenman and R.A. Eramzhyan, Sov. Phys. JETP 18 (1964) 767.
- [117] A. Fujii and Y. Yamaguchi, Progr. Theoret. Phys. 31 (1964) 107.
- [118] W. Dreschsler and B. Stech, Z. Phys. 178 (1964) 1.
- [119] K.-T. Chen, Acta Phys. Sinica 21 (1965) 1897.
- [120] C.W. Kim and H. Primakoff, Phys. Rev. 140 (1965) B566.
- [121] E.A. Peterson, Phys. Rev. 167 (1968) 971.
- [122] P. Pascual and R. Pascual, Nuovo Cimento 48 (1967) 963.
- [123] R. Pascual, Nuclear Phys. B3 (1967) 561.
- [124] S.P. Goreslavskii and G.V. Rozhnov, Sov. J. Nuclear Phys. 9 (1969) 225.
- [125] A.C. Phillips, F. Roig and J. Ros, Nuclear Phys. A237 (1975) 493.
- [126] A. Santisteban and R. Pascual, Nuclear Phys. A260 (1976) 392.
- [127] I.V. Falomkin, A.I. Filippov, M.M. Kołyukein, B. Pontecorvo, Yu.A. Schezbakov, R.M. Sulyeaev, V.M. Tsupko-Sitnikov and O.A. Zaimidiroga, Phys. Letters 3 (1963) 229.
- [128] L.B. Auerbach, R.J. Esterling, R.E. Hill, D.A. Jenkins, J.T. Lach and N.Y. Lipman, Phys. Rev. 138 (1965) B127.
- [129] D.B. Clay, J.W. Keuffel, R.L. Wagner and R.M. Edelstein, Phys. Rev. 140 (1965) B856.
- [130] L.M. Delves and A.C. Phillips, Rev. Mod. Phys. 41 (1969) 49;
S.N. Yang and A.D. Jackson, Phys. Letters 36B (1971) 1;
R.A. Brandenburg, Y.E. Kim and A. Tubis, Phys. Letters 49B (1974) 205;
W.M. Kloet and J.A. Tjon, Phys. Letters 49B (1974) 419.
- [131] A. Placci, E. Polacco, E. Zavattini, K. Ziöck, G. Carboni, U. Gastaldi, G. Gorini, G. Neri and G. Torelli, Nuovo Cimento 1A (1971) 445.

- [132] C. Jarlskog and F.J. Ynduráin, Nuovo Cimento 12A (1972) 81.
See also Kopeliovich [367].
- [133] N.C. Mukhopadhyay, Phys. Letters 40B (1972) 157.
- [134] N.C. Mukhopadhyay, Phys. Letters 44B (1973) 33.
- [135] N.C. Mukhopadhyay, Phys. Letters 45B (1973) 309.
- [136] N.C. Mukhopadhyay, Lett. Nuovo Cimento 7 (1973) 460.
- [137] N.C. Mukhopadhyay and F. Cannata, Phys. Letters 51B (1974) 225.
- [138] J.D. Immele and N.C. Mukhopadhyay, Phys. Letters 56B (1975) 13.
- [139] N.C. Mukhopadhyay and J. Martorell, to be published.
- [139a] A. Figureau and N.C. Mukhopadhyay, to be published.
- [140] V.A. Vartanian, T.A. Dmitrieva, H.-U. Jager, G.R. Kissener and R.A. Eramzhyan, Sov. J. Nuclear Phys. 11 (1970) 295.
- [141] J. Bernabéu, Nuovo Cimento 4A (1971) 715.
- [142] C.W. Kim and S.L. Mintz, Nuclear Phys. B27 (1971) 621.
- [143] J. Delorme, Compt. Rend. 256 (1963) 3568; Nuclear Phys. B19 (1970) 573.
- [144] J. Delorme and M. Ericson, Phys. Letters 32B (1970) 443.
- [145] J.S. O'Connell, T.W. Donnelly and J.D. Walecka, Phys. Rev. C6 (1972) 719.
- [146] T.W. Donnelly and J.D. Walecka, Phys. Letters 44B (1973) 330;
J.B. Cammarata, Nuclear Phys. A254 (1975) 422;
J.B. Cammarata and T.W. Donnelly, Nucl. Phys. A267 (1976) 365.
- [147] C.W. Kim and L. Armstrong, Phys. Rev. C6 (1972) 1924.
- [148] K. Kubodera and C.W. Kim, Phys. Letters 43B (1973) 275.
- [149] J.D. Vergados, Nuclear Phys. A220 (1974) 259.
- [150] V. Devanathan, R. Parthasarathy and P.R. Subramanian, Ann. Phys. (N.Y.) 73 (1972) 291; 92 (1975) 25; Nucl. Phys. A262 (1976) 433.
- [151] T.N.K. Godfrey, Ph.D. Thesis, Princeton Univ., 1954 (unpublished).
- [152] J.O. Burgman, J. Fischer, B. Leontic, A. Lundby, R. Meunier, J.P. Stroot and J.D. Teja, Phys. Rev. Letters 1 (1958) 469.
- [153] H.V. Argo, F.B. Harrison, H.W. Kruse and J. McGuire, Phys. Rev. 114 (1959) 626.
- [154] J.G. Fetkovich, T.H. Fields and R.L. McIlwain, Phys. Rev. 118 (1960) 319.
- [155] G.T. Reynolds, D.B. Scarl, R.A. Swanson, J.R. Waters and R.A. Zdanis, Phys. Rev. 129 (1963) 1790.
- [156] E.J. Maier, R.M. Edelstein and R.T. Siegel, Phys. Rev. 133B (1964) 663.
- [157] J.P. Deutsch, L. Grenacs, P. Igo-Kemenes, P. Lipnik and P.C. Macq, Phys. Letters 26B (1968) 315.
- [158] A. Babaev, V.S. Evseev, G.G. Myashicheva et al., JINR preprint R14-4241 (1968), unpublished.
- [159] Yu.G. Budyashov, V.G. Zinov, A.D. Konin, S.V. Medved', A.I. Mukhin, E.B. Ozenov, A.M. Chatzchyan and R.A. Eramzhyan, Sov. Phys. JETP 31 (1970) 651.
- [160] G.H. Miller, M. Eckhause, F.R. Kane, P. Martin and R.E. Welsh, Phys. Rev. Letters 29 (1972) 1194.
- [161] D. Kurath, Phys. Rev. 106 (1957) 975.
- [162] A.N. Boyarkina, Izv. Akad. Nauk. SSSR, ser. Fiz. 28 (1964) 335.
- [163] S. Cohen and D. Kurath, Nuclear Phys. 73 (1965) 1;
P.S. Hauge and S. Maripuu, Phys. Rev. C8 (1973) 1609, and references therein.
- [164] D. Kurath, Phys. Rev. 130 (1963) 1525.
- [165] See L. Fagg, Rev. Mod. Phys. 47 (1975) 705, and references therein.
- [166] S. Skupsky, Phys. Letters 36B (1971) 271; Nuclear Phys. A178 (1971) 289;
J.A. Bistirlich, K.M. Crowe, A.S.L. Parsons, P. Skarek and P. Truöl, Phys. Rev. C5 (1972) 1867;
H. Baer et al., Phys. Rev. C12 (1975) 921;
H. Baer, K. Crowe and P. Truöl, Radiative pion capture in nuclei, to be published in Advances in Nuclear Physics.
- [167] N.M. Kroll and M.A. Ruderman, Phys. Rev. 93 (1954) 233;
G. Chew, M.L. Goldberger, F.E. Low and Y. Nambu, Phys. Rev. 106 (1957) 1345;
see also J. Delorme and T.E.O. Ericson, Phys. Letters 21 (1966) 98.
- [168] A. Possoz, D. Favart, L. Grenacs, J. Lehmann, P.C. Macq, D. Meda, L. Palfy, J. Julien and C. Samour, Phys. Letters 50B (1974) 438;
L. Grenacs, private communication (December 1975).
- [169] R.E. MacDonald, J.A. Becker, R.A. Chalmers and D.H. Wilkinson, Phys. Rev. C10 (1974) 333.
- [170] G. Flamand and K.W. Ford, Phys. Rev. 116 (1959) 1591.
- [171] L.L. Foldy and J.D. Walecka, Phys. Rev. 140 (1965) B1339; 147 (1966) 886E.
- [172] X. Campi and D.W.L. Sprung, Nuclear Phys. A194 (1972) 401;
M. Beiner, H. Flocard, N.V. Giai and P. Quentin, Nuclear Phys. A238 (1975) 29.
- [173] J.C. Bergstrom, I.P. Auer and R.S. Hicks, Nuclear Phys. A251 (1975) 401.
- [174] J.P. Deutsch, D. Favart, R. Priels, B. Van Ostaeyen, G. Audit, N. de Button, J.-L. Faure, C. Schuhl, G. Tamas and C. Tzara, Phys. Rev. Letters 33 (1974) 316.

- [175] F. Cannata, C.W. Lucas and C. Werntz, Phys. Rev. Letters 33 (1974) 1316.
- [176] J.P. Deutsch, Invited talk at the TRIUMF School (1975), to be published, and private communications (December 1975).
- [177] H.-G. Clerc and E. Kuphal, Z. Physik 211 (1968) 451.
- [178] E. Fiorini, R. Engfer and H.K. Walter, private communications (April 1976);
E. Fiorini, Zuoz (1976) Lectures, to be published.
- [179] O. Nalcioğlu, D.J. Rowe and C. Ngo-Trong, Nuclear Phys. A218 (1974) 495.
- [180] B. Goulard, J. Joseph and F.O. Ledoyen, Phys. Rev. Letters 27 (1971) 1238.
- [181] B. MacDonald, J.A. Diaz, S.N. Kaplan and R.V. Pyle, Phys. Rev. 139 (1965) B1253.
- [182] G. Bunyatyan, V.S. Evseev, L.N. Nikityuk, A.A. Nikolina, V.N. Pokrovskii, V.S. Roganov, L.M. Smirnova and I.A. Yutlandov, Sov. J. Nuclear Phys. 9 (1969) 457;
G. Bunyatyan, Sov. J. Nuclear Phys. 11 (1970) 441.
- [183] G. Bunyatyan, Sov. J. Nuclear Phys. 2 (1966) 619; 3 (1966) 613.
- [183a] J.D. Walecka, Nuclear Phys. A258 (1976) 397.
- [184] R. Parthasarathy, private communications (October 1975).
- [185] N.P. Popov, Sov. Phys. JETP 17 (1963) 1130.
- [186] Z. Oziewicz and A. Pikulski, Acta Phys. Polon. 32 (1967) 873; 34 (1968) 291;
G. Hock and Z. Oziewicz, ibid. B4 (1973) 43;
A.P. Bukhvostov et al., ibid. B4 (1973) 495;
S. Ciechanowicz, Nucl. Phys. A267 (1976) 472.
V. Devanathan and P.R. Subramanian, Ann. Phys. 92 (1975) 25.
- [187] Z. Oziewicz, Dubna preprint JINR-E4-8350 (1974), unpublished, and private communications (October 1975).
- [188] L. Grenacs, J.P. Deutsch, P. Lipnik and P.C. Macq, Nuclear Instrum. Methods 58 (1968) 164.
- [189] B.H. Wildenthal and J.B. McGrory, Phys. Rev. C7 (1973) 714;
M.J.A. De Voigt and B.H. Wildenthal, Nuclear Phys. A206 (1973) 305.
- [190] P.M. Endt and C. van der Leun, Nuclear Phys. A214 (1973) 188 (see table 28-4 of this paper).
- [191] I.S. Shapiro and L.D. Blokhintsev, Zh. Eksp. Teor. Fiz. 39 (1960) 1113.
- [192] T. Ericson, J.C. Sens and H.P.C. Rood, Nuovo Cimento 34 (1964) 51.
- [193] M. Rho, Phys. Rev. 161 (1967) 955.
- [194] A.M. Green and M. Rho, Nuclear Phys. A130 (1969) 112.
- [195] T.W. Donnelly and J.D. Walecka, Phys. Letters 41B (1972) 275.
- [196] O. Nalcioğlu, A. Goswami and R.D. Graves, Lett. Nuovo Cimento 7 (1973) 897.
- [197] A. Rej, to be published and private communications (1975).
- [198] A. Astbury, L.B. Auerbach, D. Cutts, R.J. Esterling, D.A. Jenkins, L.H. Lipman and R.E. Shafer, Nuovo Cimento 33 (1964) 1020.
- [199] R.C. Cohen, S. Devons and A.D. Kanaris, Nuclear Phys. 57 (1964) 255.
- [200] J.P. Deutsch, L. Grenacs, P. Igo-Kemenes, P. Lipnik and P.C. Macq, Nuovo Cimento 52B (1967) 557.
- [201] J.P. Deutsch, L. Grenacs, J. Lehmann, P. Lipnik and P.C. Macq, Phys. Letters 29B (1969) 66.
- [202] F.R. Kane, M. Eckhouse, G.H. Miller, B.L. Roberts, M.E. Vislay and R.E. Welsh, Phys. Letters 45B (1973) 292.
- [203] F. Ajzenberg-Selove, Nuclear Phys. A166 (1971) 1.
- [204] L. Palfy, J.P. Deutsch, L. Grenacs, J. Lehmann and M. Steels, Phys. Rev. Letters 34 (1975) 212.
- [205] I. Sick, E.B. Hughes, T.W. Donnelly, J.D. Walecka and G.E. Walker, Phys. Rev. Letters 23 (1969) 1117.
- [206] M. Stroetzel, Z. Physik 214 (1968) 357.
- [207] J.C. Kim, R.P. Singhal and H.S. Kaplan, Can. J. Phys. 48 (1970) 83.
- [208] G.H. Miller, M. Eckhouse, P. Martin and R.E. Welsh, Phys. Rev. C6 (1972) 487.
- [209] V. Devanathan, M. Rho, K. Srinivasa Rao and S.C.K. Nair, Nuclear Phys. B2 (1967) 329;
F. Cannata, Lett. Nuovo Cimento 4 (1970) 35.
- [210] M. Goldhaber and E. Teller, Phys. Rev. 74 (1948) 1046.
- [211] M.H. Macfarlane, in: Isobaric spin in nuclear physics, eds. J.D. Fox and D. Robson (Academic Press, New York, 1966) p. 383; in: Nuclear isospin, eds. J.D. Anderson et al. (Academic Press, New York, 1969) p. 591.
- [212] A.M. Lane and A.Z. Mekjian, Phys. Rev. C8 (1973) 1981.
- [213] A. Lodder and C.C. Jonker, Phys. Letters 18 (1965) 310; Nuclear Phys. B2 (1967) 383.
- [214] J. Bernabéu, Nuclear Phys. A201 (1973) 41;
J. Bernabéu and F. Cannata, Phys. Letters 45B (1973) 445; Nuclear Phys. A215 (1973) 424.
- [215] J.D. Vergados, Penn. preprint (1975).
- [216] Yu.I. Bely, R.A. Eramzhyan, L. Majling, J. Rizek and V.A. Vartanyan, Nuclear Phys. A204 (1973) 357.
- [217] R.J. McCarthy and G.E. Walker, Phys. Rev. C11 (1975) 383.
- [218] J. Joseph, F. Ledoyen and B. Goulard, Phys. Rev. C6 (1972) 1742.
- [219] J.R. Luyten, H.P.C. Rood and H.A. Tolhoek, Nuclear Phys. 41 (1963) 236.
- [220] D. Duplain, B. Goulard and J. Joseph, Phys. Rev. C12 (1975) 28.

- [221] V. Evseev, T. Kozlowski, V. Roganov and J. Wojtlowska, Phys. Letters 28B (1969) 553; in: High-energy physics and nuclear structure, ed. S. Devons (Plenum Press, New York, 1970) p. 157.
- [222] M.E. Plett and S.E. Sobottka, Phys. Rev. C3 (1971) 1003.
- [223] S.N. Kaplan, R.V. Pyle, L.E. Temple and G.F. Valby, Phys. Rev. Letters 22 (1969) 795; private communications (1975).
- [224] T.A.E. Pratt, Nuovo Cimento 61B (1969) 119.
- [225] P. Igo-Kemenes, J.P. Deutsch, D. Favart, L. Grenacs, P. Lipnik and P.C. Macq, Phys. Letters 34B (1971) 286.
- [226] E.D. Earle and G.A. Bartholomew, Nuclear Phys. A176 (1971) 363.
- [227] G. Backenstoss, S. Charalambus, H. Daniel, W.D. Hamilton, V. Lynen, C. Malsburg, G. Poelz and H. Povel, Nuclear Phys. A162 (1971) 541.
- [228] H.P. Povel, H. Koch, W.D. Hamilton, S. Charalambus and G. Backenstoss, Phys. Letters 33B (1970) 620.
- [229] R. Raphael, H. Überall and C. Werntz, Phys. Letters 24B (1967) 15.
- [230] B. Goulard and J. Joseph, Phys. Letters 45B (1973) 27.
- [231] H. Baer, Invited talk at the New York APS meeting (February 1976), Bull. Am. Phys. Soc. 21 (1976) 80.
- [232] A. Bertin, A. Vitale and A. Placci, Phys. Rev. A7 (1973) 2214.
- [233] See, for example, J.C. Sens, Phys. Rev. 113 (1958) 679.
- [234] K.W. Ford and J.C. Wills, Nuclear Phys. 35 (1962) 295.
- [235] P. Christillin, A. Dellafiore and M. Rosa-Clot, Phys. Rev. Letters 31 (1973) 1012; Phys. Rev. C12 (1975) 691; Nuovo Cimento 34A (1976) 272, 289, 296, and private communications (1976); A. Dellafiore, Oxford preprint (1976).
- [236] F. Cannata and N.C. Mukhopadhyay, Phys. Rev. C10 (1974) 379 and C12 (1975) 1096E.
- [237] B. Goulard and H. Primakoff, Phys. Rev. C10 (1974) 2034; C11 (1975) 1894.
- [237a] J.S. Bell and J. Løvseth, Nuovo Cimento 32 (1964) 433;
H.P.C. Rood [C15];
Shuster and Rho [239];
See also E. Lubkin, Ann. Phys. 11 (1960) 414 for a detailed discussion of the Fermi gas model.
- [238] N.C. Mukhopadhyay, to be published.
- [239] P.J.S. Watson, Phys. Letters 58B (1975) 431.
- [240] A. Salam and J. Strathdee, Nature 252 (1975) 569;
J.C. Hardy and S. Towner, Phys. Letters 58B (1975) 261.
- [241] G. Do Dang, Phys. Letters 38B (1972) 397.
- [242] R. Bizzari, E. Di Capua, U. Dore, G. Gialanella, P. Guidoni and I. Laasko, Nuovo Cimento 33 (1964) 1497.
- [243] M.M. Block, T. Tikuchi, S. Koetke, C.R. Sun, R. Walker, G. Culligan, V.L. Telegdi and R. Winston, Nuovo Cimento 55A (1968) 501.
- [243a] M. Eckhouse, Carnegie Tech. Report 9286 (1962).
- [244] R.A. Reiter, T.A. Romanowski, R.B. Sutton and B.G. Chidley, Phys. Rev. Letters 5 (1960) 22.
- [245] J.L. Lathrop, R.A. Lundy, V.L. Telegdi, R. Winston and D.D. Yovanovitch, Phys. Rev. Letters 7 (1961) 107.
- [246] J. Barlow, J.C. Sens, P.J. Duke and M.A.R. Kemp, Phys. Letters 9 (1964) 84.
- [247] V.D. Bovrov, V.G. Verlamov, Yu.M. Grashin, B.A. Dolgoshein, V.G. Kirilov-Ugryumov, V.G. Roganov, A.V. Samoilov and S.V. Somov, Sov. Phys. JETP 21 (1965) 799.
- [248] C. Petitjean, H. Backe, R. Engfer, V. Jahnke, K.H. Lindenberger, H. Schneuwly, W.U. Schröder and H.K. Walter, Nuclear Phys. A178 (1971) 193.
- [249] M. Eckhouse, R.T. Siegel, R.E. Welsh and T.A. Filippas, Nuclear Phys. 81 (1966) 575;
M. Eckhouse et al., Phys. Rev. 132 (1963) 422.
- [250] O. Hashimoto, S. Nagamiya, K. Nagamine and T. Yamazaki, Contribution II.16 Sante Fe (1975).
- [250a] B.M. Aleksandrov, S. Polikanov et al., Dubna preprint E15-8628 (1975), to be published.
- [251] R.B. Kinsey et al., private communications (1975).
- [252] H. Backe, R. Engfer, U. Jahnke, E. Kankeleit, R.M. Pearce, C. Petitjean, L. Schellenberg, H. Schneuwly, W.U. Schröder, H.K. Walter and A. Zehnder, Nuclear Phys. A189 (1972) 472.
- [253] E. Wigner, Phys. Rev. 51 (1937) 106 and 947; 56 (1939) 519.
- [254] P. Franzini and L.A. Radicati, Phys. Letters 6 (1963) 322.
- [255] J.I. Fujita and K. Ikeda, Nuclear Phys. 67 (1965) 145.
- [256] B. Goulard and H. Primakoff, Phys. Rev. 135 (1964) B1139.
- [257] P. Hraskó, Phys. Letters 28B (1969) 470.
- [258] J. Krüger and P. Van Leuven, Phys. Letters 28B (1969) 623.
- [259] N.C. Mukhopadhyay, to be published.
- [260] M. Ademollo and R. Gatto, Phys. Rev. Letters 13 (1963) 264;
See R. Leonardi and M. Rosa-Clot, Riv. Nuovo Cimento 1 (1971) 1 and ref. [137] for a discussion in the present context.
- [261] J.B. French and J.C. Parikh, Phys. Letters 35B (1971) 1.
- [262] J.D. Walecka, in: Proc. of the International School of Physics "Enrico Fermi", Course XXXVIII, ed. T.E.O. Ericson (Academic Press, New York, 1967) p. 17.

- [263] F. Cannata, R. Leonardi and M. Rosa-Clot, Phys. Letters 32B (1970) 6;
See also F. Cannata and J.I. Fujita, Progr. Theoret. Phys. 51 (1974) 811
and F. Cannata, Lett. Nuovo Cimento 13 (1975) 319.
- [264] G. Heusser and T. Kirsten, Nuclear Phys. A195 (1972) 369.
- [265] H.J. Evans, Nuclear Phys. A207 (1973) 379;
L.E. Temple, S.N. Kaplan, R.V. Pyle and G.F. Valley, preprint LBL 24 (1971) unpublished.
- [266] I. Bobodyanov, Acta Phys. Acad. Sci. Hung. 29 (1970) 151.
- [267] P. Singer, Phys. Rev. 124 (1961) 1602; Nuovo Cimento 23 (1962) 669.
- [267a] B. MacDonald, J.A. Diaz, S.N. Kaplan and R.V. Pyle, Phys. Rev. 139 (1965) B1253;
S.N. Kaplan et al., Phys. Rev. 112 (1958) 968.
- [268] B.D. Day, Rev. Mod. Phys. 39 (1967) 719;
S.-O. Bäckman, A.D. Jackson and J. Speth, Phys. Letters 56B (1975) 209.
- [269] J. Hadermann, Phys. Letters 55B (1975) 141;
J. Hadermann and K. Junker, Nucl. Phys., in press.
- [270] K.J. Le Coultre, in: Nuclear reactions, eds. P.M. Endt and M. Demeur (North-Holland, Amsterdam, 1959);
V.S. Evseev and T.N. Mamedov, JINR preprint P1-7115 (Dubna, 1973).
- [271] A. Bouyssy and N. Vinh-Mau, Nuclear Phys. A185 (1972) 32;
A. Bouyssy, H. Ngo and N. Vinh-Mau, Phys. Letters 44B (1973) 139.
- [272] J. Bernabéu, T.E.O. Ericson and C. Jarlskog, Contribution No. V.A.22 to the Santa Fe meeting (1975), and private communications (December 1975).
- [273] See, for example, R.M. Sundelin and R.M. Edelstein, Phys. Rev. C7 (1973) 1037 and discussions therein.
- [274] V.S. Evseev, F. Kilbinger, V.S. Roganov, V.A. Chernogorova and M. Szymbczak, Sov. J. Nuclear Phys. 4 (1967) 387.
- [275] E.W. Anderson, Columbia University Report No. NEVIS-136 (1965), unpublished.
- [276] V.S. Evseev, private communications (August, 1975).
- [277] J. Sculli, Columbia University Report NEVIS-168 (1969), unpublished.
- [278] R. Klein, T. Neal and L. Wolfenstein, Phys. Rev. 138B (1965) 86.
- [279] V. Devanathan and M.E. Rose, Jour. Math. Sci. (India) 1 (1967) 137;
V. Devanathan, R. Parthasarathy and G. Ramachandran, Ann. of Phys. 72 (1972) 428;
P.R. Subramanian et al., Ann. of Phys. 73 (1972) 291.
- [280] A. Bogan, Nuclear Phys. B12 (1969) 89.
- [281] C.A. Piketty and J. Procureur, Nuclear Phys. B26 (1971) 390.
- [282] R.A. Eramzhyan, V.N. Fetisov and Yu.A. Salganic, Phys. Letters 35B (1971) 143; Nuclear Phys. B39 (1972) 216.
- [283] K. Kume, N. Ohtsuka, H. Ohtsubo and M. Morita, Nuclear Phys. A251 (1975) 465.
- [284] A. Bouyssy and N. Vinh-Mau, Phys. Letters 48B (1974) 162
- [285] V. Devanathan, private communications (1975).
- [285a] C. Ishii, Progr. Theoret. Phys. 21 (1959) 663.
- [286] H. Morinaga and W.F. Fry, Nuovo Cimento 10 (1953) 308.
- [287] D. Kotelchuck, Nuovo Cimento 35 (1964) 27;
D. Kotelchuck and J.V. Tyler, Phys. Rev. 165 (1968) 1190.
- [288] A.O. Weissenberg, E.D. Kolganova and N.V. Rabin, Sov. J. Nuclear Phys. 1 (1965) 467; 11 (1970) 464.
- [289] V.I. Komarov and O.V. Savchenko, Sov. J. Nuclear Phys. 8 (1969) 239.
- [290] S.E. Sobottka and E.L. Wills, Phys. Rev. Letters 20 (1968) 596.
- [291] Yu.G. Budyashov, V.G. Zinov, A.D. Konin, A.I. Mukhin and A.M. Chatzchyan, Sov. Phys. JETP 33 (1971) 11.
- [292] A. Wyttensbach, P. Baertschi, H.S. Pruis and E.A. Hermes, private communications (March 1976), and to be published in Helv. Phys. Acta;
See references for earlier radiochemical work in Singer [B30].
- [293] T. Kozlowski and A. Zglinski, Phys. Letters 50B (1974) 222; Nucleonika 19 (1974) 72, and to be published.
- [294] Yu.A. Batusov, S.A. Bunyatov, L. Vizireva, G.R. Gulkanyan, P. Mirsalikhova, V.M. Sidorov, Kh.M. Chernev and R.A. Eramzhyan, Yad. Fiz. 22 (1975) 320, and reference therein;
V.M. Sidorov, private communications (1975).
- [295] B.R. Wienke and S.L. Meyer, Phys. Rev. C3 (1971) 2179;
S.L. Meyer, private communications (1975).
- [296] A.R. Clark, T. Elioff, H.J. Frisch, R.P. Johnson, L.T. Kerth, G. Shen and W. Wenzel, Phys. Rev. D9 (1974) 533.
- [296a] M. Daum, L. Dubal, G.H. Eaton, R. Frosch, J. McCulloch, R.C. Minehart, E. Steiner, C. Amsler and R. Hausammann, Phys. Letters 60B (1976) 380;
R. Frosch, private communications (October 1976).
- [297] D.F. Zaretski and V.M. Novikov, Nuclear Phys. 28 (1961) 177.
- [298] G. Leander and P. Möller, Phys. Letters 57B (1975) 245.
- [299] S.D. Bloom, Phys. Letters 48B (1974) 420.
- [300] S.N. Kaplan, J.A. Monard and S. Nagamiya, Phys. Letters 64B (1976) 217, and private communications (1976);

- [301] O. Hashimoto, S. Nagamiya, K. Nagamine and T. Yamazaki, Phys. Letters 62B (1976) 233.
 [301] D. Chultem, V. Cojocaru, Dz. Gansorig, K.S. Chwan, T. Krogulski, V.D. Kuznetsov, H.G. Ortlepp, S.M. Polikanov, B.M. Sabirov, U. Schmidt and W. Wagner, Nuclear Phys. A247 (1975) 532 and references therein.
- [302] J. Hadermann and K. Junker, Nuclear Phys. A256 (1976) 521;
 J. Hadermann, K. Junker and N.C. Mukhopadhyay, to be published.
- [303] See, for example, V.S. Evseev and T.N. Mademov, Sov. J. Nuclear Phys. 19 (1974) 624;
 See other references quoted in [302].
- [304] P. Baertschi, A. Grütter, H.P. von Gunten, H.S. Pruys and M. Rajagopalan, private communications (February 1976) and Helv. Phys. Acta 49 (1976) 187.
- [305] P. Morrison and L.I. Schiff, Phys Rev. 58 (1940) 24.
- [306] K. Huang, C.N. Yang and T.D. Lee, Phys. Rev. 108 (1957) 1340.
- [307] G.K. Manacher and L. Wolfenstein, Phys. Rev. 116 (1959) 782.
- [308] S.L. Adler and Y. Dothan, Phys. Rev. 151 (1966) 1267.
- [309] F.E. Low, Phys. Rev. 110 (1958) 974.
- [310] See, for example, E. Borchi and R. Gatto, Nuovo Cimento 33 (1964) 1472;
 G. Opat, Phys. Rev. 134 (1964) B428.
- [311] H.P.C. Rood and H.A. Tolhoek, Nuclear Phys. 70 (1965) 658;
 H.P.C. Rood, A.F. Yano and F.B. Yano, Nuclear Phys. A228 (1974) 333.
- [312] E. Borchi and S. De Gennaro, Phys. Rev. C2 (1970) 1012.
- [313] P. Christillin and M. Rosa-Clot, Lett. Nuovo Cimento 4 (1972) 1; Phys. Rev. C7 (1973) 44.
- [314] D. Beder, Nuclear Phys. A258 (1976) 447, and private communications.
- [315] G. Conforto, M. Conversi and L. Di Lella, Proc. Internat. Conf. on High-Energy Physics, CERN (1962) p. 427.
- [316] W.T. Chu, I. Nadelhaft and J. Ashkin, Phys. Rev. 137 (1965) B352.
- [317] M. Conversi, R. Diebold and L. Di Lella, Phys. Rev. 136 (1964) B1077.
- [318] L. Di Lella, I. Hammerman, and L.M. Rosenstein, Phys. Rev. Letters 27 (1971) 830;
 L.M. Rosenstein and I.S. Hammerman, Phys. Rev. C8 (1973) 603.
- [319] M. Hasinoff, L. Grenacs and P. Trüol, private communications (1975–76).
- [320] R. Cutkosky, Phys. Rev. 107 (1957) 330.
- [321] A. Wullschleger, private communications (1975).
- [322] See R. Strubbe, Comp. Phys. Comm. 8 (1974) 1, and references therein.
- [323] H.W. Fearing, Phys. Rev. Letters 35 (1975) 79.
- [324] K. Ohta, Phys. Rev. Letters 33 (1974) 1507.
- [325] See, for example, B. Pontecorvo, Sov. Phys. JETP 34 (1958) 247;
 V. Gribov and B. Pontecorvo, Phys. Letters 29B (1969) 493;
 S.M. Bilenky and B. Pontecorvo, Phys. Letters 61B (1976) 248.
- [325a] G. Feinberg and S. Weinberg, Phys. Rev. 123 (1961) 1439; Phys. Rev. Letters 3 (1959) 111; 6 (1961) 381.
- [326] E.J. Konopinski and H.M. Mahmoud, Phys. Rev. 92 (1953) 1045.
- [327] M. Conversi, L. Di Lella, A. Egidi, C. Rubbia and M. Toller, Phys. Rev. 122 (1961) 687.
- [328] L. Kisslinger, Phys. Rev Letters 26 (1971) 998, and private communications (1975);
 See also H. Primakoff and S.P. Rosen, Phys. Rev. D5 (1972) 1784.
- [329] M. Shuster and M. Rho, Phys. Letters 42B (1972) 45.
- [330] D.A. Bryman, M. Blecher, R. Powers and K. Gotow, Phys. Rev. Letters 28 (1972) 1469.
- [330a] B. Hahn, private communications (1976).
- [331] N.C. Mukhopadhyay and L.D. Miller, Phys. Letters 47B (1973) 415;
 See also H.J. Strubbe and D.K. Callebaut, Nuclear Phys. A143 (1970) 537;
 H. Ohtsubo, M. Sano and M. Morita, Progr. Theoret. Phys. (Kyoto) 49 (1973) 877.
- [332] M. V. Barnhill, Nuclear Phys. A131 (1969) 106;
 J. L. Friar, Phys. Rev. C10 (1974) 955; C12 (1975) 2127;
 M. Bolsterli, W. R. Gibbs, B. F. Gibson and G. J. Stephenson, Phys. Rev. C10 (1974) 1225.
- [333] R. A. Krajcik and L. L. Foldy, Phys. Rev. Letters 24 (1970) 545, 762E;
 F. E. Close, Nuclear Phys. B19 (1970) 447.
- [334] D. H. Wilkinson, Phys. Rev. C7 (1973) 930; Nuclear Phys. A209 (1973) 470; A225 (1974) 365.
- [335] See, for example, M. Chemtob and M. Rho, Nuclear Phys. A163 (1971) 1.
- [336] J. Blomqvist, Phys. Letters 32B (1970) 1;
 D. O. Riska and G. E. Brown, Phys. letters 32B (1970) 662;
 E. Fischbach, E. P. Harper, Y. E. Kim, A. Tubis and W. K. Cheng, Phys. Letters 38B (1972) 8;
 W. Jaus, Helv. Phys. Acta 49 (1976) 475.
- [337] A. Gari and A. H. Huffman, Ap. J. Letters 174 (1972) L151; Ap. J. 178 (1972) 543.
- [338] F. Dautry, private communications (1975);
 See M. Rho, in: Effects mesoniques dans les noyaux (Saclay, 1975) p. 9 and ref. [108].

- [339] K. Ohta and M. Wakamatsu, Phys. Letters 51B (1974) 325 and 327.
- [340] M. Ericson, A. Figureau and C. Thévenet, Phys. Letters 45B (1973) 19.
- [341] See, for example, A. Barroso and R. J. Blin-Stoyle, Nuclear Phys. A251 (1975) 446.
- [342] M. Ericson, Ann. Phys. (N.Y.) 63 (1971) 562.
- [342a] T. E. O. Ericson and M. Locher, Nuclear Phys. A148 (1970) 1.
- [343] S. Weinberg, Phys. Rev. Letters 17 (1966) 616;
Y. Tomozawa, Nuovo Cimento 46A (1966) 707.
- [344] M. Rho, Nuclear Phys. A231 (1974) 493.
- [345] M. Ericson and T. E. O. Ericson, Ann. Phys. (N.Y.) 36 (1966) 323;
F. Scheck and C. Wilkin, Nuclear Phys. B49 (1972) 541;
G. Fäldt, Nuclear Phys. A206 (1973) 176.
- [346] S. Barshay, G. E. Brown and M. Rho, Phys. Rev. Letters 32 (1974) 787.
- [347] J. Delorme, M. Ericson, A. Figureau and C. Thévenet, private communications and to be published (1976);
J. Delorme and M. Ericson, Phys. Letters B60 (1976) 451.
- [348] R. J. Blin-Stoyle, Nuclear Phys. A254 (1975) 353.
- [349] J. Hüfner, Phys. Reports 21C (1975) 36;
G. E. Brown and W. Weise, Phys. Reports 22C (1975) 279, and to be published;
S.-O. Bäckman and W. Weise, Phys. Letters 55B (1975) 1;
W. Weise, private communications (1976).
- [350] K. Baba, Progr. Theoret. Phys. 43 (1970) 390.
- [351] L. P. Fulcher and N. C. Mukhopadhyay, Phys. Letters 47B (1973) 115; Nuovo Cimento 28A (1975) 487.
- [352] H. P. C. Rood and A. I. Yano, Phys. Letters 35B (1971) 59; 37B (1971) 189.
- [353] K. M. Case, Phys. Rev. 80 (1950) 797.
- [354] G. E. Brown and A. M. Green, Nuclear Phys. A137 (1969) 1;
A. M. Green and M. Rho, Nuclear Phys. A130 (1969) 112.
- [355] S. Wycech, Nuclear Phys. B14 (1969) 133.
- [356] J. Delorme, M. Ericson and G. Fäldt, Nuclear Phys. 240A (1975) 493.
- [357] L. Kissinger, Phys. Rev. 98 (1955) 761.
- [358] J. Delorme and M. Rho, Nuclear Phys. B34 (1971) 317; B46 (1972) 332E;
H.J. Lipkin, Phys. Letters 34B (1971) 202; Phys. Rev. Letters 27 (1971) 432;
L. Wolfenstein and E. M. Henley, Phys. Letters 36B (1971) 28.
- [359] K. Kubodera, J. Delorme and M. Rho, Nuclear Phys. B66 (1973) 253; B99 (1975) 545E.
- [360] D. H. Wilkinson, Phys. Letters 48B (1974) 169.
- [361] B. Holstein and S. Treiman, Phys. Rev. C3 (1971) 1921;
B. Holstein, Rev. Mod. Phys. 46 (1974) 789.
- [362] F. Calaprice, S. Freedman, W. C. Mead and H. C. Vantine, Phys. Rev. Letters 35 (1975) 1566.
- [363] R. E. Tribble and G. T. Garvey, Phys. Rev. Letters 32 (1974) 314.
- [363a] L. Grenacs, private communications (April 1976).
- [364] See G. F. Chew, *S-matrix theory of strong interactions* (Benjamin, New York, 1962).
- [365] C. W. Kim and H. Primakoff, Phys. Rev. 140B (1965) 566.
- [366] A. Galindo and P. Pascual, Nuclear Phys. B14 (1969) 37;
J. Delorme, Nuclear Phys. B19 (1970) 573.
- [367] B. Z. Kopeliovich, JINR Preprint P2-7086 (1973), unpublished.
- [368] Particle Data Group, Phys. Letters 50B (1974) 1.
- [369] G. Backenstoss, H. Daniel, K. Jentzsch, H. Koch, H.P. Povel, F. Schmeissner, K. Springer and R.L. Stearns, Phys. Letters 36B (1971) 422.
- [370] J.G. Fetkovich, T.H. Fields, G.B. Yodh and M. Derrick, Phys. Rev. Letters 4 (1960) 570.
- [371] V.P. Dzhelepov, P.F. Ermolov, V.I. Moskalev and V.V. Fil'chenkov, Sov. Phys. JETP 23 (1966) 820.
- [372] I.M. Blair, H. Muirhead, T. Woodhead and J.H. Wouds, Proc. Phys. Soc. (London) 80 (1962) 938.
- [373] G.H. Miller, M. Eckhouse, F.R. Kane, P. Martin and R.E. Welsh, Phys. Letters 41B (1972) 50.
- [374] J.P. Deutsch et al., CERN report PH III-70/9 (1970), unpublished.
- [375] O.A. Zaimidoroga, M.M. Kulyukin, B. Pontecorvo, R.M. Sulyaev, I.V. Falomkin, A.F. Filippov, V.M. Tsupko-Sitnikov and Yu.A. Scherbakov, Phys. Letters 6 (1963) 100.
- [376] S.N. Kaplan, B.J. Moyer and R.V. Pyle, Phys. Rev. 112 (1958) 968.
- [377] A.M. Rushton, Columbia Thesis (1972), unpublished, and private communication (Nov. 1976). Rushton's thesis corrects some errors in B. Budick et al., Phys. Rev. Letters 24 (1970) 604.
- [378] J.A. Diaz, S.N. Kaplan and R.V. Pyle, Nucl. Phys. 40 (1963) 54.
- [379] L. Palfy, J. Lehmann, L. Grenacs and M. Subotowicz, Nuovo Cimento 3A (1971) 505.
- [380] D. Bailin and N. Dombe, Phys. Letters 64B (1976) 304.